Mu opioid receptors and neuronal circuits of addiction : genetic approaches in mice

Pauline Charbogne

▶ **To cite this version:**

Pauline Charbogne. Mu opioid receptors and neuronal circuits of addiction : genetic approaches in mice. Neurobiology. Université de Strasbourg, 2015. English. NNT : 2015STRAJ030 . tel-01362949

HAL Id: tel-01362949
https://theses.hal.science/tel-01362949

Submitted on 9 Sep 2016

HAL is a multi-disciplinary open access archive for the deposit and dissemination of scientific research documents, whether they are published or not. The documents may come from teaching and research institutions in France or abroad, or from public or private research centers.

L'archive ouverte pluridisciplinaire **HAL**, est destinée au dépôt et à la diffusion de documents scientifiques de niveau recherche, publiés ou non, émanant des établissements d'enseignement et de recherche français ou étrangers, des laboratoires publics ou privés.

UNIVERSITÉ DE STRASBOURG

École Doctorale des Sciences de la Vie et de la Santé

IGBMC - CNRS UMR 7104 - Inserm U 964

THÈSE présentée par :

Pauline CHARBOGNE

soutenue le : **9 juillet 2015**

pour obtenir le grade de : **Docteur de l'université de Strasbourg**

en Aspects Moléculaires et Cellulaires de la Biologie

Mention Neurosciences

Mu opioid receptors and neuronal circuits of addiction: genetic approaches in mice

THÈSE dirigée par :

Mme KIEFFER Brigitte L.	Professeure, Université de Strasbourg/McGill University

RAPPORTEURS :

M. BELIN David	Maître de conférences, University of Cambridge
Mme LE MOINE Catherine	Directrice de recherche, Université de Bordeaux
M. ZWILLER Jean	Directeur de recherche, Université de Strasbourg

Remerciements

Je tiens à dire un grand merci au professeur Brigitte Kieffer, pour m'avoir accueillie dans son équipe et guidée dans mon travail de thèse. Merci pour toutes les discussions de fond qui m'ont amenée à développer un regard critique et constructif sur mes projets. Merci pour tout le temps que vous m'avez consacré, je sais qu'il est précieux. Un grand merci également pour votre transmission du goût de l'écriture (c'était assez inattendu !).

Je tiens à remercier les docteurs David Belin, Catherine Le Moine, Jean Zwiller, Abdel Ouagazzal et Katia Befort d'avoir accepté d'évaluer mon travail.

Merci à tous les Brikiteam members strasbourgeois passés et présents, Caro, Sercan, Xav, David, Hervé, Laurie-Anne, Claire, Raph, Chihiro, Abdel, Pascale, Pierre-Eric, Yvan, Alice, Carole, Jérôme, Julie, Aline, Michel, Paul, Laurence, Megan (wooot !), Dom (mer scie bock où) et Domi. Un énooooorme merci à Olivier pour m'avoir accompagnée durant mes balbutiements scientifiques, pour les discussions enflammées et constructives et de m'avoir fait confiance aussi vite. Merci Katia, ton coachage (un anglicisme francisé ?! les québécois vont être en tabarnack…) a été terriblement précieux. Un soutien au quotidien salvateur, tant au niveau professionnel qu'humain ! Merci beaucoup Lauren, pour tes conseils scientifiques et techniques qui ont débouché sur une belle amitié. Audrey, merci d'avoir pris autant soin de nos petites souris et de m'avoir supportée dans ton dos au quotidien ! Anne. Une page complète de remerciements rien que pour toi se trouve en annexe (Pauline's thesis, Edition collector, Gold limited version). Merci Pascal pour ton aide précieuse en microscopie et tes blagues douteuses. Merci Gilles et Djemo, vous êtes l'équivalent en gentillesse d'une licorne qui vomit des arcs-en-ciel. Merci aux gens du phéno, on a bien rigolé entre deux manips !

Merci aux Brikettes pour avoir changé le monde chaque jour. Merci Greg, pour nos rigolades et ta patience sans limite pour l'explication des stats (*toctoctoc* « euh… en fait je pensais que j'avais compris mais euh… non.»). Merci Aliza, you've been a great treadmill and congress partner! Merci Aude pour ton soutien et ton investissement. Merci Sami (*bijour*!) pour ton aide et ta voix qui porte au-delà du couloir, ça nous fait rire. *Manou,* merci pour tout, tu gères grave. Tu es une des rares personnes qui peut fournir un conseil de rédaction, une référence de produit, une idée brillante, un barbeuc' et une pompe à vélo. Une seule question subsiste : qu'est-ce qu'on ferait sans toi ? Merci Raphaël pour ta bonne humeur et ton sourire à toute épreuve, ton humour (et ta bière maison). Partager le brikouloir avec toi a été un vrai plaisir. Canadian Briki team, vous êtes parfaits. Quand se lever le matin pour aller travailler est une réelle envie, c'est qu'on a tout gagné.

Merci au cercle des Doctoriales, et tout particulièrement Adrien, Céline, Julien, Mathilde et Tam, une équipe de choc qui a su démontrer qu'être doctorant, c'est beaucoup plus qu'être en doctorat !
Merci à mes collègues de tutorat Neïla, Arnaud, Salah, André, Nicolas, Joseph, Johan, Geneviève, Ludo, Benoît, Elise, et un gros merci à Pascaline, prof passionnée et passionnante que l'on aurait tous voulu avoir en cours. Et bien évidemment merci aux étudiants d'avoir été aussi sympas et attentifs, ça a été une expérience inoubliable.
Merci aux Doctoneuros, collectif de joyeux lurons pour une entraide scientifique et déconnante. Je souhaite une longue vie à cette assoc' qui n'en est pas une !

Merci à mes amis strasbourgeois pour ces années merveilleuses dans une ville si agréable. De belles rencontres tout au long de ma thèse. Spéciale kasdédi à Miré pour une amitié comico-gastronomique du tonnerre. Merci aux aléas de la vie qui m'ont fait rencontrer la formidable Laetitia ; merci à Hugh, Bridget et Merlot qui ont partagé nombre de nos soirées. Un grand merci à Camille Lulublue pour sa vision de la vie. Merci au meilleur des meilleurs, Clément, BFF et cœur à paillettes.
Merci à mes amis montréalais pour cette année de pur bonheur (dans 'yeule). Merci à ceux d'icitte qui ont partagé leur culture (et leur bouffe !) en me faisant me sentir chez moi, Phil, Jas, Pascal, Pat, Rox, Steph, Eliane et tous les autres. Et bien sûr Chlorenzo. Aaaaah Chlorenzo (autoproclamés « You rock, b*tches », avec raison). Merci aux expat' de la *joyeuse gang* Laurette, Noémie, Yoran, Auré et Jojo, pour les grosses poilades. Merci d'avoir toujours été là pour faire *de quoi*. Et souvent n'importe quoi. Vous êtes fous tout comme il faut.
Un grand merci à mes colocs verdunois, pour m'avoir donné autant d'énergie positive lors de mes retours tardifs à la maison pendant la rédaction (et de m'avoir permis de vivre dans un endroit hyper propre sans que je mette la main à la pâte).

Merci à ma famille d'avoir cru en moi et de m'avoir soutenue dans chacune des étapes de ma vie.

Et si je peux permettre à mon grain de folie de s'exprimer, je remercie de tout mon cœur les Minions qui m'ont accompagnée durant ces années, surveillant mon travail d'un regard bienveillant et déjanté (ce qui est ma définition d'une combinaison parfaite).

Altogether, merci à ceux qui m'ont aidé à conduire mon travail, merci à ceux qui m'ont permis de m'en échapper et un merci incommensurable à ceux qui se trouvent dans les deux catégories à la fois.

Et je m'excuse pour mon rire.

Abbreviations

Δ9-THC	Δ9-tetrahydrocannabinol
AC	adenylyl cyclase
aCSF	artificial cerebrospinal fluid
Amy	amygdala
AOD	anterior olfactory nucleus, dorsal part
AOL	anterior olfactory nucleus, lateral part
AOM	anterior olfactory nucleus, medial part
Arc	arcuate hypothalamic nucleus
ASD	autism spectrum disorder
BLA	basolateral amygdala
BNST	bed nucleus of the stria terminalis
CaMKII	Ca^{2+}/calmodulin-dependent protein kinase type II
CB1	cannabinoid receptor 1
CeA	central nucleus of the amygdala
Cg	cingulate cortex
CMV	cytomegalovirus
CPA	conditioned place aversion
CPP	conditioned place preference
CPP	3-((R)-2-carboxypiperazin-4-yl)-propyl-1-phosphonic acid
CPu	caudate putamen
CREB	cAMP response element-binding protein
CS	conditioned stimulus
CTAP	Cys-Tyr-D-Trp-Arg-Thr-Pen-Thr-NH2
DAG	diacylglycerol
DAMGO	(D-Ala^2, N-$MePhe^4$, Gly-ol)-enkephalin
DG	dentate gyrus
DRG	dorsal root ganglia
DSM	Diagnostic & Statistical Manual of Mental Disorder of the American Psychiatric Association
EA	extended amygdala

EC	entorhinal cortex
eIPSCs	evoked inhibitory postsynaptic currents
ER	endoplasmic reticulum
FR	fixed ratio
GABA	gamma-aminobutyric acid
Gad	glutamic acid decarboxylase
GFP	green fluorescent protein
GIRK	particularly G protein-activated inwardly rectifying potassium channel
GPCR	G-protein coupled receptor
Hb	habenula
Hp(D)	(dorsal) hippocampus
IP	interpeduncular nucleus
KO	knockout
LH	lateral hypothalamus
M	motor cortex
M3G	morphine-3-glucuronide
M6G	morphine-6-glucuronide
MAPK	mitogen-activated protein kinase
MM	medial mammillary nucleus, medial part
MnPO	median preoptic nucleus
N6-CPA	N^6-Cyclopentyladenosine
NAc	nucleus accumbens
NBQX	2,3-dihydroxy-6-nitro-7-sulfamoyl-benzo[f]quinoxaline-2,3-dione
PAG	periacqueductal grey
PFA	paraformaldehyde
PFC	prefrontral cortex
PI3K	phosphatidylinositol 3 kinase
pir	piriform cortex
PR	progressive ratio
PVN	paraventricular thalamic nucleus
Pyr	pyramidal cell layer of the hippocampus
RMTg	rostromedial tegmental nucleus

Rt	reticular thalamic nucleus
S	somatosensorial cortex
SC	spinal cord
SuMM	supramammillary nucleus, medial part
TF	tail flick
TH	tyrosine hydroxylase
TI	tail immersion
tTA	tetracycline transactivator
VMH	ventromedial hypothalamic nucleus
VMPO	ventromedial preoptic nucleus
VP	ventral pallidum
VTA	ventral tegmental area
WT	wild type

Contents

General introduction

Part I: Opiate addiction and analgesia in Dlx-mu mice

Part II: Autistic-like syndrome in Dlx-mu mice

Part III: Target glutamatergic forebrain mu receptors in adult mice

Part IV: Create a Cre mouse line to target the extended amygdala

GENERAL INTRODUCTION

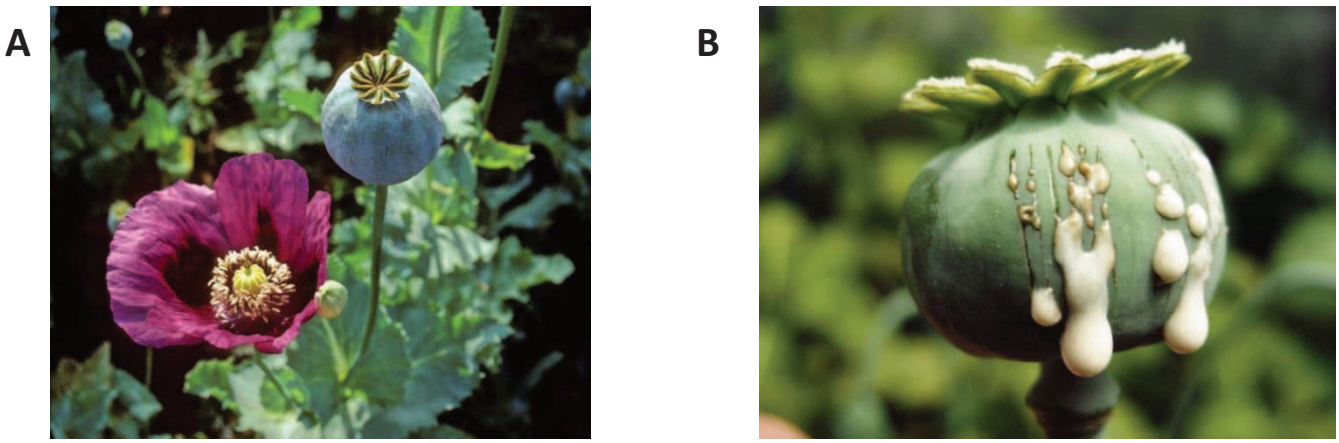

Figure 1. Opium poppy plant
(**A**) Opium poppy plant flower (*Papaver somniferum*)
(**B**) After incision of the green seed pod, the latex is collected. Alkaloids are extracted from the dried material.

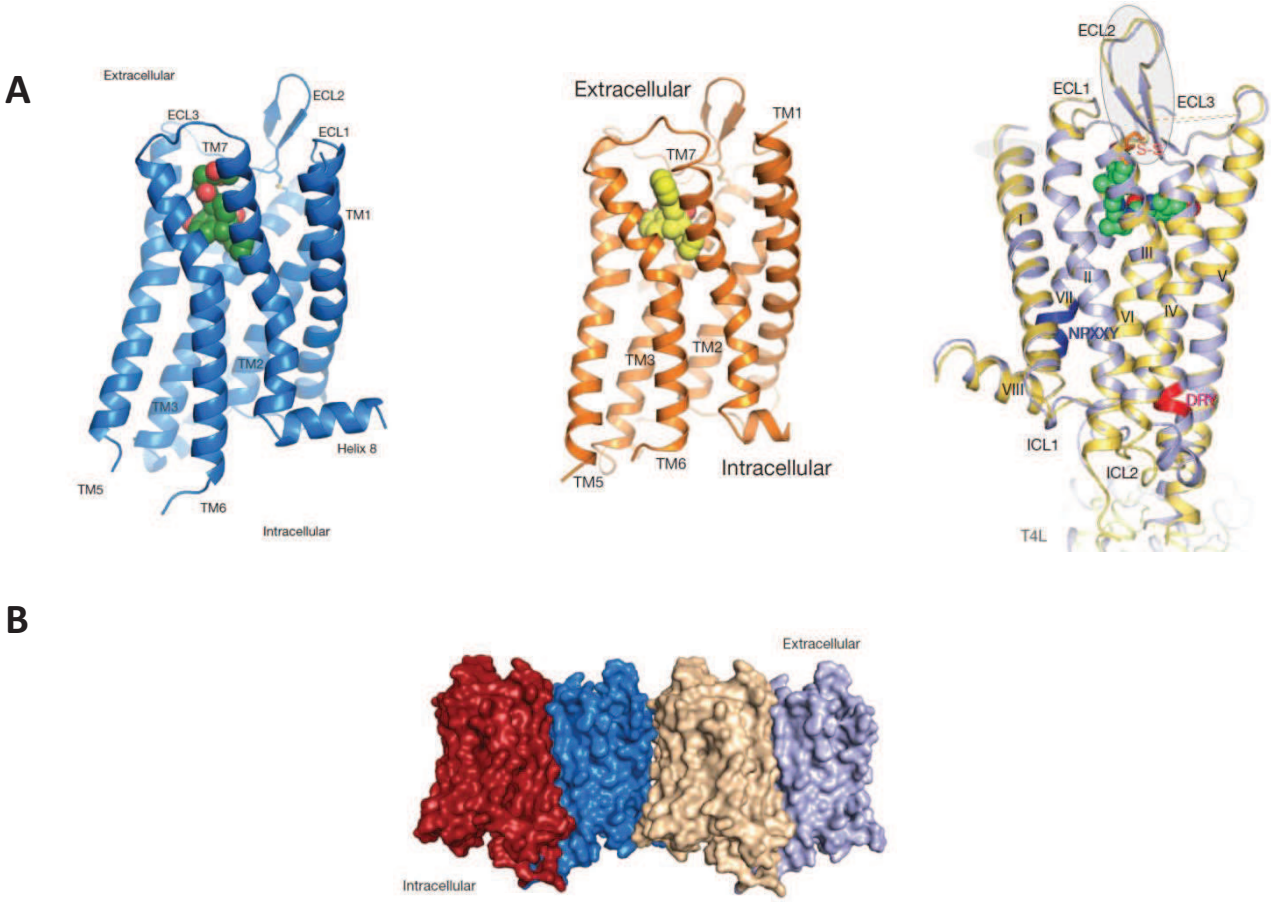

Figure 2. Overall view of the mu, delta and kappa opioid receptors structure
(**A**) Views from within the membrane plane show the typical seven-pass transmembrane GPCR architecture of the mu, delta and kappa opioid receptors (Adapted from Manglik et al., 2012, Granier et al., 2012 and Wu et al., 2012).
(**B**) Mu receptor oligomeric arrangement (Adapted from Manglik et al., 2012).

I. The opioid system

1. Overview

The opium extracted from the latex of poppy seeds (*papaver somniferum*), possesses powerful analgesic and euphoric properties (**Figure 1**). Morphine, isolated by Friedrich Sertürner in 1805, is the most active and abundant compound of opium. This alkaloid is used clinically to treat acute (i.e. open fracture or post-surgery care) and severe chronic pain (cancers, rheumatism). Despite strong adverse side effects (constipation, respiratory depression, nausea, dizziness, tolerance and dependence), morphine is the most commonly used analgesic (Brownstein, 1993).

Pharmacological studies have led to the identification of 3 opioid receptors: mu (*Oprm1*), delta (*Oprd1*) and kappa (*Oprk1*) (Pert and Snyder, 1973; Simon et al., 1973; Terenius, 1973). In the early 80's, genes encoding opioid peptide precursors were isolated: proenkephalin (*pEnk*) for enkephalins, prodynorphyn (*pDyn*) for dynorphins and pro-opiomelanocortin (*POMC*) for β-endorphin. The opioid peptides share a common amino-terminal sequence Tyr-Gly-Gly-Phe, called the "opioid motif" (Akil et al., 1998). These three receptors share about 60% sequence identity (Waldhoer et al., 2004). For an overview of the milestone discoveries in opioid research, please see review after p.21 (Charbogne et al., 2013).

Opioid receptors have been classified into the class A G-protein coupled receptor superfamily (GPCR), because they share homology with the rhodopsin receptor sequence (Fredriksson et al., 2003). The transmembrane core is formed out of a bundle of 7 α-helices that is critical for ligand binding and receptor signaling (Befort et al., 1996). Recently, the crystal structure of mu (Manglik et al., 2012), delta (Granier et al., 2012) and kappa (Wu et al., 2012) receptors was discovered (**Figure 2**), revealing a message/address model that describes conserved elements of ligand recognition as well as structural features associated with ligand-subtype selectivity.

2. Anatomical distribution

Opioid receptors are broadly expressed throughout the central nervous system and are also localized in many peripheral tissues of the mammalian organism (Wittert et al., 1996). This is evidenced by *in situ* hybridization, since the early 90's this technique has been used to detect mRNA in cell bodies expressing opioid receptors (Mansour et al., 1994). To characterize anatomical distribution of opioid

A

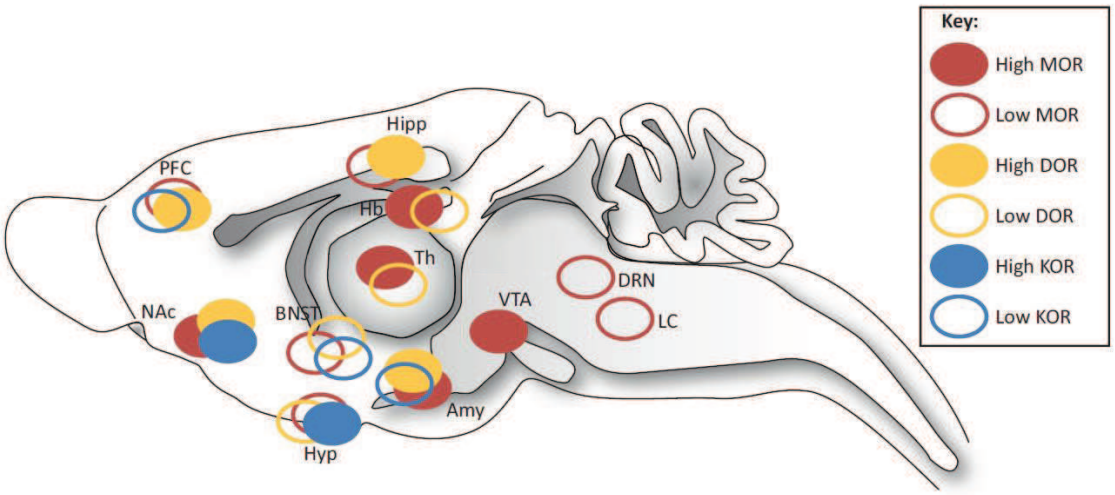

Amy, amygdala; BNST, bed nucleus of the stria terminalis; DRN, dorsal raphe nucleus; Hb, habenula; Hipp, hippocampus; Hyp hypothalamus; LC locus coeruleus; Th, thalamus; VTA, ventral tegmental area.

B

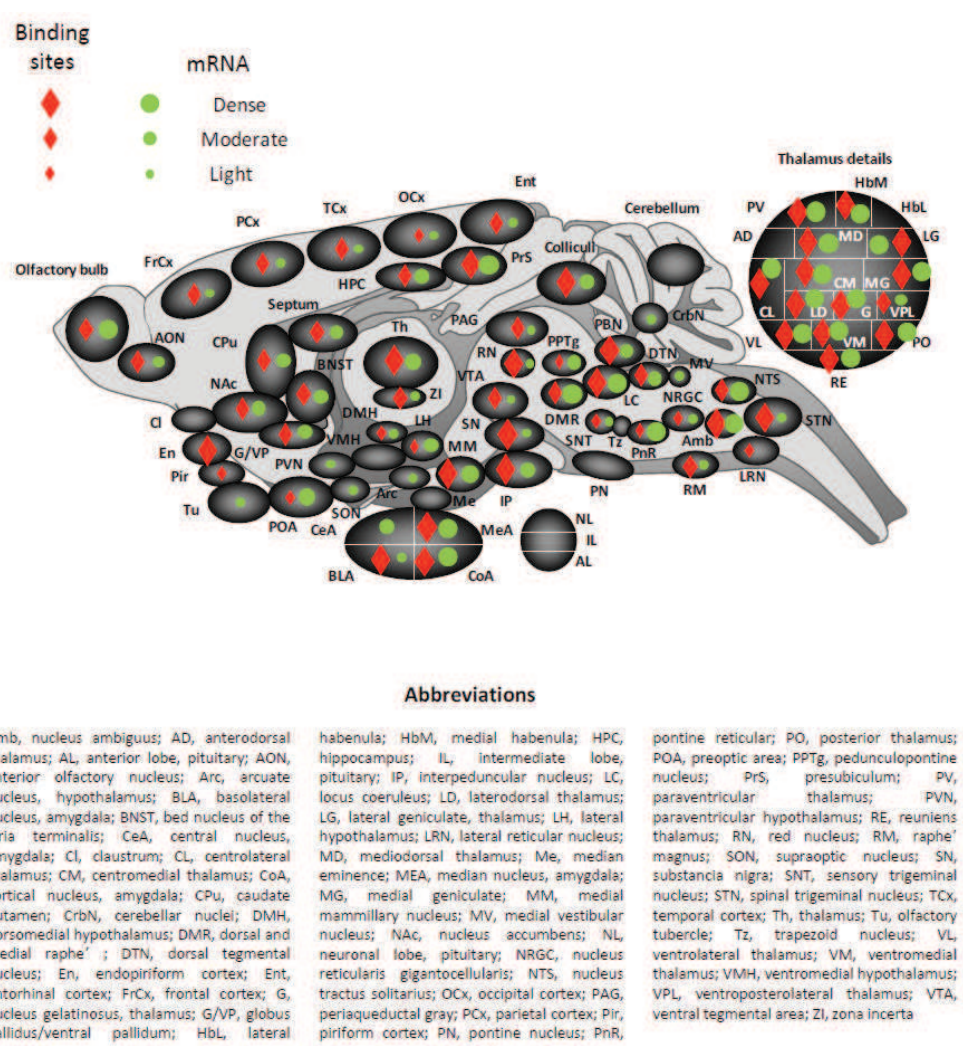

Abbreviations

Amb, nucleus ambiguus; AD, anterodorsal thalamus; AL, anterior lobe, pituitary; AON, anterior olfactory nucleus; Arc, arcuate nucleus, hypothalamus; BLA, basolateral nucleus, amygdala; BNST, bed nucleus of the stria terminalis; CeA, central nucleus, amygdala; Cl, claustrum; CL, centrolateral thalamus; CM, centromedial thalamus; CoA, cortical nucleus, amygdala; CPu, caudate putamen; CrbN, cerebellar nuclei; DMH, dorsomedial hypothalamus; DMR, dorsal and medial raphe' ; DTN, dorsal tegmental nucleus; En, endopiriform cortex; Ent, entorhinal cortex; FrCx, frontal cortex; G, nucleus gelatinosus, thalamus; G/VP, globus pallidus/ventral pallidum; HbL, lateral habenula; HbM, medial habenula; HPC, hippocampus; IL, intermediate lobe, pituitary; IP, interpeduncular nucleus; LC, locus coeruleus; LD, laterodorsal thalamus; LG, lateral geniculate, thalamus; LH, lateral hypothalamus; LRN, lateral reticular nucleus; MD, mediodorsal thalamus; Me, median eminence; MEA, median nucleus, amygdala; MG, medial geniculate; MM, medial mammillary nucleus; MV, medial vestibular nucleus; NAc, nucleus accumbens; NL, neuronal lobe, pituitary; NRGC, nucleus reticularis gigantocellularis; NTS, nucleus tractus solitarius; OCx, occipital cortex; PAG, periaqueductal gray; PCx, parietal cortex; Pir, piriform cortex; PN, pontine nucleus; PnR, pontine reticular; PO, posterior thalamus; POA, preoptic area; PPTg, pedunculopontine nucleus; PrS, presubiculum; PV, paraventricular thalamus; PVN, paraventricular hypothalamus; RE, reuniens thalamus; RN, red nucleus; RM, raphe' magnus; SON, supraoptic nucleus; SN, substancia nigra; SNT, sensory trigeminal nucleus; STN, spinal trigeminal nucleus; TCx, temporal cortex; Th, thalamus; Tu, olfactory tubercle; Tz, trapezoid nucleus; VL, ventrolateral thalamus; VM, ventromedial thalamus; VMH, ventromedial hypothalamus; VPL, ventroposterolateral thalamus; VTA, ventral tegmental area; ZI, zona incerta

Figure 3. Opioid receptor distribution

(**A**) Mu, delta and kappa receptor proteins show overlapping but distinct distribution. (Adapted from Lutz and Kieffer, 2013)

(**B**) Mu receptor protein and *mu receptor* mRNA show overlapping anatomical distribution, but differences in mRNA/protein distribution were found in several structures, suggesting that some presynaptic receptors are transported to projection areas (Adapted from Olivier Gardon and Le Merrer et al, 2009)

receptor binding sites, a classical method is ligand autoradiography that allows for description of the macroscopic distribution of receptors across the brain (Kitchen et al., 1997). Cellular localization of opioid receptors is more difficult to examine, since commercially available antibodies against opioid receptors show low *in vivo* selectivity, as is the case for other GPCRs (Michel et al., 2009). Antibody evaluation by the use of receptor knockout (KO) mice is absolutely required to assess specificity of new antibodies (Huang et al., 2015). Recently, a new tool has emerged to aid in the detection of opioid receptors, knockin mice for delta and mu receptors were developed, providing a great approach to study opioid receptor neuroanatomy (Erbs et al., 2014; Scherrer et al., 2006).

The three opioid receptors are found in the cortex, limbic system and brain stem (Le Merrer et al., 2009). They have a widespread and overlapping distribution, with some exceptions (**Figure 3A**). Delta is the most abundant receptor in the olfactory tract and amygdala (olfactory bulb, olfactory tubercle, basolateral, cortical and medial amygdala), as well as in the striatum. Kappa receptors are mainly expressed in the basal anterior forebrain (olfactory tubercle, striatum, preoptic area, hypothalamus and pituitary). Mu receptors are most broadly and abundantly expressed in the mesencephalon and some brain stem nuclei (Le Merrer et al., 2009). Analysis of [^{3}H]DAMGO (tritiated mu agonist) binding experiments has revealed the presence of mu receptors in caudate putamen (CPu), nucleus accumbens (NAc), endopiriform nucleus, amygdala, habenula, thalamus, hypothalamus, zona incerta, ventral tegmental area (VTA), interpeduncular nucleus, central grey, dentate gyrus, substantia nigra and the superior colliculus (Kitchen et al., 1997).

Opioid receptor mRNA expression generally matches the receptor protein distribution, suggesting that many opioid-containing neurons are local (**Figure 3B**, i.e. olfactory bulb, thalamus). In some cases, mRNA but not the receptor is observed in a brain region, suggesting that presynaptic receptors are transported to projection areas. Differences in mu opioid receptor mRNA/protein distribution were found in several structures such as the olfactory bulb, cortex, hippocampus, superior colliculus (A. Mansour et al., 1994).

The distribution of opioid peptide immunoreactivity is similar to opioid receptor localization. PENK is the most expressed opioid precursor, overlapping with mu receptor in the thalamus. PDYN is also widely distributed, with the highest concentration in the NAc. POMC is the most restricted, absent from cortical regions except amygdala, POMC cell bodies are limited to only three regions. There is an important mismatch between peptide immunoreactivity and cell body localization, suggesting that a substantial portion of peptides are released by projection neurons (Le Merrer et al., 2009).

3. Roles of opioid system in reward and addiction

Importantly, knockout mice have been generated for each opioid receptor and peptide, helping to decipher their roles in several aspects of drug reward and addiction. For this section, please see review (Charbogne et al., 2013).

The following sections will focus on the mu opioid receptor, which is essential for rewarding effects of opiates and non-opiate drugs of abuse.

II. The mu opioid receptor

1. Pharmacology

Mu opioid receptors have numerous ligands, such as morphine (used in the clinic), heroin (a highly addictive drug), or DAMGO (synthetic ligand for study of mu receptor function).

After the discovery of morphine and its effects, chemists tried to develop opiate molecules that would possess analgesic properties without inducing dependence. Therefore, Charles Robert Alder Wright in 1874 synthesized morphine analogues, including heroin. Contrary to the intended goal, heroin appeared to be at best an analgesic like morphine, but above all more prone to induce strong addiction.

Morphine is the prototypic mu agonist used in clinic, being a very effective pain killer (Spetea et al., 2013). Oral morphine is the analgesic of choice, in immediate or modified release form, to relief moderate to severe cancer pain (Wiffen et al., 2013). Morphine is metabolized to morphine-3-glucuronide (M3G), morphine-6-glucuronide (M6G) and nor-morphine. Those three metabolites are active; M6G strongly participates to morphine analgesia (Pergolizzi et al., 2008). Codeine, as morphine, is a natural product of opium; it is partly metabolized into morphine by the liver (Crews et al., 2014). Codeine is prescribed to treat mild to moderate pain, as well as cancer pain (Straube et al., 2014). Transdermal fentanyl seems to be an effective treatment for cancer pain management, as indicated by reduced pain to tolerable levels in patients on treatment. In addition, transdermal fentanyl produces less constipation than oral morphine (Hadley et al., 2013). Oxycodone is a semi-synthetic opioid drug that is effective in cancer (Pergolizzi et al., 2008) or post-operative (Cavalcanti et al., 2014) pain management, and has similar side effects to other opioids (Raffa et al., 2010).

Buprenorphine, a semi-synthetic high-affinity mu opioid receptor partial agonist (better known commercially as Subutex®), has a slow agonist-receptor dissociation, permitting long-lasting effects. It is used for medically assisted opioid withdrawal but mostly in maintenance therapy of opioid addiction (Li et al., 2004). Transdermal formulations can be prescribed for managing pain (Davis, 2012). To prevent intravenous abuse of buprenorphine, combination of buprenorphine and naloxone (sublingual tablets Suboxone®, Zubsolv® or BUNAVAIL®) is also used to treat opioid addiction. Methadone is a high-affinity full mu receptor agonist, used for maintenance therapy, as Subutex®, as well as chronic pain (Modesto-Lowe et al., 2010). It remains the gold standard to take charge of opioid abuse (Connery, 2015). Naltrexone is a high-affinity mu antagonist that is prescribed for opioid use disorder in extended release

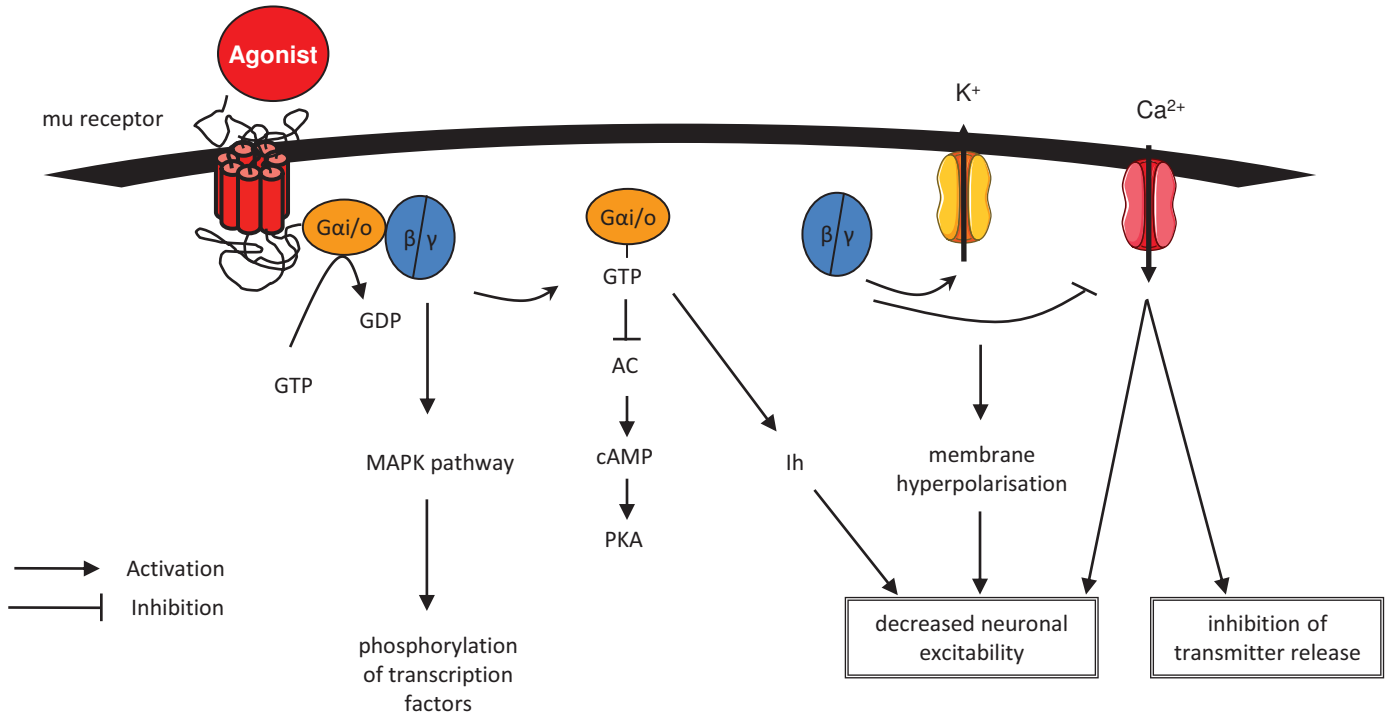

Figure 4. Signal transduction induced by mu receptor activation
Ligand-induced mu receptor activation leads to activation of G-protein subunits. Consequences are inhibition of AC, activation of potassium conductance, inhibition of calcium conductance and inhibition of transmitter release. (Adapted from Williams *et al*., 2001)
AC, adenylate cyclase; cAMP, cyclic adenosine monophosphate; GDP, guanosine diphosphate; GTP, guanosine triphosphate; Ih, voltage-dependant current; MAPK, mitogen-activated protein kinase; PKA, protein kinase A.

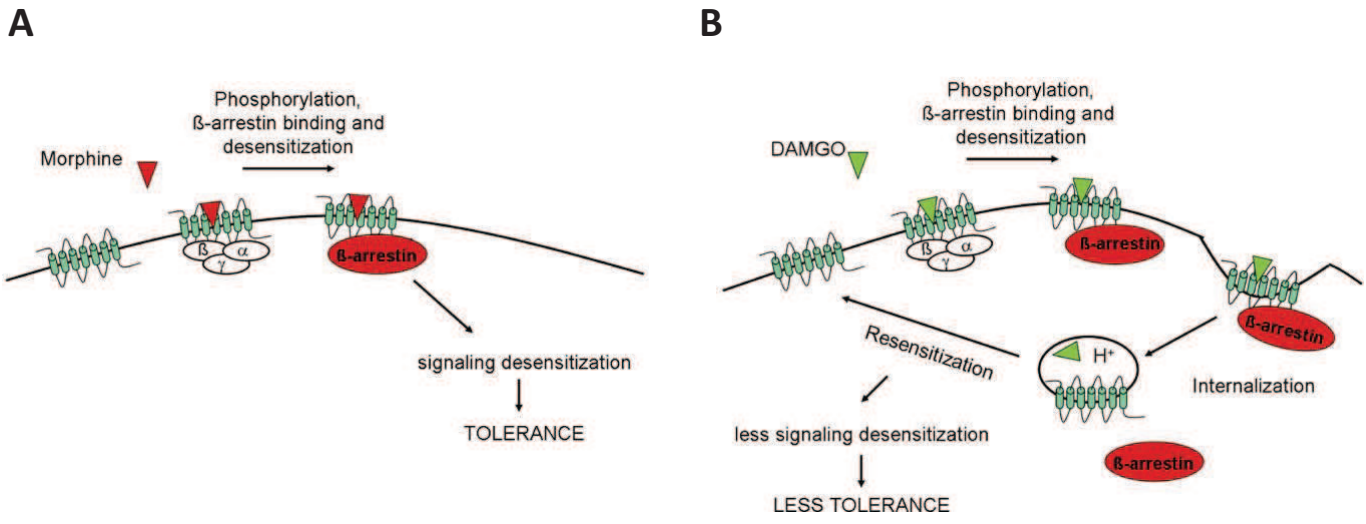

Figure 5. Different internalization potentials of morphine (**A**) and DAMGO (**B**). (Adapted from Koch et al., 2008)

form (Connery, 2015). Naloxone is a competitive opioid antagonist, clinically used to treat opioid overdose, either by intramuscular injection or nasal spray (Wermeling, 2015).

2. Cellular mechanisms

Signals transduced by opioid receptors are preferentially inhibitory through the receptors coupling to $G_{i/o}$-proteins. Activation of these receptors provokes activation and dissociation of α and βγ-G-protein subunits, through GDP-GTP exchange (**Figure 4).** When mu receptor agonists are applied acutely, the α-unit activation induces inhibition of adenylyl cyclase (AC), that decreases cAMP levels, and by modulating a voltage-dependent current (I_h), decreases neuronal excitability. Another consequence of AC inhibition is the inhibition of neurotransmitter release via PKA-dependent mechanisms (Williams et al., 2001). Opioid receptors also activate potassium channels, particularly G protein-activated inwardly rectifying potassium channels (GIRKs) through the binding of βγ-subunits released from $G_{i/o}$-proteins contributing to the hyperpolarization of neurons. Another signalling pathway activated by all the opioid receptors is the blockade of calcium channels through the release of βγ-subunits leading to the production of IP3, which releases intracellular calcium, and diacylglycerol (DAG), which activates PKC (Williams et al., 2001). Depending on the brain region, opioids inhibit excitatory or inhibitory neurotransmitter release (Fields and Margolis, 2015). βγ-subunits recruit intracellular effectors, leading to activation of mitogen-activated protein kinase (MAPK) pathway, such as phospholipase C or phosphatidylinositol 3 kinase (PI3K). MAPK activation induces enhanced phosphorylation of transcription factors, i.e. CREB (p-CREB), -ERK (p-ERK), and c-Fos (Haghparast et al., 2011). To sum up, activation of opioid receptors decreases neurotransmitter release and cell excitability at first, and modifies gene expression for long-term adaptations.

Ligand binding of mu receptors leads to activation of multiple downstream pathways, and not all agonists equally promote the same signalling cascade or receptor regulation. Functional selectivity at the mu receptor can effect G-protein coupling, activation of second messengers, mu phosphorylation, recruitment of β-arrestin2 and its signaling, receptor desensitization, and internalization (Raehal et al., 2011; for review see Williams et al., 2013). Morphine has been shown to induce poor receptor internalization, compared to DAMGO or fentanyl (**Figure 5),** leading to more receptor desensitization and thus tolerance (Koch and Höllt, 2008). In contrast, internalization of mu receptors following DAMGO application leads to dephosphorylation and recycling to the cell surface, suggesting internalization

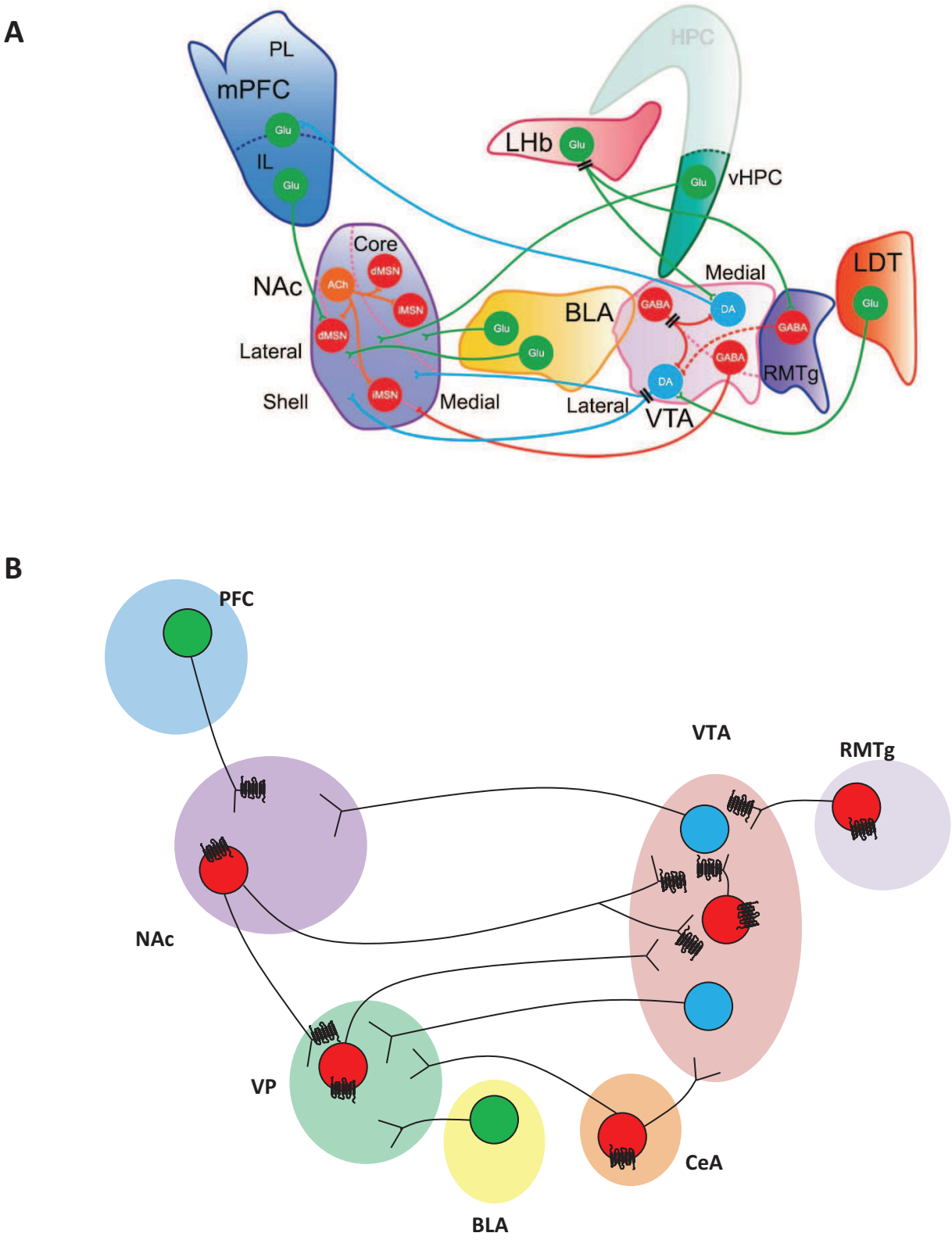

Figure 6. The mesolimbic dopamine system
(**A**) characterized by optogenetics (adapted from Nieh et al., 2013)
(**B**) with position of mu receptors ( )(for description, see text) (adapted from Meye et al., 2014)

counteracts desensitization and tolerance (Koch and Höllt, 2008). Morphine preferably recruits β-arrestin2-mediated pathways *in vivo*, methadone and fentanyl activate both β-arrestin1 and 2 pathways (Groer et al., 2011). β-arrestin2 negatively regulates mu receptor responsiveness, as shown by enhanced morphine-induced antinociception in β-arrestin2-KO mice (Bohn et al., 1999) but neither with fentanyl nor with methadone. In contrast to morphine, DAMGO leads to a strong mu receptor phosphorylation and β-arrestin recruitment (for review, see Pradhan et al., 2012; Zhou and Bohn, 2014). Mu receptor ligand-directed signalling results in diverse biological responses and is of primary importance for development of new analgesic pharmacotherapies, with or without reduced side effects (for review, see Allouche et al., 2014; Pradhan et al., 2012; Zhou and Bohn, 2014).

3. Mu receptor localization

The mu receptor is expressed in the dopaminergic mesocorticolimbic circuitry (Kitchen et al., 1997). This pathway is composed of neurons whose cell bodies are in the VTA, and project to the forebrain (NAc, olfactory tubercle, frontal cortex, amygdala, septal area)(**Figure 6**)(Meye et al., 2014; Nieh et al., 2013).

3.1 Mu receptors in the VTA

Both cell bodies and terminals of GABAergic interneurons of the VTA contain mu receptors (Lowe and Bailey, 2014). Combining double-fluorescence *in situ* hybridization for mu receptor and VGluT2, GAD67-GFP knockin mice with immunofluorescence for TH (tyrosine hydroxylase), mu receptor mRNA has been shown to be located in GABAergic (75%) and glutamatergic (25%) cells of the VTA (Kudo et al., 2014). VTA mu receptor immunoreactivity is found in dendrites, axons and terminals of GABAergic neurons as well as in glutamatergic terminals (Kudo et al., 2014). Mu receptor activation in GABAergic interneurons hyperpolarizes the cell, reducing the spontaneous GABA-mediated synaptic input to dopaminergic cells, leading to dopamine cells excitation (Johnson and North, 1992). One of the proposed mechanisms of presynaptic mu receptor-induced GABA release inhibition within the VTA (Lecca et al., 2012) is through inhibition of the secretory process at the nerve terminal level (Bergevin et al., 2002). In mu receptor KO mice, GABA overflow is increased and glutamate overflow is decreased, supporting that the mu opioid system is tonically active in the VTA (Chefer et al., 2009) maintaining glutamate/GABA balance of DA neurons.

In vivo, morphine targets mu receptor-sensitive GABAergic neurons in the tail of the VTA (also called rostromedial tegmental nucleus, RMTg) to increase VTA dopamine firing, as shown by electrophysiological recordings (Jalabert et al., 2011; Jhou et al., 2009; Matsui and Williams, 2011).

Opioid-sensitive GABA inputs to dopamine neurons can also project from the NAc (Cui et al., 2014; Watabe-Uchida et al., 2012), even if this represents a less dense population (Xia et al., 2011). Optogenetically controlled activation of terminals of the NAc showed a direct GABAergic input from the NAc to the VTA, which is mu receptor and D2 receptor sensitive (Matsui et al., 2014).

3.2 Mu receptors in the NAc

The first evidence of NAc involvement in mu receptor effects was shown by intra-NAc self-administration of morphine in rats (Olds, 1982). Mu receptors are located in NAc medium spiny neurons (MSNs) (A. Mansour et al., 1994) and are restricted to striosome (patch) compartment (Cui et al., 2014). Retrograde tracing from NAc shell labeled cell bodies in the VTA (Ford et al., 2006). A combined conditional gene expression system with trans-synaptic retrograde tracing permitted the visibility of most inputs to VTA dopamine neurons originating from NAc neurons in patch compartments; those in dopamine-projecting neurons are a very small and specific striatal population (Watabe-Uchida et al., 2012). Activation of the mu receptor differentially modulates patch and matrix compartments (Miura et al., 2007) with inhibitory actions in corticostriatal excitatory inputs and with presynaptic inhibition of IPSCs are observed only in the striosomes (Miura et al., 2007).

3.3 Mu receptors in the ventral pallidum

Optogenetic studies have revealed opioid modulation of ventral pallidal projections to dopamine and non-dopamine VTA neurons (DAMGO-sensitive neurons) (Hjelmstad et al., 2013). Ventral pallidum (VP) is reciprocally innervated by the VTA and the NAc, and is critically involved in morphine-induced sensitization, as shown by lack of induction and expression of morphine sensitization with intra-VP mu receptor blockade (Mickiewicz et al., 2009). Whole-cell patch-clamp of VP neurons experiments have demonstrated presynaptic regulation of GABAergic transmission in VP neurons by DAMGO (Kupchik et al., 2014). Opioid receptor activation in the VP modulates accumbal GABAergic neurotransmission, glutamatergic influences from the amygdala and dopaminergic inputs from the VTA (Napier and Mitrovic, 1999).

3.4 Mu receptors in the extended amygdala

The extended amygdala (EA) is composed of the bed nucleus of the stria terminalis (BNST), central nucleus of the amygdala (CeA) and a transition zone in the medial NAc (Heimer and Alheid, 1991); those structures send projections to VP, VTA lateral hypothalamus and brainstem structures (Heimer and Alheid, 1991). The mu receptor is pre- and postsynaptically expressed in the CeA and BNST, mostly in inhibitory neurons (Jaferi and Pickel, 2009). The mu receptor is found in somatodendritic sites of CeA, including those projecting to the BNST (Beckerman and Glass, 2012). Mu is the most prominent opioid receptor in the BNST, mainly in the anterior part (Poulin et al., 2009). The presence of mu receptor in the EA has been confirmed in nonhuman primates (Daunais et al., 2001).

4. Role in physiology

Consistent with the fact that mu opioid receptors are widely expressed in the central and peripheral nervous systems, their effects on physiological functions are diverse. The following sections examine the mu opioid receptor function in gastro-intestinal/renal/hepatic functions, cardiovascular responses, immunological responses, respiration, pain responses, stress and mood, social life, food consumption, sexual activity, tolerance, activity and locomotion (Bodnar, 2014). Implications of mu receptors in those functions were revealed with numerous approaches, such as knockout mice, mu specific agonists and antagonists, or mu knockdown.

4.1 Autonomic, endocrinal and immune functions

Opioids, such as morphine, are a common treatment for moderate to severe pain, but lead to adverse effects, such as opioid-induced bowel dysfunction (Mehendale and Yuan, 2006). The mu opioid receptor has a role in renal and hepatic functions (Atici et al., 2005), as shown by acute morphine-induced stimulation of diuresis and natriuresis (Gutkowska et al., 1993). The endogenous opioid peptides, β-endorphin and enkephalins, modulate hematopoiesis via mu receptors that are involved in blood cell production mostly as negative regulators (Tian et al., 1997). Opiates are known to suppress immune responses and increase susceptibility to infections (Adler et al., 1993). The mu opioid receptor

is essential for chronic morphine action on the immune system (Gavériaux-Ruff et al., 1998). For review of all the physiological functions of mu receptors, see (Bodnar, 2014) and previous reviews.

4.2 Central mu opioid receptor functions

Respiration

Mu opioid receptors are expressed on respiratory neurons in the central nervous system (Pattinson, 2008). The activation of these receptors leads to depression of ventilator responses, hypercapnia, hypoxia, irregular breathing and suppression of pharyngeal muscle function. In clinics, new studies point out that opioid-induced respiratory depression may be reversed by non-opioid drugs (van der Schier et al., 2014), for example using serotonin agonist (Manzke et al., 2003).

Pain responses

The roles of the mu opioid receptors in pain responses are due to both peripheral and central expression in the nervous system (Spetea et al., 2013). Mu opioid receptor knockout mice have been a helpful tool to demonstrate that morphine produces analgesia via mu receptors (Matthes et al., 1996). The endogenous opioid peptides acting on mu receptors mediate pain modulation in drug-free animals, as shown by shorter latencies to nociception tests in mu KO mice (Sora et al., 1997). Recently, it has been shown that tissue injury produces a constitutive activation of the mu opioid receptor (Corder et al., 2013). This prolonged endogenous mu receptor signaling provokes psychological (aversion associated with pain) and physical withdrawal (Corder et al., 2013). Stress-induced analgesia is decreased in mu receptor KO mice, indicating an implication of mu receptors in this mechanism (LaBuda et al., 2000). In the periphery, mu opioid receptors are expressed in the dorsal root ganglia (DRG). During inflammation, DRG mu receptor expression is upregulated (Stein et al., 2009). In humans, it has been reported that peripherally active opioids (that don't cross the blood-brain barrier) can produce pain relief in patients suffering from visceral and neuropathic pain (Stein et al., 2009). With the development of conditional knockout for the mu opioid receptor, we have shown that mu receptors in Nav1.8-positive sensory neurons partly mediate opiate analgesia (Weibel et al., 2013).

Stress, anxiety, depression-like behavior, mood, impulsivity

Mu opioid receptors are involved in stress-induced emotional responses, as shown by lower level of stress-induced corticosterone and behavioral responses in mu receptor KO mice after stress

exposure (tail-suspension, repeated forced-swim and restraint stress) (Ide et al., 2010). Basal corticosterone levels in these animals are equivalent to wild type controls (Ide et al., 2010). Anxiety-like behavior in mu receptor KO is still controversial. Depending on the tests used and the parameters investigated, mu receptors seem to play a positive or negative role in anxiety (Becker et al., 2014; Filliol et al., 2000). Mu receptors may have a role in the modification of emotional responses to novelty and emergence behavior (Yoo et al., 2004b). Endogenous opioid peptides are involved in the modulation of depression-like behavior, as shown by naloxone-induced facilitation of induction of learned helplessness. Activation of mu receptors with morphine reversed the escape deficit (Tejedor-Real et al., 1995)(for review, see Lutz and Kieffer, 2013). The mu opioid receptor plays also a role in disinhibition, as revealed by decreased motor impulsivity in mu receptor KO animals (Olmstead et al., 2009). For a review on the implication of mu receptors in mood disorders, see (Lutz and Kieffer, 2013).

Natural rewards

Mu opioid receptors are essential for attributing a positive value to sensory experiences like the taste of food. For instance, administration of mu opioid receptor agonists or antagonists in different species (from rodents to humans) potently modulates palatability ratings of food (Peciña and Smith, 2010). Opioids targeting mu receptors enhance the hedonic properties of food in the rostrodorsal nucleus accumbens medial shell, caudal ventral pallidum, but can also enhance food motivation (the "wanting") in a larger network (Peciña and Smith, 2010). In rabbits, mu receptors in the nucleus accumbens are essential for the hedonic eating properties (Ward et al., 2006). Human studies support animal studies, showing an effect of mu opioid receptor antagonists in food hedonic responses, and a decrease in the frequency and severity of binge eating (Nathan and Bullmore, 2009). Furthermore, the motivation to eat is decreased in mu receptor knockout mice (Papaleo et al., 2007).

Mu opioid receptors have a role in sexual behavior. In fact, opioids seem to impact on the acquisition and expression of copulation-induced conditioned place preference (CPP) (Coolen et al., 2004). Mu receptor KO males show a reduced mating activity, sperm counts and motility, and litter size (Tian et al., 1997). Moreover, opioid agonist systemic injections produce a clear and specific naloxone-reversible inhibition of sexual performance in males (Van Furth et al., 1995).

The mu opioid receptor is involved in numerous social behaviors, including maternal care, attachment behavior and social interaction. In rats, it has been shown that morphine can disrupt maternal behavior during lactation, a behavior reversed by naloxone (Bridges and Grimm, 1982), more precisely in the periacqueductal grey (PAG) (Miranda-Paiva et al., 2003). Mu knockout mice pups neither

show a preference for their mother's cues nor reach the same isolation-induced vocalization emission than the wild type pups. This study characterized a deficit in attachment behavior (that can be a component of autism syndrome) (Moles et al., 2004). Mu receptors are involved in psychosocial stress, as shown by reduced aversion to social contact post social defeat stress in mu KO mice (Komatsu et al., 2011). Permanent (KO) and transient (naltrexone treatment) disruptions of mu receptor neurotransmission impair positive effects from social contact and affiliations, showed by a reduced interest in peers or absence of socially rewarding environment preference in mice (Cinque et al., 2012). Also, mu KO mice have been proposed as a monogenic model of autism, demonstrating numerous ASD symptoms such as social interaction deficits, perseverative behaviors, and exacerbated anxiety (Becker et al., 2014). Finally, mice with the *Oprm1* A112G single nucleotide polymorphism showed increased dominance and social affiliation, that is blocked by pretreatment with naloxone (Briand et al., 2015). In human beings, the mu receptor is also associated with social attachment. Individuals expressing the minor allele (G) of the A118G polymorphism have an increased tendency to become engaged in affectionate relationships and experienced more pleasure in social situations in comparison with major allele (A) subjects (Troisi et al., 2011). Using positron emission tomography, the mu receptor has been shown to be regulated by social distress (rejection) and reward (acceptance) in humans (Hsu et al., 2013).

Drug reward

Activation of the mu receptor is responsible for the rewarding effects of morphine (Matthes et al., 1996; Sora et al., 2001) and heroin (Contarino et al., 2002) in CPP, as well as motivation to get morphine in self-administration procedure (Nguyen et al., 2012). Mu receptors are also essential for rewarding properties of non-opiate drugs of abuse, as shown by abolished CPP in mu KO mice with Δ9-tetrahydrocannabinol (Δ9-THC) (Ghozland et al., 2002) and nicotine (Berrendero et al., 2002; Walters et al., 2005), altered CPP with cocaine (Becker et al., 2002), as well as decreased alcohol 2-bottle choice (Becker et al., 2002; Hall et al., 2001; Roberts et al., 2000). For more details, please see section REVIEW.

Locomotion and sensitization

Spontaneous locomotor activity is either maintained (Ide et al., 2010; Sora et al., 1997) or reduced in mu receptor KO mice (Hall et al., 2003; Matthes et al., 1996; Tian et al., 1997). Mu receptors mediate morphine- (Hall et al., 2003) and heroin-induced (Contarino et al., 2002) hyperlocomotion. Locomotor activation induced by other drugs of abuse is differently modulated by the mu receptor. Mu

receptors do not mediate locomotor tolerance to Δ9-THC, as shown by the lack of difference between wildtype and mu KO mice in locomotion task (Ghozland et al., 2002). Locomotor sensitization is abolished in mu KO mice treated with nicotine (Yoo et al., 2004a). Depending on the study, cocaine-induced locomotion and sensitization is either impaired (Yoo et al., 2003) or unchanged (Becker et al., 2002; Contarino et al., 2002) in mu receptor KO animals. Mu receptor has a prominent role in mediating locomotor effects of ethanol (Ghozland et al., 2005). For more information, please see review (Charbogne et al., 2013).

III. Animal models of addiction

Until recently, several animal models have been described to study specific aspects of addiction that involve mu receptors. These models will be reviewed in the following sections. Animal models are key tools permitting valuable investigation in research. Reliable models are complex to build in psychiatric disorders (for comments and discussion, see (Nestler and Hyman, 2010)). To be the optimal model, an experimental design would meet 3 types of validity: face (similarity in observable outcomes, i.e. symptoms), construct (theoretical rationale), predictive (treatments will be effective in both model and humans) (Willner, 1986). In the field of drugs of abuse, behavioural models have been developed that address different stages of addiction process. During the binge/intoxication stage, we can list intracranial electrical self-stimulation, conditioned place preference (CPP) and drug self-administration. The negative affect stage can be studied using anxiety-like responses, scoring of physical signs of withdrawal or conditioned place aversion (CPA). Preoccupation/anticipation can be tested by drug-, cue- or stress-induced reinstatement (for review, see (Koob et al., 2009)). Hyperlocotomor activity induced by opiates is a measure of opiate effects and adaptations that is classically used in animal research but is less relevant to the clinic.

Substance use disorders have been defined in the DSM V (Diagnostic and Statistical Manual of Mental Disorder of the American Psychiatric Association) as the occurrence of at least 2 symptoms in an 11-criterion list. Criteria are grouped into 4 clusters: impaired control over substance use (criteria 1-4), social impairment (5-7), risky use of the substance (8-9), and pharmacological criteria (10-11). Addiction-like behavior has been observed in other species than humans. Three of the essential addiction criteria developed after prolonged cocaine self-administration in rats: the motivation to take the drug is increased, the animal has difficulties to refrain from drug-seeking, the drug use is maintained despite aversive consequences (Deroche-Gamonet et al., 2004). Moreover, addicted animals are more likely to relapse after a prolonged withdrawal period, and the percentage of addicted animals is similar to the one of diagnosed human cocaine addicts. The transition from controlled to compulsive drug use was also modeled in mice with oral morphine self-administration (Berger and Whistler, 2011).

The following sections will focus on models and tasks that I used for my project.

1. Place conditioning

Place conditioning is a pavlovian (or classical) conditioning. In drug-induced CPP or CPA, the animal learns to associate the context (environment) and the drug effect (Tzschentke, 2007). In a two-compartment box, the drug is associated to a particular compartment (with injections prior to the conditioning), a vehicle solution in another distinctive one, on alternate sessions. After the conditioning phase, the animal is re-exposed to the environment in a drug-free state and can express attraction or repulsion to drug-paired compartments. Time spent in the different boxes is measured. If the drug is rewarding, animal will explore the drug-paired compartment more than the vehicle-paired compartment, and thus has developed CPP. If the drug has aversive properties, a rodent will avoid the drug-paired box (CPA). The positive reinforcement of a drug measured in CPP can be interpreted as rewarding properties of the substance (van Ree et al., 1999).

2. Self-administration

One of the well-known instrumental (or operant) conditioning used in addiction research is the drug self-administration paradigm. Unlike the CPP procedure, in which the drug is injected by the experimenter, here the self-administration permits a non-forced exposure to the drug. Administration of the drug is contingent upon the animal behavior. This model resembles the human consumption (face validity). There are several possible routes of administration (i.v., i.c.v., intragastric, pellet, drop, etc.). Usually, an i.v. catheter is implanted in the animal vein; the animal can freely move in a Skinner box and has access to a lever (or sometimes a nose-poke), linked to the drug delivering system. The rodent has to work to receive a drug dose. With that paradigm, different parameters can be measured. First, the acquisition models the initiation of drug-taking. The animal learns that a fixed number of lever pressings (one or more) leads to a drug infusion, so drug effects. This is called the Fixed Ratio schedule. Motivation to get the drug is assessed by determining the breaking point. Also called Progressive Ratio, the number of lever pressings needed to obtain the drug infusion increases, until the animal gives up. The highest number of actions (“breaking point”) is determined and reflects the motivational properties of the drug (Sanchis-Segura and Spanagel, 2006).

Oral self-administration is very useful in alcohol research. Most of the time, ethanol consumption is measured in a two-bottle choice paradigm. Animal has access to 2 bottles, filled with drinking water or ethanol solution. The access can be either continuous (24h) or limited (few hours a day or few days a week for instance). The limited-access, in many cases leading to a high blood alcohol concentration, models the binge drinking often found in human consumption, with a good face and

construct validity. We can measure the ethanol quantity ingested (i.e. grams of ethanol per kg of rodent per time) or the preference over water (Crabbe et al., 2011). This technique gives information about the consumption of a reward.

3. Locomotor activity and sensitization

Sensitization to a drug of abuse is the increased responses after repeated exposure of the drug. Regarding addiction research, incentive sensitization theory proposes that psychomotor as well as incentive salience attributed to the drug is progressively enhanced (Sanchis-Segura and Spanagel, 2006).

4. Withdrawal

Physical signs of withdrawal can be revealed after discontinuation of drug administration. Chronic drug exposure can produce physical dependence with opioid drugs, Δ9-THC, alcohol and nicotine, but not for cocaine. Spontaneous withdrawal is observed after the cessation of the acute effects of the abused drug, but scoring is easier when physical dependence is precipitated by an antagonist. For instance, during opiate withdrawal, we can record wet-dog shakes, jumping, sniffing, paw tremor, teeth chattering, diarrhoea, and ptosis. A general physical dependence index is calculated, giving a specific value to each sign (Maldonado et al., 1997).

Aversive stimulus effect of drug withdrawal can be assessed using place aversion (Koob and Volkow, 2010).

5. Reinstatement

Reinstatement in a self-administration procedure is used as animal model of relapse. When drug self-administration is reliable, extinction sessions (lever is available, but not the drug) are conducted. Then, when the rodent does not respond in those new conditions, a stimulus is applied and lever-pressing responses are assessed. The stimulus can be either a priming injection of the drug (internal stimulus), or a stimulus that was previously paired with the drug delivery during acquisition phase (external stimulus, often a light), or a stressor. It has been shown that reinstatement can occur for a wide range of drug abuse such as cocaine, alcohol and heroin (Erb et al., 1996; Lê et al., 1998; Shaham et al., 1996). Reinstatement can also be studied after CPP procedure. The animal is exposed to the CPP box

in absence of the drug (vehicle in both compartment) during extinction (or latent inhibition), and reinstatement of drug-seeking behavior is induced by priming (Sanchis-Segura and Spanagel, 2006).

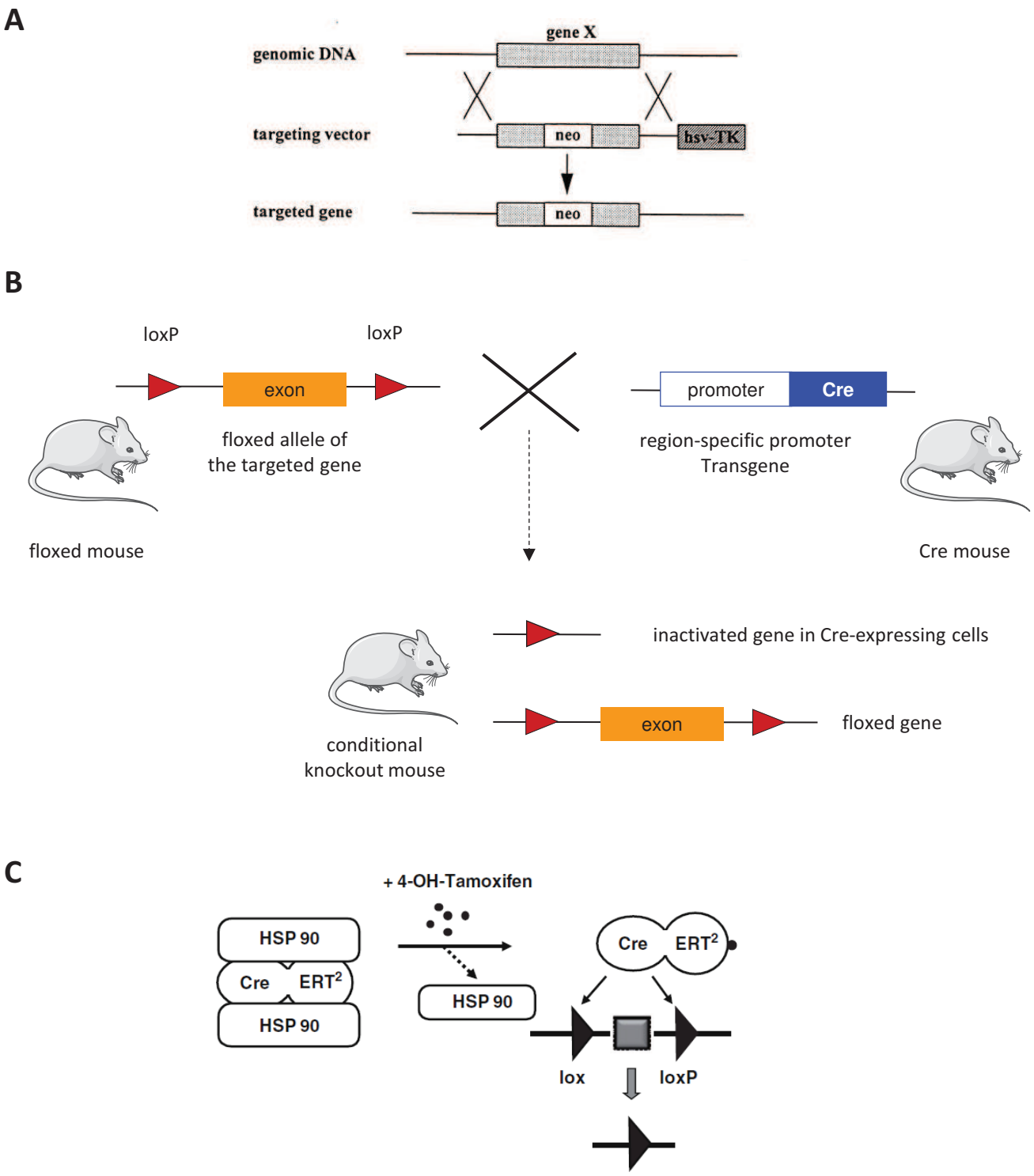

Figure 7. Genetic approaches to create mouse models

(**A**) Gene KO by homologous recombination: a gene is replaced by a disrupted form of the gene by homologous recombination. Neo cassette is used to disrupt the gene. (Adapted from Brusa et al., 1999)

(**B**) Specific gene inactivation by Cre-loxP system. The promoter drives the expression of the Cre recombinase that excises the sequence between the 2 loxP sites of the gene of interest. (Adapted from Gavériaux-Ruff and Kieffer, 2007)

(**C**) Specific gene inactivation by tamoxifen-inducible CreER^{T2} system. Cre-ER^{T2} protein is constitutively expressed in the targeted cell population, but remains inactive. The 4-OH-tamoxifen (tamoxifen is metabolised in 4-OH tamoxifen by the liver) activates ER^{T2}, leading to dissociation of HSP90 and removal of HSP90-induced interference (Adapted from Friedel et al., 2011)

IV. The use of genetic mouse models in neuroscience research

1. Total knockout approaches

Knockout mice (KO) are very useful tools for understanding gene function at systems level. For a long time, pharmacology was the only available approach, but is hampered by a number of factors, including *in vivo* selectivity, pharmacokinetics or metabolic properties of the compounds (Kieffer, 1999). Gene-targeting technology is a powerful method that completes pharmacological studies. The first idea of disrupting a gene in a mouse was proposed by the developmental geneticist Mario Capecchi in the 1980's, introducing site-directed mutagenesis into specific mammalian genes via homologous recombination (Capecchi, 1989; Mansour et al., 1988; Thomas and Capecchi, 1987) (**Figure 7A**). The first nervous system expressing gene KO mouse was generated a few years later, targeting the PrP gene, in spongiform encephalopathies research (Weissmann et al., 1993). Nowadays, this technique is widely used.

Regarding the opioid system, several constructs were generated for each receptor and peptide precursor (for review, see Befort, 2015). For mu receptors, six different lines were created, targeting either exon 1 (Schuller et al., 1999; Sora et al., 2001; Tian et al., 1997), 2 (Matthes et al., 1996) or 2 and 3 (Loh et al., 1998).

Total invalidation of a gene may have limitations (Gavériaux-Ruff and Kieffer, 2007). First, the gene can be crucial for the development and lead to the death of the animal. Moreover, genetic redundancy could lead to misinterpretations of a phenotype. Also, knockout of a gene can provoke compensatory mechanisms during development. For example, mu and delta receptor expression is upregulated in some regions of enkephalin KO mice (Brady et al., 1999). In addition, some genes are expressed in the central nervous system and in the periphery, making it difficult to target cerebral functions. To better address the question of the role of genes in the brain, with more accurate interpretations of phenotypical changes, the logical next step is to generate spatial- and temporal-specific deletion.

2. The Cre/loxP system

A more sophisticated method is a system in which the gene of interest can be disrupted in a cell-type or tissue specific manner. This approach is based on the Cre/loxP recombination system (Galli-

Taliadoros et al., 1995). The Cre recombinase is an enzyme isolated from the bacteriophage P1. This enzyme catalyzes the recombination between two 34-base pair motifs, called loxP sites, leading to an irreversible excision of the genetic DNA segment comprised between those, allowing excision of crucial segment in a gene of interest. In brief, one or several exons are "flanked" in intronic sequences in embryonic stem cells using homologous recombination. The resulting "floxed" mouse should have fully functional alleles and no phenotypic differences with wildtype congeners. Second, the Cre recombinase is expressed under the control of a specific promoter, driving the excision in a location- and time-specific manner. The expression of the Cre is ectopic, engineered by pronuclear injection. To conditionally target a gene, two mouse lines are needed: one is a transgenic line carrying the Cre driver; the other one is a mouse line carrying the floxed gene. By breeding those lines (until homozygous floxed offspring), the Cre expressed only in the targeted cells will permanently excise the floxed gene segment, leading to specific gene inactivation (**Figure 7B**) (for review Brusa, 1999; Galli-Taliadoros et al., 1995; Gavériaux-Ruff and Kieffer, 2007). The method was well described by the group of Rajewski, who generated the first conditional KO lines (Gu et al., 1993). This technique is widely used and expanding, utilizing new promoters to target neuronal tissues, brain regions or cell types. According to the Gensat website (http://www.gensat.org), 288 Cre lines are currently available in the nervous system. To date, the only existing conditional KO for the mu receptor gene is targeting Nav1.8-positive neurons, in order to address the question of mu-mediated analgesia in primary afferent nociceptive neurons (Weibel et al., 2013).

An interesting alternative to Cre/loxP classical conditional KO is the virally mediated expression of the recombinase. For instance, Cre-expressing adeno-associated or lenti- viruses are injected in the targeted region of a floxed mouse, leading to a different site- and temporal-specific gene inactivation. A limiting feature is the virus spreading and efficacy, and the reproducibility of injections.

3. Inducible Cre systems

In the Cre-flox breeding strategy, the Cre expression occurs as soon as the promoter is activated. The temporal inactivation of the gene of interest is controlled by a promoter and can lead to developmental issues, compensations or inadequate KO if the gene is expressed early. For instance, a transient ubiquitous expression of the promoter leads to a total KO line. To avoid that situation, inducible Cre were generated (**Figure 7C**). This method is based on the temporal control of the Cre recombinase driver, via ligand-dependent recombinase (Brocard et al., 1998). Here, the enzyme is

coupled to either estrogen- or progesterone-mutated ligand biding sites. Those Cre-fused sites are inactive at basal state. Activation of the Cre is induced by a specific ligand of the modified receptor (RU486 or tamoxifen) (Brocard et al., 1998). Only the ligand-treated fusion Cre is translocated from the cytoplasm into the nucleus (Friedel et al., 2011). The chimeric protein is not activated by endogenous steroids. Recombination occurs after administration of tamoxifen to transgenic mice expressing the fusion protein; the excision could not be detected in untreated animals, suggesting that this approach constitutes a very controlled and specific tool to induce the disruption of a gene of interest. In the brain, this technique is less efficient than in other tissues (Casanova et al., 2002).

Another conditional KO method uses the tetracycline transactivator (tTA). With this construct, in the presence of tetracycline or its highly efficient analog doxycycline, the transcription is disrupted, creating an on/off situation for gene reversible disruption (Gossen and Bujardt, 1992).

V. Aim of the thesis

Our laboratory investigates involvement of GPCRs in psychiatric disorders, and particularly the role of opioid receptors in drug abuse. Our research uses genetic, molecular, cellular and behavioral approaches. The total knockout of the mu receptor is very useful in deciphering the role of this receptor in reward, motivation, physical dependence, locomotor activity and analgesic properties of morphine and heroin. The goal of my thesis is to elucidate the role of selected mu receptor populations, expressed in neurons that belong to reward circuits, in opiate effects and addiction-related behaviors. To this aims, we have used conditional Cre-lox-based gene knockout approaches to inactivate the mu receptor in targeted neurons, and studied molecular, cellular and behavioral properties of mutant mice.

Aim 1: opiate addiction and analgesia in Dlx-mu mice

The first aim of my thesis was to investigate the role of the mu opioid receptors expressed in GABAergic forebrain neurons in opioid effects. The mu receptor is highly present in the limbic structures such as the NAc, PFC, amygdala, VP, hippocampus and the VTA, and mostly in GABAergic neurons (Austin and Kalivas, 1990; Johnson and North, 1992). For these reasons, we created a conditional mouse line where the Cre recombinase under the Dlx5/6 promoter, coming from a gene that is required for the differentiation and migration of most telencephalon and diencephalon GABAergic neurons, drives excision of the mu receptor gene in GABAergic forebrain neurons. I characterized the anatomical distribution of the mu receptor mRNA in this mouse model, as well as the protein distribution (collaboration with Pr. Kitchen, University of Surrey). The receptor pattern of deletion was as expected, restricted to the forebrain. To better understand the implication of GABAergic forebrain mu receptors, I examined classical opiate responses in those mutant mice, including analgesic and rewarding properties, physical dependence, locomotor effects and motivation for drugs of abuse (collaboration with Pr. Maldonado, PRBB Barcelona), as well as cellular responses (neuronal activation). This work is presented in Part I in the form of a manuscript: *Mu opioid receptors in GABAergic forebrain neurons are necessary for heroin hyperlocomotion and reduce motivation for heroin and palatable food*. Charbogne P, Gardon O, Martín-García E, Keyworth H, Matsui A, Matifas A, Befort K, Kitchen I, Bailey A, Alvarez VA, Maldonado R, Kieffer BL.

Aim 2: autistic-like syndrome in Dlx-mu mice

In a second part of my thesis, I focused on the role of mu receptors in autistic-like behaviors. As recently shown by our team, total mu receptor KO presents an autistic-like phenotype (Becker et al., 2014). I evaluated these socio-emotional behaviors in our conditional model. Important components of this syndrome were studied, such as the deficit in social interaction, the enhanced anxiety-like and conflict responses. This work is presented in Part II in another manuscript in preparation: *Mu opioid receptors in GABAergic forebrain neurons are not involved in autistic-like symptoms*. Charbogne P, Matifas A, Befort K, Kieffer BL.

Aim 3: target glutamatergic forebrain mu receptors in adult mice

In a third part, we developed a mouse line where the Cre recombinase is expressed under the control of the CaMKIIα gene promoter that targets glutamatergic forebrain neurons. This Cre is fused with ER^{T2} protein and permits expression of the enzyme only after tamoxifen treatment. I characterized the Cre recombinase pattern of expression using a reporter mouse line after tamoxifen injections, as well as the expression of the mu receptor gene.

Aim 4: create a Cre mouse line to target the extended amygdala

In the fourth part of my thesis, I contributed to develop a new mouse model to tackle gene function in the extended amygdala (EA), a brain structure heavily involved in drug reward and relapse to drug abuse. A previous work in our laboratory found a gene, named *Wfs1* (wolframin gene), whose expression is enriched in EA (Becker et al., 2008). We used a short version of the wolframin promoter, fused with eGFP protein, to generate conditional mice. Two different constructs were produced. The first one is a fusion protein eGFP-$CreER^{T2}$; the second one is eGFP-T2A-$CreER^{T2}$, permitting dissociation between the Cre (nucleus) and the eGFP (cytoplasm). I characterized the eGFP pattern of expression, illustrating Cre expression, of several founders for those constructs.

Neuropharmacology 76 (2014) 204–217

Contents lists available at ScienceDirect

Neuropharmacology

journal homepage: www.elsevier.com/locate/neuropharm

Invited review

15 years of genetic approaches *in vivo* for addiction research: Opioid receptor and peptide gene knockout in mouse models of drug abuse

Pauline Charbogne [a, b, c, d], Brigitte L. Kieffer [a, b, c, d, *], Katia Befort [a, b, c, d]

[a] IGBMC Institut de Génétique et de Biologie Moléculaire et Cellulaire, CNRS UMR 7104 – Inserm U964, Illkirch F-67404, France
[b] CNRS, UMR7104, Illkirch F-67404, France
[c] UdS Université de Strasbourg, CNRS UMR 7104 – Inserm U964, Illkirch F-67404, France
[d] Inserm U964, Illkirch F-67404, France

ARTICLE INFO

Article history:
Received 29 March 2013
Received in revised form
19 August 2013
Accepted 23 August 2013

Keywords:
Opioid receptors
Opioid peptides
Knockout mice
Drugs of abuse
Addiction
Reward

ABSTRACT

The endogenous opioid system is expressed throughout the brain reinforcement circuitry, and plays a major role in reward processing, mood control and the development of addiction. This neuromodulator system is composed of three receptors, mu, delta and kappa, interacting with a family of opioid peptides derived from POMC (β-endorphin), preproenkephalin (pEnk) and preprodynorphin (pDyn) precursors. Knockout mice targeting each gene of the opioid system have been created almost two decades ago. Extending classical pharmacology, these mutant mice represent unique tools to tease apart the specific role of each opioid receptor and peptide *in vivo*, and a powerful approach to understand how the opioid system modulates behavioral effects of drugs of abuse. The present review summarizes these studies, with a focus on major drugs of abuse including morphine/heroin, cannabinoids, psychostimulants, nicotine or alcohol. Genetic data, altogether, set the mu receptor as the primary target for morphine and heroin. In addition, this receptor is essential to mediate rewarding properties of non-opioid drugs of abuse, with a demonstrated implication of β-endorphin for cocaine and nicotine. Delta receptor activity reduces levels of anxiety and depressive-like behaviors, and facilitates morphine-context association. pEnk is involved in these processes and delta/pEnk signaling likely regulates alcohol intake. The kappa receptor mainly interacts with pDyn peptides to limit drug reward, and mediate dysphoric effects of cannabinoids and nicotine. Kappa/dynorphin activity also increases sensitivity to cocaine reward under stressful conditions. The opioid system remains a prime candidate to develop successful therapies in addicted individuals, and understanding opioid-mediated processes at systems level, through emerging genetic and imaging technologies, represents the next challenging goal and a promising avenue in addiction research.

This article is part of a Special Issue entitled 'NIDA 40th Anniversary Issue'.

© 2013 Elsevier Ltd. All rights reserved.

1. Introduction

Opiates, including morphine, are potent analgesic compounds and represent major therapeutic drugs to treat severe pain. In addition, opiates induce strong euphoria and repeated exposure often leads to dependence and eventually opioid addiction. Milestones in discoveries of the opioid system are shown in Fig. 1. Morphine, the most active component of opium, was isolated in 1805 by Serturner. Opioid receptors were described in 1973, based on opioid binding sites referred as mu, delta and kappa (Pert and Snyder, 1973; Simon et al., 1973; Terenius, 1973). Met- and Leu-enkephalins were characterized in 1975, and altogether three families of endogenous opioid peptides precursors (pre-proenkephalin pEnk, pre-prodynorphin pDyn and proopiomelanocortin POMC) were identified in the late 70's (Goldstein et al., 1979; Guillemin et al., 1976; Hughes et al., 1975; Li and Chung, 1976). Genes encoding opioid peptide precursors were isolated in the early 80's (pEnk (Comb et al., 1982; Gubler et al., 1982; Noda et al., 1982); pDyn (Kakidani et al., 1982); POMC (Nakanishi et al., 1979)). The first opioid receptor gene, encoding delta receptors, isolated by expression cloning in 1992 (Evans et al., 1992; Kieffer et al., 1992), and the two other receptor genes were cloned by homology (Mestek et al., 1995; Simonin et al., 1994, 1995). Opioid receptors belong to the superfamily of G-protein coupled receptors (Kieffer, 1995; Trigo et al., 2010), with coupling to Gi/Go proteins (Law et al., 2000),

* Corresponding author. Institut de Génétique et de Biologie Moléculaire et Cellulaire, Department of Neurobiology and Genetics, 1 Rue Laurent Fries, 67404 Illkirch, France. Tel.: +33 (0) 3 88 65 56 93; fax: +33 (0) 3 88 65 56 04.
E-mail address: briki@igbmc.fr (B.L. Kieffer).

0028-3908/$ – see front matter © 2013 Elsevier Ltd. All rights reserved.
http://dx.doi.org/10.1016/j.neuropharm.2013.08.028

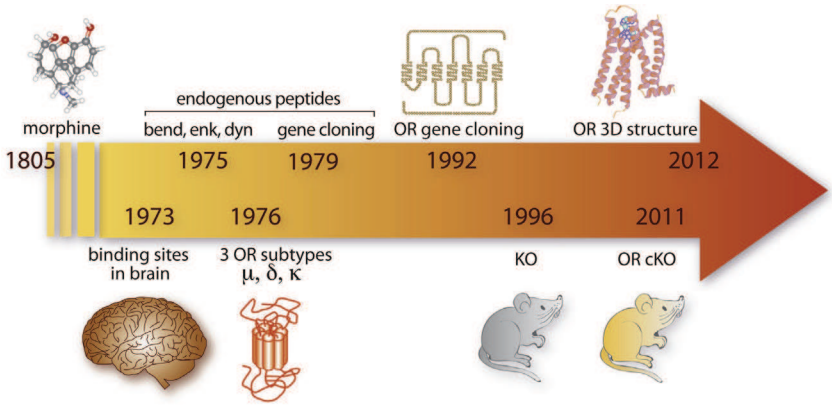

Fig. 1. Milestone discoveries in opioid research. Opium is extracted from poppy seeds (*Papaver somniferum*) and consumed for several thousand years to relieve pain and produce euphoria. Morphine, the most active alkaloid extracted from opium, was the first opioid to be isolated (1805). Opiates act on the nervous system, where they specifically activate receptors (1973), which are normally stimulated by a family of endogenous neurotransmitters, β-endorphin, enkephalins and dynorphins (1975). Several opioid receptors subtypes were further described based on receptor pharmacology (1976). Gene cloning occurred in early 80's for peptide precursors (1979) and early 90's for opioid receptors (1992). Opioid receptors genes (*Oprm1, Oprd1* and *Oprk* encoding mu-, delta- and kappa-opioid receptor; *pomc*, *pEnk* and *pDyn* encoding peptide precursors) were targeted in mice by homologous recombination, and mice lacking the mu receptor and enkephalins were available first (1996). Recently, refinement of *in vivo* targeted mutagenesis techniques led to the first conditional knockout mouse for the opioid system, with a delta receptor deletion restricted to primary afferent nociceptive neurons (2011). The 3D crystal structure of all three receptors was elucidated very recently (2012). OR: opioid receptor, KO: knockout mouse, cKO: conditional knockout mouse. Detailed references are in the text.

and their structure was solved at high-resolution by X-ray crystallography (Granier et al., 2012; Manglik et al., 2012; Wu et al., 2012). The opioid system is broadly expressed in the nervous system, particularly within the neurocircuitry of addiction (Koob and Volkow, 2010). Both peptides and receptors are present in areas associated with reward, motivation, learning and stress (Le Merrer et al., 2009; Mansour et al., 1995), and therefore play a key role in many aspects of addictive behaviors (see Lutz and Kieffer, 2013).

All the known drugs of abuse activate reinforcing brain circuitries (Koob and Volkow, 2010). These drugs, however, recruit distinct molecular targets in the brain and show notable differences in their pharmacological actions, which has led researchers and physicians to classify them into distinct groups. Opiates, acting directly at opioid receptors, produce sedative effects in addition to euphoria, and are therefore known as narcotics. In contrast, psychostimulants that include cocaine, amphetamine and methamphetamine, provide immediate euphoria with a feeling of intellectual and physical power, and indifference to pain and fatigue, mainly via direct stimulation of dopaminergic transmission. Nicotine, a major component of tobacco, is also considered a mild stimulant and α-nicotinic receptors constitute their molecular target. Relaxing and euphoric sensations searched by marijuana users arise from the stimulation of CB1 receptors by cannabinoids, including the most active component delta9-tetrahydrocannabinol (THC). Finally, the most widely abused licit drug is alcohol, targeting several receptors and ion channels in the brain and representing a major health problem (Hyman, 2008). It is now well established that the endogenous opioid system plays an important role in acute and chronic effects of all these drugs. The exact nature of opioid receptor or peptide involved has been clarified over the years, largely owing to genetic approaches, and this large set of data is overviewed here.

Drug abuse is a major threat to public health (Compton et al., 2007; Gustavsson et al., 2011). For 40 years, NIDA has supported extensive research towards understanding molecular bases of drug abuse (Everitt et al., 2008; Nestler, 2005; Pierce and Wolf, 2013), and developing innovative strategies for treatment (Heilig et al., 2011; Kalivas and Volkow, 2011; Koob et al., 2009; Pierce et al., 2012; Volkow and Skolnick, 2012). We are extremely grateful to NIDA for long-standing support to our efforts in developing genetic mouse models for opioid research. Knockout (KO) mice for the opioid system, developed by others and us, have been extensively studied and broadly shared within our research community. In this review, we have gathered data from these KO mice that have accumulated in the past fifteen years (for previous reviews see Contet et al., 2004; Kieffer and Gaveriaux-Ruff, 2002), and enabled identification or clarification of the specific role of each component of the opioid system in drug reward and addiction. Note that the opioid system plays a central role in pain processing, but this particular aspect will not be reviewed here (see recent reviews in Bodnar, 2012; Gaveriaux-Ruff and Kieffer, 2011; Woolf, 2011).

We will first summarize behavioral responses of null mutant mice to opiates, then overview reports investigating the effects of other drugs of abuse, including cannabinoids, psychostimulants (cocaine, MDMA, amphetamine), nicotine and alcohol in these mice, and finally conclude on the respective roles of opioid peptides and receptors, and perspectives of opioid research in the area of drug abuse. Whereas data from receptor KO mice have unambiguously clarified receptor roles *in vivo*, data from peptide KO mice are by essence more complex (low receptor selectivity) and the latter mutants still deserve further investigations.

2. Behavioral measures in the mouse

At present, behavioral paradigms to model distinct aspects of addiction (for a review see Everitt et al., 2008; Koob et al., 2009) in rodents remain limited, particularly for mice (see Box). Several well-described behavioral models in rats have nevertheless been successfully adapted to mice, and largely applied to mutant animals. Among these, voluntary/operant testing (two-bottle choice, TBC and self-administration, SA) addresses some aspects of binge intoxication and/or excessive consumption, and conditioned place preference (CPP) examines drug reward. Withdrawal and the negative effect of drug abstinence can be revealed by conditioned place aversion (CPA) and drug-induced physical withdrawal, and preoccupation/anticipation can be tested by drug-, cue- or stress-induced reinstatement of CPP. Finally locomotor activation by drugs of abuse, and sensitization to this effect upon repeated treatment, are also typical responses studied in rodents although no human correlate exists for this behavior. Data from all these tests are summarized in Tables 1–6, and main findings are summarized below.

Box
Behavioral measures in the mouse.

Behavioral responses examined in mutant mice (Tables 1–6) are briefly explained below.

Conditioned place preference (CPP) or aversion (CPA): pavlovian conditioning based on capacity of the animal to associate the drug effect with the context. If the drug has rewarding effects, mice explore the drug-paired compartment more than the vehicle-paired compartment, and thus show a conditioned place preference (CPP). If the drug is aversive mice avoid the drug-paired box (Conditioned place aversion or CPA). Reinstatement can be measured after a CPP paradigm: drug priming or stress can reinstate preference for the initially drug-paired box after extinction. This test models drug-seeking behavior (Tzschentke, 2007).

Self-administration (SA): operant paradigms model several elements of human drug consumption, and are therefore largely used in rodents. Drug SA in mice (except oral SA), however, is technically difficult, and studies remain scarce. In drug SA models, the animal works to obtain the drug and learns an action/outcome association. Various aspects are investigated: acquisition (under fixed ratio schedule); motivation (under progressive ratio schedule and determination of a breaking point, corresponding to the highest response possible for a single delivery); extinction (response rate after end of drug-delivery); reinstatement (as for CPP). In addition to rewarding effects of the drug, this model enables investigation of motivational aspects of drug intake (Sanchis-Segura and Spanagel, 2006).

Two-bottle choice: In this test, mostly used for measuring alcohol consumption, the animal has access to a water-containing bottle and an alcohol-containing bottle. This access is either continuous (24 h/day) or intermittent (few hours a day or few days a week). The latter closely mimics binge drinking and can be used as a model of relapse by including phases of deprivation (Crabbe et al., 2011).

Locomotor effects and sensitization: Many drugs of abuse increase locomotor activity after acute treatment. Repeated administration of the drug, classically increases this locomotor response, a phenomenon referred to as sensitization that may reflect the transition from voluntary intake to compulsive use (Robinson and Berridge, 2008; Vanderschuren and Pierce, 2010), or vulnerability to drug addiction or drug-induced psychosis in humans (Loweth and Vezina, 2011).

Withdrawal: Chronic drug administration produces physical dependence, which is revealed after cessation of drug exposure. Spontaneous withdrawal is difficult to detect and quantify in animals, therefore physical withdrawal is typically precipitated by treatment with an antagonist, followed by scoring of withdrawal signs. The latter vary with the drug (ptosis, teeth chattering, tremor, paw tremor, wet-dog shakes, sniffing, jumping, diarrhea) and a global score is calculated to measure a general dependence index (Maldonado et al., 1996).

3. Opioid system and opiate drugs

Morphine reward and withdrawal data are shown for the six KO lines in Table 1. Locomotor effects of morphine are presented in Table 6 together with stimulant effects of other drugs of abuse. Genetic studies have definitely established that the mu opioid receptor is required for therapeutic effects as well as unwanted effects of morphine (see Contet et al., 2004). Hence, morphine (Matthes et al., 1996; Nguyen et al., 2012a, 2012b; Sora et al., 2001) and heroin (Contarino et al., 2002) CPPs were abolished in mu KO mice at all the tested doses. Intravenous as well as intra-VTA infusions of the drug observed in wild type animals were also abolished in mutants (Sora et al., 2001; David et al., 2008). In another study, mu KO mice self-administered morphine at levels lower than control mice self-administering saline, perhaps unmasking a kappa/dynorphin-mediated aversive state in these mutants (Becker et al., 2000). Locomotor responses to morphine (Tian et al., 1997; Sora et al., 2001; Chefer et al., 2003; Yoo et al., 2003, 2006; Becker et al., 2000) and heroin administration (Contarino et al., 2002) were eliminated in mu KO animals (see Table 6). Together all the data demonstrate that mu receptors indeed represent the primary *in vivo* molecular target for both most clinically useful (morphine) and most largely abused (heroin) opiates.

The role of delta receptor in reward is debated. Delta KO mice developed a place preference when morphine was paired with the initially non-preferred compartment, but failed to do so when paired to the preferred side of the apparatus (Chefer and Shippenberg, 2009). The authors interpreted this result as a ceiling effect in the biased CPP protocol that was used more than a decrease of rewarding properties of morphine. In another study, using unbiased CPP, delta KO animals did not develop place preference to morphine (Le Merrer et al., 2011). In the same study, mutant mice showed impaired place conditioning to lithium, an aversive stimulus, and showed normal motivation to obtain morphine in a SA paradigm (Le Merrer et al., 2011). Together with a previous study showing intact intra-VTA SA in delta KO mice (David et al., 2008), the data concur to indicate that morphine reward and motivation to obtain the drug are intact in these animals, however drug-context association is impaired. A subsequent study showed that internal or external non-spatial cues (circadian, drug, auditory) predicting drug or food reward restored morphine CPP in delta KO mice, suggesting that only contextual learning is impaired in these mice (Le Merrer et al., 2012). Considering locomotor effects, the stimulant effect of acute morphine was unchanged in delta KO mice (Chefer et al., 2003). However, sensitization or tolerance to this effect, observed upon distinct regimen of chronic morphine administration, was enhanced and reduced respectively (Chefer and Shippenberg, 2009), indicating a role for delta receptors in these adaptive responses to chronic morphine. Otherwise, physical dependence was unchanged in delta KO mice (Nitsche et al., 2002). In conclusion, the delta receptor does not directly mediate morphine reward and likely facilitates contextual learning. Also, as many other systems, this receptor contributes to chronic morphine-induced neuroplasticity. Mechanisms underlying a potential cross talk between delta receptor activity and mu opioid receptor signaling *in vivo* remain unclear (see Pradhan et al., 2011; Stockton and Devi, 2012).

β-endorphin KO animals compared with wild-type controls spent equal (Niikura et al., 2008) or more (Skoubis et al., 2005) time in the drug-paired compartment, depending on the dose and paradigm used. No modification of morphine CPP could be detected in proenkephalin (pEnk) KO mice (Skoubis et al., 2005), and physical dependence was either decreased (Shoblock and Maidment, 2007) or enhanced in these mice (Nitsche et al., 2002). These results suggest paradoxical negative modulatory roles for the two endogenous peptides in morphine reward (βend) and withdrawal (pEnk), or that compensatory mechanisms have developed in knockout animals.

Morphine CPP was unchanged in mice lacking the kappa opioid receptor (Simonin et al., 1998), as well as dynorphin (Mizoguchi et al., 2010; Zimmer et al., 2001). Prodynorphin KO mice showed unchanged (Mizoguchi et al., 2010; Zimmer et al., 2001) or increased hyperlocomotor activity upon morphine administration (Mizoguchi et al.,

Table 1
Behavioral effects of morphine and heroin in opioid receptor and peptide knockout mice.

Gene KO	Drug of abuse	Behavioral test	Drug of abuse dose, route	Genotype effect	Ref
mu	Morphine	CPP	3 mg/kg, s.c.	Abolished	Matthes et al., 1996
		CPP	10 mg/kg, s.c.	Abolished	Sora et al., 2001
		CPP	10 mg/kg, s.c.	Abolished	Nguyen et al., 2012a
		CPP	10 mg/kg, s.c.	Abolished	Nguyen et al., 2012b
		+ *challenge on d14*	5 mg/kg, s.c.	Abolished	
		SA	2 or 4 mg/0.2 mL, i.c.v. FR1	Lower than saline groups	Becker et al., 2000
		SA	0.1 or 0.3 mg/kg/injection, i.v. FR4	Abolished	Sora et al., 2001
		VTA SA	50 or 100 ng/infusion	Abolished	David et al., 2008
		Withdrawal	20–100 mg/kg, i.p. *(2x/d, 5d)*	Abolished	Matthes et al., 1996
	Heroin	CPP	1 mg/kg, i.p.	Abolished	Contarino et al., 2002
delta	Morphine	CPP preferred side	10 mg/kg, s.c.	Abolished	Chefer and Shippenberg, 2009
		CPP non-preferred side	10 mg/kg, s.c.	Unchanged	
		CPP drug free state	5 mg/kg, s.c.	Abolished	Le Merrer et al., 2011
		CPP under morphine	5 mg/kg, s.c.	Unchanged	
		CPP without cue	10 mg/kg, s.c.	Abolished	Le Merrer et al., 2012
		CPP with cue	5, 10 and 20 mg/kg, s.c.	Unchanged/restored	
		SA	0.25 or 0.5 mg/kg/infusion, i.v. FR1	Unchanged	Le Merrer et al., 2011
			0.25 mg/kg/infusion, i.v. PR	Unchanged	
			0.5 mg/kg/infusion, i.v. PR	Increased	
		VTA SA	50 ng/infusion	Unchanged	David et al., 2008
		Withdrawal	75 mg, pellet *(3d)*	Unchanged	Nitsche et al., 2002
kappa	Morphine	CPP	1 mg/kg, s.c.	Unchanged	Simonin et al., 1998
		Withdrawal	20–100 mg/kg, i.p. *(2x/d, 6d)*	Abolished	Simonin et al., 1998
βend	Morphine	CPP	10 mg/kg, s.c.	Increased	Skoubis et al., 2005
		CPP	5 mg/kg, s.c.	Unchanged	Niikura et al., 2008
pEnk	Morphine	CPP	10 mg/kg, s.c.	Unchanged	Skoubis et al., 2005
		Withdrawal	75 mg, pellet *(3d)*	Increased	Nitsche et al., 2002
		Withdrawal jumping	20 mg/kg, s.c. *(1 injection)*	Decreased	Shoblock and Maidment, 2007
			100 mg/kg, s.c. *(2d)*	Abolished	
pDyn	Morphine	CPP	5 mg/kg, s.c.	Unchanged	Zimmer et al., 2001
		CPP	3.5 mg/kg, s.c.	Unchanged	Mizoguchi et al., 2010
		Withdrawal	20–100 mg/kg, i.p. *(2x/d, 5d)*	Unchanged	Zimmer et al., 2001

Data are shown for each knockout (gene KO) mouse line. Behavioral tests are detailed in the Box. Unchanged: no genotype effect; increased: KO shows higher response compared to wild-type (WT); decreased: KO shows lower response compared to WT; abolished: no response in KO. CPP: Conditioned Place Preference; d: day; SA: self-administration; VTA: ventral tegmental area; FR: fixed ratio; PR: progressive ratio.

2010), suggesting that dynorphin opposes mu receptor signaling for the control of locomotor effects. Several signs of naloxone-induced withdrawal were decreased in morphine-dependent kappa KO mice (Simonin et al., 1998), an effect that could not be observed in pDyn mutants (Zimmer et al., 2001). A tonic role for the kappa/dynorphin system is therefore detected in dependent animals, at receptor level, in agreement with pharmacological studies suggesting protective role of kappa receptor blockade in morphine dependence (Wee and Koob, 2010). Involvement of this anti-reward system (Koob and Le Moal, 2008) is overall better detected in knockout mice under conditions of stress (Bruchas et al., 2010) and in response to non-opioid drugs of abuse (see below).

Table 2
Behavioral effects of cannabinoid in opioid receptor and peptide knockout mice.

Gene KO	Drug of abuse	Behavioral test	Drug of abuse dose, route	Genotype effect	Ref
mu	THC	CPP	1 mg/kg, i.p.	Abolished	Ghozland et al., 2002
		CPA	5 mg/kg, i.p.	Decreased	Ghozland et al., 2002
		Withdrawal	10 mg/kg, s.c. *(5d)*	Unchanged	Lichtman et al., 2001
			30 or 100 mg/kg, s.c. *(5d)*	Decreased	
		Withdrawal	20 mg/kg, i.p. *(2x/d, 6d)*	Unchanged	Ghozland et al., 2002
delta	THC	CPP	1 mg/kg, i.p.	Unchanged	Ghozland et al., 2002
		CPA	5 mg/kg, i.p.	Unchanged	Ghozland et al., 2002
		Withdrawal	20 mg/kg, i.p. *(2x/d, 6d)*	Unchanged	Ghozland et al., 2002
mu delta	THC	CPP	1 mg/kg, i.p.	Decreased	Castane et al., 2003
		Withdrawal	20 mg/kg, i.p. *(2x/d, 6d)*	Decreased	Castane et al., 2003
kappa	THC	CPP	1 mg/kg, i.p.	Unchanged	Ghozland et al., 2002
		CPP without priming	1 mg/kg, i.p.	Present, absent in WT	
		CPA	5 mg/kg, i.p.	Abolished	Ghozland et al., 2002
		Withdrawal	20 mg/kg, i.p. *(2x/d, 6d)*	Unchanged	Ghozland et al., 2002
pEnk	THC	Withdrawal	20 mg/kg, i.p. *(2x/d, 6d)*	Decreased	Valverde et al., 2000
pDyn	THC	CPA	5 mg/kg, i.p.	Abolished	Zimmer et al., 2001
		Withdrawal	20 mg/kg, i.p. *(2x/d, 6d)*	Decreased (trend)	Zimmer et al., 2001
	WIN	SA	6.25 mg/kg/infusion, i.v. FR1	Increased	Mendizabal et al., 2006
			12.5 mg/kg/infusion, i.v. FR1	Abolished	

Data are shown for each knockout (gene KO) mouse line. Behavioral tests are detailed in the Box. Unchanged: no genotype effect; increased: KO shows higher response compared to wild-type (WT); decreased: KO shows lower response compared to WT; abolished: no response in KO. THC: Δ^9-tetrahydrocannabinol; WIN: WIN 55,212-2; CPP: Conditioned Place Preference; CPA: Conditioned Place Aversion; d: day; SA: self-administration; FR: fixed ratio.

Table 3
Behavioral effects of psychostimulant in opioid receptor and peptide knockout mice.

Gene KO	Drug of abuse	Behavioral test	Drug of abuse dose, route	Genotype effect	Ref
mu	Cocaine	CPP	5–10 mg/kg i.p.	Rightward shift	Becker et al., 2002
		CPP	10 mg/kg, i.p.	Unchanged	Contarino et al., 2002
		CPP	5 mg/kg, s.c.	Unchanged	Hall et al., 2004
			10 mg/kg, s.c.	Decreased	
		CPP	30 mg/kg, i.p.	Unchanged	Nguyen et al., 2012a
		SA	0.4, 0.8 or 1.6 μg/inf, i.v. FR1	Decreased	Mathon et al., 2005
	MDMA	CPP	10 mg/kg, i.p.	Unchanged	Robledo et al., 2004
	Amphetamine	CPP	1 mg/kg, i.p.	Unchanged	Marquez et al., 2007
kappa	Cocaine	CPP ± forced swim stress	15 mg/kg, s.c.	Unchanged/no effect of stress	McLaughlin et al., 2006a
		CPP	15 mg/kg, s.c.	Unchanged	Redila and Chavkin, 2008
		Stress-induced reinstatement		Abolished	
		Cocaine prime test	15 mg/kg, s.c.	Unchanged	
βend	Cocaine	CPP	30–60 mg/kg i.p.	Rightward shift	Marquez et al., 2008
		CPP	30 mg/kg, i.p.	Abolished	Nguyen et al., 2012a
pDyn	Cocaine	CPP ± forced swim stress	15 mg/kg, s.c.	Unchanged/no effect of stress	McLaughlin et al., 2003
		CPP + social defeat stress	15 mg/kg, s.c.	Decreased	McLaughlin et al., 2006b
		CPP	15 mg/kg, s.c.	Unchanged	Redila and Chavkin, 2008
		Stress-induced reinstatement		Abolished	
		Cocaine prime test	15 mg/kg, s.c.	Decreased	

Data are shown for each knockout (gene KO) mouse line. Behavioral tests are detailed in the Box. Unchanged: no genotype effect; increased: KO shows higher response compared to wild-type (WT); decreased: KO shows lower response compared to WT; abolished: no response in KO. CPP: Conditioned Place Preference; d: day; SA: self-administration; FR: fixed ratio.

4. Opioid system and cannabinoids

Both pharmacological studies and genetic approaches provide considerable evidence suggesting that cannabinoid and opioid systems interact bi-directionally to regulate both neurochemical effects of drug and behavioral responses (Trigo et al., 2010; Vigano et al., 2005). Although mechanisms underlying functional interactions remain unclear, receptors from the two systems show overlapping distribution in various brain structures, and potential heterodimer formation between CB1 and mu opioid receptors has been suggested from *in vitro* studies (Maldonado et al., 2011; Solinas et al., 2008). Data summarizing cannabinoid effects in KO mice for the opioid system are shown in Table 2.

THC-induced CPP was unchanged in delta or kappa KO mice (Ghozland et al., 2002), but was abolished in mu KO mutants (Ghozland et al., 2002) and the double mu–delta KO line (Castane et al., 2003), suggesting that mu receptors mediate rewarding properties of THC. Interestingly conditioned place aversion (CPA), typically observed at a high dose of THC in wild-type mice, was abolished in both pDyn (Zimmer et al., 2001) and kappa KO mice (Ghozland et al., 2002). The latter observations indicate that the kappa/dynorphin system mediates aversive effects of THC, another facet of cannabinoid effects. This was further supported by facilitated self-administration of WIN, a cannabinoid agonist, in pDyn KO mice (Mendizabal et al., 2006). It has long been established that mu and kappa receptors oppositely regulate hedonic homeostasis (Spanagel et al., 1992) and it is therefore possible that the same opposing activities of the two opioid receptors mediate the well-known dual euphoric/aversive effects of cannabinoids. Notably, the delta receptor does not seem involved in all these THC effects, at least from knockout mice analysis (Ghozland et al., 2002).

THC withdrawal upon chronic THC treatment was reduced in pEnk KO mice (Valverde et al., 2000) and double mu–delta KO mice (Castane et al., 2003). Reduced THC withdrawal was also detected in mu KO animals, at high doses of THC (Lichtman et al., 2001). Single mutants for pDyn (Zimmer et al., 2001), mu, delta or kappa

Table 4
Behavioral effects of nicotine in opioid receptor and peptide knockout mice.

Gene KO	Behavioral test	Drug of abuse dose, route	Genotype effect	Ref
mu	CPP	0.5 or 0.7 mg/kg, s.c.	Abolished	Berrendero et al., 2002
	CPP	1 mg/kg, i.p.	Abolished	Walters et al., 2005
		2 mg/kg, i.p.	Unchanged	
	Withdrawal	10 mg/kg/d, minipump *(6d)*	Decreased	Berrendero et al., 2002
delta	CPP	0.17 mg/kg, s.c.	Abolished	Berrendero et al., 2012
	SA	15 μg/kg/infusion 10d, i.v. FR1	Unchanged	Berrendero et al., 2012
		30 μg/kg/infusion 10d, i.v. FR1	Decreased	
		30 μg/kg/infusion, i.v. PR	Decreased	
	Withdrawal	8.77 mg/kg/d, minipump *(6d)*	Unchanged	Berrendero et al., 2012
βend	CPP	0.5 mg/kg, s.c.	Abolished	Trigo et al., 2009
	Withdrawal	10 mg/kg/d, minipump *(6d)*	Unchanged	Trigo et al., 2009
pEnk	CPP	0.5 mg/kg, s.c.	Abolished	Berrendero et al., 2005
	Withdrawal	25 mg/kg/d, minipump *(6d)*	Decreased	Berrendero et al., 2005
pDyn	CPP	0.5 mg/kg, s.c.	Unchanged	Galeote et al., 2009
	SA	5.2–85.5 mg/kg/infusion, i.v. FR1	Leftward shift	Galeote et al., 2009
		5.2, 10.6, 21.3 or 85.5 mg/kg/infusion, i.v. PR	Unchanged	
		42.7 mg/kg/infusion, i.v. PR	Decreased	
	Withdrawal	25 mg/kg/d, minipump *(6d)*	Unchanged	Galeote et al., 2009

Data are shown for each knockout (gene KO) mouse line. Behavioral tests are detailed in the Box. Unchanged: no genotype effect; increased: KO shows higher response compared to wild-type (WT); decreased: KO shows lower response compared to WT; abolished: no response in KO. CPP: Conditioned Place Preference; d: day; SA: self-administration; FR: fixed ratio; PR: progressive ratio.

Table 5
Alcohol behavioral effects in opioid receptor and peptide knockout mice.

Gene KO	Behavioral test	Drug of abuse dose, route	Genotype effect	Ref
mu	TBC limited access	10%	Unchanged	van Rijn and Whistler, 2009
	TBC	10%	Decreased	Becker et al., 2002
	TBC	2–32%	Decreased (female)	Hall et al., 2001
	TBC	10%	Decreased	Roberts et al., 2000
	Oral SA	5–10%	Abolished	
	Oral SA following TBC		Abolished	
	CPP	2 or 4 g/kg	Unchanged	Becker et al., 2002
	CPP	2 g/kg	Abolished (female)	Hall et al., 2001
	Withdrawal	liquid diet 0.8–5%	Earlier signs	Ghozland et al., 2005
delta	TBC limited access	10%	Increased	van Rijn and Whistler, 2009; van Rijn et al., 2010
	Oral SA	5–10%	Increased	Roberts et al., 2001
	TBC following SA	10%	Increased	
kappa	TBC limited access	10%	Decreased	van Rijn and Whistler, 2009
	TBC	3–12%	Decreased	Kovacs et al., 2005
βend	TBC	7%	Increased	Grisel et al., 1999
	TBC +/− mild foot shock	8%	Decreased/no effect of stress	Racz et al., 2008
	SA	75 mg/kg; 2h session/9d; i.v. FR3	Acquisition in KO but not WT	Grahame et al., 1998
	Oral SA	3–6%	Unchanged	Hayward et al., 2004
	Withdrawal	forced drinking 16%	Unchanged	Racz et al., 2008
pEnk	TBC	2–10%	Unchanged	Koenig and Olive, 2002
	TBC	8%	Unchanged	Racz et al., 2008
	TBC + foot shock		Decreased (male)	
	Oral SA	3–6%	Unchanged	Hayward et al., 2004
	CPP	2 g/kg, i.p.	Unchanged	Koenig and Olive, 2002
	Withdrawal	forced drinking 16%	Unchanged	Racz et al., 2008
pDyn	TBC	2–8%	Increased	Femenia and Manzanares, 2012
	TBC	3–12%	Decreased (female)	Blednov et al., 2006
	TBC	8%	Increased	Racz et al., 2012
	TBC + foot shock		Prolonged/WT	
	TBC	4–10%	Unchanged	Sperling et al., 2010
	CPP	2 g/kg, i.p.	Increased	Femenia and Manzanares, 2012
	CPP drug free state	2 g/kg, i.p.	Unchanged (female)	Nguyen et al., 2012c
	CPP priming	2 g/kg, i.p. challenge 1 g/kg	Increased (female)	
	CPP	2 g/kg, i.p.	Unchanged	Blednov et al., 2006
	Conditioned taste aversion	2.5 g/kg, i.p.	Unchanged	
	Withdrawal	4 g/kg, p.o.	Increased	Femenia and Manzanares, 2012
		4 g/kg, i.p.	Unchanged	Blednov et al., 2006

Data are shown for each knockout (gene KO) mouse line. Behavioral tests are detailed in the Box. Unchanged: no genotype effect; increased: KO shows higher response compared to wild-type (WT); decreased: KO shows lower response compared to WT; abolished: no response in KO; CPP: Conditioned Place Preference; d: day; SA: self-administration; TBC: two-bottle choice; FR: fixed ratio.

receptors (Ghozland et al., 2002) otherwise showed normal THC withdrawal. The data together suggest that an endogenous enkephalinergic tone, acting jointly at mu and delta receptors, contributes to the development of physical dependence to THC.

5. Opioid system and psychostimulants

Multiple studies have pointed out a role for opioid receptors and their endogenous ligands in psychostimulant – particularly cocaine-addiction (for a recent review, see Yoo et al., 2012, and Table 3). Cocaine self-administration was dose-dependently reduced in mu KO mice (Mathon et al., 2005), and cocaine CPP was maintained (Contarino et al., 2002; Hall et al., 2004; Nguyen et al., 2012a) or decreased (Hall et al., 2004) depending on dose and experimental conditions (number of pairings, number and duration of conditioning sessions). These data indicate that mu receptors mediate, at least in part, cocaine reward. A rightward shift of the CPP dose–response curve was observed in both mu (Becker et al., 2002) and β-endorphin (Marquez et al., 2007) KO mice, suggesting decreased cocaine sensitivity in the two lines and a possible implication of mu/βend signaling in cocaine reinforcement. Place preference studies were also conducted in mu KO for amphetamine (Marquez et al., 2007) and MDMA (Robledo et al., 2004) but no phenotype could be detected.

The rewarding properties of cocaine were examined using CPP in mice lacking either kappa receptors or preprodynorphin. Preference for the drug-paired compartment was maintained in both animal models (McLaughlin et al., 2006a, 2003; Redila and Chavkin, 2008). In presence of stress, cocaine CPP is typically increased in wild type mice but remained unchanged in kappa and pDyn KO mice (forced-swim stress in McLaughlin et al. (2006a); McLaughlin et al. (2003); social defeat stress in McLaughlin et al. (2006b), indicating that the kappa/dynorphin system contributes to the stress-mediated response. Within this line, stress-induced reinstatement of extinguished cocaine CPP was decreased in pDyn KO, although this was not observed in kappa KO mice (Redila and Chavkin, 2008).

Another well-known effect of psychostimulants is drug-induced hyperlocomotion (Table 6). In some reports, the locomotor response to cocaine was reduced in mu KO mice (Chefer et al., 2004; Yoo et al., 2006, 2003) as well as in βend KO mice (Marquez et al., 2008), while in many other mu KO studies, this cocaine effect was unchanged (Becker et al., 2002; Chefer et al., 2004; Contarino et al., 2002; Hall et al., 2004; Lesscher et al., 2005). Furthermore, sensitization to locomotor effects of cocaine was reduced (Yoo et al., 2006, 2003), maintained (Lesscher et al., 2005), or enhanced (Hummel et al., 2004), depending on the mouse genetic background (Hummel et al., 2004) and the pattern of drug exposure (administration regimen and timing of injections) (Allouche et al., 2013; Puig et al., 2012). In mu KO mice also, methamphetamine-induced locomotion, was decreased at one dose, maintained in lower and higher doses, and no behavioral

Table 6
Drugs of abuse locomotor effects in opioid receptor and peptide knockout mice.

Gene KO	Drug of abuse	Locomotor stimulation	Drug of abuse dose, route	Genotype effect	Ref
mu	Morphine	Locomotion	2.3 mg/kg, i.p.	Abolished	Tian et al., 1997
		Locomotion	5 or 10 mg/kg, s.c.	Decreased/saline	Becker et al., 2000
		Locomotion	10 mg/kg, s.c.	Abolished	Sora et al., 2001
		Locomotion	10 or 20 mg/kg, s.c.	Abolished	Chefer et al., 2003
		Locomotor sensitization *(6d inj)*	10 mg/kg, s.c. *d1*	Abolished locomotion	Yoo et al., 2003, 2006
		+ *challenge on day 12*	10 mg/kg, s.c. *d12*	Abolished	
	Heroin	Locomotion	3 mg/kg, i.p.	Abolished	Contarino et al., 2002
	THC	Locomotor tolerance *(2x/d, 5d)*	20 mg/kg, i.p.	Unchanged	Ghozland et al., 2002
	Cocaine	Locomotion	20 or 40 mg/kg, i.p.	Unchanged	Becker et al., 2002
		Locomotion	30 mg/kg, i.p.	Unchanged	Contarino et al., 2002
		Locomotion	15 mg/kg, i.p.	Abolished	Yoo et al., 2003, 2006
		Locomotion	10 mg/kg, i.p.	Unchanged	Chefer et al., 2004
			20 mg/kg, i.p.	Decreased	
		Locomotion	20 mg/kg, s.c.	Unchanged	Hall et al., 2004
		Locomotion	3, 10, 20, or 30 mg/kg i.p.	Unchanged	Lesscher et al., 2005
		Locomotor sensitization *(6d inj)*	15 mg/kg, i.p.		Yoo et al., 2003, 2006
		+ *challenge on day 12*	15 mg/kg, i.p.	Decreased	
		Locomotor sensitization *(10d inj)*	15 mg/kg, i.p.		Hummel et al., 2004
		+ *challenge on day 17*	15 mg/kg, i.p.	Decreased in 129S6xC57BL/6J Increased in C57BL/6J	
		Locomotor sensitization *(5d inj)*	20 mg/kg, s.c.	Unchanged	Hall et al., 2004
		Locomotor sensitization *(11d inj)*	20 mg/kg, i.p.		Lesscher et al., 2005
		+ *challenge on day 14*	10 mg/kg, i.p.	Unchanged	
	Methamphetamine	Locomotion	1.25 mg/kg, i.p.	Unchanged	Shen et al., 2010
			2.5 mg/kg, i.p.	Decreased	
			10 mg/kg, i.p.	Unchanged	
		Locomotor sensitization *(7d inj)*	0.62 mg/kg, i.p.	Abolished	
	Nicotine	Locomotion	0.7, 1 or 3 mg/kg, s.c.	Unchanged	Berrendero et al., 2002
		Locomotor sensitization *(2x/d, 7d)*	0.05 mg/kg, s.c. *d1*	No effect (WT and KO)	Yoo et al., 2004
			0.05 mg/kg, s.c. *d7*	Abolished	
		+ *challenge on day 11*	0.05 mg/kg, s.c.	Abolished	
		Locomotor sensitization *(2x/d, 7d)*	0.05 mg/kg, s.c. *d1*	No effect (WT and KO)	Yoo et al., 2005
			0.05 mg/kg, s.c. *d7*	Abolished	
	Alcohol	Locomotion	0.75, 1.25 or 1.75 g/kg, i.p.	Abolished	Ghozland et al., 2005
		Locomotion	0.5 or 1.2 g/kg, i.p.	Decreased (trend)	Hall et al., 2001
delta	Morphine	Locomotion	10 or 20 mg/kg, s.c.	Unchanged	Chefer et al., 2003
		Locomotor sensitization *(5d inj)*	20 mg/kg, s.c.	Unchanged, faster	Chefer and Shippenberg, 2009
		Challenge on day +7	5 mg/kg, s.c.	Increased	
		Challenge on day +33	5 mg/kg, s.c.	Unchanged	
		Locomotor tolerance *(3d)*	25 mg pellet, s.c.	Decreased	
	THC	Locomotor tolerance *(2x/d, 5d)*	20 mg/kg, i.p.	Unchanged	Ghozland et al., 2002
	Cocaine	Locomotion	10 mg/kg, i.p.	Increased	Chefer et al., 2004
			20 mg/kg, i.p.	Unchanged	
	Nicotine	Locomotion	0.35, 1.05 or 2.10 mg/kg, s.c.	Unchanged	Berrendero et al., 2012
mu delta	THC	Locomotion	20 mg/kg, i.p.	Unchanged	Castane et al., 2003
	Cocaine	Locomotion	5 or 15 mg/kg, i.p.	Unchanged	Chefer et al., 2005
			10 mg/kg, i.p.	Increased	
		Locomotor sensitization *(5d inj)*	15 mg/kg, i.p. *d1*	Increased locomotion	
		+ *challenge on day 8*	15 mg/kg, i.p. *d8*	Abolished	
kappa	THC	Locomotor tolerance *(2x/d, 5d)*	20 mg/kg, i.p.	Decreased	Ghozland et al., 2002
	Cocaine	Locomotion	5 or 15 mg/kg, i.p.	Unchanged	Chefer et al., 2005
			10 mg/kg, i.p.	Increased	
		Locomotor sensitization *(5d inj)*	15 mg/kg, i.p. *d1*	Increased locomotion	
		+ *challenge on day 8*	15 mg/kg, i.p. *d8*	Abolished	
βend	Cocaine	Locomotion	15, 30, or 60 mg/kg, i.p.	Decreased	Marquez et al., 2008
	Nicotine	Locomotion (horizontal)	1 or 3 mg/kg, s.c.	Unchanged	Trigo et al., 2009
		Locomotion (vertical)	1 mg/kg, s.c.	Increased	
			3 mg/kg, s.c.	Unchanged	
	Alcohol	Locomotor sensitization *(12d inj)*	2 g/kg, i.p.		Sharpe and Low, 2009
		+ *challenge on day 13 or 14*	1.2 g/kg, i.p.	Unchanged	
pEnk	THC	Locomotion	20 mg/kg, i.p.	Unchanged	Valverde et al., 2000
	Nicotine	Locomotion	1, 3 or 6 mg/kg, s.c.	Unchanged	Berrendero et al., 2005

Table 6 (*continued*)

Gene KO	Drug of abuse	Locomotor stimulation	Drug of abuse dose, route	Genotype effect	Ref
pDyn	Morphine	Locomotion	5 mg/kg, s.c.	Unchanged	Zimmer et al., 2001
		Locomotion	4.2 mg/kg, s.c.	Increased	Mizoguchi et al., 2010
			5 mg/kg, s.c.	Unchanged	
	THC	Locomotion	20 mg/kg, i.p.	Unchanged	Zimmer et al., 2001
	Cocaine	Locomotion	10 or 15 mg/kg, i.p.	Decreased	Chefer and Shippenberg, 2006
		Locomotor sensitization *(14d inj)*	15 mg/kg, i.p. *d1*	Unchanged	Bailey et al., 2007
			15 mg/kg, i.p. *d3, 7 and 14*	Increased	
	Nicotine	Locomotion	1, 3 or 6 mg/kg, s.c.	Unchanged	Galeote et al., 2009
	Alcohol	Locomotion	2 g/kg, i.p.	Unchanged	Nguyen et al., 2012c

Data are shown for each knockout (gene KO) mouse line. Measures of locomotor stimulation and sensitization are detailed in the Box. Unchanged: no genotype effect; increased: KO shows higher response compared to wild-type (WT); decreased: KO shows lower response compared to WT; abolished: no response in KO; d: day; inj: injection.

sensitization was found (Shen et al., 2010), therefore altogether, evidence exists that mu receptor activity contributes to locomotor effects of cocaine, and the adaptive response to repeated exposure to the drug.

Cocaine-induced locomotion was also investigated in delta KO mice, showing an increased response to cocaine in these mutant animals (Chefer et al., 2004). Locomotion stimulation upon cocaine administration was maintained or increased (Chefer et al., 2005) in kappa KO animals depending on the dose, and maintained (Bailey et al., 2007) or decreased (Chefer and Shippenberg, 2006) in pDyn KO mice, indicating contrasting effects of the kappa/dynorphin system in this response. Similarly, locomotor sensitization was abolished in kappa KO mice (Chefer et al., 2005), and increased in pDyn KO animals (Bailey et al., 2007), suggesting a dissociation of kappa receptors and dynorphins in the locomotor stimulant effect of cocaine.

6. Opioid system and nicotine

Among psychostimulants, nicotine is the primary component of tobacco that maintains smoking habits. The drug acts as a nicotinic acetylcholine receptor agonist to produce relaxation and enhanced cognitive performance, and is strongly addictive. Pharmacological and genetic studies have provided evidence for a critical role for the opioid system in nicotine addiction (for recent reviews, see Berrendero et al., 2010; Drews and Zimmer, 2010; Hadjiconstantinou and Neff, 2011; Tuesta et al., 2011), and knockout studies addressing nicotine reward and withdrawal are summarized in Table 4.

Rewarding properties of nicotine were altered in pEnk, βend, mu and delta KO mice, as shown by decreased nicotine CPP in these mutant mice (Berrendero et al., 2002, 2005, 2012; Trigo et al., 2009; Walters et al., 2005). In agreement, enhanced extracellular dopamine induced by nicotine in the nucleus accumbens was attenuated in mice lacking pEnk (Berrendero et al., 2005) and delta receptors (Berrendero et al., 2012). Also, the acquisition of nicotine SA was decreased in delta KO mice (Berrendero et al., 2012), further substantiating the notion that delta/pEnk receptor signaling contributes to reinforcing properties of nicotine. In contrast, self-administration of a low nicotine dose was increased in pDyn KO mice (Galeote et al., 2009) suggesting that, as for THC, dynorphin may contribute to aversive effects of nicotine. It would be interesting to pursue similar experiments in kappa KO mice to confirm this hypothesis.

mu/pEnk signaling seems involved in nicotine dependence. Withdrawal signs of chronically nicotine-treated pEnk (Berrendero et al., 2005) and mu KO (Berrendero et al., 2002) mice were attenuated, while no difference with wild-type controls was observed for pDyn (Galeote et al., 2009), delta (Berrendero et al., 2012) and βend (Trigo et al., 2009) KO mice. Finally, the mu receptor also contributes to nicotine-induced locomotor sensitization (Yoo et al., 2005, 2004), see Table 6.

7. Opioid system and alcohol

Alcohol produces euphoria, among many other effects, and acts on several molecular targets in the brain. A recent analysis of 37 KO mouse lines has provided evidence that alcohol consumption is controlled by multiple physiological systems (Blednov et al., 2012). Among these, endogenous opioids represent an important neurobiological component of alcohol intake and dependence (Gianoulakis, 2009; Koob et al., 2003). Extensive research has implicated endogenous opioid peptide release in alcohol consumption, and naltrexone, a general opioid antagonist, showed some efficacy in the treatment of alcoholism (Koob et al., 2009). Knockout mice have provided key insights into opioid mechanisms underlying alcohol-related behaviors (see Table 5). Mice lacking mu opioid receptors did not self-administer alcohol under several conditions, including oral self-administration and the two-bottle choice, and did not display conditioned place preference to alcohol (Becker et al., 2002; Hall et al., 2001; Roberts et al., 2000), demonstrating that mu receptors are essential to consumption and motivation for alcohol. mu receptor also plays a role in alcohol withdrawal as the absence of mu receptor accelerated the progression of physical signs of withdrawal (Ghozland et al., 2005). Finally, no locomotor stimulation was observed following alcohol administration in mu KO mice (Ghozland et al., 2005 and Table 6), and altogether data show a prominent role of mu receptors in many aspects of alcohol effects.

Opposing mu receptor mutants, delta KO mice showed increased alcohol consumption in TBC (Roberts et al., 2001; van Rijn et al., 2010; van Rijn and Whistler, 2009) and oral SA combined with TBC (Roberts et al., 2001) paradigms and their innate anxiety returned to wild-type levels after alcohol SA (Roberts et al., 2001). Given the important role of delta in reducing emotional responses (Filliol et al., 2000), increased alcohol intake in these mutants may reflect a self-medication approach to alleviate high levels of anxiety (for a recent review, see Chu Sin Chung and Kieffer, 2013). Interestingly, pEnk KO animals showed intact rewarding effect of alcohol and a normal pattern of alcohol consumption (Koenig and Olive, 2002), however alcohol drinking was modified in pEnk KO under stressful conditions. The latter observation supports a role for delta/pEnk signaling in regulating emotional responses that may impact on alcohol consumption. β-endorphin may also be involved since alcohol intake was reduced (Racz et al., 2008), unchanged (Hayward et al., 2004) or increased (Grahame et al., 1998; Grisel et al., 1999) in βend KO mice.

Paradoxically, mice lacking the kappa receptor showed reduced preference and alcohol consumption in TBC paradigms (Kovacs et al., 2005; van Rijn and Whistler, 2009), which contrast with increased reinforcing effects of other drugs of abuse in these mice. Using similar

TBC testing, pDyn KO mice showed increased voluntary consumption (Femenia and Manzanares, 2012; Racz et al., 2012) suggesting that the kappa receptor and dynorphins regulate alcohol intake via distinct mechanisms. Alcohol CPP was unchanged (Blednov et al., 2006; Nguyen et al., 2012c; Sperling et al., 2010) or increased (Femenia and Manzanares, 2012) in mice lacking pDyn. The latter observation is in agreement with the TBC data and the reported aversive-like activity of dynorphin peptides. pDyn KO mice otherwise showed normal increase in stress-induced alcohol preference (Racz et al., 2012; Sperling et al., 2010), but developed stronger withdrawal signs after chronic alcohol (Femenia and Manzanares, 2012). As mu receptors therefore, pDyn influences several aspects of responses to alcohol, and future studies will examine whether kappa/pDyn signaling indeed operates in alcohol abuse.

8. Discussion and concluding remarks

Knockout studies have highlighted very distinct roles for each component of the opioid system in drug reward and dependence: the mu receptor is a convergent molecular target mediating rewarding properties of all drugs of abuse, the kappa receptor opposes mu receptor signaling in the control of hedonic homeostasis, and also mediates aversive effects of cannabinoids and nicotine, and the delta receptor most likely modulates drug consumption indirectly, by improving emotional states or facilitating drug-context association (see Lutz and Kieffer, 2012, 2013). Confronting data from receptor KO and peptide KO mice is a difficult task, since ideally behavioral responses of the six knockout lines should be examined in parallel, using the same experimental setting. This was performed with the three receptor lines for some responses, but was never achieved for the six lines together. Also studies from constitutive gene deletions have sometimes yielded results which are discordant with behavioral pharmacology, often attributed to compensatory mechanisms that may develop in genetically modified animals (Kieffer and Gaveriaux-Ruff, 2002; Portugal and Gould, 2008). Altogether however, data analysis across the literature allows identification of potential endogenous receptor/peptide systems operating in drug reinforcement processes, and reveals differing mechanisms across the distinct classes of drugs of abuse (Figs. 2 and 3).

8.1. Role of mu signaling in drug reward

mu receptor is essential for rewarding effects of opiates as well as non-opiate drugs (cannabinoids, psychostimulants and alcohol). Both pEnk and βend (Roth-Deri et al., 2008) are involved in rewarding effects of non-opioid drugs of abuse, with a demonstrated implication of βend for cocaine and alcohol, whereas nicotine or cannabinoid reward has been little explored so far for the two peptides.

8.2. Role of kappa signaling in drug aversion

The important role of kappa/dynorphin in dysphoric effects of drugs of abuse has been reviewed recently (Shippenberg et al., 2007; Wee and Koob, 2010). The set of data summarized here supports the notion that kappa receptors mainly interact with pDyn-derived peptides to limit drug reward and mediate dysphoric aspects for some drugs (cannabinoids, nicotine). Moreover, and only under stressful conditions, kappa/dynorphin activity increases sensitivity to cocaine reward. The kappa/dynorphin partnership regulating alcohol intake, however, requires further studies.

8.3. Role of delta signaling in drug reward

Data indicate that delta receptor activity reduces levels of anxiety and depressive-like behaviors, and that enkephalin is involved in this process (Chu Sin Chung and Kieffer, 2013; Lutz and Kieffer, 2012; Pradhan et al., 2011), and it is likely that delta/pEnk signaling also regulates alcohol intake through similar mechanisms.

8.4. Clinical perspectives

Many pharmacotherapies to treat addiction have been developed in the past decades, but have often shown modest efficacy or acted on sub-populations of patients (Potenza et al., 2011; Volkow and Skolnick, 2012). Clinical studies also showed reduced relapse rate in patients receiving behavioral therapy (alcohol), and in general individual differences, including genetic vulnerability, need be considered (Heilig et al., 2011). The question of whether novel opioid compounds could lead to more efficient treatments is under intense investigations. Naltrexone, a general opioid antagonist, was the first opioid medication with FDA approval to reduce the level or frequency of drug intake (Pettinati and Rabinowitz, 2006). Methadone treatment, targeting mu receptors, was a pioneering substitution approach to treat heroin addiction, and a recent report describing eight compounds effective in the treatment of alcohol (acamprosate, naltrexone), opioid (buprenorphine, methadone, naloxone) and nicotine (nicotine, varenicline, bupropion) addiction, shows that mu receptors remain a prime target in most successful treatments for addiction (Pierce et al., 2012). Delta agonists may be efficient to limit disruption of emotional responses in addicted

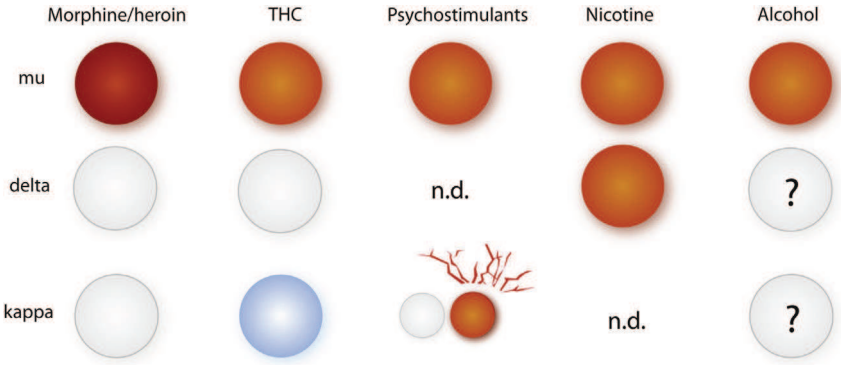

Fig. 2. Involvement of opioid receptors in drug reward. The scheme summarizes data from receptor KO mice and highlights the role of each receptor in drug reward. The mu opioid receptor mediates rewarding properties of both opioid and non-opioid drugs of abuse. With the exception of nicotine, the delta receptor does not seem involved in drug reward. The kappa receptor mediates dysphoric effects of THC and favors cocaine reward after stress (red lines). The role of delta and kappa receptor in alcohol intake is under investigation (see text). Circles indicate euphoria (red/orange), no effect (white) or dysphoria (blue); n.d: not determined in receptor KO mice.

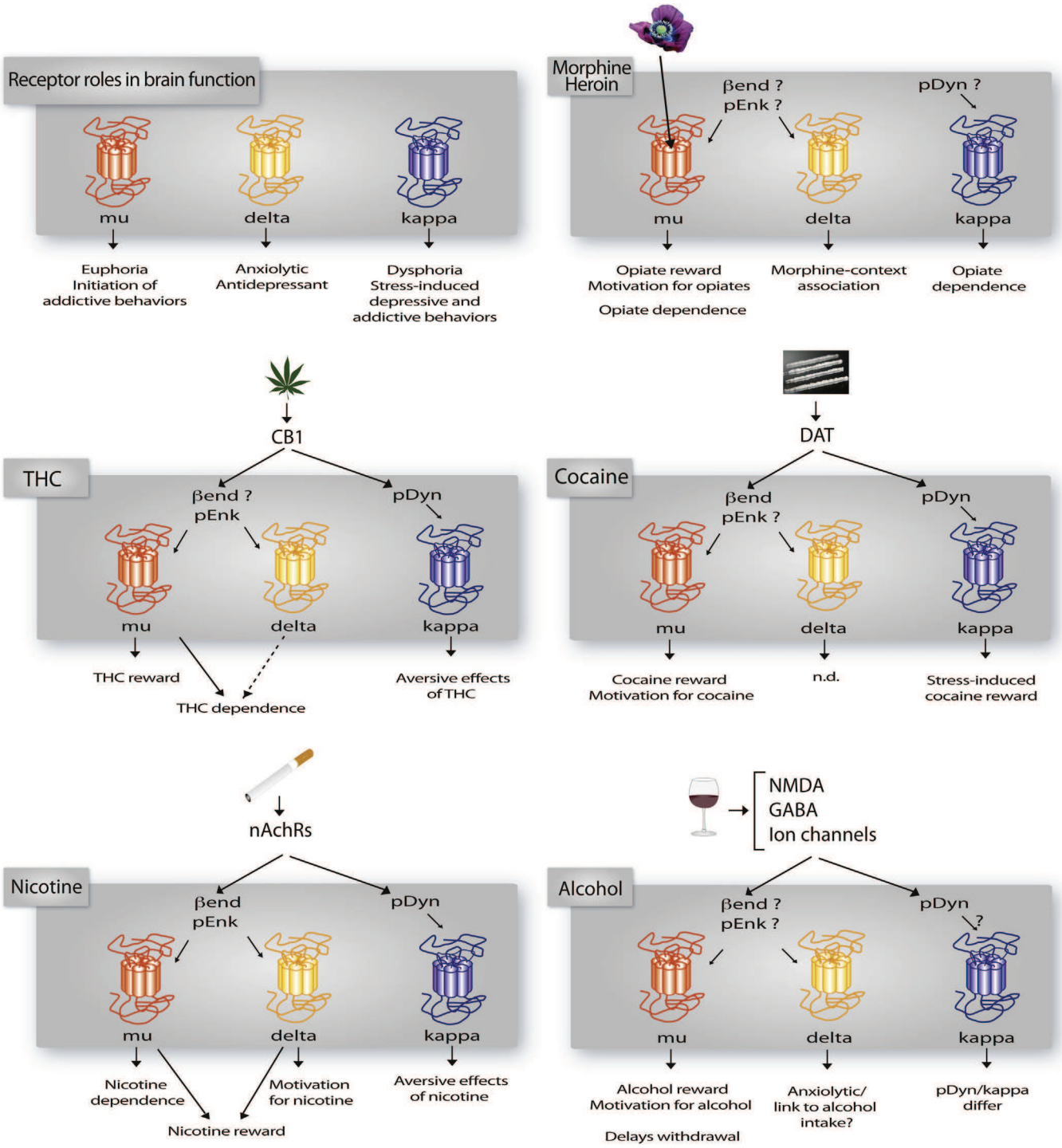

Fig. 3. Distinct roles of opioid receptors and peptides in addiction-related effects of drugs of abuse. The upper left scheme summarizes known roles of opioid receptors in brain functions related to hedonic homeostasis and mood (from Lutz and Kieffer, 2012). In the five other panels, we propose mechanisms implicating opioid receptors and/or peptides in addiction liability of each class of drugs of abuse, as inferred from both receptor and peptide knockout mouse data reviewed here. "Reward" and "drug-context association" refer to CPP data, "aversive effects" to CPA data, "motivation for the drug" to SA experiments, and "dependence" to scores of physical withdrawal under antagonist treatment. Data from locomotor studies are not included (see summary in Table 6). Opiates: peptide KO mice show paradoxical (β-end/reward, pEnk/withdrawal) or no (pDyn/withdrawal) phenotype. THC: β-end KO mice not tested; cocaine: pEnk KO mice not tested; nicotine: β-end KO mice tested for reward but not withdrawal; alcohol: β-end KO mice show contrasting phenotypes and pEnk show a phenotype under stress. Altogether, data from peptide KO mice, combined with those from receptor KO mice, concur to substantiate involvement of a kappa/dynorphin system in dysphoric states associated to drugs of abuse, although this may not apply to alcohol. Data also suggest a role for mu/β-end signaling in cocaine and nicotine reward, and implication of delta/pEnk signaling to regulate alcohol intake.

individuals (Lutz and Kieffer, 2012). Delta drugs have been developed to treat chronic pain and depression, and are currently being tested in the clinic, but their use in indications related to drug abuse has not been considered, as yet (Gaveriaux-Ruff and Kieffer, 2011). Preclinical research has definitely established that kappa receptor activity plays a role in addiction-related behaviors, with a prodepressant-like activity (see review Lutz and Kieffer, 2013). Kappa antagonists are therefore promising candidates for pharmacotherapies in stress- and

addiction-related disorders, and may attenuate compulsive drug intake (Wee and Koob, 2010) or specific symptoms of depressive disorders, depending on the administration time point (Knoll and Carlezon, 2010). Finally, considering the growing evidence of co-morbidity between addiction and depression, possible improvement of addiction therapies may arise from the combination of substitution treatments (mu agonists such as methadone, or partial agonists such as buprenorphine) with kappa antagonists or delta agonists, for treating patients with comorbid conditions (Lutz and Kieffer, 2013).

Further development of delta and kappa opioid drugs will join the growing body of studies addressing other targets, such as gamma-aminobutyric acid receptors and voltage-gated ion channels. These drugs will likely complete other non-pharmacological therapies, including transcranial magnetic stimulation or behavioral, cognitive therapies and group therapies considered very effective in long-term treatments (Addolorato et al., 2012; Volkow and Skolnick, 2012).

9. Future directions – addressing the neural circuit by genetic approaches

9.1. Conditional knockout

Conventional knockout approaches have proved valuable to tease apart respective contributions of opioid receptor and peptides in several aspects of drug abuse. Further important developments in addiction research involve investigation of molecular mechanisms operating at the level of neuronal circuits underlying the distinct aspects of addiction (Koob and Volkow, 2010). Therefore, genetic approaches targeted at specific brain sites or neuronal populations are required (Fowler and Kenny, 2012; Gaveriaux-Ruff and Kieffer, 2007; Heldt and Ressler, 2009), among which conditional gene knockout using the Cre/loxP system has received great attention (Nagy, 2000). In the addiction field, several studies using this technology have provided invaluable insights into circuit mechanisms of drug reward. Site-specific deletion of α4-containing nAChR (McGranahan et al., 2011) as well as NMDA receptor NR1 subunit (Wang et al., 2010) has revealed involvement of NMDA receptors expressed in dopaminergic neurons in nicotine reward. Mice lacking CREB specifically in the cerebral cortex were tested for cocaine self-administration and showed a role for CREB in mediating cocaine reinforcement in this brain structure (McPherson et al., 2010). A comprehensive analysis of behavioral and autonomic effects of THC in several conditional lines has revealed implication of the CB1 receptor expressed at the level of forebrain glutamatergic neurons (CB1CamKIIa-Cre mice), cortical glutamatergic neurons (CB1NEX-Cre mice) and dopaminergic neurons (CB1Drd1a-Cre mice), but not GABAergic neurons (CB1Dlx5/6-Cre mice) (Monory et al., 2007). Also a conditional knockout approach using Pet1-Cre mice, targeting the transcription factor *Lmx1b* in developing serotonergic neurons of the hindbrain, showed that central serotonergic neurons modulate supraspinal pain but are not involved in morphine reward (Zhao et al., 2007). So far, only one conditional line has been reported for opioid receptors and peptides, demonstrating a key role of delta receptors expressed in primary nociceptive neurons in delta analgesia and the control of chronic pain (Gaveriaux-Ruff et al., 2011). It is expected that conditional lines for the opioid system, targeting the neurocircuitry of addiction, will be instrumental to understand circuit mechanisms underlying opioid-mediated drug effects and plasticity.

9.2. Optogenetics and brain imaging

More recently, a novel area of investigation has emerged with the development of optogenetic approaches to manipulate specific neuronal populations in live animals (Fowler and Kenny, 2012). For example, light-mediated phasic activation of dopaminergic neurons in the VTA produced a place preference in a CPP paradigm (Tsai et al., 2009) and the specific light-activation of cholinergic neurons from nucleus accumbens reduced cocaine reward (Witten et al., 2010). The specific manipulation of mu, delta or kappa receptor expressing neurons will be of great interest towards understanding neuronal connectivity and plasticity while addiction develops. Within this line, non-invasive neuroimaging and functional connectivity techniques, now developed in small rodents, offer promises in translational medicine (Dalley et al., 2009; Jasinska et al., 2013), and neuroimaging of opioid receptor and peptide genetic mutants may provide invaluable information towards understanding the human disease.

9.3. New animal models

Behavioral testing in mice is limited, however new models have been developed to better characterize several stages of the addiction cycle, or protracted abstinence and relapse (for example: Goeldner et al., 2011; for reviews see O'Brien and Gardner, 2005; Spanagel, 2003) Animal research is expanding in this direction for brain disorders in general (Ahmed, 2010; Berton et al., 2012; Nestler and Hyman, 2010). Also, automated multidimensional systems now enable recording behavior of mice living in social groups to characterize novelty-seeking trait, anxiety, impulsivity, compulsivity and motivation, and such systems can be successfully applied to study behavioral adaptations to drugs of abuse (Radwanska and Kaczmarek, 2011). Also, drosophila or zebra fish are model organisms that allow rapid genetic screens and are being developed in the context of drug abuse (Kaun et al., 2012; Klee et al., 2012; Stewart et al., 2011).

Ultimately, the combination of emerging technologies at molecular, circuit and behavioral levels holds enormous potential to discover novel mechanisms operating at integrated level. The opioid system remains a prime candidate to develop successful therapies in addicted individuals, and understanding opioid-mediated processes at systems levels represents a challenging goal in addiction research.

Acknowledgments

We would like to thank Sandra Bour for her help with figure preparation and Dominique Massotte for critical reading of the manuscript. This work was supported by CNRS, INSERM, and Université de Strasbourg. We also thank the Mouse Clinical Institute (ICS, Illkirch, France), the European Union (Grant No. GENADDICT/FP6 005166), and the National Institutes of Health (National Institute of Drug Addiction, grant #05010 and National Institute on Alcohol Abuse and Alcoholism, grant #16658) for financial support.

References

Addolorato, G., Leggio, L., Hopf, F.W., Diana, M., Bonci, A., 2012. Novel therapeutic strategies for alcohol and drug addiction: focus on GABA, ion channels and transcranial magnetic stimulation. Neuropsychopharmacology 37, 163–177.

Ahmed, S.H., 2010. Validation crisis in animal models of drug addiction: beyond non-disordered drug use toward drug addiction. Neurosci. Biobehav. Rev. 35, 172–184.

Allouche, S., Le Marec, T., Noble, F., Marie, N., 2013. Different patterns of administration modulate propensity of methadone and buprenorphine to promote locomotor sensitization in mice. Prog. Neuropsychopharmacol. Biol. Psychiatry 40, 286–291.

Bailey, A., Yoo, J.H., Racz, I., Zimmer, A., Kitchen, I., 2007. Preprodynorphin mediates locomotion and D2 dopamine and mu-opioid receptor changes induced by chronic 'binge' cocaine administration. J. Neurochem. 102, 1817–1830.

Becker, A., Grecksch, G., Brodemann, R., Kraus, J., Peters, B., Schroeder, H., Thiemann, W., Loh, H.H., Hollt, V., 2000. Morphine self-administration in mu-

opioid receptor-deficient mice. Naunyn Schmiedebergs Arch. Pharmacol. 361, 584–589.
Becker, A., Grecksch, G., Kraus, J., Loh, H.H., Schroeder, H., Hollt, V., 2002. Rewarding effects of ethanol and cocaine in mu opioid receptor-deficient mice. Naunyn Schmiedebergs Arch. Pharmacol. 365, 296–302.
Berrendero, F., Kieffer, B.L., Maldonado, R., 2002. Attenuation of nicotine-induced antinociception, rewarding effects, and dependence in mu-opioid receptor knock-out mice. J. Neurosci. 22, 10935–10940.
Berrendero, F., Mendizabal, V., Robledo, P., Galeote, L., Bilkei-Gorzo, A., Zimmer, A., Maldonado, R., 2005. Nicotine-induced antinociception, rewarding effects, and physical dependence are decreased in mice lacking the preproenkephalin gene. J. Neurosci. 25, 1103–1112.
Berrendero, F., Plaza-Zabala, A., Galeote, L., Flores, A., Bura, S.A., Kieffer, B.L., Maldonado, R., 2012. Influence of delta-opioid receptors in the behavioral effects of nicotine. Neuropsychopharmacology 37, 2332–2344.
Berrendero, F., Robledo, P., Trigo, J.M., Martin-Garcia, E., Maldonado, R., 2010. Neurobiological mechanisms involved in nicotine dependence and reward: participation of the endogenous opioid system. Neurosci. Biobehav. Rev. 35, 220–231.
Berton, O., Hahn, C.G., Thase, M.E., 2012. Are we getting closer to valid translational models for major depression? Science 338, 75–79.
Blednov, Y.A., Mayfield, R.D., Belknap, J., Harris, R.A., 2012. Behavioral actions of alcohol: phenotypic relations from multivariate analysis of mutant mouse data. Genes Brain Behav. 11, 424–435.
Blednov, Y.A., Walker, D., Martinez, M., Harris, R.A., 2006. Reduced alcohol consumption in mice lacking preprodynorphin. Alcohol 40, 73–86.
Bodnar, R.J., 2012. Endogenous opiates and behavior: 2011. Peptides 38, 463–522.
Bruchas, M.R., Land, B.B., Chavkin, C., 2010. The dynorphin/kappa opioid system as a modulator of stress-induced and pro-addictive behaviors. Brain Res. 1314, 44–55.
Castane, A., Robledo, P., Matifas, A., Kieffer, B.L., Maldonado, R., 2003. Cannabinoid withdrawal syndrome is reduced in double mu and delta opioid receptor knockout mice. Eur. J. Neurosci. 17, 155–159.
Chefer, V.I., Czyzyk, T., Bolan, E.A., Moron, J., Pintar, J.E., Shippenberg, T.S., 2005. Endogenous kappa-opioid receptor systems regulate mesoaccumbal dopamine dynamics and vulnerability to cocaine. J. Neurosci. 25, 5029–5037.
Chefer, V.I., Kieffer, B.L., Shippenberg, T.S., 2003. Basal and morphine-evoked dopaminergic neurotransmission in the nucleus accumbens of MOR- and DOR-knockout mice. Eur. J. Neurosci. 18, 1915–1922.
Chefer, V.I., Kieffer, B.L., Shippenberg, T.S., 2004. Contrasting effects of mu opioid receptor and delta opioid receptor deletion upon the behavioral and neurochemical effects of cocaine. Neuroscience 127, 497–503.
Chefer, V.I., Shippenberg, T.S., 2006. Paradoxical effects of prodynorphin gene deletion on basal and cocaine-evoked dopaminergic neurotransmission in the nucleus accumbens. Eur. J. Neurosci. 23, 229–238.
Chefer, V.I., Shippenberg, T.S., 2009. Augmentation of morphine-induced sensitization but reduction in morphine tolerance and reward in delta-opioid receptor knockout mice. Neuropsychopharmacology 34, 887–898.
Chu Sin Chung, P., Kieffer, B.L., 2013. Delta opioid receptors in brain function and diseases. Pharmacol. Ther. 40, 112–120.
Comb, M., Seeburg, P.H., Adelman, J., Eiden, L., Herbert, E., 1982. Primary structure of the human Met- and Leu-enkephalin precursor and its mRNA. Nature 295, 663–666.
Compton, W.M., Thomas, Y.F., Stinson, F.S., Grant, B.F., 2007. Prevalence, correlates, disability, and comorbidity of DSM-IV drug abuse and dependence in the United States: results from the national epidemiologic survey on alcohol and related conditions. Arch. Gen. Psychiatry 64, 566–576.
Contarino, A., Picetti, R., Matthes, H.W., Koob, G.F., Kieffer, B.L., Gold, L.H., 2002. Lack of reward and locomotor stimulation induced by heroin in mu-opioid receptor-deficient mice. Eur. J. Pharmacol. 446, 103–109.
Contet, C., Kieffer, B.L., Befort, K., 2004. Mu opioid receptor: a gateway to drug addiction. Curr. Opin. Neurobiol. 14, 370–378.
Crabbe, J.C., Harris, R.A., Koob, G.F., 2011. Preclinical studies of alcohol binge drinking. Ann. N. Y. Acad. Sci. 1216, 24–40.
Dalley, J.W., Fryer, T.D., Aigbirhio, F.I., Brichard, L., Richards, H.K., Hong, Y.T., Baron, J.C., Everitt, B.J., Robbins, T.W., 2009. Modelling human drug abuse and addiction with dedicated small animal positron emission tomography. Neuropharmacology 56 (Suppl. 1), 9–17.
David, V., Matifas, A., Gavello-Baudy, S., Decorte, L., Kieffer, B.L., Cazala, P., 2008. Brain regional Fos expression elicited by the activation of mu- but not delta-opioid receptors of the ventral tegmental area: evidence for an implication of the ventral thalamus in opiate reward. Neuropsychopharmacology 33, 1746–1759.
Drews, E., Zimmer, A., 2010. Modulation of alcohol and nicotine responses through the endogenous opioid system. Prog. Neurobiol. 90, 1–15.
Evans, C.J., Keith Jr., D.E., Morrison, H., Magendzo, K., Edwards, R.H., 1992. Cloning of a delta opioid receptor by functional expression. Science 258, 1952–1955.
Everitt, B.J., Belin, D., Economidou, D., Pelloux, Y., Dalley, J.W., Robbins, T.W., 2008. Review. Neural mechanisms underlying the vulnerability to develop compulsive drug-seeking habits and addiction. Philos. Trans. R. Soc. Lond. B Biol. Sci. 363, 3125–3135.
Femenia, T., Manzanares, J., 2012. Increased ethanol intake in prodynorphin knockout mice is associated to changes in opioid receptor function and dopamine transmission. Addict Biol. 17, 322–337.
Filliol, D., Ghozland, S., Chluba, J., Martin, M., Matthes, H.W., Simonin, F., Befort, K., Gaveriaux-Ruff, C., Dierich, A., LeMeur, M., Valverde, O., Maldonado, R., Kieffer, B.L., 2000. Mice deficient for delta- and mu-opioid receptors exhibit opposing alterations of emotional responses. Nat. Genet. 25, 195–200.
Fowler, C.D., Kenny, P.J., 2012. Utility of genetically modified mice for understanding the neurobiology of substance use disorders. Hum. Genet. 131, 941–957.
Galeote, L., Berrendero, F., Bura, S.A., Zimmer, A., Maldonado, R., 2009. Prodynorphin gene disruption increases the sensitivity to nicotine self-administration in mice. Int. J. Neuropsychopharmacol. 12, 615–625.
Gaveriaux-Ruff, C., Kieffer, B.L., 2007. Conditional gene targeting in the mouse nervous system: insights into brain function and diseases. Pharmacol. Ther. 113, 619–634.
Gaveriaux-Ruff, C., Kieffer, B.L., 2011. Delta opioid receptor analgesia: recent contributions from pharmacology and molecular approaches. Behav. Pharmacol. 22, 405–414.
Gaveriaux-Ruff, C., Nozaki, C., Nadal, X., Hever, X.C., Weibel, R., Matifas, A., Reiss, D., Filliol, D., Nassar, M.A., Wood, J.N., Maldonado, R., Kieffer, B.L., 2011. Genetic ablation of delta opioid receptors in nociceptive sensory neurons increases chronic pain and abolishes opioid analgesia. Pain 152, 1238–1248.
Ghozland, S., Chu, K., Kieffer, B.L., Roberts, A.J., 2005. Lack of stimulant and anxiolytic-like effects of ethanol and accelerated development of ethanol dependence in mu-opioid receptor knockout mice. Neuropharmacology 49, 493–501.
Ghozland, S., Matthes, H.W., Simonin, F., Filliol, D., Kieffer, B.L., Maldonado, R., 2002. Motivational effects of cannabinoids are mediated by mu-opioid and kappa-opioid receptors. J. Neurosci. 22, 1146–1154.
Gianoulakis, C., 2009. Endogenous opioids and addiction to alcohol and other drugs of abuse. Curr. Top. Med. Chem. 9, 999–1015.
Goeldner, C., Lutz, P.E., Darcq, E., Halter, T., Clesse, D., Ouagazzal, A.M., Kieffer, B.L., 2011. Impaired emotional-like behavior and serotonergic function during protracted abstinence from chronic morphine. Biol. Psychiatry 69, 236–244.
Goldstein, A., Tachibana, S., Lowney, L.I., Hunkapiller, M., Hood, L., 1979. Dynorphin-(1-13), an extraordinarily potent opioid peptide. Proc. Natl. Acad. Sci. U. S. A. 76, 6666–6670.
Grahame, N.J., Low, M.J., Cunningham, C.L., 1998. Intravenous self-administration of ethanol in beta-endorphin-deficient mice. Alcohol Clin. Exp. Res. 22, 1093–1098.
Granier, S., Manglik, A., Kruse, A.C., Kobilka, T.S., Thian, F.S., Weis, W.I., Kobilka, B.K., 2012. Structure of the delta-opioid receptor bound to naltrindole. Nature 485, 400–404.
Grisel, J.E., Mogil, J.S., Grahame, N.J., Rubinstein, M., Belknap, J.K., Crabbe, J.C., Low, M.J., 1999. Ethanol oral self-administration is increased in mutant mice with decreased beta-endorphin expression. Brain Res. 835, 62–67.
Gubler, U., Seeburg, P., Hoffman, B.J., Gage, L.P., Udenfriend, S., 1982. Molecular cloning establishes proenkephalin as precursor of enkephalin-containing peptides. Nature 295, 206–208.
Guillemin, R., Ling, N., Burgus, R., 1976. Endorphins, hypothalamic and neurohypophysial peptides with morphinomimetic activity: isolation and molecular structure of alpha-endorphin. C. R. Acad. Sci. Hebd Seances Acad. Sci. D 282, 783–785.
Gustavsson, A., Svensson, M., Jacobi, F., Allgulander, C., Alonso, J., Beghi, E., Dodel, R., Ekman, M., Faravelli, C., Fratiglioni, L., Gannon, B., Jones, D.H., Jennum, P., Jordanova, A., Jonsson, L., Karampampa, K., Knapp, M., Kobelt, G., Kurth, T., Lieb, R., Linde, M., Ljungcrantz, C., Maercker, A., Melin, B., Moscarelli, M., Musayev, A., Norwood, F., Preisig, M., Pugliatti, M., Rehm, J., Salvador-Carulla, L., Schlehofer, B., Simon, R., Steinhausen, H.C., Stovner, L.J., Vallat, J.M., den Bergh, P.V., van Os, J., Vos, P., Xu, W., Wittchen, H.U., Jonsson, B., Olesen, J., 2011. Cost of disorders of the brain in Europe 2010. Eur. Neuropsychopharmacol. 21, 718–779.
Hadjiconstantinou, M., Neff, N.H., 2011. Nicotine and endogenous opioids: neurochemical and pharmacological evidence. Neuropharmacology 60, 1209–1220.
Hall, F.S., Goeb, M., Li, X.F., Sora, I., Uhl, G.R., 2004. mu-Opioid receptor knockout mice display reduced cocaine conditioned place preference but enhanced sensitization of cocaine-induced locomotion. Brain Res. Mol. Brain Res. 121, 123–130.
Hall, F.S., Sora, I., Uhl, G.R., 2001. Ethanol consumption and reward are decreased in mu-opiate receptor knockout mice. Psychopharmacology (Berl.) 154, 43–49.
Hayward, M.D., Hansen, S.T., Pintar, J.E., Low, M.J., 2004. Operant self-administration of ethanol in C57BL/6 mice lacking beta-endorphin and enkephalin. Pharmacol. Biochem. Behav. 79, 171–181.
Heilig, M., Goldman, D., Berrettini, W., O'Brien, C.P., 2011. Pharmacogenetic approaches to the treatment of alcohol addiction. Nat. Rev. Neurosci. 12, 670–684.
Heldt, S.A., Ressler, K.J., 2009. The use of lentiviral vectors and Cre/loxP to investigate the function of genes in complex behaviors. Front. Mol. Neurosci. 2, 22.
Hughes, J., Smith, T.W., Kosterlitz, H.W., Fothergill, L.A., Morgan, B.A., Morris, H.R., 1975. Identification of two related pentapeptides from the brain with potent opiate agonist activity. Nature 258, 577–580.
Hummel, M., Ansonoff, M.A., Pintar, J.E., Unterwald, E.M., 2004. Genetic and pharmacological manipulation of mu opioid receptors in mice reveals a differential effect on behavioral sensitization to cocaine. Neuroscience 125, 211–220.
Hyman, S.E., 2008. A glimmer of light for neuropsychiatric disorders. Nature 455, 890–893.
Jasinska, A.J., Zorick, T., Brody, A.L., Stein, E.A., 2013. Dual role of nicotine in addiction and cognition: a review of neuroimaging studies in humans. Neuropharmacology. http://dx.doi.org/10.1016/j.neuropharm.2013.02.015 [Epub ahead of print].

Kakidani, H., Furutani, Y., Takahashi, H., Noda, M., Morimoto, Y., Hirose, T., Asai, M., Inayama, S., Nakanishi, S., Numa, S., 1982. Cloning and sequence analysis of cDNA for porcine beta-neo-endorphin/dynorphin precursor. Nature 298, 245–249.
Kalivas, P.W., Volkow, N.D., 2011. New medications for drug addiction hiding in glutamatergic neuroplasticity. Mol. Psychiatry 16, 974–986.
Kaun, K.R., Devineni, A.V., Heberlein, U., 2012. *Drosophila melanogaster* as a model to study drug addiction. Hum. Genet. 131, 959–975.
Kieffer, B.L., 1995. Recent advances in molecular recognition and signal transduction of active peptides: receptors for opioid peptides. Cell Mol. Neurobiol. 15, 615–635.
Kieffer, B.L., Befort, K., Gaveriaux-Ruff, C., Hirth, C.G., 1992. The delta-opioid receptor: isolation of a cDNA by expression cloning and pharmacological characterization. Proc. Natl. Acad. Sci. U. S. A. 89, 12048–12052.
Kieffer, B.L., Gaveriaux-Ruff, C., 2002. Exploring the opioid system by gene knockout. Prog. Neurobiol. 66, 285–306.
Klee, E.W., Schneider, H., Clark, K.J., Cousin, M.A., Ebbert, J.O., Hooten, W.M., Karpyak, V.M., Warner, D.O., Ekker, S.C., 2012. Zebrafish: a model for the study of addiction genetics. Hum. Genet. 131, 977–1008.
Knoll, A.T., Carlezon Jr., W.A., 2010. Dynorphin, stress, and depression. Brain Res. 1314, 56–73.
Koenig, H.N., Olive, M.F., 2002. Ethanol consumption patterns and conditioned place preference in mice lacking preproenkephalin. Neurosci. Lett. 325, 75–78.
Koob, G.F., Kenneth Lloyd, G., Mason, B.J., 2009. Development of pharmacotherapies for drug addiction: a Rosetta stone approach. Nat. Rev. Drug Discov. 8, 500–515.
Koob, G.F., Le Moal, M., 2008. Addiction and the brain antireward system. Annu. Rev. Psychol. 59, 29–53.
Koob, G.F., Roberts, A.J., Kieffer, B.L., Heyser, C.J., Katner, S.N., Ciccocioppo, R., Weiss, F., 2003. Animal models of motivation for drinking in rodents with a focus on opioid receptor neuropharmacology. Recent Dev. Alcohol 16, 263–281.
Koob, G.F., Volkow, N.D., 2010. Neurocircuitry of addiction. Neuropsychopharmacology 35, 217–238.
Kovacs, K.M., Szakall, I., O'Brien, D., Wang, R., Vinod, K.Y., Saito, M., Simonin, F., Kieffer, B.L., Vadasz, C., 2005. Decreased oral self-administration of alcohol in kappa-opioid receptor knock-out mice. Alcohol Clin. Exp. Res. 29, 730–738.
Law, P.Y., Wong, Y.H., Loh, H.H., 2000. Molecular mechanisms and regulation of opioid receptor signaling. Annu. Rev. Pharmacol. Toxicol. 40, 389–430.
Le Merrer, J., Becker, J.A., Befort, K., Kieffer, B.L., 2009. Reward processing by the opioid system in the brain. Physiol. Rev. 89, 1379–1412.
Le Merrer, J., Faget, L., Matifas, A., Kieffer, B.L., 2012. Cues predicting drug or food reward restore morphine-induced place conditioning in mice lacking delta opioid receptors. Psychopharmacology (Berl.) 223, 99–106.
Le Merrer, J., Plaza-Zabala, A., Del Boca, C., Matifas, A., Maldonado, R., Kieffer, B.L., 2011. Deletion of the delta opioid receptor gene impairs place conditioning but preserves morphine reinforcement. Biol. Psychiatry 69, 700–703.
Lesscher, H.M., Hordijk, M., Bondar, N.P., Alekseyenko, O.V., Burbach, J.P., van Ree, J.M., Gerrits, M.A., 2005. Mu-opioid receptors are not involved in acute cocaine-induced locomotor activity nor in development of cocaine-induced behavioral sensitization in mice. Neuropsychopharmacology 30, 278–285.
Li, C.H., Chung, D., 1976. Isolation and structure of an untriakontapeptide with opiate activity from camel pituitary glands. Proc. Natl. Acad. Sci. U. S. A. 73, 1145–1148.
Lichtman, A.H., Sheikh, S.M., Loh, H.H., Martin, B.R., 2001. Opioid and cannabinoid modulation of precipitated withdrawal in delta(9)-tetrahydrocannabinol and morphine-dependent mice. J. Pharmacol. Exp. Ther. 298, 1007–1014.
Loweth, J.A., Vezina, P., 2011. Sensitization. In: Olmstead, M.C. (Ed.), Animal Models of Drug Addiction. Humana Press, Saskatoon, SK, Canada, pp. 191–205.
Lutz, P.E., Kieffer, B.L., 2012. Opioid receptors: distinct roles in mood disorders. Trends Neurosci. 36, 195–206.
Lutz, P.E., Kieffer, B.L., 2013. The multiple facets of opioid receptor function: implications for addiction. Curr. Opin. Neurobiol. 23, 473–479.
Maldonado, R., Berrendero, F., Ozaita, A., Robledo, P., 2011. Neurochemical basis of cannabis addiction. Neuroscience 181, 1–17.
Maldonado, R., Blendy, J.A., Tzavara, E., Gass, P., Roques, B.P., Hanoune, J., Schutz, G., 1996. Reduction of morphine abstinence in mice with a mutation in the gene encoding CREB. Science 273, 657–659.
Manglik, A., Kruse, A.C., Kobilka, T.S., Thian, F.S., Mathiesen, J.M., Sunahara, R.K., Pardo, L., Weis, W.I., Kobilka, B.K., Granier, S., 2012. Crystal structure of the micro-opioid receptor bound to a morphinan antagonist. Nature 485, 321–326.
Mansour, A., Fox, C.A., Akil, H., Watson, S.J., 1995. Opioid-receptor mRNA expression in the rat CNS: anatomical and functional implications. Trends Neurosci. 18, 22–29.
Marquez, P., Baliram, R., Dabaja, I., Gajawada, N., Lutfy, K., 2008. The role of beta-endorphin in the acute motor stimulatory and rewarding actions of cocaine in mice. Psychopharmacology (Berl.) 197, 443–448.
Marquez, P., Baliram, R., Kieffer, B.L., Lutfy, K., 2007. The mu opioid receptor is involved in buprenorphine-induced locomotor stimulation and conditioned place preference. Neuropharmacology 52, 1336–1341.
Mathon, D.S., Lesscher, H.M., Gerrits, M.A., Kamal, A., Pintar, J.E., Schuller, A.G., Spruijt, B.M., Burbach, J.P., Smidt, M.P., van Ree, J.M., Ramakers, G.M., 2005. Increased gabaergic input to ventral tegmental area dopaminergic neurons associated with decreased cocaine reinforcement in mu-opioid receptor knockout mice. Neuroscience 130, 359–367.
Matthes, H.W., Maldonado, R., Simonin, F., Valverde, O., Slowe, S., Kitchen, I., Befort, K., Dierich, A., Le Meur, M., Dolle, P., Tzavara, E., Hanoune, J., Roques, B.P., Kieffer, B.L., 1996. Loss of morphine-induced analgesia, reward effect and withdrawal symptoms in mice lacking the mu-opioid-receptor gene. Nature 383, 819–823.
McGranahan, T.M., Patzlaff, N.E., Grady, S.R., Heinemann, S.F., Booker, T.K., 2011. alpha4beta2 nicotinic acetylcholine receptors on dopaminergic neurons mediate nicotine reward and anxiety relief. J. Neurosci. 31, 10891–10902.
McLaughlin, J.P., Land, B.B., Li, S., Pintar, J.E., Chavkin, C., 2006a. Prior activation of kappa opioid receptors by U50,488 mimics repeated forced swim stress to potentiate cocaine place preference conditioning. Neuropsychopharmacology 31, 787–794.
McLaughlin, J.P., Li, S., Valdez, J., Chavkin, T.A., Chavkin, C., 2006b. Social defeat stress-induced behavioral responses are mediated by the endogenous kappa opioid system. Neuropsychopharmacology 31, 1241–1248.
McLaughlin, J.P., Marton-Popovici, M., Chavkin, C., 2003. Kappa opioid receptor antagonism and prodynorphin gene disruption block stress-induced behavioral responses. J. Neurosci. 23, 5674–5683.
McPherson, C.S., Mantamadiotis, T., Tan, S.S., Lawrence, A.J., 2010. Deletion of CREB1 from the dorsal telencephalon reduces motivational properties of cocaine. Cereb. Cortex 20, 941–952.
Mendizabal, V., Zimmer, A., Maldonado, R., 2006. Involvement of kappa/dynorphin system in WIN 55,212-2 self-administration in mice. Neuropsychopharmacology 31, 1957–1966.
Mestek, A., Hurley, J.H., Bye, L.S., Campbell, A.D., Chen, Y., Tian, M., Liu, J., Schulman, H., Yu, L., 1995. The human mu opioid receptor: modulation of functional desensitization by calcium/calmodulin-dependent protein kinase and protein kinase C. J. Neurosci. 15, 2396–2406.
Mizoguchi, H., Watanabe, C., Osada, S., Yoshioka, M., Aoki, Y., Natsui, S., Yonezawa, A., Kanno, S., Ishikawa, M., Sakurada, T., Sakurada, S., 2010. Lack of a rewarding effect and a locomotor-enhancing effect of the selective mu-opioid receptor agonist amidino-TAPA. Psychopharmacology (Berl.) 212, 215–225.
Monory, K., Blaudzun, H., Massa, F., Kaiser, N., Lemberger, T., Schutz, G., Wotjak, C.T., Lutz, B., Marsicano, G., 2007. Genetic dissection of behavioural and autonomic effects of Delta(9)-tetrahydrocannabinol in mice. PLoS Biol. 5, e269.
Nagy, A., 2000. Cre recombinase: the universal reagent for genome tailoring. Genesis 26, 99–109.
Nakanishi, S., Inoue, A., Kita, T., Nakamura, M., Chang, A.C., Cohen, S.N., Numa, S., 1979. Nucleotide sequence of cloned cDNA for bovine corticotropin-beta-lipotropin precursor. Nature 278, 423–427.
Nestler, E.J., 2005. Is there a common molecular pathway for addiction? Nat. Neurosci. 8, 1445–1449.
Nestler, E.J., Hyman, S.E., 2010. Animal models of neuropsychiatric disorders. Nat. Neurosci. 13, 1161–1169.
Nguyen, A.T., Marquez, P., Hamid, A., Kieffer, B., Friedman, T.C., Lutfy, K., 2012a. The rewarding action of acute cocaine is reduced in beta-endorphin deficient but not in mu opioid receptor knockout mice. Eur. J. Pharmacol. 686, 50–54.
Nguyen, A.T., Marquez, P., Hamid, A., Lutfy, K., 2012b. The role of mu opioid receptors in psychomotor stimulation and conditioned place preference induced by morphine-6-glucuronide. Eur. J. Pharmacol. 682, 86–91.
Nguyen, K., Tseng, A., Marquez, P., Hamid, A., Lutfy, K., 2012c. The role of endogenous dynorphin in ethanol-induced state-dependent CPP. Behav. Brain Res. 227, 58–63.
Niikura, K., Narita, M., Okutsu, D., Tsurukawa, Y., Nanjo, K., Kurahashi, K., Kobayashi, Y., Suzuki, T., 2008. Implication of endogenous beta-endorphin in the inhibition of the morphine-induced rewarding effect by the direct activation of spinal protein kinase C in mice. Neurosci. Lett. 433, 54–58.
Nitsche, J.F., Schuller, A.G., King, M.A., Zengh, M., Pasternak, G.W., Pintar, J.E., 2002. Genetic dissociation of opiate tolerance and physical dependence in delta-opioid receptor-1 and preproenkephalin knock-out mice. J. Neurosci. 22, 10906–10913.
Noda, M., Furutani, Y., Takahashi, H., Toyosato, M., Hirose, T., Inayama, S., Nakanishi, S., Numa, S., 1982. Cloning and sequence analysis of cDNA for bovine adrenal preproenkephalin. Nature 295, 202–206.
O'Brien, C.P., Gardner, E.L., 2005. Critical assessment of how to study addiction and its treatment: human and non-human animal models. Pharmacol. Ther. 108, 18–58.
Pert, C.B., Snyder, S.H., 1973. Opiate receptor: demonstration in nervous tissue. Science 179, 1011–1014.
Pettinati, H.M., Rabinowitz, A.R., 2006. New pharmacotherapies for treating the neurobiology of alcohol and drug addiction. Psychiatry (Edgmont.) 3, 14–16.
Pierce, R.C., O'Brien, C.P., Kenny, P.J., Vanderschuren, L.J., 2012. Rational development of addiction pharmacotherapies: successes, failures, and prospects. Cold Spring Harb Perspect. Med. 2, a012880.
Pierce, R.C., Wolf, M.E., 2013. Psychostimulant-induced neuroadaptations in nucleus accumbens AMPA receptor transmission. Cold Spring Harb Perspect. Med. 3, a012021.
Portugal, G.S., Gould, T.J., 2008. Genetic variability in nicotinic acetylcholine receptors and nicotine addiction: converging evidence from human and animal research. Behav. Brain Res. 193, 1–16.
Potenza, M.N., Sofuoglu, M., Carroll, K.M., Rounsaville, B.J., 2011. Neuroscience of behavioral and pharmacological treatments for addictions. Neuron 69, 695–712.
Pradhan, A.A., Befort, K., Nozaki, C., Gaveriaux-Ruff, C., Kieffer, B.L., 2011. The delta opioid receptor: an evolving target for the treatment of brain disorders. Trends Pharmacol. Sci. 32, 581–590.
Puig, S., Noble, F., Benturquia, N., 2012. Short- and long-lasting behavioral and neurochemical adaptations: relationship with patterns of cocaine administration and expectation of drug effects in rats. Transl. Psychiatry 2, e175.

Racz, I., Markert, A., Mauer, D., Stoffel-Wagner, B., Zimmer, A., 2012. Long-term ethanol effects on acute stress responses: modulation by dynorphin. Addict. Biol 18, 678–688.
Racz, I., Schurmann, B., Karpushova, A., Reuter, M., Cichon, S., Montag, C., Furst, R., Schutz, C., Franke, P.E., Strohmaier, J., Wienker, T.F., Terenius, L., Osby, U., Gunnar, A., Maier, W., Bilkei-Gorzo, A., Nothen, M., Zimmer, A., 2008. The opioid peptides enkephalin and beta-endorphin in alcohol dependence. Biol. Psychiatry 64, 989–997.
Radwanska, K., Kaczmarek, L., 2011. Characterization of an alcohol addiction-prone phenotype in mice. Addict Biol. 17, 601–612.
Redila, V.A., Chavkin, C., 2008. Stress-induced reinstatement of cocaine seeking is mediated by the kappa opioid system. Psychopharmacology (Berl.) 200, 59–70.
Roberts, A.J., Gold, L.H., Polis, I., McDonald, J.S., Filliol, D., Kieffer, B.L., Koob, G.F., 2001. Increased ethanol self-administration in delta-opioid receptor knockout mice. Alcohol Clin. Exp. Res. 25, 1249–1256.
Roberts, A.J., McDonald, J.S., Heyser, C.J., Kieffer, B.L., Matthes, H.W., Koob, G.F., Gold, L.H., 2000. mu-Opioid receptor knockout mice do not self-administer alcohol. J. Pharmacol. Exp. Ther. 293, 1002–1008.
Robinson, T.E., Berridge, K.C., 2008. Review. The incentive sensitization theory of addiction: some current issues. Philos. Trans. R. Soc. Lond. B Biol. Sci. 363, 3137–3146.
Robledo, P., Mendizabal, V., Ortuno, J., de la Torre, R., Kieffer, B.L., Maldonado, R., 2004. The rewarding properties of MDMA are preserved in mice lacking mu-opioid receptors. Eur. J. Neurosci. 20, 853–858.
Roth-Deri, I., Green-Sadan, T., Yadid, G., 2008. Beta-endorphin and drug-induced reward and reinforcement. Prog. Neurobiol. 86, 1–21.
Sanchis-Segura, C., Spanagel, R., 2006. Behavioural assessment of drug reinforcement and addictive features in rodents: an overview. Addict Biol. 11, 2–38.
Sharpe, A.L., Low, M.J., 2009. Proopiomelanocortin peptides are not essential for development of ethanol-induced behavioral sensitization. Alcohol Clin. Exp. Res 33, 1202–1207.
Shen, X., Purser, C., Tien, L.T., Chiu, C.T., Paul, I.A., Baker, R., Loh, H.H., Ho, I.K., Ma, T., 2010. mu-Opioid receptor knockout mice are insensitive to methamphetamine-induced behavioral sensitization. J. Neurosci. Res. 88, 2294–2302.
Shippenberg, T.S., Zapata, A., Chefer, V.I., 2007. Dynorphin and the pathophysiology of drug addiction. Pharmacol. Ther. 116, 306–321.
Shoblock, J.R., Maidment, N.T., 2007. Enkephalin release promotes homeostatic increases in constitutively active mu opioid receptors during morphine withdrawal. Neuroscience 149, 642–649.
Simon, E.J., Hiller, J.M., Edelman, I., 1973. Stereospecific binding of the potent narcotic analgesic (3H) etorphine to rat-brain homogenate. Proc. Natl. Acad. Sci. U. S. A. 70, 1947–1949.
Simonin, F., Befort, K., Gaveriaux-Ruff, C., Matthes, H., Nappey, V., Lannes, B., Micheletti, G., Kieffer, B., 1994. The human delta-opioid receptor: genomic organization, cDNA cloning, functional expression, and distribution in human brain. Mol. Pharmacol. 46, 1015–1021.
Simonin, F., Gaveriaux-Ruff, C., Befort, K., Matthes, H., Lannes, B., Micheletti, G., Mattei, M.G., Charron, G., Bloch, B., Kieffer, B., 1995. kappa-Opioid receptor in humans: cDNA and genomic cloning, chromosomal assignment, functional expression, pharmacology, and expression pattern in the central nervous system. Proc. Natl. Acad. Sci. U. S. A. 92, 7006–7010.
Simonin, F., Valverde, O., Smadja, C., Slowe, S., Kitchen, I., Dierich, A., Le Meur, M., Roques, B.P., Maldonado, R., Kieffer, B.L., 1998. Disruption of the kappa-opioid receptor gene in mice enhances sensitivity to chemical visceral pain, impairs pharmacological actions of the selective kappa-agonist U-50,488H and attenuates morphine withdrawal. EMBO J. 17, 886–897.
Skoubis, P.D., Lam, H.A., Shoblock, J., Narayanan, S., Maidment, N.T., 2005. Endogenous enkephalins, not endorphins, modulate basal hedonic state in mice. Eur. J. Neurosci. 21, 1379–1384.
Solinas, M., Goldberg, S.R., Piomelli, D., 2008. The endocannabinoid system in brain reward processes. Br. J. Pharmacol. 154, 369–383.
Sora, I., Elmer, G., Funada, M., Pieper, J., Li, X.F., Hall, F.S., Uhl, G.R., 2001. Mu opiate receptor gene dose effects on different morphine actions: evidence for differential in vivo mu receptor reserve. Neuropsychopharmacology 25, 41–54.
Spanagel, R., 2003. Alcohol addiction research: from animal models to clinics. Best Pract. Res. Clin. Gastroenterol. 17, 507–518.
Spanagel, R., Herz, A., Shippenberg, T.S., 1992. Opposing tonically active endogenous opioid systems modulate the mesolimbic dopaminergic pathway. Proc. Natl. Acad. Sci. U. S. A. 89, 2046–2050.
Sperling, R.E., Gomes, S.M., Sypek, E.I., Carey, A.N., McLaughlin, J.P., 2010. Endogenous kappa-opioid mediation of stress-induced potentiation of ethanol-conditioned place preference and self-administration. Psychopharmacology (Berl.) 210, 199–209.
Stewart, A., Wong, K., Cachat, J., Gaikwad, S., Kyzar, E., Wu, N., Hart, P., Piet, V., Utterback, E., Elegante, M., Tien, D., Kalueff, A.V., 2011. Zebrafish models to study drug abuse-related phenotypes. Rev. Neurosci. 22, 95–105.
Stockton Jr., S.D., Devi, L.A., 2012. Functional relevance of mu-delta opioid receptor heteromerization: a role in novel signaling and implications for the treatment of addiction disorders: from a symposium on new concepts in mu-opioid pharmacology. Drug Alcohol Depend. 121, 167–172.
Terenius, L., 1973. Characteristics of the "receptor" for narcotic analgesics in synaptic plasma membrane fraction from rat brain. Acta Pharmacol. Toxicol. (Copenh.) 33, 377–384.
Tian, M., Broxmeyer, H.E., Fan, Y., Lai, Z., Zhang, S., Aronica, S., Cooper, S., Bigsby, R.M., Steinmetz, R., Engle, S.J., Mestek, A., Pollock, J.D., Lehman, M.N., Jansen, H.T., Ying, M., Stambrook, P.J., Tischfield, J.A., Yu, L., 1997. Altered hematopoiesis, behavior, and sexual function in mu opioid receptor-deficient mice. J. Exp. Med 185, 1517–1522.
Trigo, J.M., Martin-Garcia, E., Berrendero, F., Robledo, P., Maldonado, R., 2010. The endogenous opioid system: a common substrate in drug addiction. Drug Alcohol Depend 108, 183–194.
Trigo, J.M., Zimmer, A., Maldonado, R., 2009. Nicotine anxiogenic and rewarding effects are decreased in mice lacking beta-endorphin. Neuropharmacology 56, 1147–1153.
Tsai, H.C., Zhang, F., Adamantidis, A., Stuber, G.D., Bonci, A., de Lecea, L., Deisseroth, K., 2009. Phasic firing in dopaminergic neurons is sufficient for behavioral conditioning. Science 324, 1080–1084.
Tuesta, L.M., Fowler, C.D., Kenny, P.J., 2011. Recent advances in understanding nicotinic receptor signaling mechanisms that regulate drug self-administration behavior. Biochem. Pharmacol. 82, 984–995.
Tzschentke, T.M., 2007. Measuring reward with the conditioned place preference (CPP) paradigm: update of the last decade. Addict Biol. 12, 227–462.
Valverde, O., Maldonado, R., Valjent, E., Zimmer, A.M., Zimmer, A., 2000. Cannabinoid withdrawal syndrome is reduced in pre-proenkephalin knock-out mice. J. Neurosci. 20, 9284–9289.
van Rijn, R.M., Brissett, D.I., Whistler, J.L., 2010. Dual efficacy of delta opioid receptor-selective ligands for ethanol drinking and anxiety. J. Pharmacol. Exp. Ther. 335, 133–139.
van Rijn, R.M., Whistler, J.L., 2009. The delta(1) opioid receptor is a heterodimer that opposes the actions of the delta(2) receptor on alcohol intake. Biol. Psychiatry 66, 777–784.
Vanderschuren, L.J., Pierce, R.C., 2010. Sensitization processes in drug addiction. Curr. Top. Behav. Neurosci. 3, 179–195.
Vigano, D., Rubino, T., Parolaro, D., 2005. Molecular and cellular basis of cannabinoid and opioid interactions. Pharmacol. Biochem. Behav. 81, 360–368.
Volkow, N.D., Skolnick, P., 2012. New medications for substance use disorders: challenges and opportunities. Neuropsychopharmacology 37, 290–292.
Walters, C.L., Cleck, J.N., Kuo, Y.C., Blendy, J.A., 2005. Mu-opioid receptor and CREB activation are required for nicotine reward. Neuron 46, 933–943.
Wang, L.P., Li, F., Shen, X., Tsien, J.Z., 2010. Conditional knockout of NMDA receptors in dopamine neurons prevents nicotine-conditioned place preference. PLoS One 5, e8616.
Wee, S., Koob, G.F., 2010. The role of the dynorphin-kappa opioid system in the reinforcing effects of drugs of abuse. Psychopharmacology (Berl.) 210, 121–135.
Witten, I.B., Lin, S.C., Brodsky, M., Prakash, R., Diester, I., Anikeeva, P., Gradinaru, V., Ramakrishnan, C., Deisseroth, K., 2010. Cholinergic interneurons control local circuit activity and cocaine conditioning. Science 330, 1677–1681.
Woolf, C.J., 2011. What is this thing called pain? J. Clin. Invest. 120, 3742–3744.
Wu, H., Wacker, D., Mileni, M., Katritch, V., Han, G.W., Vardy, E., Liu, W., Thompson, A.A., Huang, X.P., Carroll, F.I., Mascarella, S.W., Westkaemper, R.B., Mosier, P.D., Roth, B.L., Cherezov, V., Stevens, R.C., 2012. Structure of the human kappa-opioid receptor in complex with JDTic. Nature 485, 327–332.
Yoo, J.H., Cho, J.H., Lee, S.Y., Lee, S., Loh, H.H., Ho, I.K., Jang, C.G., 2006. Differential effects of morphine- and cocaine-induced nNOS immunoreactivity in the dentate gyrus of hippocampus of mice lacking mu-opioid receptors. Neurosci. Lett. 395, 98–102.
Yoo, J.H., Cho, J.H., Lee, S.Y., Loh, H.H., Ho, I.K., Jang, C.G., 2005. Reduced nNOS expression induced by repeated nicotine treatment in mu-opioid receptor knockout mice. Neurosci. Lett. 380, 70–74.
Yoo, J.H., Kitchen, I., Bailey, A., 2012. The endogenous opioid system in cocaine addiction: what lessons have opioid peptide and receptor knockout mice taught us? Br. J. Pharmacol. 166, 1993–2014.
Yoo, J.H., Lee, S.Y., Loh, H.H., Ho, I.K., Jang, C.G., 2004. Loss of nicotine-induced behavioral sensitization in micro-opioid receptor knockout mice. Synapse 51, 219–223.
Yoo, J.H., Yang, E.M., Lee, S.Y., Loh, H.H., Ho, I.K., Jang, C.G., 2003. Differential effects of morphine and cocaine on locomotor activity and sensitization in mu-opioid receptor knockout mice. Neurosci. Lett. 344, 37–40.
Zhao, Z.Q., Gao, Y.J., Sun, Y.G., Zhao, C.S., Gereau, R.W.T., Chen, Z.F., 2007. Central serotonergic neurons are differentially required for opioid analgesia but not for morphine tolerance or morphine reward. Proc. Natl. Acad. Sci. U. S. A. 104, 14519–14524.
Zimmer, A., Valjent, E., Konig, M., Zimmer, A.M., Robledo, P., Hahn, H., Valverde, O., Maldonado, R., 2001. Absence of delta-9-tetrahydrocannabinol dysphoric effects in dynorphin-deficient mice. J. Neurosci. 21, 9499–9505.

PART I

Opiate addiction and analgesia in Dlx-mu mice

Introduction

I. Mu receptor in GABAergic forebrain neurons

The mu receptor is highly present in the limbic structures such as the NAc, prefrontral cortex (PFC), amygdala, VP, hippocampus and the VTA, and mostly in GABAergic neurons. The first evidence was claimed in 1990 by Austin and Kalivas. Motor stimulation induced by the mu receptor agonist DAMGO was attenuated by intra-ventral pallidum GABA-A agonist muscimol pretreatment (Austin and Kalivas, 1990), indicating that mu receptor agonists could act by inhibiting GABAergic transmission within this brain structure. Since then, evidence has been growing for mu receptor expression in GABAergic neurons in many different regions. Mu receptors have been shown to be located in GABAergic interneurons within the VTA (Johnson and North, 1992; Kudo et al., 2014; Lowe and Bailey, 2014), as well as the RMTg (Lecca et al., 2012; Matsui and Williams, 2011), the BNST (Kudo et al., 2014), the VP (Kupchik et al., 2014), and the striatum (Miura et al., 2007).

II. Dlx5/6-Cre mouse line

Dlx is a group of genes from Homeobox gene superclass (Holland, 2013). *Dlx* genes are expressed/implicated in/ during mouse forebrain development. Studies have revealed that the *Dlx* genes are required for the differentiation and migration of most telencephalon and diencephalon GABAergic neurons. In the mouse forebrain, *Dlx5* and *Dlx6* genes are expressed starting around embryonic day 9.5 (Yu et al., 2011). The mouse and zebrafish *Dlx* genes share highly overlapping expression within the forebrain which mostly correlates with Gad (glutamic acid decarboxylase) expression (MacDonald et al., 2013). In these two developing animals, *Dlx5/Dlx6* (corresponding to *dlx5a/dlx6a* in the zebrafish) expression is modulated by the *cis*-regulatory elements (enhancers) I56i and I56ii) that are present within the intergenic region (Yu et al., 2011). To drive excision of the mu receptor gene in GABAergic forebrain neurons, we created a conditional mouse line where the Cre recombinase is under the Dlx5/6 promoter. This Cre recombinase driver was previously used to successfully delete the cannabinoid receptor 1 (CB1)(Monory et al., 2006) and the delta opioid receptor in forebrain GABAergic neurons (Chu Sin Chung et al., 2015).

III. Aim of the chapter

The first aim of my thesis was to investigate the role of mu opioid receptors expressed in GABAergic forebrain neurons in opioid effects, using Dlx-mu mice. I characterized the anatomical distribution of the mu receptor mRNA in this mouse model. The protein distribution was conducted by Helen Keyworth from Pr. Kitchen laboratory, University of Surrey, Guilford, UK. I examined classical opiate responses in those mutant mice, including analgesic properties, physical dependence, motor effects, conditioned place preference and cellular responses (neuronal activation). Motivation to get heroin and chocolate experiments were performed by Elena Martín-García from Pr. Maldonado laboratory, PRBB, Barcelona, Spain. Electrophysiological recordings were done in collaboration with Aya Matsui, from Dr. Alvarez laboratory, NIH, Bethesda, USA. This work is presented in the form of a manuscript in the following section: *Mu opioid receptors in GABAergic forebrain neurons are necessary for heroin hyperlocomotion and reduce motivation for heroin and palatable food*. Charbogne P, Gardon O, Martín-García E, Keyworth H, Matsui A, Matifas A, Befort K, Kitchen I, Bailey A, Alvarez VA, Maldonado R, Kieffer BL.

Manuscript 1

Mu opioid receptors in GABAergic forebrain neurons are necessary for heroin hyperlocomotion and reduce motivation for heroin and palatable food

Pauline Charbogne[1,2], Olivier Gardon[1], Elena Martín-García[3], Helen L. Keyworth[4], Aya Matsui[5], Audrey Matifas[1], Katia Befort[6], Ian Kitchen[4], Alexis Bailey[4], Veronica A. Alvarez[5], Rafael Maldonado[3], Brigitte L. Kieffer[1,2*].

[1] Institut de Génétique et de Biologie Moléculaire et Cellulaire, CNRS/INSERM/Université de Strasbourg, 1 rue Laurent Fries, 67404 Illkirch, France

[2] Douglas Mental Health Institute, Department of Psychiatry, McGill University, 6875 boulevard LaSalle, H4H 1R3 Montreal, QC, Canada

[3] Departament de Ciencies Experimentals i de la Salut, Universitat Pompeu Fabra, PRBB, C/Dr. Aiguader 88, 08003 Barcelona, Spain

[4] Faculty of Health and Medical Sciences, AY Building, University of Surrey, Guildford, Surrey GU2 7XH, UK

[5] Section on Neuronal Structure, National Institute on Alcohol Abuse and Alcoholism, National Institute of Health, Bethesda, MD, USA

[6] CNRS, Laboratoire de Neurosciences Cognitives et Adaptatives – UMR7364, Faculté de Psychologie, Neuropôle de Strasbourg – Université de Strasbourg, Strasbourg, France

* Corresponding author. Douglas Mental Health Institute, Department of Psychiatry, McGill University, 6875 boulevard LaSalle, H4H 1R3 Montreal, QC, Canada

Phone: 514 761-6131 ext.: 3175; fax: 514 762-3033

brigitte.kieffer@douglas.mcgill.ca

ABSTRACT

BACKGROUND: Mu opioid receptors are broadly expressed throughout the nervous system and are key players in pain control, as well as reward and motivation. Neural circuits underlying mu receptor effects have been poorly explored by genetic approaches. Here we used conditional knockout of the *Oprm1* gene to determine whether mu receptors expressed in GABAergic neurons of the forebrain are essential to these processes.

METHODS: We characterized mu receptor expression in the brain of Dlx5/6-Cre X *Oprm1*$^{fl/fl}$ (Dlx-mu) mice and examined behavioral responses to major opiate effects. We also examined c-Fos activation at the level of mesolimbic circuits and electrophysiological responses to mu agonists in VTA slices of mutant mice.

RESULTS: In Dlx-mu mice, *Oprm1* mRNA expression was strongly decreased in the forebrain, particularly in striatum and amygdala, but remained intact in midbrain and hindbrain including notably the ventral tegmental area. Morphine-induced analgesia and physical dependence were maintained, but heroin-induced locomotor activation was abolished in mutant mice, concomitant with enhanced heroin-induced catalepsy. Intriguingly, Dlx-mu mice showed increased motivation to self-administer heroin and palatable food. Conditioned place preference to morphine and heroin was otherwise indistinguishable from controls. c-Fos induction after acute heroin was modified at the level of the entire dopaminergic mesolimbic circuit, and electrophysiological recordings showed lack of DAMGO-induced eIPSCs in VTA GABA neurons, concordant with the lack of mu receptor expression in the striatum of Dlx-mu animals.

CONCLUSIONS: We demonstrate that mu receptors expressed in GABAergic neurons of the forebrain play key but distinct roles on locomotor and motivational effects of heroin. While mediating heroin-induced locomotor stimulation, this particular receptor population exerts an inhibitory activity on drug and food self-administration. This study, therefore, reveals for the first time a specific mu opioid receptor subpopulation, whose activity opposes the well-established facilitating function of the receptor on motivational processes.

Keywords: conditional gene knockout, mu opioid receptor, GABAergic forebrain neurons, analgesia, locomotion, catalepsy, reward, motivation.

INTRODUCTION

Mu opioid receptors mediate all the biological effects of morphine (Matthes et al., 1996) and heroin (Contarino et al., 2002; Kitanaka et al., 1998), notably their strong analgesic and addictive properties. These receptors are therefore major therapeutic targets for the treatment of severe pain, and also contribute to recreational drug use, as well as rewarding effects of natural stimuli including social interactions (Becker et al., 2014; Moles et al., 2004).

Mu receptors are broadly expressed in both central and peripheral nervous systems (see Erbs et al., 2014; Kitchen et al., 1997), and therefore regulate nociceptive pathways and reward processing at multiple sites. Within mesolimbic circuits for example (reviewed in Le Merrer et al., 2009), local pharmacological mu opioid receptor blockade at the level of the nucleus accumbens (NAc) reduces hedonic, motivational and reinforcing values of food (Castro and Berridge, 2014; Katsuura and Taha, 2014; Shin et al., 2010), and also positively regulate food reward and intake in the basolateral amygdala (BLA), ventral pallidum (VP) and ventral tegmental area (VTA) (Echo et al., 2002; Taha et al., 2009; Wassum et al., 2011). Further, mu receptor activation in the VP suppresses ethanol self-administration (Kemppainen et al., 2012) while receptor blockade in the VP inhibited induction and expression of opiate-induced behavioral sensitization (Mickiewicz et al., 2009). Intra-VTA and intra-rostromedial tegmental nucleus (RMTg) application of mu agonists elicits reward and motivation (David et al., 2008; Jhou et al., 2012), and mu receptor blockade in the NAc decreases cocaine reward (Soderman and Unterwald, 2008).

At present, brain sites where mu receptors mediate *in vivo* opioid effects, or regulate behavior, have been mostly examined by local pharmacological manipulations, and little is known about cellular bases of underlying circuit mechanisms. Conditional gene knockout in specific neuron populations represents a most suitable approach to this goal. We previously targeted mu receptors expressed in Nav1.8-positive primary afferent neurons, and demonstrated that these peripheral mu receptors mediate morphine analgesia under conditions of inflammatory pain only (Weibel et al., 2013). Here, we targeted central mu receptors expressed in forebrain GABAergic neurons, and examined morphine and heroin effects with a particular focus on rewarding, motivational and locomotor responses.

METHODS AND MATERIALS

Animals

Mu floxed mouse line (*Oprm1*$^{fl/fl}$) has been previously described by our group (Weibel et al., 2013). Briefly, exons 2 and 3 of mu receptor gene *Oprm1* are flanked by loxP sites. *Oprm1*$^{fl/fl}$ mice show intact mu receptor expression (Weibel et al., 2013). To generate a conditional knockout for *Oprm1* in GABAergic forebrain neurons, the Dlx5/6-Cre-*Oprm1*$^{-/-}$ mouse line was created in our vivarium (Institut Clinique de la Souris - Institut de Génétique et de Biologie Moléculaire et Cellulaire, Illkirch, France) by breeding the Dlx5/6-Cre mice (obtained from Beat Lutz laboratory, Institute of Physiological Chemistry, Johannes Gutenberg University, Germany) with mu floxed mice. Dlx5/6-Cre line was successfully used in previous studies to conditionally invalidate cannabinoid CB1 receptors (Monory et al., 2006) and delta opioid receptors (Chu Sin Chung et al., 2015). Resulting Cre positive (Cre(+), Dlx5/6-Cre-*Oprm1*$^{-/-}$) animals are called Dlx-mu, and Cre negative animals (Cre(-), *Oprm1*$^{fl/fl}$) are Controls. Dlx-mu and littermates controls have the same genetic background (63% C57BL/6J-37% 129SvPas).

CMV-Cre-*Oprm1*$^{-/-}$ (CMV-mu) mice were used as total knockout for the mu receptor gene, by breeding mu floxed mice with CMV-Cre mice, expressing the Cre recombinase under the control of the cytomegalovirus (CMV, ubiquitous) promoter (Metzger and Chambon, 2001). This line has a 75% C57BL/6J-25% 129SvPas background. In locomotor activity experiments, we also tested mu opioid receptor knockout (KO) and their controls (named wild type, WT), previously described in (Matthes et al., 1996). The latter mutants have a different genetic background (50% C57BL/6J-50% 129SvPas) compared to Dlx-mu and Controls (63% C57BL/6J-37% 129SvPas).

All experiments were carried out according to the recommendations of the IASP (Zimmermann, 1983) and the European Communities Council Directive of September 22, 2010 (directive 2010/63/UE). The study protocols were approved by the local bioethics committee (Comité d'Éthique pour l'Expérimentation Animale, Institut Clinique de la Souris - Institut de Génétique et de Biologie Moléculaire et Cellulaire, Illkirch, France). Experiments were performed on male and female mice 8/20-week old at the beginning of the study, habituated to the experimental environment and handled for 2 days before behavioral testing. Experimental room light was set at 15 lux. All behavioral testing was performed with the observer blind to the genotype or treatment. All animals were housed in a room maintained at 21±2°C and 45±5% humidity, with a 12h light-dark cycle (lights on at 7:00 AM). Food and water were available *ad libitum*. For self-administration procedures, all experiments were carried out with 8/18-week old males and only males were used. Mice were housed individually in controlled

laboratory conditions with the temperature maintained at 21±1 ºC and humidity at 55±10%. Mice were tested during the first hours of the dark phase of a reversed light/dark cycle (lights off at 8.00 h and on at 20.00 h). For experiments of operant conditioning maintained by chocolate, mice were food-deprived (85 % of the initial weight) and water was available *ad libitum*. Animal procedures were conducted in strict accordance with the guidelines of the European Communities Directive 86/609/EEC regulating animal research and were approved by the local ethical committee (CEEA-PRBB, Barcelona, Spain).

Treatments

The mu agonists morphine (hydrochloride, Francopia, Cepia Sanofi, France) and heroin (diacetylmorphine hydrochloride, kindly provided by Francopia, Cepia Sanofi, France), the opioid antagonist naloxone (hydrochloride, Sigma-Aldrich, St Louis, USA), and the catecholamine-releasing molecule amphetamine (D-amphetamine hemisulfate, A-5880, Sigma-Aldrich, St Louis, USA) were used in the present study. For analgesia, physical dependence, locomotion, catalepsy, and c-Fos immunoreactivity tests, compounds were intraperitoneally (i.p.) injected. Naloxone in withdrawal procedure was injected subcutaneously (s.c.). For conditioned place preference (CPP) experiments, morphine and heroin were administrated s.c. In the heroin self-administration procedure, the solution was delivered by an intravenous catheter (i.v.). All the pharmacological substances were dissolved in NaCl 0.9% and administered in a 10 mL/kg volume.

Genotyping-PCR

PCR analysis on genomic DNA were performed in order to genotype the mice for presence of 1) Cre recombinase, 2) loxP sites and 3) excision of *Oprm1*. PCR was achieved on DNA from mouse digested digit sample (NaCl 0.2M; Tris-HCl 100 mM pH8.5; EDTA 5mM; SDS 0.2%; proteinase K (Sigma) 10 mg/mL; overnight at 55°C).

The Cre PCR reaction was performed by adding 0.5 µL lysate to 49.5 µL reaction mix (1X PCR buffer (Sigma); $MgCl_2$ (Sigma) 2.5 mM; dNTPs 0.2 mM (Thermo Scientific); TAQ DNA polymerase 2.5 U (Sigma); forward *Cre* primer (5'-GAT CGC TGC CAG GAT ATA CG-3'), reverse *Cre* primer (5'-CAT CGC CAT CTT CCA GCA G-3'), forward *myosin* gene primer (5'-TTA CGT CCA TCG TGG ACA GC-3'), reverse *myosin* gene primer (5'-TGG GCT GGG TGT TAG CCT TA-3') 0.5 µM). PCR reaction was performed with temperature cycling parameters consisting of initial denaturation at 94°C for 5 min followed by 30 cycles of denaturation at 94°C for 1 min, annealing at 62°C for 1 min, extension at 72°C for 1 min, and a final incubation at 72°C for 10 min.

The loxP sites PCR reaction was performed by adding 0.5 µL lysate to 49.5 µL reaction mix (1X PCR buffer GoTaq (Promega); $MgCl_2$ (Sigma) 1 mM; dNTPs 0.4 mM (Thermo Scientific); TAQ DNA polymerase 2.5 U (Promega); forward *mu floxed* gene primer (5'-GTT ACT GGA GAA TCC AGG CCA AGC-3'), reverse *mu floxed* gene primer (5'-TGC TAG AAC CTG CGG AGC CAC A-3') 1 µM). PCR reaction was performed with temperature cycling parameters consisting of initial denaturation at 94°C for 5 min followed by 30 cycles of denaturation at 95°C for 1 min, annealing at 60°C for 1 min, extension at 72°C for 1 min, and a final incubation at 72°C for 10 min.

The mu excision PCR reaction was performed by adding 0.2 µL lysate to 49.8 µL reaction mix (1X PCR buffer (Sigma); $MgCl_2$ (Sigma) 2.5 mM; dNTPs 0.2 mM (Thermo Scientific); TAQ DNA polymerase 2.5 U (Sigma); forward excision primer (5'-ACC AGT ACA TGG ACT GGA TGT GCC-3'), reverse excision primer (5'-GAG ACA AGG CTC TGA GGA TAG TAA C-3'), forward *myosin* gene primer (5'-TTA CGT CCA TCG TGG ACA GC-3'), reverse *myosin* gene primer (5'-TGG GCT GGG TGT TAG CCT TA-3') 0.5 µM). PCR reaction was performed with temperature cycling parameters consisting of initial denaturation at 94°C for 5 min followed by 35 cycles of denaturation at 94°C for 30 sec, annealing at 61°C for 30sec, extension at 72°C for 30 sec, and a final incubation at 72°C for 10 min.

Tissue collection for mRNA analysis

Mice were sacrificed by cervical dislocation. Brains were extracted, rinsed in cold 1X PBS (phosphate-buffered saline solution, Sigma) and 1-mm thick slices were cut with a stainless steel coronal brain matrix chilled on ice (Harvard apparatus, Holliston, MA, USA). Different brain regions were collected from 3 to 5 mice per genotype and treatment according to the stereotaxic atlas of mouse brain (Paxinos and Franklin, 2001). The caudate putamen (CPu) was bilaterally punched using a 2-mm diameter tissue corer; NAc, VTA, amygdala, lateral hypothalamus (LH) were bilaterally punched with a 1.2-mm tissue corer; prefrontal cortex (PCF) and periacqueducal grey (PAG) were centrally punched using a 2-mm diameter tissue corer; habenula (Hb) and dorsal raphe nucleus (DRN) were centrally punched using a 1.2-mm diameter tissue corer; and the hippocampus and spinal cord were dissected. Samples were immediately frozen on dry ice and kept at -80°C until processing.

Quantitative real-time PCR

Samples were processed to extract total RNA, using TRIzol reagent (Invitrogen, Cergy Pontoise, France) according to manufacturer's instructions. The quality and quantity of RNA was measured with ND-1000 NanoDrop (Thermo Fisher Scientific, Wilmington, USA) spectrophotometer. Reverse

transcription of 800 ng to 1 µg total RNA was performed on bilateral pooled brain samples in triplicate, in a 20 µL final volume, with Superscript II kit (Superscript II RT, Invitrogen). Real-time PCR was performed on the resulting cDNA using a Light Cycler 480 apparatus (Roche, Meylan, France) and iQ SYBR Green supermix (Biorad, Marnes-la-Coquette, France). Primers sequences were: CCGAAATGCCAAAATTGTCA (*Oprm1* forward), GGACCCCTGCCTGTATTTTGT (*Oprm1* reverse), GACGGCCAGGTCATCACTAT (*ß-actin* forward), CCACCGATCCACACAGAGTA (*ß-actin* reverse), TGAGATTCGGGATATGCTGTTG (*arbp* gene "36B4" forward), TTCAATGGTGCCTCTGGAGAT (*arbp* gene "36B4" reverse), TGACACTGGTAAAACAATGCA (*HPRT* forward), GGTCCTTTTCACCAGCAAGCT (*HPRT* reverse), GTCTCCCAGATCGGGCATTT (*drd1* forward), TTCTGGGTTCAGTGCTCCAG (*drd1* reverse), ATCGTCTCGTTCTACGTGCC (*drd2* forward), GTGGGTACAGTTGCCCTTGA (*drd2* reverse), GCTCGTCATGTTTGGCATC (*Oprd1* forward), AAGTACTTGGCGCTCTGGAA (*Oprd1* reverse), TCCTTGGAGGCACCAAAGTCAG (*Oprk1* forward), TGGTGATGCGGCGGAGATTTCG (*Oprk1* reverse), ATGCCGAGATTCTGCTACAGT (*pomc* forward), TCCAGCGAGAGGTCGAGTTT (*pomc* reverse), CGACATCAATTTCCTGGCGT (*penk* forward), AGATCCTTGCAGGTCTCCCA (*penk* reverse), ATGATGAGACGCCATCCTTC (*pdyn* forward), TTAATGAGGGCTGTGGGAAC (*pdyn* reverse). Thermal cycling parameters were 1 min at 95°C followed by 40 amplification cycles of 15 sec at 95°C, 15 sec at 60°C and 30 sec at 72°C. Expression levels were normalized to *ß-actin* housekeeping gene levels. Two reference genes (*HPRT*, *arbp*) were tested in each run as an internal control. The $2^{-\Delta\Delta Ct}$ method was used to evaluate differential expression levels (Livak and Schmittgen, 2001) of Control, Dlx-mu and CMV-mu mice. Control Cre(-) (*Oprm1*$^{fl/fl}$) animals were used as baseline to normalize. A first cohort of Control, Dlx-mu and CMV-mu mice was used to study the mu receptor mRNA distribution in a large range of regions; a second cohort, composed of Control and Dlx-mu mice, was used to investigate opioid system and dopamine receptors mRNA modifications in the NAc and CPu.

Autoradiography binding assay

Following decapitation, intact brains were removed, snap frozen at -20°C in isopentane and then stored at -80°C until sectioned. Adjacent sections were cut from control, Dlx-mu and constitutive KO brains for determination of total binding for mu receptors using [^{3}H]DAMGO (D-Ala^2-MePhe^4-Gly-ol^5 enkephalin). Brains were sectioned in a cryostat (Zeiss Hyrax C 25, Carl Zeiss MicroImaging GmbH, Germany), with an internal temperature of -21°C. 20 µm coronal sections were cut at 300 µm intervals, from rostral to caudal levels, and thaw-mounted onto gelatine coated ice-cold microscope slides and processed for autoradiography. Adjacent sections were cut for determination of total and non-specific

(NSB) binding. Sections were stored at -20°C prior to radioligand binding. Mu receptor binding was carried out as described previously (Slowe et al., 1999) with minor modifications.

For mu receptor binding, slides were pre-incubated for 30 mins in 50 mM Tris-HCl pre-incubation buffer, containing 0.9% w/v NaCl, pH 7.4 at room temperature. The slides were then incubated in 50 mM Tris-HCl buffer, pH 7.4 at room temperature in the presence of 4 nM [3H]DAMGO (specific activity 51.5 Ci/mmol) for 60 mins. Non-specific binding (NSB) was determined in adjacent sections in the presence of 1 µM naloxone. Incubation was terminated by rapid rinses (3 x 5 mins) in ice-cold 50 mM Tris-HCl buffer, pH 7.4 at room temperature and distilled water (3 x 5 mins), then rapidly cool-air dried.

Following binding, sections were rapidly dried under cold air for 2 hours, and dried for up to 7 days using anhydrous calcium sulphate (BDH Chemicals, Poole, UK). Adjacent total and non-specific labelled sections were apposed to Kodak BioMax MR-1 film alongside autoradiographic microscale standards of known concentration. [^{125}I]epibatidine and [^{125}I]α-bungarotoxin bound sections were exposed to film for 24 hours and 7 days, respectively, with a set of ^{14}C microscale standards which had been cross-calibrated to iodinated standards (Baskin and Wimpy, 1989; Miller and Zahniser, 1987). [^{3}H]-bound sections were exposed to film with ^{3}H microscale standards for a period of 10 weeks.

For development, films were covered with an aqueous solution of 50 % v/v Kodak D19 developer for 3 mins. The reaction was stopped by 1 min rinse in distilled water containing a drop of glacial acetic acid. Images were fixed by submersion in Kodak rapid fix solution for 5 mins. Films were then rinsed in distilled water and dried overnight in a fume cupboard.

Films were analysed by video-based densiometry using an MCID image analyser (Imaging Research, Canada) as previously described (Kitchen et al., 1997). In brief, fmol/mg tissue equivalents for receptor binding were derived from either ^{3}H or ^{14}C microscale standards, and the relationship between tissue radioactivity and optical density was calculated using MCID software, with appropriate adjustments to allow for radioactive decay of both the standards and the radioligands. Specific receptor binding was derived by subtraction of NSB from total binding for mu receptors.

For each region quantified measures were taken from both left and right hemispheres, therefore receptor binding represents a duplicate determination for each brain region and the *n* values listed refer to the number of animals analysed. The following structures were analysed by sampling 5 – 20 times with a box tool: cortex (8 x 8 mm), olfactory tubercle (6 x 6 mm) and hippocampus (5 x 5 mm). All other regions were analysed by free-hand drawing. Brain structures were identified by reference to the mouse atlas of Franklin and Paxinos (Paxinos and Franklin, 2001).

Electrophysiological recordings

All procedures were performed in accordance with the guidelines of National Institute on Alcohol Abuse and Alcoholism and the Animal Care and Use Committees approved all of the experimental procedures.

Dlx-mu mice and littermate controls were anesthetized with isoflurane and transcardially perfused with ice-cold artificial cerebrospinal fluid (aCSF) containing the following (in mM): 124 NaCl, 2.5 KCl, 1.3 MgCl2, 2.5 CaCl2, 1.0 NaH2PO4, 26.2 NaHCO3, 20 D-glucose, 0.4 Ascorbate and 3 Kynurenic Acid. Brains were removed and placed in a vibratome (Leica). Sagittal slices (220-230 µm) were prepared in ice-cold aCSF. Slices were incubated in warm (33°C) 95%O2/5%CO2 oxygenated aCSF containing Kyrurenic acid (3 mM) for 30 min and moved to room temperature (22-24°C) in aCSF with kyrurenic acid until used. Slices containing midbrain were then transferred to the recording chamber that was constantly perfused with oxygenated aCSF 33°C 95%O2/5%CO2 at the rate of 1.5-2 mL/min. Midbrain neurons were visualized with a 40x water-immersion objective on an upright fluorescent microscope (BX51WI, Olympus USA) equipped with gradient contrast infrared optics. Whole-cell voltage clamp recording was performed from dopamine and GABA neurons in VTA using an Axopatch-200B amplifier (Molecular Devices). Physiological identification of dopamine neurons was based on the presence of D2-autoreceptor-mediated GIRK currents and the rate of spontaneous action potential activity (1-5 Hz) with spike widths ≥1.2 ms (Chieng et al., 2011; Ford et al., 2006; Li et al., 2012; Ungless et al., 2004). Identification of GABA neurons was based on the absence of D2-autoreceptor mediated GIRK current, and the range of spontaneous action potential activity (>10 Hz) with spike widths <1.0 ms. GABA-A IPSCs were recorded with patch pipettes (2.0-3.5 MΩ) filled with an internal solution containing the following (in mM): 57.5 KCl, 57.5 K-methylsulfate, 20 NaCl, 1.5 MgCl2, 5 HEPES, 10 BAPTA, 2 ATP, 0.2 GTP, and 10 phosphocreatine, pH 7.35, 290 mOsM. All neurons were voltage clamped at -60 mV. Series resistance was monitored throughout the experiment (range; 3-15 MΩ). GABA-A IPSCs were evoked by electrical stimulation using a paired pulse (2 stimuli at 20 Hz) delivered every 20 s via monopolar electrode placed 100-200 µm rostroventral location from the recorded neuron cell body. All recordings were performed in the presence of NBQX 5 µM and 3-((R)-2-carboxypiperazin-4-yl)-propyl-1-phosphonic acid (CPP 5 µM) to isolate GABA-A IPSCs.

c-Fos protein immunoreactivity

Animals were weighted and handled for 2 days and injected daily for 2 days prior to the experiment to avoid stress-induced c-Fos expression (Reichmann et al., 2013; Ziółkowska et al., 2012). Mice were deeply anesthetized with ketamine-xylazine (1g/kg and 100mg/kg respectively, i.p.) 2h after either saline or heroin (10 mg/kg, i.p.) administration (Bontempi and Sharp, 1997). They were perfused transcardially with 10mL of ice-cold phosphate buffer (PB, 0.1 M, pH 7.4) followed by 100 mL of fresh cold 4% paraformaldehyde (PFA) in 0.1 M PB. Brains were dissected, post-fixated 24 to 48h in 4% PFA and cryoprotected in 30% sucrose (in 1X PB solution) for 48h. Brains were frozen and cut in a cryostat into 50-µm thick coronal sections, collected in 0.1 M PB. Free-floating sections were incubated overnight at room temperature with a primary rabbit polyclonal antibody (Ab-5, Calbiochem, Merck, Darmstadt, Germany, 1:20,000) targeting sequence 4-17 of the Fos protein. The sections were then incubated 2h with a biotinylated goat anti-rabbit IgG secondary antibody (Jackson Immunoresearch, West Baltimore Pike, PA, USA, 1:2,000). C-Fos immunoshistochemistry was revealed with a standard avidin-biotin peroxidase method (ABC, Elite Vectastain Kit, Vector Laboratories, Burlingame, CA, USA). Detection of the peroxidase was performed with the chromogen diaminobenzidine (Sigma-Aldrich, Saint-Quentin, France). Images were acquired using Hamamatsu Nanozoomer 2-HT (Hamamatsu Photonics, Hamamatsu, Japan) slide scanner. Brightfield 20x magnification images were analysed with NDP View software and Fos-immunoreactive cells were manually counted using NDP View Ex counter plugin. The second cohort images were acquired using MIRAX Scan 150 BF/FL (Zeiss, Germany). Comparison of the two acquisition methods showed no difference between cohorts (data not shown) and data were pooled. The number of positive nuclei, expressed per mm^2, were evaluated bilaterally using 4 to 7 sections per animal (n=6 mice per group), in 7 brain regions (NAc core and shell, CPu dorsomedial, dorsolateral, ventromedial and vendrolateral, and VTA) (Franklin and Paxinos).

Behavioral assays

Nociception. TI-TF: Analgesic effects of morphine on thermal nociception were assessed using tail immersion (TI) and tail flick (TF) tests. Mice received i.p. injections of cumulative doses of morphine (0, 2, 4, 6 and 10 mg/kg) every 30 minutes. All the 3 tests are done successively, with one-minute interval between each test (TI 52°C, then TI 54°C and finally TF). Mice were restrained in a tube during the 3 tests. For TI tests (Matthes et al., 1996), the bottom half of the mouse tail was dipped in a 52°C/54°C water bath and the latency for the mouse to withdraw its tail was measured. For TF test, the mouse tail is placed on a heating laser (intensity setting 40, radial heat, Tail Flick apparatus, DL Instrument International) and the latency for the tail flick was measured. To avoid tissue damage, a cut-

off is determined according to basal nociceptive threshold (respectively 20, 15 and 15 sec). Hot plate: The animals were placed on a 54◦C hot plate (Bioseb, France), surrounded by a Plexiglas cylinder, 30 minutes after morphine injection (0, 2 or 5 mg/kg, i.p.) (Matthes et al., 1996). The latency to show the first signs of discomfort (forepaw lick, hindpaw lick and jump) was measured. Jump is defined as no contact of the 4 paws with the plate. We applied a 240-sec cut-off time.

Physical dependence and withdrawal. Mice received chronic escalating morphine treatment during 6 days (10, 20, 40, 60, 80 and 100 mg/kg, i.p.) (adapted from Matthes et al., 1996). The twice daily injections are separated from 8h minimum. On day 7, a last morphine 100 mg/kg dose was injected 2 hours prior testing. In a room lighted at 15 lux, mice were placed in Plexiglas observation boxes (30 x 15 x 15cm) and basal activity is observed during 5 min. Withdrawal is precipitated by a naloxone injection (1 mg/kg, s.c.) for both morphine and vehicle-treated animals, and mice were placed back into the observation boxes for 20 min. Number of paw tremors, jumps, head shakes, wet dog shakes and sniffing were counted; ptosis, teeth chattering and piloerection presence was evaluated during each 5-min period. A general withdrawal score is calculated, giving a coefficient for each component (jumping x 0.8; wet dog shakes x 1; paw tremor x 0.35; sniffing x 0.5; ptosis x 1.5; teeth chattering x 1.5; body tremor x 1.5; piloerection x 1.5) (adapted from Berrendero et al., 2003). Additional signs are scored to complete the observation (activity, grooming, rearing).

Locomotor activity. Mice locomotion was assessed in clear Plexiglas boxes (21 × 11 × 17 cm) placed over an infrared platform, light intensity of the room set at 15 lux. Animal traveling distances were analyzed and recorded via an automated tracking system equipped with an infrared-sensitive camera (Videotrack; View Point, Lyon, France). Speed sensitivity was set at 6 cm/sec, to take into account only large movements for the locomotion measure. Mice were placed individually in the activity boxes for a 60 min-habituation period to reach a stable basal activity. Then, mice received injection of vehicle, heroin (0.5, 2, 4, 6, 8 or 10 mg/kg, i.p.) or amphetamine (2.5 or 5 mg/kg, i.p.) and were placed back in the same boxes. Drug-induced locomotor effects were recorder for further 120 min. In a supplementary experiment, we assessed horizontal and vertical activity of mu KO, WT, Control and Dlx-mu mice following the same protocol as previously described. Here, individual cages (Imetronic, Pessac, France) were equipped with infrared captors ~2 and ~8.5 cm from the floor, allowing measurements of both locomotor activity and rears.

Locomotor sensitization. Mice sensitization to heroin was assessed in the same conditions as acute heroin locomotion recordings. Briefly, during the first session, mice basal locomotion was measured during a 60 min-habituation period. Mice received then a heroin injection (0, 0.5, 2 or 10

mg/kg, i.p.) and were placed back in the locomotor boxes for 2h. The same experiment is conducted in the same mice every 4 days, to produce a locomotor sensitization during 5 sessions (day 1 to day 17).

Bar test. Animals received injection of either saline or heroin (2, 6 or 10 mg/kg, i.p.) 30 min prior to the test (Tzschentke and Schmidt, 1996). Muscular rigidity is assessed by placing the forepaws of the mice on a horizontal bar (0.4 cm diameter, 4.5 cm above the surface). Latency for the mouse to withdraw its forepaws is measured, using a cut-off time of 2 min.

Conditioned place preference. CPP boxes (Imétronic, Pessac, France) were composed of 2 compartments (15.5 x 16.5 x 20 cm) separated by a corridor (6 x 16.5 x 20 cm). The 2 boxes had the same size and distinct shape and floor texture. Dim light was used to diminish stress level (30 lux). Automated movement detection was recorded by infrared beams (Place Preference, Imétronic). Procedure consisted of pre-conditioning, conditioning and test phases. During a 20-min pre-conditioning, mice were allowed to freely explore the entire apparatus. Time spent in both boxes is calculated. Animals spending more than 67% in one compartment are excluded. According to pre-conditioning results, a drug-paired box is assigned to each mouse to balance groups in an unbiased procedure. Day 2 to 4, on the morning, mice received either saline, morphine (10 mg/kg, s.c.) or heroin (0.5, 2 or 10 mg/kg, s.c.) injection and are confined in the drug-paired compartment for 20 min. Seven hours later, during the 20-min afternoon conditioning session, mice were all injected with saline solution and confined in the other chamber. Test occurred on day 5 on the morning. Mice were free to explore the apparatus during 20 min and time spent in both compartment was recorded. A preference ratio is calculated as the time spent in the drug-paired compartment divided by the time spent in both compartments.

Heroin self-administration apparatus. Drug self-administration training and testing occurred in operant chambers (Model ENV-307A-CT, MED Associates, Inc., Georgia, VT, USA) equipped with two holes, one randomly selected as the active hole and the other as the inactive. Pump noise and stimuli lights (cues), one located inside the active hole and the other above it were paired with the delivery of the reinforcer. Chambers were made of aluminium and clear acrylic, had grid floors and were housed in sound- and light-attenuated boxes equipped with fans to provide ventilation and ambient noise. When mice responded on the reinforced hole, the stimulus light went on, and a drug infusion was delivered. Heroin was infused via a syringe that was mounted on a microinfusion pump (PHM-100A, MED Associates, Inc., Georgia, VT, USA) and connected via Tygon tubing (0.96 mm o.d., Portex Fine Bore Polythene Tubing, Portex Limited, Hythe, Kent, UK) to a single channel liquid swivel (375/25, Instech

Laboratories, Plymouth Meeting, PA, USA) and to the mouse intravenous (i.v.) catheter. The swivel was mounted on a counterbalanced arm above the operant chamber.

Food self-administration apparatus. Operant responding maintained by food was performed in mouse operant chambers (Model ENV-307A-CT, Med Associates, Georgia, VT, USA) equipped with two holes, one randomly selected as the active hole and the other as the inactive. Stimuli lights (cues), one located inside the active hole and the other above it were paired with the delivery of the reinforcer. Nose-poking on the active hole resulted in a pellet delivery together with a stimulus-light named conditioned stimulus (CS), located above the active hole and inside the hole while pressing on the inactive lever had no consequences. The chambers were made of aluminum and acrylic, and were housed in sound- and light-attenuated boxes equipped with fans to provide ventilation and white noise. A food dispenser equidistant between the two levers permitted delivery of food pellets when required.

Surgery. Mice were anaesthetized with a ketamine/xylazine mixture (1g/kg and 100mg/kg respectively, i.p.) and then implanted with indwelling i.v. silastic catheters (Soria et al., 2005). Briefly, a 6 cm length of silastic tubing (0.3 mm inner diameter, 0.6 mm outer diameter) (Silastic®, Dow Corning, Houdeng-Goegnies, Belgium) was fitted to a 22-gauge steel cannula (Semat, Herts, UK) that was bent at a right angle and then embedded in a cement disk (Dentalon Plus, Heraeus Kulzer, Wehrheim, Germany) with an underlying nylon mesh. The catheter tubing was inserted 1.3 cm into the right jugular vein and anchored with suture. The remaining tubing ran subcutaneously to the cannula, which exited at the midscapular region. All incisions were sutured and coated with antibiotic ointment (Bactroban, GlaxoSmithKline, Madrid, Spain). After surgery, animals were allowed to recover for 3 days prior to initiation of self-administration sessions. The catheter was flushed daily with a heparinised saline (30 USP units/mL). The patency of intravenous catheters was evaluated after the PR session and whenever drug self-administration behavior appeared to deviate dramatically from that observed previously by infusion of 0.1 mL thiopental sodium (5 mg/mL) through the catheter. If prominent signs of anaesthesia were not apparent within 3 s of the infusion, the mouse was removed from the experiment. The success rate for maintaining patency of the catheter (mean of duration of 11 days) until the end of the heroin self-administration training was 90 %. The verification of the catheter patency was not necessary for the extinction and reinstatement phases since heroin was not available.

Drugs in self-administration procedures. Heroin was obtained from Ministerio de Sanidad y Consumo (Spain) and dissolved in sterile 0.9 % physiological saline. Ketamine hydrochloride (100 mg/kg) (Imalgène 1000; Rhône Mérieux, Lyon, France) and xylazine hydrochloride (20 mg/kg) (Sigma, Madrid, Spain) were mixed and dissolved in ethanol (5 %) and distilled water (95 %). This anaesthetic mixture was

administered intraperitoneally in an injection volume of 20 mL/kg of body weight. Thiopental sodium (5 mg/mL) (Braun Medical S.A, Barcelona, Spain) was dissolved in distilled water and delivered by infusion of 0.1 mL through the i.v. catheter.

Acquisition of operant responding maintained by heroin. Heroin self-administration sessions were performed in accordance to protocols previously described (Burokas et al., 2012; Martín-García et al., 2009; Soria et al., 2008, 2005). Acquisition of operant conditioning maintained by heroin was performed by using different doses in decreasing order (0.1, 0.05, 0.025, 0.0125 and 0.006 mg/kg per injection, i.v.) delivered in 23.5 µl over 2 sec. Mice were given 1-h daily self-administration sessions during 20 consecutive days under fixed ratio (FR) 1 schedule of reinforcement. Nose-poking on the active hole resulted in the delivery of a reinforcer (heroin), while nose-poking on the inactive hole had no consequences. The side of active and inactive hole was counterbalanced between animals. The house light was on at the beginning of the session for 3 sec and off during the remaining time of the session. No extra houselight was turned on during session. Each daily session started with a priming injection of the drug. At the dose off 0.0125 mg/kg per injection i.v., animals were tested in a progressive ratio (PR) schedule where the response requirement to earn the reinforcer escalated according to the following series: 1-2-3-5-12-18-27-40-60-90-135-200-300-450-675-1000. The maximum duration of the PR session was 3 h or until mice did not respond on any hole within 1 h, and was performed only once. Mice were feed *ad libitum* during the whole experiment. The stimuli light together with the pump noise (environmental cues) signaled delivery of the heroin infusion. The timeout period after infusion delivery was 10 sec. During this 10 sec period, the cue light was off and no reward was provided after nose-poking on the active hole. Responses on the inactive hole and all the responses elicited during the 10 s timeout period were also recorded. The session was terminated after 50 reinforcers were delivered or after one hour, whichever occurred first. As previously described (Burokas et al., 2012; Martín-García et al., 2009; Soria et al., 2008, 2005), the criteria for self-administration behavior was achieved when all of the following conditions were met: 1) mice maintained a stable responding with less than 20 % deviation from the mean of the total number of reinforcers earned in three consecutive sessions (80 % of stability); 2) at least 75 % responding on the active hole, and 3) a minimum of 5 reinforcers per session. After each session, mice were returned to their home-cages. Each chamber was cleaned at the end of each session to prevent the presence of odor of the previous mouse. On day 21, after operant conditioning maintained by heroin at the dose of 0.006 mg/kg/infusion mice were moved from the heroin self-administration/training phase to the extinction phase.

Extinction of operant responding maintained by heroin. The experimental conditions during the extinction phase were similar to the acquisition of operant responding sessions except that heroin was not available and stimuli lights (environmental cues) were not presented after nose-poking in the active hole. Mice were given 1-h daily sessions (7 days per week) until reaching the extinction criterion. The criterion for extinction was achieved when mice made during 3 consecutive sessions a mean number of nose-poking in the active hole of less than 30 % of the responses obtained during the mean of the three days of achievement of the acquisition criteria of heroin self-administration training. All animals were run during 10 consecutive daily sessions. Then after, all mice were test under reinstatement induced by cue.

Cue-induced reinstatement. The presentation of conditioned environmental cue was performed to evaluate the reinstatement of heroin-seeking behavior. Test for cue-induced reinstatement was conducted under the same conditions used in the training phase except that heroin was not available. Each nose-poke in the active hole led to the presentation of both stimuli lights for 2 sec. The reinstatement criterion was achieved when nose-pokes in the active hole were double than nose-pokes in the active hole during the three 3 consecutive days that mice acquired extinction criteria or a minimum of 10 nose-pokes in the active hole.

Acquisition of operant responding maintained by chocolate. Control and Dlx-mu male mice (n=33) were trained during 1 h for 10 consecutive days to nose-poke for chocolate-flavored food-pellets as reward, paired with the presentation of a cue-light serving as CS, on a FR1 schedule of reinforcement followed by 5 sessions under FR5. Each chocolate-flavored pellet (TestDiet, Richmond, IN, USA) of 20 mg (20.5% protein, 12.7% fat, 66.8% carbohydrate, with a caloric value of 3.48 kcal/g) contained the addition of chocolate flavor (2% pure unsweetened cocoa), and the proportion of sugars within the carbohydrate part included a sucrose content of 50.11%. The criteria for acquisition of operant responding were achieved when mice maintained a stable responding with less than 20 % deviation from the mean of the total number of food-pellets earned in three consecutive sessions, with at least 75 % responding on the reinforced lever, and a minimum of 10 reinforcements per session (Burokas et al., 2012; Martín-García et al., 2011). Mice were food-deprived during the whole experiment at 85 % of their *ad libitum* initial weight adjusted for growth. After the 15 FR sessions, animals were tested in a PR schedule during one session where the response requirement to earn the reinforcer escalated according to the following series: 1-5-12-21-33-51-75-90-120-155-180-225-260-300-350-410-465-540-630-730-850-1000-1200-1500-1800-2100-2400-2700-3000-3400-3800-4200-4600-5000-5500. The maximum duration of the PR session was 5 h or until mice did not respond on any lever within 1 h. After each

session, mice were returned to their home-cages. Each chamber was cleaned at the end of each session to prevent the presence of odor of the previous mouse. After PR session, mice were moved to the extinction phase.

Statistical analyses

Data are presented as mean ± standard error (SEM) and statistical significance was achieved by $p<0.05$. Statistical analyses were performed using Prism6 (GraphPad Software) and post hoc analyses were followed with Bonferroni multiple comparisons test when appropriate. Gene expression was performed by a one-way ANOVA when comparing more than 2 genotypes and by two-tailed t-tests when 2. Comparison of specific binding in Control and Dlx-mu mice was carried out using two-way ANOVA followed where appropriate with Holm-Šídák multiple comparisons. Comparison of neuronal activation of the two genotypes (Control and Dlx-mu) was performed by a two-way ANOVA. Behavioral experiments were analysed by a two-way ANOVA with repeated measures for tail immersion and tail flick tests with morphine doses as within factor; the same analysis was used for locomotor sensitization with sessions as within factor. Two-way ANOVA was used for withdrawal scoring, locomotor activity, bar test and CPP experiments. For self-administration procedures, statistical analyses were performed using the Statistical Package for Social Science program SPSS® 15.0 (SPSS Inc, Chicago, USA). Analysis of the data during the acquisition phase of operant conditioning maintained by heroin or chocolate was conducted using three-way ANOVA of repeated measures with day and hole (active/inactive) as within-subjects factors and genotype as between-subjects factor. Post-hoc analysis (Newman-Keuls) was also performed when required. For operant conditioning maintained by heroin, three-way ANOVA was performed separately for each dose. For operant conditioning maintained by chocolate three-way ANOVA was performed separately for FR1 and FR5. Data of the breaking point achieved during the PR session was analysed with one-way ANOVA with genotype as between-subjects factor. To evaluate the extinction and cue-induced reinstatement, three-way ANOVA of repeated measures was performed with experimental phase and hole as within-subjects factors, and genotype as between-subject factor. Post-hoc analysis (Newman-Keuls) was performed when required. For electrophysiological recording, data were acquired using pClamp 10 software (sampled at 50 kHz, filtered at 1 kHz) and post hoc analysis was performed with AxoGraphX (Axograph Scientific). The peak amplitude of GABA-A IPSC was measured using AxoGraphX peak measurement software after subtracting the baseline.

RESULTS

Dlx-mu mice show a deletion of the mu receptor in the forebrain

We crossed the mu floxed mouse line (*Oprm1*$^{fl/fl}$) with the Dlx5/6-Cre mouse line expressing the Cre recombinase in forebrain GABAergic neurons, to generate the conditional knockout line Dlx5/6-Cre-*Oprm1*$^{-/-}$ (or Dlx-mu). The Dlx5/6-Cre mouse line has been successfully used to conditionally inactivate cannabinoid 1 (CB1) and delta opioid receptor in GABAergic forebrain neurons (Chu Sin Chung et al., 2015; Monory et al., 2006). We analysed *Oprm1* mRNA expression from homozygous mu floxed animals ((Cre(-), *Oprm1*$^{fl/fl}$), Control), conditional knockout (Dlx-mu) mice and constitutive knockout (CMV-mu) mice (**Figure 1A**). One-way ANOVA showed a genotype effect in all the investigated regions. Bonferroni *post hoc* analysis revealed that *mu receptor* mRNA expression of Dlx-mu mice was different from Control mice in the NAc ($p<0.001$), CPu, amygdala (Amy), dorsal hippocampus (HpD) ($p<0.001$) and ventral hippocampus (HpV) ($p<0.05$). Mu transcripts of all the regions studied is abolished in CMV-mu mice ($p<0.01$). In Dlx-mu animals, mu receptor transcripts were not different from CMV-mu in the NAc, CPu, Amy and Hp ($p>0.05$). It has been previously shown that constitutive deletion of mu receptors can trigger genetic modulation in mutant mice (Befort et al., 2008; Park et al., 2001). To explore the integrity of the opioid system, we tested mRNA expression of opioid peptide precursors and receptor transcripts (proenkephalin *pEnk*, prodynorphin *pDyn*, delta receptor *Oprd1*, kappa receptor *Oprk1*) in the CPu (**Figure 1B**) and NAc (**Figure 1C**) in Control and Dlx-mu mice. *POMC* expression, the precursor of β-endorphin, was too low to be measured. No changes in mRNA expression were detected in Dlx-mu mice in comparison to Control mice. Thus, the Dlx-mu presents a specific decrease of *mu receptor* mRNA expression in the striatum, the amygdala and the hippocampus.

Then, we quantified mu receptor protein distribution in Dlx-mu, CMV-mu and Control mice using autoradiography binding of the tritiated mu receptor agonist [^{3}H]DAMGO (**Figure 1D-F**). Analysis of constitutive KO samples confirmed genotype with complete mu receptor deletion. Two-way ANOVA revealed significant effect of genotype [$F_{(1,259)}=33.75$], region [$F_{(50,\ 259)}=24.28$] and genotype x region interaction [$F_{(50,\ 259)}=1.81$]; where $p<0.001$ in all cases. There was a mean reduction of 21% in Dlx-mu compared to Control mice. Holm-Šídák multiple comparisons found significant decrease of [^{3}H]DAMGO binding in Dlx-mu mice in NAc shell and core ($p<0.001$), external plexiform and internal granular layers of the olfactory bulbs, CPu, olfactory tubercles, medial septum, preoptic area, ventral pallidum, basomedial amygdala, hypothalamus and medial geniculate nucleus ($p<0.05$), relative to Control mice. Two-way ANOVA found no significant effects for any of the factors analysed in spinal cords (**Table 1**).

These results show that, as expected, our Cre/LoxP strategy lead to *Oprm1* gene inactivation specifically in the forebrain.

Dlx-mu mice show intact morphine-induced analgesia and physical dependence

We first examined the phenotypic consequences of the conditional mu receptor knockout on nociception responses to acute morphine administration. To do so, we investigated morphine analgesia in the tail immersion test and tail flick test, classical thermal nociception paradigms used to assess acute analgesic effects of opiates. We compared the analgesic properties of four doses of morphine in Control and Dlx-mu animals (**Figure 2A-C**). Two-way repeated measures ANOVA of tail immersion (52 and 54°C) and tail flick tests revealed a treatment effect [$F_{(5,\ 110)}$=122.6; p<0.001; $F_{(5,\ 110)}$=149.7; p<0.001; $F_{(5,\ 110)}$=91.30; p<0.001 respectively], but neither genotype effect [$F_{(1,\ 22)}$=0.20; p=0.66; $F_{(1,\ 22)}$=0.157; p=0.70; $F_{(1,\ 22)}$=0.027; p=0.87] nor interaction genotype x treatment [$F_{(5,\ 110)}$=0.29; p=0.92; $F_{(5,\ 110)}$=0.25; p=0.94; $F_{(5,\ 110)}$=0.12; p=0.99] (**Figure 2A-C**). Bonferroni *post hoc* analysis showed morphine treatment was effective from 4mg/kg (p<0.001) in the three behavioral tests. Similarly, 2-way ANOVA revealed a treatment effect in the hot plate test in latency to lick forepaws [$F_{(2,\ 35)}$=13.44; p<0.001], latency to lick the hindpaws (flinching) [$F_{(2,\ 32)}$=18.71; p<0.001] and latency to jump [$F_{(2,\ 35)}$=47.73; p<0.001] (**Figure 2D**). Neither genotype nor interaction genotype x treatment effects were detected in the hot plate test for the 3 criteria measured: latency to lick forepaws [$F_{(1,\ 35)}$=1.21; p=0.28; $F_{(2,\ 35)}$=0.39; p=0.68], flinching latency [$F_{(1,\ 32)}$=0.038; p=0.85; $F_{(2,\ 32)}$=0.32; p=0.73] and latency to jump [$F_{(1,\ 35)}$=0.36; p=0.55; $F_{(2,\ 35)}$=0.096; p=0.91]. Thus, selective inactivation of the mu receptor in forebrain GABAergic neurons does not alter analgesic properties of morphine.

We also determined whether the conditional deletion of mu alters the development of physical dependence to chronic morphine treatment, a syndrome that engages broad adaptations throughout brain circuits. We induced physical dependence to morphine by repeated injections of ascending doses of morphine (10–100mg/kg), twice daily over 6 days. Two hours after the last morphine or saline injection, a single naloxone dose (1 mg/kg, s.c.) was administered and withdrawal signs were scored. A global withdrawal score was calculated (adapted from (Berrendero et al., 2003)) for Control and cKO animals (**Figure 2E**). The global withdrawal score revealed a morphine effect [$F_{(1,\ 45)}$=104.0, p<0.001, 2-way ANOVA] that is not different between genotypes [$F_{(1,\ 45)}$=0.17, p=0.68, 2-way ANOVA, interaction genotype x treatment $F_{(1,\ 45)}$=0.31, p=0.58] (**Figure 2E**). No sign-of opiate withdrawal was observed during the 5-minute observation session before naloxone administration (data not shown). All the individual signs of withdrawal scored were similar in both genotypes (**Figure S1 and Table S1 in Supplementary**).

Deletion of mu receptor in forebrain GABAergic neurons did not alter the physical dependence induced by chronic morphine administration.

Dlx-mu mice show no locomotor response to heroin, but enhanced heroin-induced catalepsy

We examined heroin-induced hyperlocomotion in conditional knockout mice and their controls during a 2h-recording session, at doses from 0.5 to 20 mg/kg (**Figure 3A**). Two-way ANOVA revealed treatment effect [$F_{(7,\ 160)}$=7.37, p<0.001], genotype effect [$F_{(1,\ 160)}$=23.79, p<0.001] and interaction [genotype x treatment, $F_{(7,\ 160)}$=7.44, p<0.001]. *Post hoc* analysis showed no locomotor effect of heroin in Dlx-mu mice (p>0.05, Bonferroni). Treatment effect in Control mice was observed at 6, 8 and 10 mg/kg heroin (p<0.01, p<0.05 and p<0.001 respectively, Bonferroni). Genotype effect was observed at 6 and 10 mg/kg (p<0.05 and 0.001 respectively, Bonferroni). No heroin locomotor effects were found in mu total KO mice (see **Figure S2**). We then determined whether sensitization to heroin develops in Dlx-mu mice (**Figure 3B**). Control and Dlx-mu mice received heroin treatment (0 or 10 mg/kg, i.p.) every 4-5 days, during 5 sessions. Two-way ANOVA repeated measures revealed a genotype effect [$F_{(1,\ 78)}$=39.51; p<0.001], a treatment effect [$F_{(1,\ 78)}$=52.91; p<0.001] as well as session x genotype x treatment interaction [$F_{(3.085,\ 240.623)}$=11.01; p<0.001]. *Post hoc* analysis between the four groups showed no differences between Control group treated with saline and Dlx-mu groups (p<0.001). Control heroin group showed a significant difference with the three other groups (p<0.001, Bonferroni). The two other doses (0.5 and 2 mg/kg) produced no locomotor effects in any group at all days of treatment (data not shown). Mu receptor knockout in forebrain GABAergic neurons abolished locomotor effect as well as locomotor sentitization to heroin.

Previous studies showed that opiates induce catalepsy (Tzschentke and Schmidt, 1996), an effect that involves limbic and basal ganglia sites (Havemann and Kuschinsky, 1982; Manning et al., 1994). We examined the cataleptic effect of heroin in Dlx-mu and Control mice (**Figure 3C**). Thirty minutes after drug administration, heroin induced catalepsy differently in the two groups. Two-way ANOVA revealed genotype effect [$F_{(1,\ 116)}$=14.78; p=0.002], treatment effect [$F_{(3,\ 116)}$=39.12; p<0.001] as well as genotype x treatment interaction [$F_{(3,\ 116)}$=12.78; p<0.001]. *Post hoc* analysis showed a significant heroin effect at 6 and 10 mg/kg (p<0.001, Bonferroni) and a difference between Dlx-mu and Control mice at 10 mg/kg heroin (p<0.001, Bonferroni). Therefore, the lack of mu receptors in forebrain GABAergic neurons potentiated the heroin-induced catalepsy. Locomotor activation and catalepsy induced by heroin were also tested in constitutive mu receptor knockout and corresponding wild type mice, and no heroin effect could be detected in mutant animals (data not shown).

Hyperlocomotion and catalepsy are motor outputs that are both modulated by the dopaminergic system (Serrano et al., 2002; Vanderwende and Spoerlein, 1979). To explore the integrity of the dopamine system, we first determined *dopamine receptors* mRNA expression from Control and conditional knockout (Dlx-mu) mice in CPu (**Figure 3D**) and NAc (**Figure 3E**). No changes in dopamine receptor transcripts (dopamine D1 *drd1*, dopamine D2 *drd2*) expression were detected in Dlx-mu mice in comparison to Control mice. To then explore the functionality of the dopamine system, we next examined the effect of amphetamine in locomotor activity in Dlx-mu and Control mice (**Figure 3F**). Treatment effect was significant [$F_{(2, 41)}$=26.37, p<0.001, 2-way ANOVA], but there was neither genotype effect nor genotype x treatment interaction [$F_{(1, 41)}$=0.56, p=0.90; $F_{(2, 41)}$=0.54, p=0.59, respectively). *Post hoc* analysis revealed a difference between 5 mg/kg amphetamine administration and the other doses (p<0.001, Bonferroni). The conditional gene knockout did not produce any change in dopamine receptor expression or in the classical effect of amphetamine. The different heroin motor responses found in Dlx-mu mice are therefore not due to dopamine responsiveness differences.

Dlx-mu mice show increased motivation to self-administer heroin and palatable food

Previous studies showed an absence of rewarding effects of morphine (Matthes et al., 1996) and heroin (Contarino et al., 2002) in mu total knockout animals. The NAc and VTA are key structures of the reward circuit, and for opiate reward (Le Merrer et al., 2009). In our mouse model, deletion of the mu receptor occurred in the NAc but its expression was intact in the VTA. We assessed the contribution of the NAc receptor population in morphine and heroin reward using the CPP paradigm. After 6 conditioning sessions, preference for the drug-paired compartment was determined. In morphine CPP (**Figure 4A**), statistical analysis (two-way ANOVA) revealed a treatment effect [$F_{(1, 38)}$=5.32; p=0.03], but neither effect of genotype [$F_{(1, 38)}$= 0.031, p=0.86] nor genotype x treatment interaction [$F_{(1, 38)}$=0.11, p=0.74]. In heroin CPP, two-way ANOVA also revealed a treatment effect [$F_{(3, 83)}$=4.26, p=0.008], but neither effect of genotype [$F_{(1, 83)}$=0.16, p=0.69] nor genotype x treatment interaction [$F_{(3, 83)}$=0.28, p=0.84]. *Post hoc* analysis showed a main treatment effect at 2 and 10 mg/kg compared to saline groups (p<0.05, Bonferroni). The targeted mu receptor deletion in Dlx-mu mice, therefore, did not modify reinforcing properties of any of the two opiates in the CPP paradigm.

Mu constitutive knockout mice showed no self-administration of morphine (Becker et al., 2000; Sora et al., 2001). We assessed the contribution of mu receptors in forebrain GABAergic neurons in heroin reward and motivation, using heroin self-administration paradigm (**Figure 4B**). We first examined the acquisition of operant responding maintained by heroin. Three-way ANOVA of the active and

inactive nose-poking responses during the 20 days of self-administration was performed separately for each dose (see **Table S2** for three-way ANOVA). During operant conditioning maintained by heroin at the dose of 0.1 mg/kg/infusion, three-way ANOVA revealed no significant main effects of genotype, or the interaction between genotype, hole and day. There were no interactions between genotype and hole, genotype and day, or hole and day. Only a significant main effect of day and a significant main effect of hole were obtained, meaning that the number of nose-pokes decreased across days similarly in both genotypes and all mice discriminated between active and inactive hole. At the dose of 0.05 mg/kg/infusion, a significant effect of hole independent of day or genotype was obtained. Thus, mice from both genotypes discriminated between the active and the inactive holes during the whole period of training at the same dose (**Figure 4B**). At the dose of 0.025 mg/kg/infusion, a general main effect of genotype was detected and a significant main effect of hole, independent of day, was maintained but this effect was dependent of the genotype as shown by the significant interaction between genotype and hole. Thus, Dlx-mu mice showed significantly higher active nose-pokes than Control mice. With the dose of 0.0125 mg/kg/infusion, only a significant main effect of hole was observed independent of genotype or day, meaning that all mice discriminated similarly independently of the day. Finally, at the dose of 0.006 mg/kg/infusion, a general main effect of hole was maintained, but additionally a significant main effect of day and an interaction between hole and day was observed independent of the genotype, meaning that both genotypes discriminated between holes but this discrimination evolved across days. Thus, active nose-pokes increased across days similarly in both genotypes. Motivation for heroin was assessed in the PR schedule of reinforcement (**Figure 4C**). Here, the breaking point values were significantly increased in Dlx-mu mice when compared to Control littermates [$F_{(1,7)}$=4.02; p<0.05] revealing an increased motivation for heroin in Dlx-mu mice compared to Control. Following extinction period, cue-induced reinstatement was assessed. Three-way ANOVA of the active and inactive nose-poking responses during acquisition, extinction and cue-induced reinstatement phases was performed (**Figure 4D**). Significant main effect of genotype, hole and phase were obtained in addition to significant interactions between the two factors of genotype and hole, genotype and day, day and hole and the interaction between the three factors of genotype, hole and day (see **Table S2** for three-way ANOVA). Newman-Keuls *post hoc* test revealed that after extinction, the exposure to the associated cue reinstated heroin-seeking behavior only in Dlx-mu mice. During the reinstatement test, the number of active nose-poking responses was significantly higher in Dlx-mu mice than that obtained the day achieving the extinction criterion and animals reached a higher level of responses than that during the

acquisition training (**Figure 4D**). In cue-induced reinstatement, active nose-poking responses were higher in Dlx-mu mice when compared to Control littermates.

We then evaluated acquisition and maintenance of operant responding maintained by chocolate, a highly palatable food reward (Martín-García et al., 2011). Two-way ANOVA of the number of pellets during the 15 days of self-administration revealed a significant main effects of genotype [$F_{(1,31)}$=5.27; p<0.01], significant effects of day [$F_{(14,434)}$=83.44; p<0.001] and no interaction between genotype and day [$F_{(14,434)}$=0.99; p>0.05]. The number of pellets intake was higher in Dlx-mu mice. On FR1 schedule, the acquisition criteria of the operant responding maintained by chocolate-flavored pellets were achieved by 100 % of both genotypes. Active nose-poking responses were similar in Dlx-mu than in Control mice (see **Table S3** for three-way ANOVA). Mice from both genotypes discriminated between the active and the inactive holes during most of the whole period of training and the number of active nose-poking responses increased across days while the inactive nose-poking responses decreased over time (**Figure 4E**). The mean number of active nose-poking for chocolate reinforcement during the stable phase of self-administration was 213.30 ± 25.13 in Control and 270.18 ± 39.34 in Dlx-mu mice. On FR5 schedule, the acquisition criteria were achieved by 100 % of both genotypes. Active nose-poking responses were similar in both genotypes (see **Table S3** for three-way ANOVA). All mice discriminated between the active and the inactive holes during the whole period of FR5, and the number of active nose-poking remained stable across days (**Figure 4E**). A significant main effect of genotype was revealed with high number of active nose-poking responses in the Dlx-mu mice. The mean number of active nose-poking for chocolate reinforcement during the stable phase of self-administration was 635.80 ± 48.55 in Control and 925.05 ± 97.50 in Dlx-mu mice. Motivation for chocolate was evaluated in the PR schedule of reinforcement (**Figure 4F**). The breaking point values were significantly increased in Dlx-mu mice when compared to Control littermates [$F_{(1,31)}$=9.64; p<0.01] revealing an increased motivation for chocolate in Dlx-mu mice.

Together, these data demonstrate that Dlx-mu mice display a remarkable increase in their motivation to seek both heroin and chocolate in the self-administration procedures, a phenotype that was not detected in the CPP experiments.

Dlx-mu mice show altered heroin-induced c-Fos responses

Because the absence of mu opioid receptors in striatal but not VTA GABAergic neurons modifies both opiate locomotor effects and motivation to seek opiates, we examined whether opiate-induced neuronal activation is modified within the mesolimbic dopaminergic circuit using c-Fos immunoreactivity

(Dragunow and Faull, 1989) (**Figure 5**). Acute injection of opiate induces c-fos activation in mice, notably in the NAc and CPu as well as VTA (Singh et al., 2004; Ziółkowska et al., 2012). We administered acutely 10mg/kg of heroin and the animals were sacrificed 2 hrs after. We analysed c-Fos immunoreactivity in the NAc (core and shell), CPu (dorsolateral, dorsomedial, ventrolateral, ventromedial) and VTA. In the NAc shell, two-way ANOVA revealed a genotype effect [$F_{(1, 20)}$=12.92, p=0.0018], and a treatment effect [$F_{(1, 20)}$=17.72, p<0.001] but no interaction [$F_{(1, 20)}$=1.769, p=0.19] (**Figure 5G**). In the VTA, two-way ANOVA revealed a genotype effect [$F_{(1, 19)}$=8.44, p=0.0018], a treatment effect [$F_{(1, 19)}$=44.65, p<0.001] and a genotype x treatment interaction [$F_{(1, 19)}$=5.697, p=0.03]. *Post hoc* analysis showed that Control mice treated with heroin had greater c-Fos induction in the VTA than the three other groups (p<0.01) (**Figure 5E**). Heroin increased significantly c-Fos induction in the VTA of Dlx-mu in comparison to saline group of the same genotype (p<0.05). In the dorsolateral CPu, two-way ANOVA revealed a genotype effect [$F_{(1, 20)}$=8.032, p=0.010], a treatment effect [$F_{(1, 20)}$=4.718, p=0.042] and a genotype x treatment interaction [$F_{(1, 20)}$=8.71, p=0.008]. *Post hoc* analysis showed that Control mice treated with heroin had greater c-Fos induction in the dorsolateral CPu than the three other groups (p<0.05) (**Figure 5C**). No effects were found in the other regions investigated (p>0.05). Altogether these results show that neuronal activity induced by heroin is blunted at the level of dorsolateral CPu, NAc shell and the VTA, indicating that mesolimbic circuitry activity is modified in Dlx-mu mice.

Dlx-mu mice show no DAMGO-induced decrease of eIPSCs in VTA GABAergic neurons

To determine cellular mechanisms underlying the intriguing enhanced motivation for both heroin and food in Dlx-mu mice, we further performed electrophysiological analysis at the level of the VTA. Our hypothesis was that the targeted Dlx-mu knockout in NAc GABAergic neurons would impact the physiology of VTA DA neurons, whose role in mediating motivation for drugs of abuse is well-established (Bromberg-Martin et al., 2010; Cachope and Cheer, 2014). In our model, mu receptor is deleted in NAc neurons (Dlx-mu *Oprm1* mRNA expression did not differ from CMV-mu mice, **Figure 1A**), known to send projections to the VTA (Xia et al., 2011). A paired electrical stimulation was applied to evoke GABA-A IPSCs in GABA neurons of the VTA in Control and Dlx-mu mice (**Figure 6A**). Application of mu opioid receptor agonist DAMGO (1 µM) decreased the amplitude of GABA-A IPSCs to 45.1±8.1% of baseline in wild type littermate (p<0.001, $t_{(7)}$=6.74, Student t-test); however, DAMGO failed to inhibit IPSCs in GABA neurons from Dlx-mu mice (103.0±4.3% of baseline, p=0.51, $t_{(9)}$=0.69). The inhibition induced by DAMGO was significantly different between two groups (p<0.001, $t_{(16)}$=6.65). Previous study showed that striatal inputs to midbrain dopamine neurons were highly sensitive to adenosine A1

receptor agonists (Matsui et al., 2014). When the A1 receptor agonist N^6-CPA (1 μM) was applied to the slices, IPSCs were significantly inhibited to 59.1±11.2% of baseline (p=0.005, $t_{(9)}$=3.66) in Control littermate mice, and 60.1±14.3% of baseline (p=0.03, $t_{(6)}$=2.80) Dlx-mu mice. The degree of N^6-CPA induced inhibition was similar between the genotypes (p=0.96, $t_{(15)}$=0.05). GABA-A IPSCs were also recorded in dopamine neurons (**Figure 6B**). Application of DAMGO inhibited GABA-A IPSC to 41.9±11.6% and 46.2±11.7% of baseline in Control littermate and Dlx-mu mice, respectively (Control: p=0.0016, $t_{(7)}$=5.00; Dlx-mu: p=0.0013, $t_{(9)}$=4.59). The amplitude of DAMGO-mediated inhibition was similar between the two groups (p=0.80, $t_{(16)}$=0.26), indicating that the mu opioid sensitive GABA inputs to dopamine neurons was not altered in the Dlx-mu mice. This result suggested that the majority of GABA inputs to dopamine neurons do not originate from striatum/forebrain region but rather represent inputs from local or other mu opioid expressing GABA neurons. The effect of Adenosine A1 receptor agonist N^6-CPA on GABA inputs to dopamine neurons was also tested. N^6-CPA application had no significant effect on the amplitude of GABA-A IPSCs in Control or mutant mice (Control: 79.0±11.1% of baseline, p=0.11, $t_{(6)}$=1.886; Dlx-mu: 98.3±6.77% of baseline, p=0.80, $t_{(11)}$=0.25). The inhibitions were not significantly different from 100% baseline in both groups. Altogether, our results suggest that presynaptic mu receptors of MSN neurons projecting to VTA GABAergic neurons are lacking in Dlx-mu mice (**Figure 6C**).

DISCUSSION

We used Dlx5/6-Cre mice to target the mu receptor gene in forebrain GABAergic neurons, and obtained conditional knockout mice with a deletion of *Oprm1* mRNA expression in the striatum (NAc and CPu), amygdala and hippocampus, while *Oprm1* mRNA level in the VTA is unchanged. In these animals, we observed that morphine-induced analgesia and physical dependence are preserved. These data indicate that mu receptors in GABAergic neuron of the forebrain do not play a role in morphine nociception and withdrawal. Furthermore, our behavioral analysis showed no heroin-induced hyperlocomotion and increased heroin-induced catalepsy in conditional mutants, suggesting an important role for these mu receptors in heroin-mediated motor–responses. Finally, our results demonstrate that the lack of mu receptors on forebrain GABAergic neurons increases seeking behaviour for heroin and palatable food, apparently without modifying their rewarding value, indicating that this particular population of mu receptors also contributes to regulate motivational processes.

Numerous studies reported expression of mu receptors mostly within GABAergic neurons, including in the VTA (Johnson and North, 1992; Lowe and Bailey, 2014), bed nucleus of the stria

terminalis (BNST) (Kudo et al., 2014), VP (Kupchik et al., 2014) and striatum (Miura et al., 2007). Kalyuzhny and Wessendorf (1998) identified double-labelling of mu receptor and GABA in piriform and parietal cortices, hippocampal and thalamic nuclei (Kalyuzhny and Wessendorf, 1998). Also, an mRNA study showed that all mu receptor mRNA positive neurons from the hippocampal formation were GAD positive (Stumm et al., 2004). Here we used the Dlx-mu mice, which were previously used to invalidate the cannabinoid receptor CB1 and the delta opioid receptor in forebrain GABAergic neurons (Chu Sin Chung et al., 2015; Monory et al., 2006). In accordance with the literature, our approach indeed led to delete mu opioid receptor expression in forebrain regions with reported mu receptor expression in GABAergic neurons. The conditional mu receptor KO was particularly strong in the striatum. Notably, most mu opioid receptor mRNA was deleted in NAc and CPu (≈96%), but a substantial protein level was left (28 to 48%). The remaining mu receptor proteins may come from a small population of cholinergic interneurons (Jabourian et al., 2005; Svingos et al., 2001) and to a greater extent from presynaptic receptors on glutamatergic projecting neurons from cortex and amygdala (O'Donnell and Grace, 1995).

Constitutive deletion of a gene can lead to compensatory mechanisms. For instance, it was previously shown that in mu total KO, D1/D2 mRNA expression is increased in different brain regions, notably in NAc and CPu (Park et al., 2001). Here, mRNA levels for other opioid receptors, opioid peptides or D1/D2 receptors are unchanged, suggesting that the behavioral phenotypes that we observed are not due to modifications in their expression.

Total invalidation of the mu opioid receptor led to the suppression of morphine analgesic effects (Matthes et al., 1996; Sora et al., 1997). In the present study, Dlx-mu mice displayed similar morphine-induced antinociception to control littermates, indicating that mu receptors located within forebrain GABAergic neurons are not implicated in analgesic effects of morphine. Mu opioid receptors are expressed throughout nociceptive pathways in the brain, spinal cord and sensory neurons (Mansour et al., 1995). Previous studies have shown that PAG is a major site of action of morphine-induced analgesia (Jensen and Yaksh, 1986; Manning et al., 1994; Meyer et al., 2009; Morgan et al., 2014). In fact, mu receptors that are expressed in the PAG are spared in the conditional knockout mouse line. Recently, corticostriatal circuit has been proposed to play a role in the regulation of chronic pain (Lee et al., 2015), and it may therefore be interesting to evaluate the development of persistent pain in Dlx-mu mice under inflammatory or neuropathic pain conditions.

Physical dependence induced by chronic morphine administration is abolished in mu receptor knockout mice (Matthes et al., 1996), however Dlx-mu mice develop the full spectrum of physical withdrawal signs. Neuronal substrates of opioid withdrawal include locus coeruleus and PAG for somatic

signs, and BNST for the aversive component of morphine withdrawal (Williams et al., 2001), and mu opioid receptor expression is intact at these sites. Nucleus accumbens and amygdala neurons also possibly participate to the withdrawal syndrome (Stinus et al., 1990), hence our data indicate that either mu receptors in these brain regions do not contribute to the expression of withdrawal signs, or that these receptors are involved to a small extent and their contribution is not detected under our conditions.

In mice, acute heroin injection produces an increase in locomotor activity (Bailey et al., 2010), and this behavior is not observed in total mu opioid receptor KO mice (Contarino et al., 2002). As for total KO mice, Dlx-mu mice in this study show no locomotor response to heroin, consistent with the lack of c-fos response to heroin in the Nac Shell (**Figure 5** and (Leite-Morris et al., 2004)). Further, we observed a weak but significant heroin-induced cataleptic state in control mice (bar test), as reported for morphine in the literature (Tzschentke and Schmidt, 1996), and this effect was dramatically enhanced in Dlx-mu mutants. It is likely that heroin-induced hyperactivity normally hides catalepsy in control mice, and that the cataleptic effect of heroin is unmasked in Dlx-mu animals that do not show locomotor activation. Heroin-induced locomotor activation and catalepsy, therefore, engage two separate neural mechanisms, a hypothesis that is supported by the clear dissociation between the locomotor phenotype and the lack of cataleptic phenotype in Dlx-mu mice at the dose of 6 mg/kg heroin. Together, we conclude that mu opioid receptors expressed in forebrain GABAergic neurons, possibly at the level of striatum, are essential for heroin-induced locomotor effects. At this stage, mu receptors contributing to heroin catalepsy remain to be identified. Mechanisms underlying locomotor effects of heroin in control mice may involve dopaminergic transmission (Kuribara, 1995; Rodríguez-Arias et al., 2000), however, the locomotor response to amphetamine was identical in Dlx-mu and control mice. Further experiments will be required to determine potential dopaminergic or other mechanisms in this particular mu opioid receptor activity.

Rewarding and motivational properties of opiates, as measured by CPP and self-administration procedures, are abolished in total mu KO mice (Becker et al., 2000; Matthes et al., 1996; Sora et al., 2001). In our study, morphine and heroin induced similar conditioned place preference in both genotypes, indicating that the association between opioid reward and the treatment context is preserved in our conditional mice. This result suggests that the two opiate drugs produce their rewarding effects via recruitment of mu receptors that have remained intact in Dlx-mu mice. Unchanged mu opioid receptor mRNA levels in the VTA, a major site for opiate reinforcement (Bozarth and Wise, 1981; Devine and Wise, 1994; for review see Le Merrer et al., 2009) likely explains our observation of

intact opiate CPP in Dlx-mu mice. Interestingly however, data from the self-administration experiments reveal a strong phenotype for Dlx-mu mice. First, the acquisition of heroin self-administration was slightly enhanced, and second, the breaking point in the PR schedule of reinforcement was remarkably increased in Dlx-mu mice compared to Control. Third, cue-induced reinstatement is also higher in our mutant mice, and altogether, these data demonstrate higher motivation to self-administer and seek heroin. In addition, the number of voluntary chocolate pellet intake, as well as the breaking point to obtain chocolate pellet in the PR schedule, were remarkably higher in Dlx-mu mice, revealing increased motivation also for high palatable food. Combining these results, our data suggest that mu opioid receptors in GABAergic neurons strongly regulate motivation for both drug-induced and natural rewards, and most intriguingly, may act as a brake on these behaviors.

We performed electrophysiological recordings to further understand circuit mechanisms that may lead to enhanced motivation for heroin and palatable food in mutant mice. In VTA slices, we found that mu opioid receptor-dependent inhibition of GABA-A IPSCs is lost selectively in GABA neurons of Dlx-mu mice, while dopamine neurons retain normal sensitivity for the mu agonist. This result first suggests that presynaptic mu opioid receptors expressed on striatal afferences to the VTA, representing a small proportion of VTA mu opioid receptors (Matsui 2014), are lacking in Dlx-mu mice (Fig 6C). This was barely detectable in the autoradiographic analysis of mu opioid receptor protein, showing a trend to reduced receptor number in the VTA. Also, electrophysiological results indicate that mu opioid sensitive GABAergic inputs from the striatum/forebrain to the midbrain contact mainly GABAergic neurons, rather than dopaminergic neurons (Fig 6C). Altogether, we propose a model where mu receptors on striatal MSN terminals normally inhibit GABA release onto VTA GABAergic interneurons, exerting a disinhibitory tone on these neurons, which limits activity of dopamine neurons. In contrast to the broadly studied mu opioid receptors expressed in VTA GABAergic neurons, this particular mu receptor population would therefore exert inhibitory control over dopamine neurons. As a consequence, specific deletion of these receptors in Dlx-mu mice, would lead to enhanced responsiveness of dopamine neurons, which may in turn underlie increased motivation of mutant mice to self-administer heroin or palatable food. This potential mechanism suggests for the first time that a specific mu opioid receptor subpopulation exerts a negative feed-back activity on mesolimbic dopaminergic circuitry, which opposes the well-established facilitating function of the receptor on motivational processes.

In conclusion, the analysis of conditional Dlx-mu mice reveals a specific role for mu opioid receptors in forebrain GABAergic neurons in both locomotor and motivational effects of heroin. This particular receptor population seems to play distinct roles for the two behavioural responses to heroin,

with an essential role to mediate the stimulant effects of heroin and an inhibitory activity on drug seeking and taking. Further investigations should definitely establish whether these particular mu opioid receptor roles take place at the level of GABAergic medium spiny neurons of the striatum, or in other GABAergic neurons of the forebrain.

Acknowledgements

We thank the Mouse clinical Institute and the animal core facility at the Institut de Génétique et de Biologie Moléculaire et Cellulaire for technical support (Illkirch, France). This work was supported by the Centre National de la Recherche Scientifique, Institut National de la Santé et de la Recherche Médicale, and Université de Strasbourg. We would also like to thank the US National Institutes of Health (National Institute of Drug Addiction, grant #05010 and National Institute on Alcohol Abuse and Alcoholism, grant #16658) for financial support. This study was funded by the Intramural Programs of National Institute on Alcohol Abuse and Alcoholism (NIAAA) and National Institute of Neurological Disorders and Stroke Grant ZIA-AA000421. This work was also supported by the Spanish 'Instituto de Salud Carlos III' (RTA, no. RD06/001/001), the Spanish 'Ministerio de Ciencia e Innovación' (no. Ministerio de Ciencia e Innovación (SAF2011-29864), the Catalan Government (SGR2009-00131) and ICREA Academia-2008.

REFERENCES

Bailey, A., Metaxas, A., Al-Hasani, R., Keyworth, H.L., Forster, D.M., Kitchen, I., 2010. Mouse strain differences in locomotor, sensitisation and rewarding effect of heroin; Association with alterations in MOP-r activation and dopamine transporter binding. Eur. J. Neurosci. 31, 742–753. doi:10.1111/j.1460-9568.2010.07104.x

Baskin, D.G., Wimpy, T.H., 1989. Calibration of [14C]plastic standards for quantitative autoradiography of [125I]labeled ligands with Amersham Hyperfilm beta-max. Neurosci. Lett. 104, 171–177. doi:10.1016/0304-3940(89)90350-9

Becker, a, Grecksch, G., Brödemann, R., Kraus, J., Peters, B., Schroeder, H., Thiemann, W., Loh, H.H., Höllt, V., 2000. Morphine self-administration in mu-opioid receptor-deficient mice. Naunyn. Schmiedebergs. Arch. Pharmacol. 361, 584–589.

Becker, J.A., Clesse, D., Spiegelhalter, C., Schwab, Y., Le Merrer, J., Kieffer, B.L., 2014. Autistic-Like Syndrome in Mu Opioid Receptor Null Mice is Relieved by Facilitated mGluR4 Activity. Neuropsychopharmacology 2049–2060. doi:10.1038/npp.2014.59

Befort, K., Filliol, D., Darcq, E., Ghate, a., Matifas, a., Lardenois, a., Muller, J., Thibault, C., Dembele, D., Poch, O., Kieffer, B.L., 2008. Gene expression is altered in the lateral hypothalamus upon activation of the mu opioid receptor. Ann. N. Y. Acad. Sci. 1129, 175–184. doi:10.1196/annals.1417.028

Berrendero, F., Castañé, A., Ledent, C., Parmentier, M., Maldonado, R., Valverde, O., 2003. Increase of morphine withdrawal in mice lacking A2a receptors and no changes in CB1/A2a double knockout mice. Eur. J. Neurosci. 17, 315–324. doi:10.1046/j.1460-9568.2003.02439.x

Bontempi, B., Sharp, F.R., 1997. Systemic morphine-induced Fos protein in the rat striatum and nucleus accumbens is regulated by mu opioid receptors in the substantia nigra and ventral tegmental area. J. Neurosci. 17, 8596–8612. doi:http://www.jneurosci.org/content/17/21/8596

Bozarth, M. a, Wise, R. a, 1981. Intracranial self-administration of morphine into the ventral tegmental area in rats. Life Sci. 28, 551–555. doi:10.1016/0024-3205(81)90148-X

Bromberg-Martin, E.S., Matsumoto, M., Hikosaka, O., 2010. Dopamine in Motivational Control: Rewarding, Aversive, and Alerting. Neuron 68, 815–834. doi:10.1016/j.neuron.2010.11.022

Burokas, A., Gutiérrez-Cuesta, J., Martín-García, E., Maldonado, R., 2012. Operant model of frustrated expected reward in mice. Addict. Biol. 17, 770–782. doi:10.1111/j.1369-1600.2011.00423.x

Cachope, R., Cheer, J.F., 2014. Local control of striatal dopamine release. Front. Behav. Neurosci. 8, 188. doi:10.3389/fnbeh.2014.00188

Castro, D.C., Berridge, K.C., 2014. Opioid hedonic hotspot in nucleus accumbens shell: mu, delta, and kappa maps for enhancement of sweetness “liking” and “wanting”. J. Neurosci. 34, 4239–50. doi:10.1523/JNEUROSCI.4458-13.2014

Chieng, B., Azriel, Y., Mohammadi, S., Christie, M.J., 2011. Distinct cellular properties of identified dopaminergic and GABAergic neurons in the mouse ventral tegmental area. J. Physiol. 589, 3775–3787. doi:10.1113/jphysiol.2011.210807

Chu Sin Chung, P., Keyworth, H.L., Martin-Garcia, E., Charbogne, P., Darcq, E., Bailey, A., Filliol, D., Matifas, A., Scherrer, G., Ouagazzal, A.-M., Gaveriaux-Ruff, C., Befort, K., Maldonado, R., Kitchen, I., Kieffer, B.L., 2015. A Novel Anxiogenic Role for the Delta Opioid Receptor Expressed in GABAergic Forebrain Neurons. Biol. Psychiatry 77, 404–415. doi:10.1016/j.biopsych.2014.07.033

Contarino, A., Picetti, R., Matthes, H.W., Koob, G.F., Kieffer, B.L., Gold, L.H., 2002. Lack of reward and locomotor stimulation induced by heroin in ??-opioid receptor-deficient mice. Eur. J. Pharmacol. 446, 103–109. doi:10.1016/S0014-2999(02)01812-5

David, V., Matifas, A., Gavello-Baudy, S., Decorte, L., Kieffer, B.L., Cazala, P., 2008. Brain regional Fos expression elicited by the activation of mu- but not delta-opioid receptors of the ventral tegmental area: evidence for an implication of the ventral thalamus in opiate reward. Neuropsychopharmacology 33, 1746–1759. doi:10.1038/sj.npp.1301529

Devine, D.P., Wise, R. a, 1994. Self-administration of morphine, DAMGO, and DPDPE into the ventral tegmental area of rats. J. Neurosci. 14, 1978–1984.

Dragunow, M., Faull, R., 1989. in neuronal pathway tracing. J. Neurosci. Methods 29, 261–265.

Echo, J. a., Lamonte, N., Ackerman, T.F., Bodnar, R.J., 2002. Alterations in food intake elicited by GABA and opioid agonists and antagonists administered into the ventral tegmental area region of rats. Physiol. Behav. 76, 107–116. doi:10.1016/S0031-9384(02)00690-X

Erbs, E., Faget, L., Scherrer, G., Matifas, A., Filliol, D., Vonesch, J.L., Koch, M., Kessler, P., Hentsch, D., Birling, M.C., Koutsourakis, M., Vasseur, L., Veinante, P., Kieffer, B.L., Massotte, D., 2014. A mu-delta opioid receptor brain atlas reveals neuronal co-occurrence in subcortical networks. Brain Struct. Funct. 1–26. doi:10.1007/s00429-014-0717-9

Ford, C.P., Mark, G.P., Williams, J.T., 2006. Properties and opioid inhibition of mesolimbic dopamine neurons vary according to target location. J. Neurosci. 26, 2788–2797. doi:10.1523/JNEUROSCI.4331-05.2006

Havemann, U., Kuschinsky, K., 1982. Review neurochemical aspects of the opioid - induced “catatonia.” Neurochem. Int. 4.

Jabourian, M., Venance, L., Bourgoin, S., Ozon, S., Pérez, S., Godeheu, G., Glowinski, J., Kemel, M.-L., 2005. Functional mu opioid receptors are expressed in cholinergic interneurons of the rat dorsal striatum: territorial specificity and diurnal variation. Eur. J. Neurosci. 21, 3301–3309. doi:10.1111/j.1460-9568.2005.04154.x

Jensen, T.S., Yaksh, T.L., 1986. Comparison of antinociceptive action of morphine in the periaqueductal gray, medial and paramedial medulla in rat. Brain Res. 363, 99–113. doi:10.1016/0006-8993(86)90662-1

Jhou, T.C., Xu, S.P., Lee, M.R., Gallen, C.L., Ikemoto, S., 2012. Mapping of reinforcing and analgesic effects of the mu opioid agonist Endomorphin-1 in the ventral midbrain of the rat. Psychopharmacology (Berl). 224, 303–312. doi:10.1007/s00213-012-2753-6

Johnson, S.W., North, R. a, 1992. Opioids excite dopamine neurons by hyperpolarization of local interneurons. J. Neurosci. 12, 483–488.

Kalyuzhny, A.E., Wessendorf, M.W., 1998. Relationship of ??- and ??-opioid receptors to GABAergic neurons in the central nervous system, including antinociceptive brainstem circuits. J. Comp. Neurol. 392, 528–547. doi:10.1002/(SICI)1096-9861(19980323)392:4<528::AID-CNE9>3.0.CO;2-2

Katsuura, Y., Taha, S. a., 2014. Mu opioid receptor antagonism in the nucleus accumbens shell blocks consumption of a preferred sucrose solution in an anticipatory contrast paradigm. Neuroscience 261, 144–152. doi:10.1016/j.neuroscience.2013.12.004

Kemppainen, H., Raivio, N., Suo-Yrjo, V., Kiianmaa, K., 2012. Opioidergic Modulation of Ethanol Self-Administration in the Ventral Pallidum. Alcohol. Clin. Exp. Res. 36, 286–293. doi:10.1111/j.1530-0277.2011.01611.x

Kitanaka, N., Sora, I., Kinsey, S., Zeng, Z., Uhl, G.R., 1998. No heroin or morphine 6beta-glucuronide analgesia in mu-opioid receptor knockout mice. Eur. J. Pharmacol. 355, R1–R3.

Kitchen, I., Slowe, S.J., Matthes, H.W., Kieffer, B., 1997. Quantitative autoradiographic mapping of mu-, delta- and kappa-opioid receptors in knockout mice lacking the mu-opioid receptor gene. Brain Res. 778, 73–88.

Kudo, T., Konno, K., Uchigashima, M., Yanagawa, Y., Sora, I., Minami, M., Watanabe, M., 2014. GABAergic neurons in the ventral tegmental area receive dual GABA/enkephalin-mediated inhibitory inputs from the bed nucleus of the stria terminalis. Eur. J. Neurosci. 39, 1796–1809. doi:10.1111/ejn.12503

Kupchik, Y.M., Scofield, M.D., Rice, K.C., Cheng, K., Roques, B.P., Kalivas, P.W., 2014. Cocaine dysregulates opioid gating of GABA neurotransmission in the ventral pallidum. J. Neurosci. 34, 1057–66. doi:10.1523/JNEUROSCI.4336-13.2014

Kuribara, H., 1995. Modification of morphine sensitization by opioid and dopamine receptor antagonists: Evaluation by studying ambulation in mice. Eur. J. Pharmacol. 275, 251–258. doi:10.1016/0014-2999(94)00787-8

Le Merrer, J., Becker, J. a J., Befort, K., Kieffer, B.L., 2009. Reward processing by the opioid system in the brain. Physiol. Rev. 89, 1379–1412. doi:10.1152/physrev.00005.2009

Lee, M., Manders, T.R., Eberle, S.E., Su, C., D'amour, J., Yang, R., Lin, H.Y., Deisseroth, K., Froemke, R.C., Wang, J., 2015. Activation of Corticostriatal Circuitry Relieves Chronic Neuropathic Pain. J. Neurosci. 35, 5247–5259. doi:10.1523/JNEUROSCI.3494-14.2015

Leite-Morris, K. a, Fukudome, E.Y., Shoeb, M.H., Kaplan, G.B., 2004. GABA(B) receptor activation in the ventral tegmental area inhibits the acquisition and expression of opiate-induced motor sensitization. J. Pharmacol. Exp. Ther. 308, 667–678. doi:10.1124/jpet.103.058412

Li, W., Doyon, W.M., Dani, J. a., 2012. Quantitative unit classification of ventral tegmental area neurons in vivo. J. Neurophysiol. 107, 2808–2820. doi:10.1152/jn.00575.2011

Livak, K.J., Schmittgen, T.D., 2001. Analysis of relative gene expression data using real-time quantitative PCR and the 2(-Delta Delta C(T)) Method. Methods 25, 402–408. doi:10.1006/meth.2001.1262

Lowe, J.D., Bailey, C.P., 2014. Functional selectivity and time-dependence of mu-opioid receptor desensitization at nerve terminals in the mouse ventral tegmental area. Br. J. Pharmacol. 1–46. doi:10.1111/bph.12605

Manning, B.H., Morgan, M.J., Franklin, K.B., 1994. Morphine analgesia in the formalin test: evidence for forebrain and midbrain sites of action. Neuroscience 63, 289–294. doi:10.1016/0306-4522(94)90023-X

Mansour, A., Fox, C. a., Akil, H., Watson, S.J., 1995. Opioid-receptor mRNA expression in the rat CNS: anatomical and functional implications. Trends Neurosci. 18, 22–29. doi:10.1016/0166-2236(95)93946-U

Martín-García, E., Barbano, M.F., Galeote, L., Maldonado, R., 2009. New operant model of nicotine-seeking behaviour in mice. Int. J. Neuropsychopharmacol. 12, 343–356. doi:10.1017/S1461145708009279

Martín-García, E., Burokas, A., Kostrzewa, E., Gieryk, A., Korostynski, M., Ziolkowska, B., Przewlocka, B., Przewlocki, R., Maldonado, R., 2011. New operant model of reinstatement of food-seeking behavior in mice. Psychopharmacology (Berl). 215, 49–70. doi:10.1007/s00213-010-2110-6

Matsui, A., Jarvie, B.C., Robinson, B.G., Hentges, S.T., Williams, J.T., 2014. Separate GABA afferents to dopamine neurons mediate acute action of opioids, development of tolerance, and expression of withdrawal. Neuron 82, 1346–1356. doi:10.1016/j.neuron.2014.04.030

Matthes, H.W., Maldonado, R., Simonin, F., Valverde, O., Slowe, S., Kitchen, I., Befort, K., Dierich, a, Le Meur, M., Dollé, P., Tzavara, E., Hanoune, J., Roques, B.P., Kieffer, B.L., 1996. Loss of morphine-induced analgesia, reward effect and withdrawal symptoms in mice lacking the mu-opioid-receptor gene. Nature. doi:10.1038/383819a0

Metzger, D., Chambon, P., 2001. Site- and time-specific gene targeting in the mouse. Methods 24, 71–80. doi:10.1006/meth.2001.1159

Meyer, P.J., Morgan, M.M., Kozell, L.B., Ingram, S.L., 2009. Contribution of dopamine receptors to periaqueductal gray-mediated antinociception. Psychopharmacology (Berl). 204, 531–540. doi:10.1007/s00213-009-1482-y

Mickiewicz, A.L., Dallimore, J.E., Napier, T.C., 2009. The ventral pallidum is critically involved in the development and expression of morphine-induced sensitization. Neuropsychopharmacology 34, 874–886. doi:10.1038/npp.2008.111

Miller, J. a, Zahniser, N.R., 1987. The use of 14C-labeled tissue paste standards for the calibration of 125I-labeled ligands in quantitative autoradiography. Neurosci. Lett. 81, 345–350. doi:10.1016/0304-3940(87)90408-3

Miura, M., Saino-Saito, S., Masuda, M., Kobayashi, K., Aosaki, T., 2007. Compartment-specific modulation of GABAergic synaptic transmission by mu-opioid receptor in the mouse striatum with green fluorescent protein-expressing dopamine islands. J. Neurosci. 27, 9721–9728. doi:10.1523/JNEUROSCI.2993-07.2007

Moles, A., Kieffer, B.L., D'Amato, F.R., 2004. Deficit in attachment behavior in mice lacking the mu-opioid receptor gene. Science 304, 1983–1986. doi:10.1126/science.1095943

Monory, K., Massa, F., Egertová, M., Eder, M., Blaudzun, H., Westenbroek, R., Kelsch, W., Jacob, W., Marsch, R., Ekker, M., Long, J., Rubenstein, J.L., Goebbels, S., Nave, K.A., During, M., Klugmann, M., Wölfel, B., Dodt, H.U., Zieglgänsberger, W., Wotjak, C.T., Mackie, K., Elphick, M.R., Marsicano, G., Lutz, B., 2006. The Endocannabinoid System Controls Key Epileptogenic Circuits in the Hippocampus. Neuron 51, 455–466. doi:10.1016/j.neuron.2006.07.006

Morgan, M.M., Reid, R. a., Stormann, T.M., Lautermilch, N.J., 2014. Opioid Selective Antinociception Following Microinjection Into the Periaqueductal Gray of the Rat. J. Pain 15, 1102–1109. doi:10.1016/j.jpain.2014.07.008

O'Donnell, P., Grace, a a, 1995. Synaptic interactions among excitatory afferents to nucleus accumbens neurons: hippocampal gating of prefrontal cortical input. J. Neurosci. 15, 3622–3639.

Park, Y., Ho, I.K., Fan, L.W., Loh, H.H., Ko, K.H., 2001. Region specific increase of dopamine receptor D1/D2 mRNA expression in the brain of mu-opioid receptor knockout mice. Brain Res. 894, 311–315.

Paxinos, G., Franklin, K.B.J., 2001. The mouse brain in stereotaxic coordinates. Acad. Press 1–350.

Reichmann, F., Painsipp, E., Holzer, P., 2013. Environmental Enrichment and Gut Inflammation Modify Stress-Induced c-Fos Expression in the Mouse Corticolimbic System. PLoS One 8, 1–13. doi:10.1371/journal.pone.0054811

Rodríguez-Arias, M., Broseta, I., Aguilar, M. a., Miñarro, J., 2000. Lack of specific effects of selective D1 and D2 dopamine antagonists vs. risperidone on morphine-induced hyperactivity. Pharmacol. Biochem. Behav. 66, 189–197. doi:10.1016/S0091-3057(00)00207-0

Serrano, A., Aguilar, M. a., Manzanedo, C., Rodríguez-Arias, M., Miarro, J., 2002. Effects of DA D1 and D2 antagonists on the sensitisation to the motor effects of morphine in mice. Prog. Neuro-Psychopharmacology Biol. Psychiatry 26, 1263–1271. doi:10.1016/S0278-5846(02)00265-8

Shin, a. C., Pistell, P.J., Phifer, C.B., Berthoud, H.R., 2010. Reversible suppression of food reward behavior by chronic mu-opioid receptor antagonism in the nucleus accumbens. Neuroscience 170, 580–588. doi:10.1016/j.neuroscience.2010.07.017

Singh, M.E., Verty, a. N. a, Price, I., McGregor, I.S., Mallet, P.E., 2004. Modulation of morphine-induced Fos-immunoreactivity by the cannabinoid receptor antagonist SR 141716. Neuropharmacology 47, 1157–1169. doi:10.1016/j.neuropharm.2004.08.008

Slowe, S.J., Simonin, F., Kieffer, B., Kitchen, I., 1999. Quantitative autoradiography of mu-,delta- and kappa1 opioid receptors in kappa-opioid receptor knockout mice. Brain Res. 818, 335–345.

Soderman, a. R., Unterwald, E.M., 2008. Cocaine reward and hyperactivity in the rat: Sites of mu opioid receptor modulation. Neuroscience 154, 1506–1516. doi:10.1016/j.neuroscience.2008.04.063

Sora, I., Elmer, G., Funada, M., Pieper, J., Li, X.F., Hall, F.S., Uhl, G.R., 2001. μ Opiate receptor gene dose effects on different morphine actions: Evidence for differential in vivo μ receptor reserve. Neuropsychopharmacology 25, 41–54. doi:10.1016/S0893-133X(00)00252-9

Sora, I., Takahashi, N., Funada, M., Ujike, H., Revay, R.S., Donovan, D.M., Miner, L.L., Uhl, G.R., 1997. Opiate receptor knockout mice define mu receptor roles in endogenous nociceptive responses and morphine-induced analgesia. Proc. Natl. Acad. Sci. U. S. A. 94, 1544–1549. doi:10.1073/pnas.94.4.1544

Soria, G., Barbano, M.F., Maldonado, R., Valverde, O., 2008. A reliable method to study cue-, priming-, and stress-induced reinstatement of cocaine self-administration in mice. Psychopharmacology (Berl). 199, 593–603. doi:10.1007/s00213-008-1184-x

Soria, G., Mendizábal, V., Touriño, C., Robledo, P., Ledent, C., Parmentier, M., Maldonado, R., Valverde, O., 2005. Lack of CB1 cannabinoid receptor impairs cocaine self-administration. Neuropsychopharmacology 30, 1670–1680. doi:10.1038/sj.npp.1300707

Stinus, L., Le Moal, M., Koob, G.F., 1990. Nucleus accumbens and amygdala are possible substrates for the aversive stimulus effects of opiate withdrawal. Neuroscience 37, 767–773. doi:10.1016/0306-4522(90)90106-E

Stumm, R.K., Zhou, C., Schulz, S., Höllt, V., 2004. Neuronal types expressing mu- and delta-opioid receptor mRNA in the rat hippocampal formation. J. Comp. Neurol. 469, 107–118. doi:10.1002/cne.10997

Svingos, a L., Colago, E.E., Pickel, V.M., 2001. Vesicular acetylcholine transporter in the rat nucleus accumbens shell: subcellular distribution and association with mu-opioid receptors. Synapse 40, 184–192. doi:10.1002/syn.1041

Taha, S. a, Katsuura, Y., Noorvash, D., Seroussi, A., Fields, L., 2009. Convergent, not serial, striatal and pallidal circuits regulate opioid-induced food intake. Neuroscience 161, 718–733. doi:10.1016/j.neuroscience.2009.03.057.Convergent

Tzschentke, T.M., Schmidt, W.J., 1996. Morphine-induced catalepsy is augmented by NMDA receptor antagonists, but is partially attenuated by an AMPA receptor antagonist. Eur. J. Pharmacol. 295, 137–146. doi:10.1016/0014-2999(95)00667-2

Ungless, M. a, Magill, P.J., Bolam, J.P., 2004. Uniform inhibition of dopamine neurons in the ventral tegmental area by aversive stimuli. Science 303, 2040–2042. doi:10.1126/science.1093360

Vanderwende, C., Spoerlein, M.T., 1979. Morphine-induced catalepsy in mice: modification by drugs acting on neurotransmitter system 18, 633–637.

Wassum, K.M., Cely, I.C., Balleine, B.W., Maidment, N.T., 2011. Micro-opioid receptor activation in the basolateral amygdala mediates the learning of increases but not decreases in the incentive value of a food reward. J. Neurosci. 31, 1591–1599. doi:10.1523/JNEUROSCI.3102-10.2011

Weibel, R., Reiss, D., Karchewski, L., Gardon, O., Matifas, A., Filliol, D., Becker, J. a J., Wood, J.N., Kieffer, B.L., Gaveriaux-Ruff, C., 2013. Mu Opioid Receptors on Primary Afferent Nav1.8 Neurons Contribute to Opiate-Induced Analgesia: Insight from Conditional Knockout Mice. PLoS One 8, 1–18. doi:10.1371/journal.pone.0074706

Williams, J.T., Christie, M.J., Manzoni, O., 2001. Cellular and synaptic adaptations mediating opioid dependence. Physiol. Rev. 81, 299–343.

Xia, Y., Driscoll, J.R., Wilbrecht, L., Margolis, E.B., Fields, H.L., Hjelmstad, G.O., 2011. Nucleus accumbens medium spiny neurons target non-dopaminergic neurons in the ventral tegmental area. J. Neurosci. 31, 7811–7816. doi:10.1523/JNEUROSCI.1504-11.2011

Zimmermann, M., 1983. Ethical guidelines for investigations of experimental pain in conscious animals. Pain 16, 109–110. doi:10.1016/0304-3959(83)90201-4

Ziółkowska, B., Korostyński, M., Piechota, M., Kubik, J., Przewołcki, R., 2012. Effects of morphine on immediate-early gene expression in the striatum of C57BL/6J and DBA/2J mice. Pharmacol. Reports 64, 1091–1104.

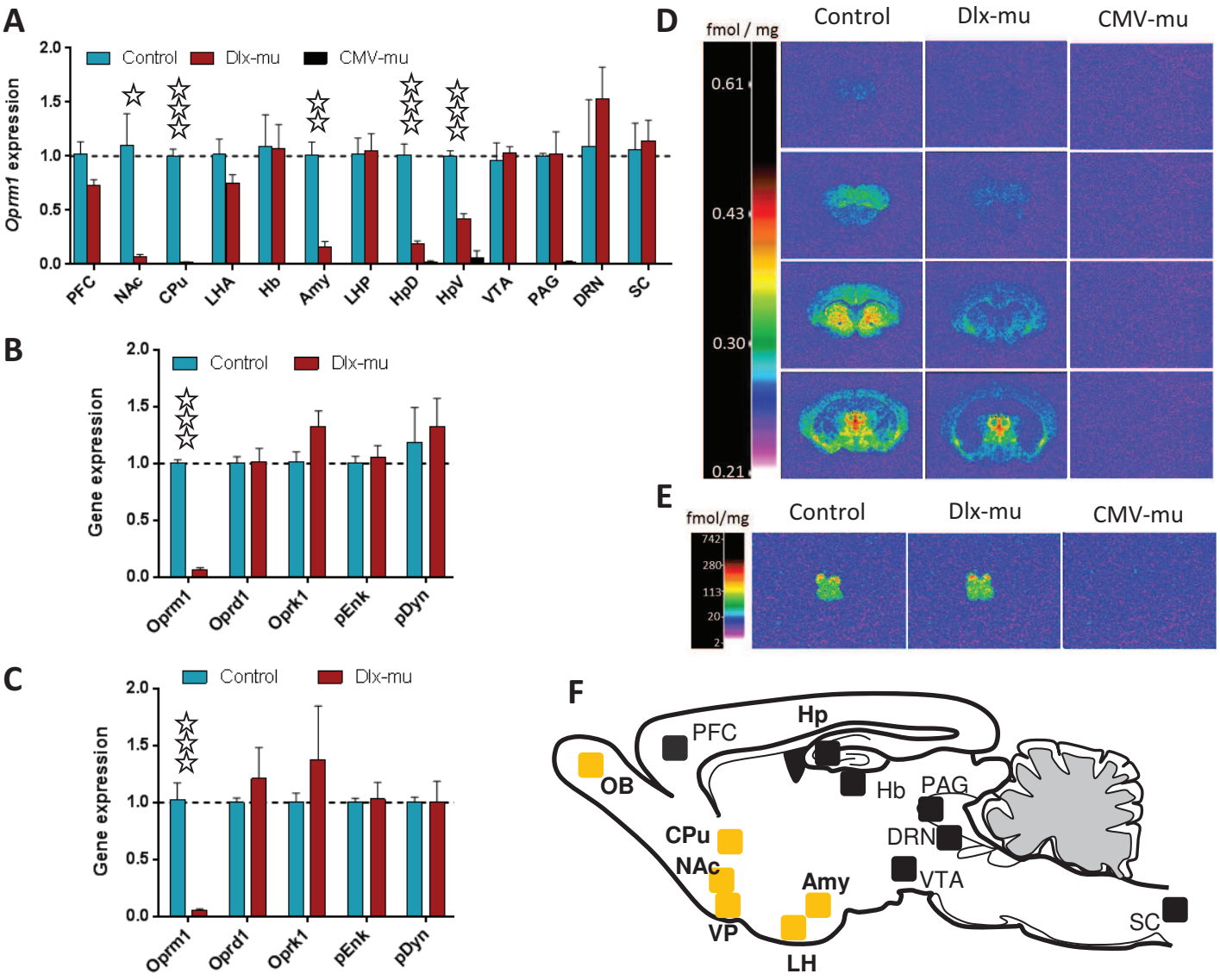

Figure 1. Neuroanatomical characterization of the conditional knockout animals. (**A-C**) Quantitative real-time polymerase chain reaction. Mu receptor gene (*Oprm1*) messenger RNA in Dlx-mu (conditional knockout) and CMV-mu (constitutive knockout) mice is represented according to the expression in Control (=1, dotted line) (**A**), normalized using β-actin as housekeeping gene. Messenger RNA expression of the opioid system genes in Dlx-mu mice is represented according to the expression in Control (=1, dotted line) in the CPu (**B**) and NAc (**C**). No *Oprm1* mRNA expression was detected in Dlx-mu mice. No changes in other genes mRNA expression were detected (one-way ANOVA). (**D, E**) Autoradiograms of brain sections (**D**) and spinal cords (**E**) in Control, Dlx-mu and CMV-mu mice. Mu receptor were labelled with [^{3}H]DAMGO. The color bar shows a pseudo-color interpretation of relative density of black and white images calibrated in fmol/mg tissue. Non-specific binding was homogenous and at background levels. The sections from the three genotypes were processed in parallel throughout binding and development of autoradiograms. (**F**) Summary of mu receptor protein deletion in Dlx-mu mice compared to Control, adapted from **Table 1**. Brain regions in yellow correspond to Dlx-mu mice structures that show a significant reduction of mu receptor protein compared to Control mice. n=3-4 per group. Open stars represent significant difference between Control and Dlx-mu mice. One star, $p<0.05$; two stars, $p<0.01$; three stars, $p<0.001$ (t-test). Amy, amygdala; CPu, caudate putamen; DRN, dorsal raphe nucleus; Hb, habenula; Hp, hippocampus; LH, lateral hypothalamus; NAc, nucleus accumbens; OB, olfactory bulbs; PAG, periaqueductal grey; PFC, prefrontal cortex; SC, spinal cord; VP, ventral pallidum; VTA, ventral tegmental area.

Table 1. Quantification of specific [^{3}H]DAMGO binding in brain sections from Control and Conditional knockout mice

Region	Bregma	[^{3}H]DAMGO-specific binding (fmol/mg tissue)		
		Control (n=3)	Dlx-mu (n=4)	% change
Olfactory bulb	3.56			
External plexiform Layer		21.4 ± 9.1	0.0 ± 0.0 ***	-100
Internal granular layer		21.8 ± 8.5	0.0 ± 0.1 ***	-100
Cortical areas				
Motor	2.1			
Superficial layers		41.8 ± 15.4	27.7 ± 9.6	-33.8
Deep layers		46.7 ± 6.9	30.2 ± 9.4	-35.4
Orbital	2.1			
Superficial layers		48.8 ± 14.6	57.2 ± 10.5	17.2
Deep layers		49.0 ± 9.0	48.1 ± 9.8	-1.7
Frontal	1.98			
Superficial layers		27.9 ± 10.4	29.9 ± 9.2	7.2
Deep layers		33.7 ± 10.6	34.4 ± 10.3	2.3
Cingulate	1.1			
Superficial layers		28.8 ± 10.9	32.1 ± 9.4	11.6
Deep layers		30.6 ± 2.6	32.7 ± 11.0	7.1
Frontal-Parietal	1.1			
Superficial layers		17.1 ± 3.7	25.9 ± 10.2	51.9
Deep layers		25.8 ± 6.2	31.4 ± 10.2	21.7
Rostral sosmatosensory	1.1			
Superficial layers		14.3 ± 4.3	22.2 ± 8.3	55.3
Deep layers		27.2 ± 7.0	28.3 ± 9.1	3.9
Parietal	-1.46			
Superficial layers		17.0 ± 9.1	16.0 ± 6.3	-5.9
Deep layers		25.0 ± 9.4	23.1 ± 8.1	-7.4
Caudal somatosensory	-2.06			
Superficial layers		14.9 ± 5.2	15.6 ± 5.1	4.7
Deep layers		25.8 ± 8.0	24.0 ± 8.3	-7
Retrosplenial	-2.06			
Superficial layers		22.6 ± 6.4	24.1 ± 8.5	6.6
Deep layers		38.0 ± 5.6	25.6 ± 7.1	-32.5
Temporal	-2.06			
Superficial layers		22.8 ± 6.6	25.7 ± 5.1	12.7
Deep layers		35.0 ± 8.8	36.9 ± 9.3	5.2
Auditory	-2.54			
Superficial layers		22.5 ± 6.7	23.3 ± 7.6	3.2
Deep layers		33.3 ± 11.1	35.6 ± 8.7	7.1
Visual	-3.52			
Superficial layers		32.9 ± 15.9	14.7 ± 7.1	-55.3
Deep layers		26.6 ± 7.2	18.1 ± 7.7	-31.8
Entorhinal	-3.64	53.5 ± 17.8	77.8 ± 9.5	45.5

Values of specific [^{3}H]DAMGO binding represent mean ± SEM fmol/mg of tissue equivalent in brain regions of wild-type (WT) and conditional mu receptor knockout mice. Bregma coordinates are taken from the mouse brain atlas of Franklin and Paxinos (1997). Specific binding was calculated after the subtraction of non-specific from total [^{3}H]DAMGO binding. Percent change in binding indicates change in conditional knockout compared to Control mice. N indicates number of animals per group. Two-way ANOVA revealed significant effect of genotype, region and genotype x region, all p<0.001. *Post hoc* Holm- ídák multiple comparisons revealed significant within-region differences compared to Control. One star, p<0.05; two stars, *p*<0.01; three stars, *p*<0.001.

Table 1. Continued

Region	Bregma	[^{3}H]DAMGO-specific binding (fmol/mg tissue) Control (n=3)	Dlx-mu (n=4)	% change
Nucleus accumbens	1.18			
Core		119.5 ± 4.5	33.7 ± 5.3 ***	-71.8
Shell		102.6 ± 4.9	32.2 ± 4.4 ***	-68.6
Caudate putamen	1.1	56.8 ± 12.7	27.2 ± 2.3 *	-52.1
Dorsal endopiriform nucleus	1.1	66.6 ± 7.3	73.3 ± 10.4	10.1
Septum	0.74			
Medial		56.6 ± 4.7	25.2 ± 8.1 *	-55.4
Lateral		35.6 ± 5.6	18.2 ± 6.7	-49
Vertical limb of the diagonal band		49.0 ± 8.2	21.9 ± 8.1	-55.4
Ventral pallidum	-0.22	66.4 ± 22.9	12.5 ± 1.3 ***	-81.1
Preoptic area	-0.22	53.4 ± 7.6	15.8 ± 6.6 *	-70.4
Amygdala	-1.46			
Basolateral		98.5 ± 14.9	104.5 ± 17.7	6.1
Basomedial		70.6 ± 13.9	32.2 ± 10.9 *	-54.4
Medial		59.6 ± 11.8	49.5 ± 13.7	-28.9
Medial habenula	-1.46	190.0 ± 19.4	221.0 ± 21.6	16.3
Thalamus	-1.46	61.0 ± 11.8	48.8 ± 11.1	-19.9
Central lateral		132.6 ± 17.5	112.1 ± 14.7	-15.5
Central medial		155.4 ± 28.3	140.8 ± 15.4	-9.4
Intermediodorsal thalamic nucleus		142.9 ± 37.2	157.8 ± 20.1	10.5
Reuniens		103.9 ± 26.5	69.6 ± 18.4	-33
Hypothalamus	-1.46	62.6 ± 10.7	24.8 ± 7.7 *	-60.4
Hippocampus	-2.06	26.1 ± 3.7	10.7 ± 7.0	-59
Dorsal hippocampus	-3.8	41.1 ± 20.2	23.9 ± 8.9	-41.8
Substantia nigra	-3.4	68.6 ± 12.5	40.1 ± 11.5	-41.6
Ventral tegmental area	-3.4	86.8 ± 9.0	67.7 ± 6.3	-22
Superficial grey	-3.4			
Superficial layer		83.0 ± 14.5	78.6 ± 7.9	-5.3
Intermediate layer		87.3 ± 7.7	74.6 ± 5.1	-14.4
Medial geniculate nucleus	-3.4	48.5 ± 12.7	11.7 ± 3.0 *	-75.9
Periaqueductal grey	-3.4	59.1 ± 6.0	39.4 ± 9.2	-33.3
Interpeduncular nucleus	-3.64	83.1 ± 18.7	67.1 ± 33.9	-19.2
Spinal cord				
Cervical (C6)				
Whole section		41.7 ± 15.9	55.3 ± 12.8	32.5
Superficial layers (lamina I and II)		80.3 ± 22.9	95.0 ± 12.9	18.3
Laminas III-IV		36.0 ± 8.5	50.7 ± 7.8	40.9
Lamina X		39.6 ± 18.6	48.2 ± 10.3	21.9
Ventral horn (laminas VII -IX)		33.2 ± 8.9	46.1 ± 7.5	38.5

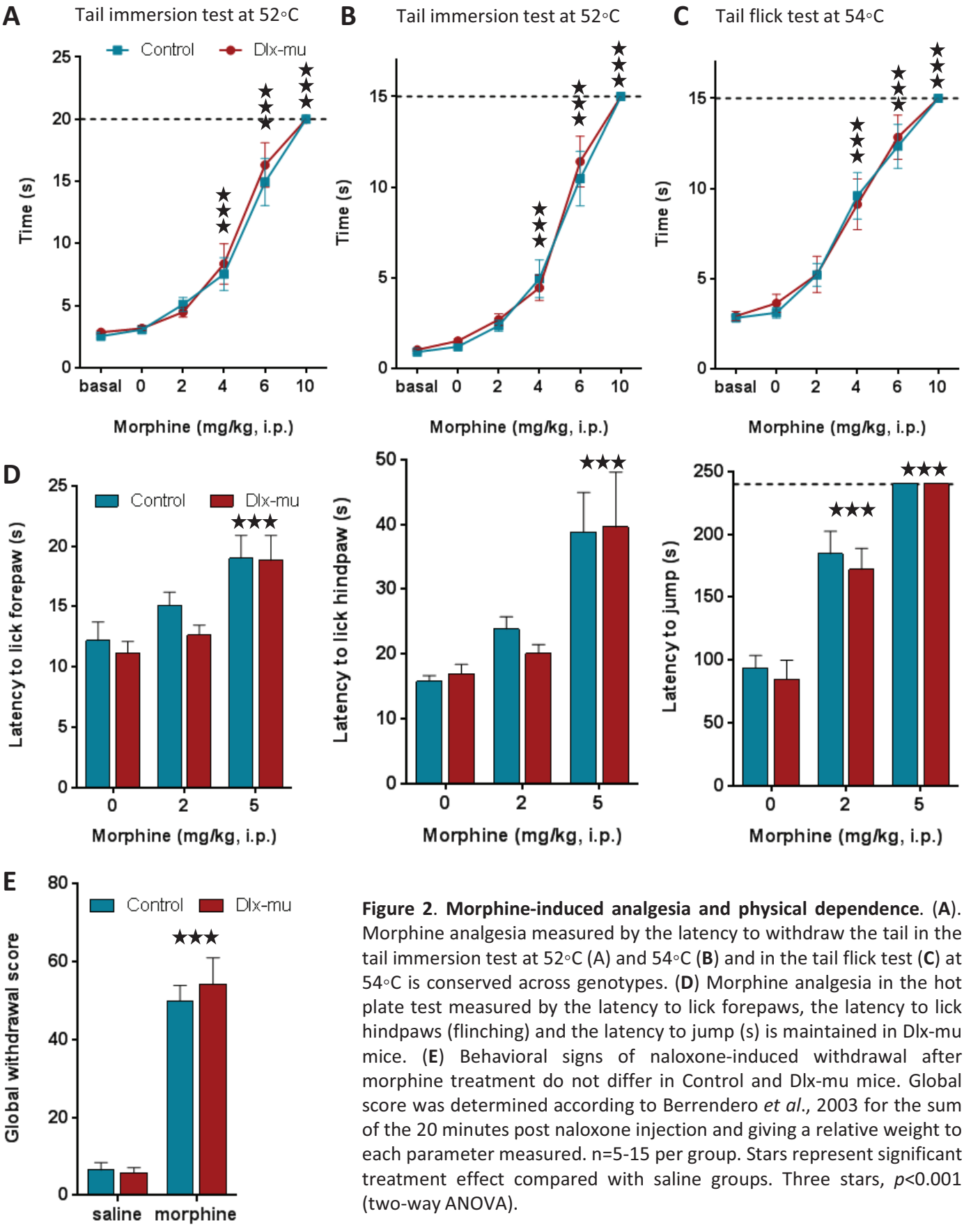

Figure 2. **Morphine-induced analgesia and physical dependence**. (**A**). Morphine analgesia measured by the latency to withdraw the tail in the tail immersion test at 52◦C (A) and 54◦C (**B**) and in the tail flick test (**C**) at 54◦C is conserved across genotypes. (**D**) Morphine analgesia in the hot plate test measured by the latency to lick forepaws, the latency to lick hindpaws (flinching) and the latency to jump (s) is maintained in Dlx-mu mice. (**E**) Behavioral signs of naloxone-induced withdrawal after morphine treatment do not differ in Control and Dlx-mu mice. Global score was determined according to Berrendero *et al*., 2003 for the sum of the 20 minutes post naloxone injection and giving a relative weight to each parameter measured. n=5-15 per group. Stars represent significant treatment effect compared with saline groups. Three stars, $p<0.001$ (two-way ANOVA).

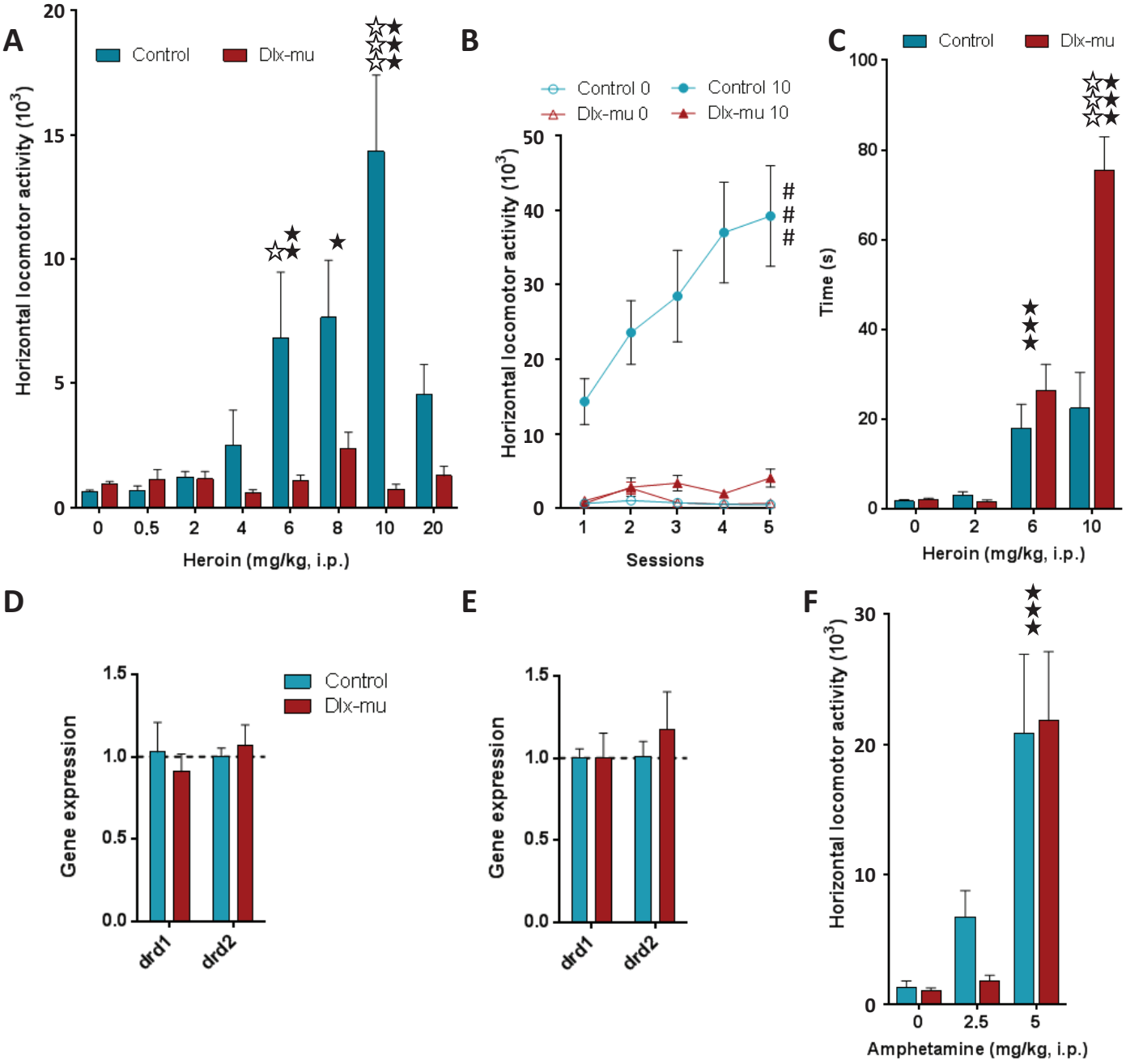

Figure 3. **Pharmacological modification of locomotion, sensitization to hyperlocomotion and catalepsy**. Upper panels show heroin motor effects, lower panels show dopaminergic compounds locomotor effects. (**A**) Activity after heroin intraperitoneal injection was measured over a 2h-session. Heroin increased locomotor activity in Control mice at 6, 8 and 10 mg/kg, but not in Dlx-mu mice. Difference between genotypes was found at 6 and 10 mg/kg. (**B**) Sensitization to 10 mg/kg heroin locomotor effects was assessed for 5 2h-sessions. Control mice showed locomotor sensitization but not Dlx-mu animals. (**C**) Catalepsy was evaluated in the bar test, 30 min after intraperitoneal heroin administration. Heroin produced catalepsy in both genotypes at 6 and 10 mg/kg, and that effect is stronger in Dlx-mu mice at the highest heroin dose tested. (**D**) Messenger RNA expression of the dopamine receptor genes in Dlx-mu mice is represented according to the expression in Control (=1, dotted line) in the CPu (**D**) and NAc (**E**). No changes in *DA receptor* mRNA expression were detected (one-way ANOVA). (**F**) Activity after amphetamine intraperitoneal injection was measured over a 2h-session. Amphetamine increased locomotor activity in Control and Dlx-mu mice at 5 mg/kg. No difference between genotypes was observed. n=5-33 per group. Black stars represent significant treatment effect compared with saline groups, open stars represent significant difference between genotypes, # represents significant difference between groups. One symbol, p<0.05; two symbols, *p*<0.01; three symbols, *p*<0.001 (two-way ANOVA for locomotion and bar test, three-way ANOVA for sensitization).

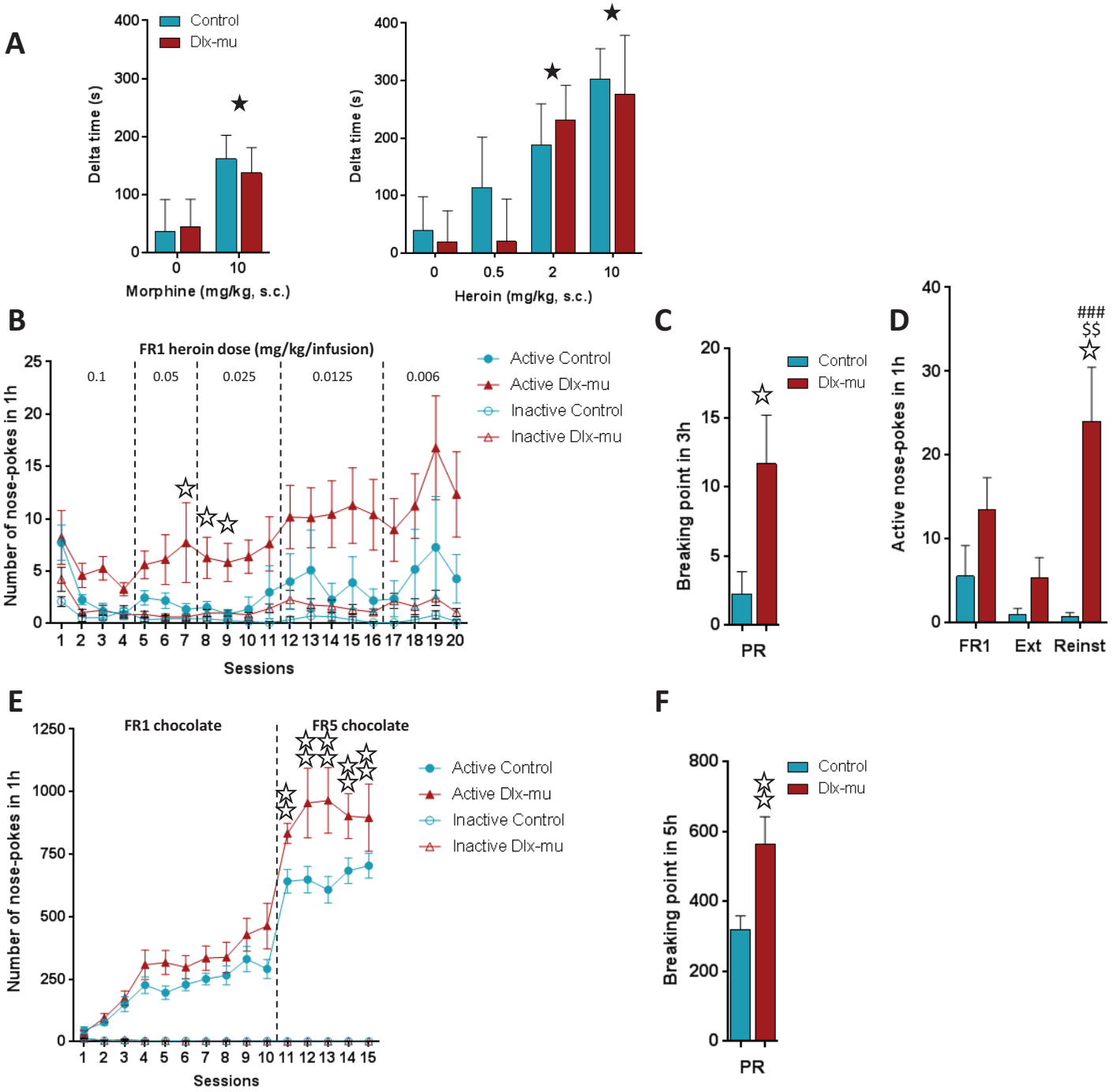

Figure 4. **Reward and motivation behavior**. (**A**) Opiate-induced reward was assessed in a 6-session conditioned place preference paradigm. Conditioned place preference is represented as a delta time (pre-conditioning minus post-conditioning time spent in the drug-paired compartment). Left, morphine was rewarding at 10 mg/kg (s.c) in both genotypes. Right, heroin induced a place preference at 2 and 10 mg/kg (s.c.) and this effect did not differ across genotypes. (**B**) Operant conditioning maintained by heroin to assess the primary reinforcing effects of the drug. Acquisition of heroin self-administration started to be significantly higher in Dlx-mu mice at sessions 7-9 at the dose of 0.025 mg/kg/infusion and was maintained in the following lower doses. (**C**) Motivation for heroin (0.0125 mg/kg/inf). Breaking point achieved in a 3h-PR session revealed an increased motivation for heroin in Dlx-mu mice. (**D**) Cue-induced reinstatement (acquisition at 0.006 mg/kg/inf). After an extinction phase, cue-induced reinstatement is only observed in Dlx-mu mice. (**E**) Operant conditioning maintained by chocolate-flavored pellets. Mean number of active and inactive nose-pokes during 10 days of FR1 and 5 days of FR5 in 1 h daily sessions. (**F**) Motivation for chocolate-flavored pellets. Mean breaking point achieved in a session of progressive ratio that was conducted once and lasted 5 h. n=4-21 per group in CPP, n=11-20 per group in operant paradigms. Black stars represent significant treatment effect compared with saline groups, open stars represent significant difference between genotypes, $ represents significant difference with acquisition phase, # represents significant difference with extinction phase. One symbol, $p<0.05$; two symbols, $p<0.01$; three symbols, $p<0.001$ (two-way ANOVA in CPP, one-way ANOVA in self-administration). FR, fixed ratio; PR, progressive ratio; ext, extinction; Reinst, reinstatement.

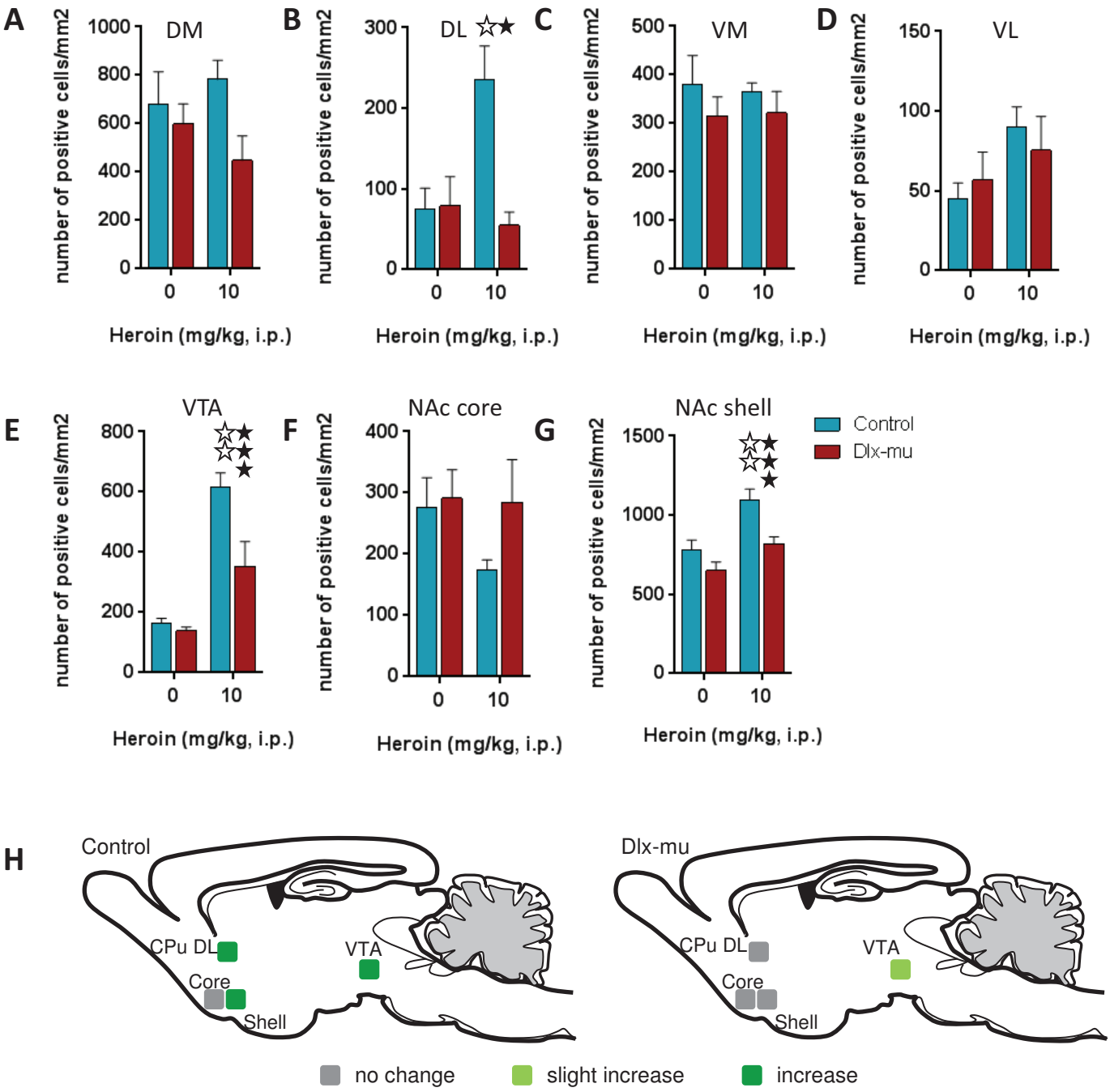

Figure 5. c-Fos immunoreactivity in Control and Dlx-mu mice. Immunohistochemistry for c-Fos protein was assessed on brain sections from animals perfused 2h after saline or heroin administration (10 mg/kg, i.p.). Number of positive neurons were manually scored on defined regions and data were expressed on c-Fos positives cells per mm2. Heroin induced c-Fos in the dorsolateral CPu (**B**), VTA (**E**) and NAc shell (**G**) of the Control group, and in the VTA in Dlx-mu group. Treatment had no effect on c-Fos induction in dorsomedial (**A**), ventrolateral (**D**) and ventromedial CPu (**C**) and NAc core (**F**). Schematic summary of c-Fos immunoreactivity in both Control and Dlx-mu groups after heroin administration (**H**).

n=5-6 per group. Black stars represent significant treatment effect, open stars represent significant genotype effect. One star, $p<0.05$; two stars, $p<0.01$; three stars, $p<0.001$ (two-way ANOVA). CPu, caudate putamen; DL, dorsolateral; DM, dorsomedial; NAc, nucleus accumbens; VL, ventrolateral; VM, ventromedial; VTA, ventral tegmental area.

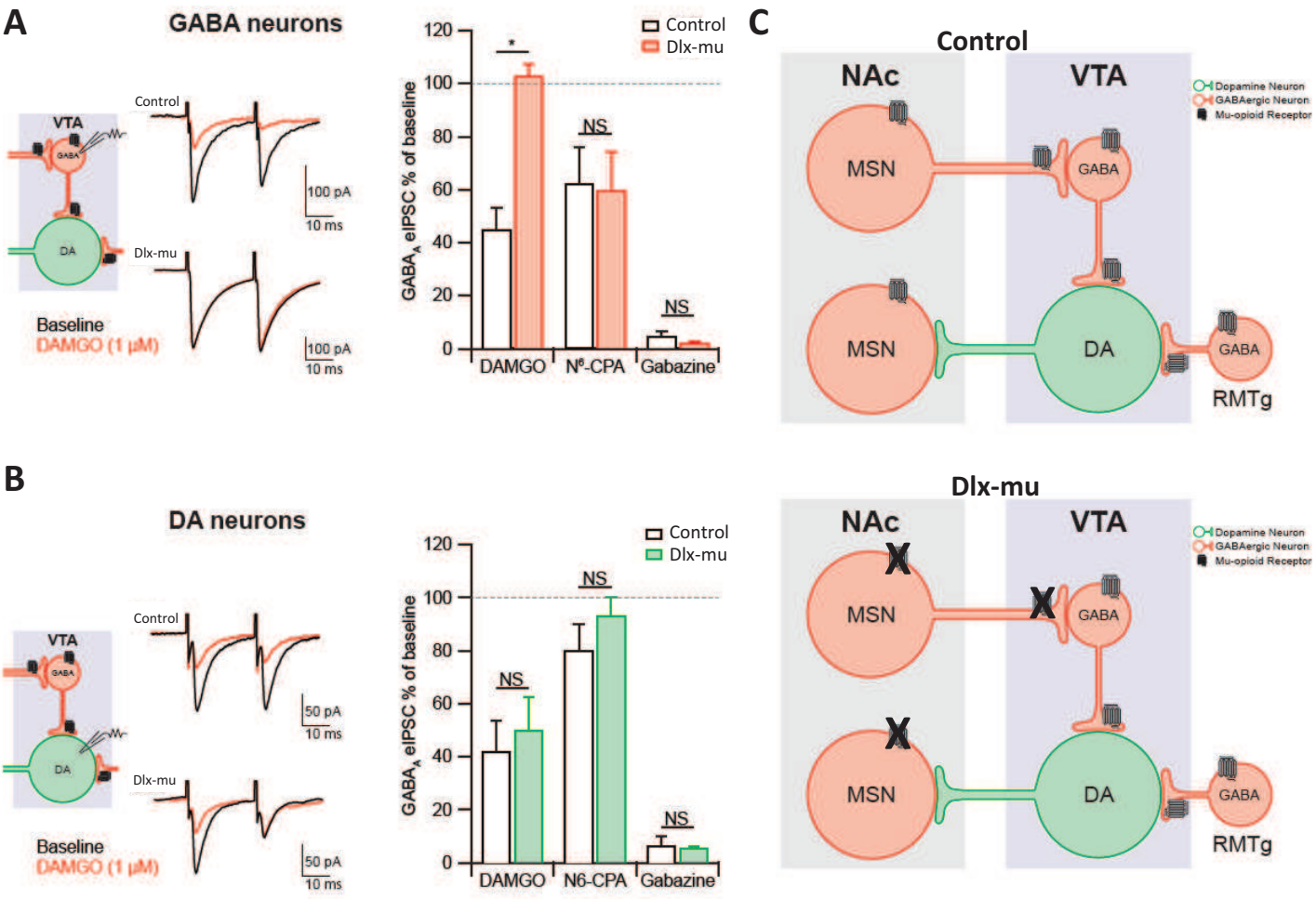

Figure 6. Electrophysiological characterization of the VTA neurons of conditional knockout animal. (**A**) Evoked IPSCs in GABAergic neurons of the VTA. Amplitude of GABA-A IPSCs was decreased after application of DAMGO (1 µM) in Control but not in Dlx-mu animals. Differences across genotypes in eIPCSs were not found after adenosine agonist application (N6-CPA, 1 µM). (**B**) Evoked IPCSs in dopaminergic neurons of the VTA. Amplitude of GABA-A IPSCs was decreased after application of DAMGO (1 µM) and N6-CPA (1 µM) in the same way in Control and Dlx-mu mice. (**C**) Schematic representation of mu receptor localization (black) in dopaminergic (green) and GABAergic (red) neurons od the VTA and NAc. Upper panel, localization in Control; lower panel, localization in Dlx-mu mice. n=8-10 per group. Stars represent significant difference between Control and Dlx-mu mice. One star, $p<0.05$ (t-test). DA, dopamine; NAc, nucleus accumbens; VTA, ventral tegmental area.

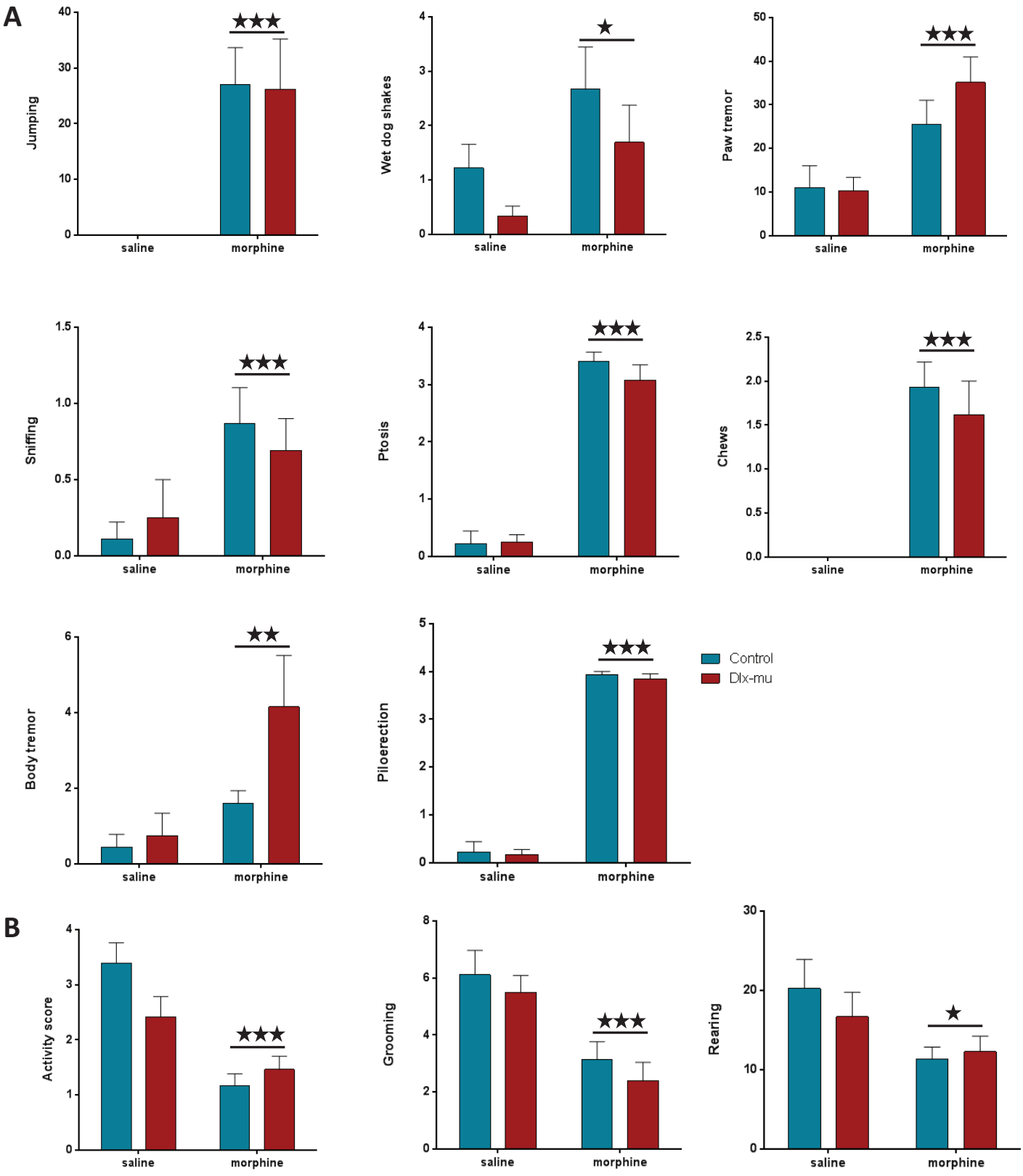

Figure S1. Behavioral signs of naloxone-induced withdrawal after chronic morphine treatment in control and Dlx-mu mice. Each sign was scored 5 minutes prior and 20 minutes post naloxone injection. Data showed the sum of the 20 minutes post naloxone injection. **(A)** Signs included in global score. **(B)** Supplementary signs scored. n=9-15 per group. Stars represent treatment effect. One star, P<0.05; two stars, P<0.01; three stars, P<0.001 (Two-way ANOVA).

		Df1	Df2	F	*p*-value	
Jump	genotype	1	45	0.004335	0.9478	
	treatment	1	45	17.11	0.0002	***
	genotype x treatment	1	45	0.004335	0.9478	
Wet dog shake	genotype	1	45	2.117	0.1526	
	treatment	1	45	4.792	0.0338	*
	genotype x treatment	1	45	0.004454	0.9471	
Paw tremor	genotype	1	45	0.7086	0.4043	
	treatment	1	45	14.01	0.0005	***
	genotype x treatment	1	45	0.9686	0.3303	
Sniffing	genotype	1	45	0.006059	0.9383	
	treatment	1	45	6.91	0.0117	*
	genotype x treatment	1	45	0.4726	0.4953	
Ptosis	genotype	1	45	0.5199	0.4746	
	treatment	1	45	215	<0.0001	****
	genotype x treatment	1	45	0.7339	0.3962	
Chews	genotype	1	45	0.3364	0.5648	
	treatment	1	45	41.9	<0.0001	****
	genotype x treatment	1	45	0.3364	0.5648	
Body tremor	genotype	1	45	2.976	0.0914	
	treatment	1	45	7.566	0.0085	**
	genotype x treatment	1	45	1.84	0.1817	
Piloerection	genotype	1	45	0.3456	0.5596	
	treatment	1	45	926.5	<0.0001	****
	genotype x treatment	1	45	0.01696	0.897	
Activity	genotype	1	45	1.303	0.2597	
	treatment	1	45	28.67	<0.0001	****
	genotype x treatment	1	45	4.56	0.0382	
Grooming	genotype	1	45	0.9898	0.3251	
	treatment	1	45	19.87	<0.0001	****
	genotype x treatment	1	45	0.010147	0.9203	
Rearing	genotype	1	45	0.2776	0.6008	
	treatment	1	45	7.214	0.01	*
	genotype x treatment	1	45	0.8326	0.3663	

Table S1. Statistical analysis (two-way ANOVA) of behavioral signs of naloxone-induced withdrawal after morphine treatment in Control and Dlx-mu mice. Upper table, signs included in the global score; lower table, supplementary signs scored.

A

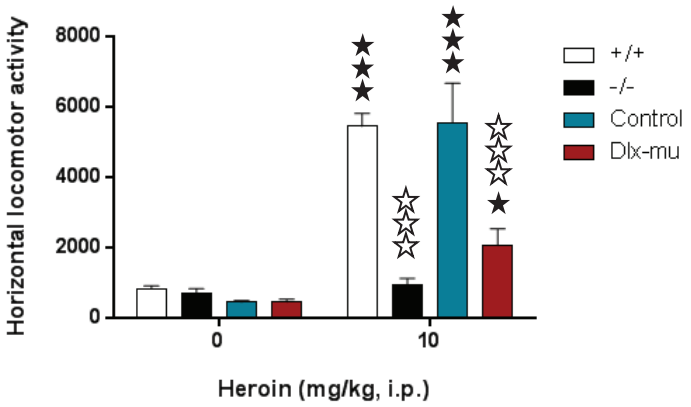

B

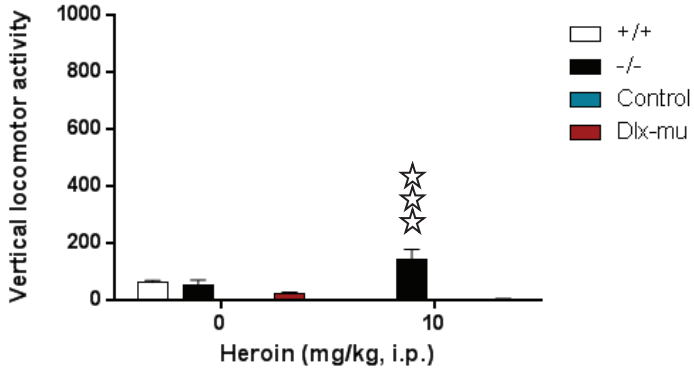

Figure S2. Heroin-induced hyperlocomotor activity in a 2-h session. **(A)** Horizontal activity after intraperitoneal heroin injection was measured over a 2h-session. Heroin increased locomotor activity in +/+, Control and Dlx-mu mice at 10 mg/kg, but not in -/- mice. Both -/- and Dlx-mu at 10 mg/kg heroin are different from +/+ and Control animals. **(B)** Vertical activity after intraperitoneal heroin injection was measured over a 2h-session. Heroin increased vertical activity only in -/- mice. Genotype difference was found between -/- and the other groups.

n=6-11 per group. Black stars represent significant treatment effect compared with saline groups, open stars represent significant difference between genotypes. One star, $p<0.05$; two stars, $p<0.01$; three stars, $p<0.001$ (two-way ANOVA).

	Three-way ANOVA			
	Acquisition 0.1 mg/kg/inf		Acquisition 0.05 mg/kg/inf	
	F-value	*P*-value	*F*-value	*P*-value
Genotype	$F_{(1,26)}$ = 3.61	*n.s.*	$F_{(1,27)}$ = 2.55	*n.s.*
Hole	$F_{(1,26)}$ = 20.40	*P* < 0.001	$F_{(1,27)}$ = 6.27	*P* < 0.001
Day	$F_{(3,78)}$ = 8.73	*P* < 0.001	$F_{(2,54)}$ =0.04	*n.s.*
Genotype × Hole	$F_{(1,26)}$ = 2.63	*n.s.*	$F_{(1,27)}$ = 2.05	*n.s.*
Genotype × Day	$F_{(3,78)}$ = 0.36	*n.s.*	$F_{(2,54)}$ = 0.43	*n.s.*
Hole × Day	$F_{(3,78)}$ = 1.58	*n.s.*	$F_{(2,54)}$ = 007	*n.s.*
Genotype × Hole × Day	$F_{(3,78)}$ = 7.14	*n.s.*	$F_{(2,54)}$ = 058	*n.s.*
	Acquisition 0.025 mg/kg/inf		Acquisition 0.0125 mg/kg/inf	
	F-value	*P*-value	*F*-value	*P*-value
Genotype	$F_{(1,2)}$ = 5.44	*P* < 0.05	$F_{(1,27)}$ = 2.81	*n.s.*
Hole	$F_{(1,2)}$ = 10.08	*P* < 0.01	$F_{(1,27)}$ = 8.64	*P* < 0.001
Day	$F_{(2,54)}$ = 0.19	*n.s.*	$F_{(5,135)}$ = 1.53	*n.s.*
Genotype × Hole	$F_{(1,2)}$ = 4.75	*P* < 0.05	$F_{(1,27)}$ = 1.91	*n.s.*
Genotype × Day	$F_{(2,54)}$ = 0.02	*n.s.*	$F_{(5,135)}$ = 0.72	*n.s.*
Hole × Day	$F_{(2,54)}$ = 0.28	*n.s.*	$F_{(5,135)}$ = 1.10	*n.s.*
Genotype × Hole × Day	$F_{(2,54)}$ = 0.01	*n.s.*	$F_{(5,135)}$ = 1.34	*n.s.*
	Acquisition 0.006 mg/kg/inf		Extinction and cue-induced reinstatement	
	F-value	*P*-value	*F*-value	*P*-value
Genotype	$F_{(1,27)}$ = 1.92	*n.s.*	$F_{(1,27)}$ = 5.88	*P* < 0.05
Hole	$F_{(1,27)}$ = 73.78	*P* < 0.01	$F_{(1,27)}$ = 10.46	*P* < 0.01
Day/Experimental phase	$F_{(3,81)}$ = 25.50	*P* < 0.01	$F_{(2,54)}$ = 4.97	*P* < 0.05
Genotype × Hole	$F_{(1,27)}$ = 1.94	*n.s.*	$F_{(1,27)}$ = 5.29	*P* < 0.05
Genotype × Day	$F_{(3,81)}$ = 1.80	*n.s.*	$F_{(2,54)}$ = 5.80	*P* < 0.01
Hole × Day	$F_{(3,81)}$ = 24.30	*P* < 0.05	$F_{(2,54)}$ = 4.06	*P* < 0.05
Genotype × Hole × Day	$F_{(3,81)}$ = 1.91	*n.s.*	$F_{(2,54)}$ = 4.61	*P* < 0.05

Three-way ANOVA with genotype as between-subjects factor and repeated measures in the factors day/experimental phase and hole (active/inactive). See materials and methods for details. *n.s.:* non significant

Table S2. Operant responding maintained by heroin during acquisition (0.1, 0.05, 0.025, 0.0125 and 0.006 mg/kg per injection, i.v.), extinction and cue-induced reinstatement.

	Three-way ANOVA			
	Acquisition FR1		Acquisition FR5	
	F-value	*P*-value	*F*-value	*P*-value
Genotype	$F_{(1,31)}$ = 2.87	*n.s.*	$F_{(1,31)}$ = 6.88	*P* < 0.01
Hole	$F_{(1,31)}$ = 122.15	*P* < 0.001	$F_{(1,31)}$ = 259.91	*P* < 0.001
Day	$F_{(9,279)}$ = 31.40	*P* < 0.001	$F_{(4,124)}$ = 0.81	*n.s.*
Genotype × Hole	$F_{(1,31)}$ = 2.79	*n.s.*	$F_{(1,31)}$ = 6.80	*P* < 0.05
Genotype × Day	$F_{(9,279)}$ = 1.75	*n.s.*	$F_{(4,124)}$ = 1.55	*n.s.*
Hole × Day	$F_{(9,279)}$ = 34.46	*P* < 0.001	$F_{(4,124)}$ = 0.78	*n.s.*
Genotype × Hole × Day	$F_{(9,279)}$ = 1.83	*n.s.*	$F_{(4,124)}$ = 1.56	*n.s.*

Three-way ANOVA with genotype as between-subjects factor and repeated measures in the factors day and hole (active/inactive). See materials and methods for details. *n.s.:* non significant

Table S3. Operant responding maintained by chocolate-flavoured food-pellets during acquisition at FR1 and FR5 schedule of reinforcement.

PART II

Autistic-like syndrome in Dlx-mu mice

Introduction

I. The autistic-like syndrome

The autism spectrum disorder (ASD) is a neurodevelopmental disorder characterized by persistent deficits in social communication, social interaction and restricted repetitive patterns of behavior, interests, or activities. Those symptoms are present in the early developmental period, and lead to significant impairment in social or occupational areas of current functioning (DSM V). In addition to main symptoms, ASD patients can present seizures, intellectual disabilities among other secondary symptoms (Johnson and Myers, 2007). Recently, the global prevalence of ASD was estimated at 62/10 000 (Elsabbagh et al., 2012).

ASD has a high genetic heterogeneity, and modeling the complete pathophysiology remains difficult. To date, there is no universally accepted animal model of autism that would recapitulate the entire syndrome. A reductionist approach helps to better understand the potential common pathological mechanisms of ASD. Many genes have been implicated in ASD, including neuroligins, neurexins, contactins, cadherins, ion channels, Shank protein family or cytoskeletal proteins (for review, see Banerjee et al., 2014; Crawley, 2012; Ellegood et al., 2014; Persico and Bourgeron, 2006) and several monogenic mouse models have been described, including the fragile X mental retardation 1 KO (*Fmr1*) mice, based on reported autistic-like phenotype (Oddi et al., 2013) or KO mice for the mu opioid receptor involved in social reward.

II. The mu opioid receptor in social behavior and autistic-like syndrome

Social motivation is composed of social orienting (preference for social world), social reward (to seek and take pleasure in social interactions) and social maintaining (foster and maintain social bond). Lack of social learning experiences can affect the development of mature social cognitive skills. The deficit in social cognition can therefore be a consequence of disrupted social interest. This statement led to the establishment of the social motivation theory of autism (Chevallier et al., 2012). The mu opioid receptor is highly implicated in reward and motivation. Mu KO mice have been proposed as a monogenic model of autism (Oddi et al., 2013), and our laboratory reported a wide array of ASD-like

behaviors, such as social interaction deficits, perseverative behaviors, and exacerbated anxiety in these mutant mice (Becker et al., 2014).

III. Aim of the study: an autistic-like syndrome in Dlx-mu mice?

I focused on the role of mu receptors in autistic-like behaviors. Based on previous work by our team (Becker et al., 2014), I evaluated the social behavior, which is a core symptom of ASD, as well as anxiety-like and conflict responses, which are secondary symptoms. This work is presented in a manuscript in preparation: *Mu opioid receptors in GABAergic forebrain neurons are not involved in autistic-like symptoms*. Charbogne P, Matifas A, Befort K, Kieffer BL. In complement, I also investigated motor impairments, which are considered secondary symptoms of ASD.

Manuscript 2

Mu opioid receptors in GABAergic forebrain neurons are not involved in autistic-like symptoms.

Pauline Charbogne[1,2], Audrey Matifas[1], Katia Befort[3], Brigitte L. Kieffer[1,2*].

[1] Institut de Génétique et de Biologie Moléculaire et Cellulaire, CNRS/INSERM/Université de Strasbourg, 1 rue Laurent Fries, 67404 Illkirch, France

[2] Douglas Mental Health Institute, Department of Psychiatry, McGill University, 6875 boulevard LaSalle, H4H 1R3 Montreal, QC, Canada

[3] CNRS, Laboratoire de Neurosciences Cognitives et Adaptatives – UMR7364, Faculté de Psychologie, Neuropôle de Strasbourg – Université de Strasbourg, Strasbourg, France

* Corresponding author. Douglas Mental Health Institute, Department of Psychiatry, McGill University, 6875 boulevard LaSalle, H4H 1R3 Montreal, QC, Canada

Phone: 514 761-6131 ext.: 3175; fax: 514 762-3033

brigitte.kieffer@douglas.mcgill.ca

ABSTRACT

Mu opioid receptor knockout mice (mu KO) have been shown to recapitulate a full spectrum of autistic-like behaviors, however neural circuit mechanisms underlying this phenotype have not been explored. To identify mu opioid receptors responsible for the autistic-like syndrome of total mu KO mice, we targeted the *Oprm1* gene in GABAergic forebrain neurons. The conditional Dlx5/6-Cre X *Oprm1*$^{fl/fl}$ (Dlx-mu) mice showed strongly reduced receptor expression mainly in striatum and amygdala, involved in social reward and anxiety. We then examined social skills and anxiety-like behaviors, representing main core and secondary symptoms of autism spectrum disorders (ASDs). As in our previous report, social interactions were impaired in mu KO mice, but there was no deficit in Dlx-mu animals. Moreover, total KO mice showed increased levels of anxiety in both marble burying and novelty-suppressed feeding tests, as shown previously, however this deficit was absent in conditional Dlx-mu mice. In addition, there was no detectable phenotype in Dlx-mu mice, whether Dlx-mu mice and controls were raised separately or together. In conclusion, the genetic deletion of mu opioid receptors expressed in GABAergic forebrain is not sufficient to induce an autistic-like syndrome in mice.

Keywords: conditional gene knockout, mu opioid receptor, GABAergic forebrain neurons, autism spectrum disorder, social interaction, anxiety-like behavior.

INTRODUCTION

The autism spectrum disorder (ASD) is a neurodevelopmental disorder characterized by persistent deficits in social communication and social interaction as well as restricted, repetitive patterns of behavior, interests, or activities (DSM V). Deficit in social motivation, that includes social orienting, social reward and social maintaining parameters, has been proposed to be a primary component of autism (Chevallier et al., 2012).

The mu opioid receptor is involved in reward, but also in numerous social behaviors, including maternal care, attachment behavior and social interaction. In rats, morphine was shown to disrupt maternal behavior during lactation, a behavior reversed by naloxone (Bridges and Grimm, 1982), more precisely by acting in the periaqueductal grey (PAG) (Miranda-Paiva et al., 2003). Mu opioid receptor knockout (mu KO) mice pups neither show a preference for their mother's cues nor reach the same level of maternal separation-induced vocalizations than the wild type pups (Moles et al., 2004). This study concluded on a deficit in attachment behavior in mu KO pups, a phenotype that could be considered as reflecting a main ASD component (Moles et al., 2004). Mu opioid receptors are involved in psychosocial stress, as revealed by the reduced aversion to social contact post social defeat stress in mu KO mice (Komatsu et al., 2011). Permanent (KO) and transient (naltrexone treatment) disruptions of mu opioid neurotransmission impair positive affect from social contact and affiliations, as shown by a reduced interest in peers or absence of socially rewarding environment preference in mice (Cinque et al., 2012). Finally, mice with the *Oprm1* A112G single nucleotide polymorphism showed increased dominance and social affiliation, that is blocked by pre-treatment with naloxone (Briand et al., 2015). In humans, mu opioid receptor is also associated to social attachment (Troisi et al., 2011). Individuals expressing the minor allele (G) of the A118G polymorphism have an increased tendency to become engaged in affectionate relationships and experienced more pleasure in social situations in comparison with major allele (A) subjects (Troisi et al., 2011). Using positron emission tomography, mu receptor was shown regulated by social distress (rejection) and reward (acceptance) in humans (Hsu et al., 2013).

Due to the high implication of the mu opioid receptor in social motivation, mu KO mice have been proposed as a monogenic model of ASD (Oddi et al., 2013). The main brain regions involved in social motivation are the amygdala, ventral striatum and prefrontal cortex (Chevallier et al., 2012). Moreover, GABA signaling is altered in ASD (reviewed in Cellot and Cherubini, 2014). In the present study, we investigated whether conditional Dlx-mu mice, which show strong reduction of mu receptors

in GABAergic neurons of the forebrain including striatum and amygdala (Charbogne et al., in preparation, Part I) are implicated in some of the ASD-like phenotypes observed in the mu KO mice.

MATERIALS AND METHODS

Animals

Experiments were performed on male and female mice aged 8-12 weeks at the beginning of the study. Dlx5/6-Cre line was successfully used in previous studies to conditionally invalidate cannabinoid CB1 receptors (Monory et al., 2006) and delta opioid receptors (Chu Sin Chung et al., 2015). The mu floxed mouse line (*Oprm1*$^{fl/fl}$) has been previously described by our group (Weibel et al., 2013). Briefly, exons 2 and 3 of the mu receptor gene *Oprm1* are flanked by loxP sites. *Oprm1*$^{fl/fl}$ mice show intact mu receptor expression (Weibel et al., 2013). To generate a conditional knockout for *Oprm1* in GABAergic forebrain neurons, the Dlx5/6-Cre-*Oprm1*$^{-/-}$ mouse line was created at the ICS-IGBMC (Institut Clinique de la Souris - Institut de Génétique et de Biologie Moléculaire et Cellulaire, Illkirch, France) by breeding the Dlx5/6-Cre mice (obtained from Beat Lutz laboratory, Institute of Physiological Chemistry, Johannes Gutenberg University, Germany) with mu floxed mice. Resulting Cre positive (Cre(+), Dlx5/6-Cre-*Oprm1*$^{-/-}$) animals are called Dlx-mu and Cre negative (Cre(-), *Oprm1*$^{fl/fl}$) are Control. To test whether Control littermates have an influence on the development of potential autistic-like phenotype in Dlx-mu animals, we separated genotypes before postnatal day 3. New born mice were genotyped quickly after birth and assigned to a separated (only one genotype among pups) or mixed (half Controls and half Dlx-mu) group. To avoid stress bias in separated genotypes groups, we also exchanged the mixed pups cages. As a control experiments (Becker 2014), we also tested mu opioid receptor knockout (KO) and their control (named wild type, WT), previously described in (Matthes et al., 1996). The latter mutants have a different genetic background (50% C57BL/6J-50% 129SvPas) compared to Dlx-mu and Controls (63% C57BL/6J-37% 129SvPas).

All experiments were carried out according to the recommendations of the European Communities Council Directive of September 22, 2010 (directive 2010/63/UE). The study protocols were approved by the local bioethics committee (Comité d'Éthique pour l'Expérimentation Animale, Institut Clinique de la Souris - Institut de Génétique et de Biologie Moléculaire et Cellulaire, Illkirch, France). Experiments were performed on male and female mice 8/12-week old at the beginning of the study, habituated to the experimental environment and handled for 2 days before behavioral testing. Experimental room light was set at 15 lux for all the tests (exceptions are indicated in the behavioral

method section). All behavioral testing was performed with the observer blind to the genotype. All animals were housed in a room maintained at 21±2°C and 45±5% humidity, with a 12h light-dark cycle. Food and water were available *ad libitum*.

Genotyping-PCR

PCR analysis on genomic DNA were performed in order to genotype the mice for presence of 1) Cre recombinase, 2) loxP sites and 3) excision of *Oprm1*. PCR was carried out on DNA DNA obtained from the collected mouse digits digested with Proteinase K (NaCl 0.2M; Tris-HCl 100 mM pH8.5; EDTA 5mM; SDS 0.2%; proteinase K (Sigma) 10 mg/mL) overnight at 55°C.

The Cre PCR reaction was performed by adding 0.5 µL lysate to 49.5 µL reaction mix (1X PCR buffer (Sigma); $MgCl_2$ (Sigma) 2.5 mM; dNTPs 0.2 mM (Thermo Scientific); TAQ DNA polymerase 2.5 U (Sigma); forward *Cre* primer (5'-GAT CGC TGC CAG GAT ATA CG-3'), reverse *Cre* primer (5'-CAT CGC CAT CTT CCA GCA G-3'), forward *myosin* gene primer (5'-TTA CGT CCA TCG TGG ACA GC-3'), reverse *myosin* gene primer (5'-TGG GCT GGG TGT TAG CCT TA-3') 0.5 µM). PCR reaction was performed with temperature cycling parameters consisting of initial denaturation at 94°C for 5 min followed by 30 cycles of denaturation at 94°C for 1 min, annealing at 62°C for 1 min, extension at 72°C for 1 min, and a final incubation at 72°C for 10 min.

The loxP sites PCR reaction was performed by adding 0.5 µL lysate to 49.5 µL reaction mix (1X PCR buffer GoTaq (Promega); $MgCl_2$ (Sigma) 1 mM; dNTPs 0.4 mM (Thermo Scientific); TAQ DNA polymerase 2.5 U (Promega); forward *mu floxed* gene primer (5'-GTT ACT GGA GAA TCC AGG CCA AGC-3'), reverse *mu floxed* gene primer (5'-TGC TAG AAC CTG CGG AGC CAC A-3') 1 µM). PCR reaction was performed with temperature cycling parameters consisting of initial denaturation at 94°C for 5 min followed by 30 cycles of denaturation at 95°C for 1 min, annealing at 60°C for 1 min, extension at 72°C for 1 min, and a final incubation at 72°C for 10 min.

The mu excision PCR reaction was performed by adding 0.2 µL lysate to 49.8 µL reaction mix (1X PCR buffer (Sigma); $MgCl_2$ (Sigma) 2.5 mM; dNTPs 0.2 mM (Thermo Scientific); TAQ DNA polymerase 2.5 U (Sigma); forward excision primer (5'-ACC AGT ACA TGG ACT GGA TGT GCC-3'), reverse excision primer (5'-GAG ACA AGG CTC TGA GGA TAG TAA C-3'), forward *myosin* gene primer (5'-TTA CGT CCA TCG TGG ACA GC-3'), reverse *myosin* gene primer (5'-TGG GCT GGG TGT TAG CCT TA-3') 0.5 µM). PCR reaction was performed with temperature cycling parameters consisting of initial denaturation at 94°C for 5 min followed by 35 cycles of denaturation at 94°C for 30 sec, annealing at 61°C for 30sec, extension at 72°C for 30 sec, and a final incubation at 72°C for 10 min.

Behavioral assays

Social interaction. Social behavior was performed in 4 equal square arenas (50 x 50 cm) separated by 35 cm-high opaque grey Plexiglas walls over a white Plexiglas platform (View Point, Lyon, France). Mice used for social interaction ("interacting mice") were 8-10-week-old gender-matched grouped-housed wild-type mice, socially naive and unfamiliar to the experimental animals. On day 1, all the animals were habituated to the arena during a 30-min session. On day 2, both interacting and experimental mice are placed into the open filed for 10 min and number of nose and paw contacts (crawling over, mounting, stepping on, pushing), grooming (overall or precisely after social event) and following, as well as total time spent in close contact (nose and paw contacts), were scored on video recordings.

Marble burying test. Mice were placed on a clear home cage filled of 4-cm deep fresh sawdust, containing 20 marbles and covered with a filtering lid for 15 min. Light intensity was set at 30 lux. The number of marbles buried (≥50%) in sawdust was scored.

Novelty-suppressed feeding. Mice were first food-deprived 24h and isolated in a new home cage 20 min prior testing. Light intensity in the experimental room was set at 60 lux. Three chew were placed in the center of a white squared tissue left in the middle of the arena (see "social interaction"), covered of 1 cm of fresh sawdust. The animals were placed in the open field and the latency to feed is measured, with a cut-off time of 15 min. The mouse was transferred back to the empty home cage immediately after reaching and eating the food pellet. The mouse was allowed to eat during 5 min in this condition and food consumption was weighed.

The time line is represented in **Figure 1**.

Statistical analysis

All statistical tests were performed using Prism6 (GraphPad Software). The effect of genotype was analysed by one-way ANOVA. Significant genotype effect was followed by multiple comparisons test. When only two genotypes were compared, we used two-tailed t-tests. We used Grubbs' test to detect and exclude outliers.

RESULTS

Mu opioid receptor deletion in forebrain GABAergic neurons is not sufficient to impair social interaction

First, we tested whether mu opioid receptors in the forebrain GABAergic neurons contribute to social interactions. To do so, we examined social abilities of WT and total KO in the social interaction test (**Figure 2A**). Student t-tests revealed that constitutive KO mice for the mu receptor show significantly less nose contacts compared to WT [$t_{(42)}$=2.50, p=0.017] as we found previously in Becker et al., 2014. We also found a tendency for shorter time in close contact [$t_{(42)}$=1.58, p=0.12] and for higher grooming events [$t_{(42)}$=1.54, p=0.13]. Then, we examined social abilities of conditional Dlx-mu mice, and found no differences between control and Dlx-mu mice (not shown). D'Amato studies suggest that siblings can influence the mouse phenotype (personal communication), in particular differences in social interactions between mutant and controls may be reduced when siblings from the two genotypes develop within a mixed group, as is the case in our breeding scheme (see methods). We therefore genotyped pups at P4 and re-created sibling groups from the same genotype. We then examined adult mouse behaviors with siblings harbouring either 100% the same genotype (Control separated and Dlx-mu separated groups) or mixed 50%-50% genotypes (Control mixed and Dlx-mu mixed groups). One-way ANOVA did not show any differences in social behavior between groups, neither for the number of nose contacts [$F_{(3, 68)}$=1.49, p=0.28], number of grooming events [$F_{(3, 68)}$=0.93, p=0.82] nor the total time spent in close contact [$F_{(3, 68)}$=1.36, p=0.91] (**Figure 2B**). Selective deletion of the mu receptor in forebrain GABAergic neurons, therefore, does not alter social interactions, and this behavior is not modified even when the conditional knockout are separated from Control siblings.

Mu opioid receptor deletion in forebrain GABAergic neurons is not sufficient to impair anxiety-like behaviors

Then, we studied whether the mu opioid receptor in forebrain GABAergic neurons is involved in the anxiety-like behavior that we previously observed in total mu KO mice. Specifically, we examined anxiety-like behavior using the marble burying, a defensive anxiety test, and novelty suppressed feeding (NSF) tests, a conflict test (**Figure 3A**). In the marble burying experiment, the number of marbles buried in a 15-min session was measured. First, we observed the anxiety like behavior in WT and total KO animals. As we found previously in Becker et al., 2014, student t-test showed a statistically higher number of marbles buried in mu receptor KO mice compared to WT [$t_{(42)}$=3.31, p=0.0019] (**Figure 3B**). In

the novelty-suppressed feeding paradigm, t-test revealed a longer latency to feed in KO compared to WT animals [$t_{(31)}$=6.28, p<0.001]. We then compared Control and Dlx-mu mice, mixed and separated (**Figure 3C**). In the marble burying test, one-way ANOVA revealed no genotype effect [$F_{(3, 69)}$=2.08, *p*=0.12]. In the NSF test, one-way ANOVA showed no genotype effect [$F_{(3, 50)}$=2.22, *p*=0.13]. Mu receptor knockout in forebrain GABAergic neurons, therefore, does not seem to contribute to anxiety-related behaviors.

DISCUSSION

Altogether, our data show that genetic deletion of the mu opioid receptor in forebrain GABAergic neurons does not produce any detectable social or anxiety deficit, which are otherwise observed upon complete gene KO (Becker et al., 2014; Oddi et al., 2013). Consequently, this particular mu opioid receptor subpopulation does not seem to contribute to the development of ASD-like symptoms.

Dlx-mu mice show blunted mu opioid receptor expression throughout the striatum (caudate putamen and nucleus accumbens), as well as reduced receptor number at the level of the amygdala. Those regions are all involved in social behaviors (Chevallier et al., 2012). Social play behavior in rats, which is highly rewarding (Trezza et al., 2011a), induces expression of the marker of cellular activity c-Fos was increased in the prefrontal cortex, dorsal and ventral striatum, lateral amygdala, some thalamic nuclei, dorsal raphe and pendunculopontine tegmental nucleus (van Kerkhof et al., 2014). Further, there is evidence for a role of mu opioid receptors in social reward at the level of ventral striatum. Social play in adolescent rats is increased by intra-NAc infusion of morphine and mu receptor agonist [D-Ala^2,*N*-MePhe^4,Gly^5-ol]encephalin (DAMGO), and decreased by intra-NAc infusion of mu receptor antagonist Cys-Tyr-D-Trp-Arg-Thr-Pen-Thr-NH_2 (CTAP) (Trezza et al., 2011b). Moreover, CTAP infusion in the NAc prevents the development of social-play conditioned place preference (Trezza et al., 2011b). In prairie voles, modulation of the mu receptor by antagonists in different subregions of the striatum suggests distinct roles of the dorsal striatum, NAc core and shell in partner preference, pair bond formation and mating (Resendez et al., 2013) and activation of mu receptors in the dorsal striatum appeared a key element of adult social attachment in prairie voles (Burkett et al., 2011). The lack of consequences of mu receptor gene KO in the NAc, therefore, was surprising. This is unlikely due to inappropriate behavioral testing conditions or sensitivity, since the social deficit phenotype was well detected in total KO mice under the same experimental conditions. Rather, remaining mu receptor populations expressed at other

brain sites, including cortex where receptor expression is almost intact or mid/hindbrain structures, may be sufficient to process rewarding stimuli and maintain normal levels of social behaviors. Alternatively, mu opioid receptors expressed in non-GABAergic neurons in the forebrain may contribute to social reward, a hypothesis that would deserve further investigation.

Anxiety-like behavior measured in the marble burying test is higher in total mu KO mice than WT animals, as reported in our previous report (Becker et al., 2014), but anxiety levels in Dlx-mu animals were similar to their control littermates. Marble burying is utilized to measure anxiety-like responses, and has also been proposed to reflect repetitive behaviors (Thomas et al., 2009). These two components of ASD-like behaviors seem to be spared in our model. To confirm the lack of increased anxiety in Dlx-mu mice, we also examined anxiety responses in the NSF test. In this conflict test, animals face a choice between approaching and consuming food, which is rewarding, and entering a novel environment, which is anxiogenic. Here, we confirmed that mu receptor KO animals show a high latency to reach and consume the food, suggesting a high level of anxiety as in our previous report (Becker et al., 2014). Again, Dlx-mu mice did not display this anxiety response, and together, data from the two tests suggest that mu receptor in forebrain GABAergic neurons do not modulate anxiety-like behaviors. A primary site for the control of negative emotional responses is the amygdala (Asan et al., 2013), and it is possible that remaining mu receptors at this site in mutant mice are sufficient to maintain anxiety-related responses at control levels. Alternatively, mu opioid receptors in the abundant GABAergic neuron population of central amygdala may not contribute to this behavior. Also, the anxiety phenotype observed in total mu KO may result from receptors operating at the level of cortico-hippocampal areas, where mu receptor expression is mostly maintained in Dlx-mu mice. Mu opioid receptor gene targeting in other neuron populations will address these hypotheses in the future.

In our previous work, to confirm whether or not the parents have an influence on ASD symptoms, mu KO pups were raised by mu WT parents and vice versa. Cross-fostering did not reverse or ameliorated ASD symptoms in mu total KO mice (Becker et al., 2014). The autistic-like syndrome observed in mu KO, therefore, has a genetic origin. Furthermore, D'Amato proposed that siblings could influence a mouse phenotype (D'Amato, personal communication), based on the observation that ASD patients enhance their communication skills by therapy involving several forms of social exposure (Weitlauf et al., 2014). In our study, sibling effects on social and anxiety-related behaviors could not be detected.

To conclude, our data suggest that mu opioid receptors in GABAergic neurons of the forebrain do not control ASD-like behaviors. Further studies will be necessary to determine which mu opioid receptor populations are important in ASD-like behaviors.

REFERENCES

Asan, E., Steinke, M., Lesch, K.P., 2013. Serotonergic innervation of the amygdala: Targets, receptors, and implications for stress and anxiety. Histochem. Cell Biol. 139, 785–813. doi:10.1007/s00418-013-1081-1

Becker, J.A., Clesse, D., Spiegelhalter, C., Schwab, Y., Le Merrer, J., Kieffer, B.L., 2014. Autistic-Like Syndrome in Mu Opioid Receptor Null Mice is Relieved by Facilitated mGluR4 Activity. Neuropsychopharmacology 2049–2060. doi:10.1038/npp.2014.59

Briand, L. a., Hilario, M., Dow, H.C., Brodkin, E.S., Blendy, J. a., Berton, O., 2015. Mouse Model of OPRM1 (A118G) Polymorphism Increases Sociability and Dominance and Confers Resilience to Social Defeat. J. Neurosci. 35, 3582–3590. doi:10.1523/JNEUROSCI.4685-14.2015

Bridges, R.S., Grimm, C.T., 1982. Reversal of morphine disruption of maternal behavior by concurrent treatment with the opiate antagonist naloxone 218, 166–168.

Burkett, J.P., Spiegel, L.L., Inoue, K., Murphy, A.Z., Young, L.J., 2011. Activation of μ-Opioid Receptors in the Dorsal Striatum is Necessary for Adult Social Attachment in Monogamous Prairie Voles. Neuropsychopharmacology 36, 2200–2210. doi:10.1038/npp.2011.117

Cellot, G., Cherubini, E., 2014. GABAergic signaling as therapeutic target for autism spectrum disorders. Front. Pediatr. 2, 70. doi:10.3389/fped.2014.00070

Chevallier, C., Kohls, G., Troiani, V., Brodkin, E.S., Schultz, R.T., 2012. The social motivation theory of autism. Trends Cogn. Sci. 16, 231–238. doi:10.1016/j.tics.2012.02.007

Chu Sin Chung, P., Keyworth, H.L., Martin-Garcia, E., Charbogne, P., Darcq, E., Bailey, A., Filliol, D., Matifas, A., Scherrer, G., Ouagazzal, A.-M., Gaveriaux-Ruff, C., Befort, K., Maldonado, R., Kitchen, I., Kieffer, B.L., 2015. A Novel Anxiogenic Role for the Delta Opioid Receptor Expressed in GABAergic Forebrain Neurons. Biol. Psychiatry 77, 404–415. doi:10.1016/j.biopsych.2014.07.033

Cinque, C., Pondiki, S., Oddi, D., Di Certo, M.G., Marinelli, S., Troisi, a, Moles, a, D'Amato, F.R., 2012. Modeling socially anhedonic syndromes: genetic and pharmacological manipulation of opioid neurotransmission in mice. Transl. Psychiatry 2, e155. doi:10.1038/tp.2012.83

Hsu, D.T., Sanford, B.J., Meyers, K.K., Love, T.M., Hazlett, K.E., Wang, H., Ni, L., Walker, S.J., Mickey, B.J., Korycinski, S.T., Koeppe, R. a, Crocker, J.K., Langenecker, S. a, Zubieta, J.-K., 2013. Response of the

μ-opioid system to social rejection and acceptance. Mol. Psychiatry 18, 1211–7. doi:10.1038/mp.2013.96

Komatsu, H., Ohara, A., Sasaki, K., Abe, H., Hattori, H., Hall, F.S., Uhl, G.R., Sora, I., 2011. Decreased response to social defeat stress in μ-opioid-receptor knockout mice. Pharmacol. Biochem. Behav. 99, 676–682. doi:10.1016/j.pbb.2011.06.008

Matthes, H.W., Maldonado, R., Simonin, F., Valverde, O., Slowe, S., Kitchen, I., Befort, K., Dierich, a, Le Meur, M., Dollé, P., Tzavara, E., Hanoune, J., Roques, B.P., Kieffer, B.L., 1996. Loss of morphine-induced analgesia, reward effect and withdrawal symptoms in mice lacking the mu-opioid-receptor gene. Nature. doi:10.1038/383819a0

Miranda-Paiva, C.M., Ribeiro-Barbosa, E.R., Canteras, N.S., Felicio, L.F., 2003. A role for the periaqueductal grey in opioidergic inhibition of maternal behaviour. Eur. J. Neurosci. 18, 667–674. doi:10.1046/j.1460-9568.2003.02794.x

Moles, A., Kieffer, B.L., D'Amato, F.R., 2004. Deficit in attachment behavior in mice lacking the mu-opioid receptor gene. Science 304, 1983–1986. doi:10.1126/science.1095943

Monory, K., Massa, F., Egertová, M., Eder, M., Blaudzun, H., Westenbroek, R., Kelsch, W., Jacob, W., Marsch, R., Ekker, M., Long, J., Rubenstein, J.L., Goebbels, S., Nave, K.A., During, M., Klugmann, M., Wölfel, B., Dodt, H.U., Zieglgänsberger, W., Wotjak, C.T., Mackie, K., Elphick, M.R., Marsicano, G., Lutz, B., 2006. The Endocannabinoid System Controls Key Epileptogenic Circuits in the Hippocampus. Neuron 51, 455–466. doi:10.1016/j.neuron.2006.07.006

Oddi, D., Crusio, W.E., D'Amato, F.R., Pietropaolo, S., 2013. Monogenic mouse models of social dysfunction: Implications for autism. Behav. Brain Res. 251, 75–84. doi:10.1016/j.bbr.2013.01.002

Resendez, S.L., Dome, M., Gormley, G., Franco, D., Nevárez, N., Hamid, A. a, Aragona, B.J., 2013. μ-Opioid receptors within subregions of the striatum mediate pair bond formation through parallel yet distinct reward mechanisms. J. Neurosci. 33, 9140–9. doi:10.1523/JNEUROSCI.4123-12.2013

Thomas, A., Burant, A., Bui, N., Graham, D., Yuva-Paylor, L. a., Paylor, R., 2009. Marble burying reflects a repetitive and perseverative behavior more than novelty-induced anxiety. Psychopharmacology (Berl). 204, 361–373. doi:10.1007/s00213-009-1466-y

Trezza, V., Campolongo, P., Vanderschuren, L.J.M.J., 2011a. Evaluating the rewarding nature of social interactions in laboratory animals. Dev. Cogn. Neurosci. 1, 444–458. doi:10.1016/j.dcn.2011.05.007

Trezza, V., Damsteegt, R., Achterberg, E.J.M., Vanderschuren, L.J.M.J., 2011b. Nucleus accumbens μ-opioid receptors mediate social reward. J. Neurosci. 31, 6362–6370. doi:10.1523/JNEUROSCI.5492-10.2011

Troisi, A., Frazzetto, G., Carola, V., Di Lorenzo, G., Coviello, M., D'Amato, F.R., Moles, A., Siracusano, A., Gross, C., 2011. Social hedonic capacity is associated with the A118G polymorphism of the mu-opioid receptor gene (OPRM1) in adult healthy volunteers and psychiatric patients. Soc. Neurosci. 6, 88–97. doi:10.1080/17470919.2010.482786

Van Kerkhof, L.W.M., Trezza, V., Mulder, T., Gao, P., Voorn, P., Vanderschuren, L.J.M.J., 2014. Cellular activation in limbic brain systems during social play behaviour in rats. Brain Struct. Funct. 219, 1181–211. doi:10.1007/s00429-013-0558-y

Weibel, R., Reiss, D., Karchewski, L., Gardon, O., Matifas, A., Filliol, D., Becker, J. a J., Wood, J.N., Kieffer, B.L., Gaveriaux-Ruff, C., 2013. Mu Opioid Receptors on Primary Afferent Nav1.8 Neurons Contribute to Opiate-Induced Analgesia: Insight from Conditional Knockout Mice. PLoS One 8, 1–18. doi:10.1371/journal.pone.0074706

Weitlauf, A.S., McPheeters, M.L., Peters, B., Sathe, N., Travis, R., Aiello, R., Williamson, E., Veenstra-VanderWeele, J., Krishnaswami, S., Jerome, R., Warren, Z., 2014. Therapies for Children With Autism Spectrum Disorder: Behavioral Interventions Update. AHRQ Publ. No. 14-EHC036-EF. Rockville, MD Agency Healthc. Res. Qual. 120.

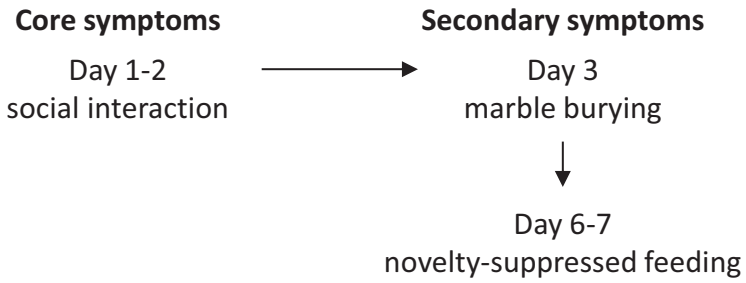

Figure 1. Test battery time lines of the ASD-like behavioral assessment.

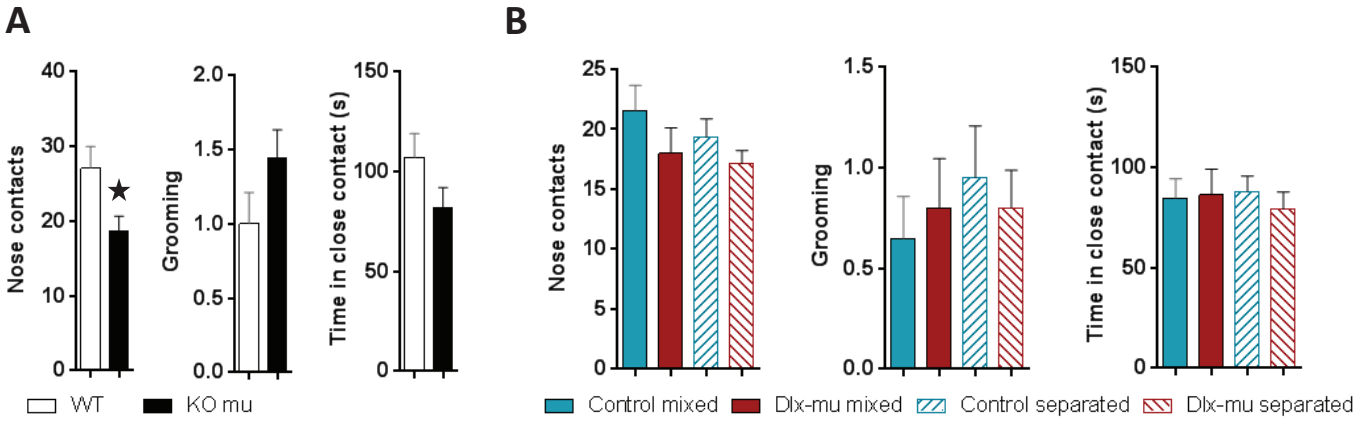

Figure 2. Social abilities assessed in the social interaction test. (**A**) n=17-18 per group. (**B**) n=15-20 per group. A social interaction deficit phenotype was found in KO mice, but not for Dlx-mu mice, raised either mixed or separated. Black stars represent significant difference compared to WT group . One star, $p<0.05$ (t-test).

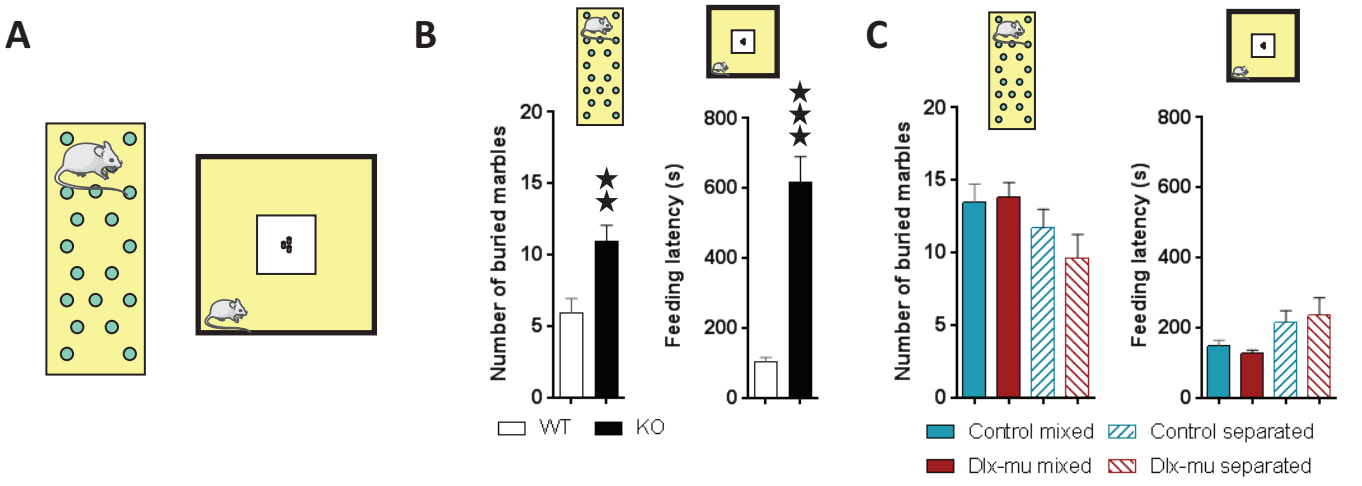

Figure 3. Anxiety-like behavior evaluated using the marble burying (**A, left**) and novelty suppressed feeding (NSF) (**A, right**) tests. (**B**) Marble burying and NSF tests showed increased anxiety-like behavior in KO mice compared to WT. (**C**) No difference was found in defensive behavior between Control and Dlx-mu mice, mixed or separated, in any of the two tests. *(**A, left**) n=15-18 per group. (**A, right**) n=10-20 per group*. Black stars represent significant difference compared to WT group. Two stars, $p<0.01$; three stars, $p<0.001$ (t-test).

Supplementary experiments

I. Materials and Methods

Animals

Experiments were performed on male and female mice aged of 8-12 weeks at the beginning of the study. Mu floxed mouse line (*Oprm1*$^{fl/fl}$) have been previously described by our group (Weibel et al., 2013). Briefly, exons 2 and 3 of mu receptor gene *Oprm1* are flanked by loxP sites. *Oprm1*$^{fl/fl}$ mice show intact mu receptor expression (Weibel et al., 2013). To generate a conditional knockout for *Oprm1* in GABAergic forebrain neurons, the Dlx5/6-Cre-*Oprm1*$^{-/-}$ mouse line was created at the ICS-IGBMC (Institut Clinique de la Souris - Institut de Génétique et de Biologie Moléculaire et Cellulaire, Illkirch, France) by breeding the Dlx5/6-Cre mice (obtained from Beat Lutz laboratory, Institute of Physiological Chemistry, Johannes Gutenberg University, Germany) with mu floxed mice. Dlx5/6-Cre line was successfully used in previous studies to conditionally invalidate cannabinoid CB1 receptors (Monory et al., 2006) and delta opioid receptors (Chu Sin Chung et al., 2015). Resulting Cre positive (Cre(+), Dlx5/6-Cre-*Oprm1*$^{-/-}$) animals are called Dlx-mu and Cre negative (Cre(-), *Oprm1*$^{fl/fl}$) are Controls. To verify the autistic-like syndrome that was found in the study of Becker et al., we used mu knockout and their control (named wild type, WT), previously described in (Matthes et al., 1996). They have a different genetic background (50% C57BL/6J-50% 129SvPas) compared to Dlx-mu and Controls (63% C57BL/6J-37% 129SvPas).

Behavioral experiments

Rotarod. On day 1, mice are allowed to stay on the rod at least 3 consecutive minutes during a habituation session at a stable speed of 4 rpm. From day 2 to 5, mice are placed back on the rod in an accelerating mode (from 4 to 40 rpm in 5 min). The latency to fall is measured. Rotarod test was assessed three trials separated by 1 min-recovery intervals.

Grip test. Mice were holding the grid of a dynamometer (BioSeb, Valbonne, France) and pulled back by their tail. We measured the maximal strength exerted by the mouse before losing grip. Muscular strength was recorder 3 times a day, separated by 30 s-recovery intervals.

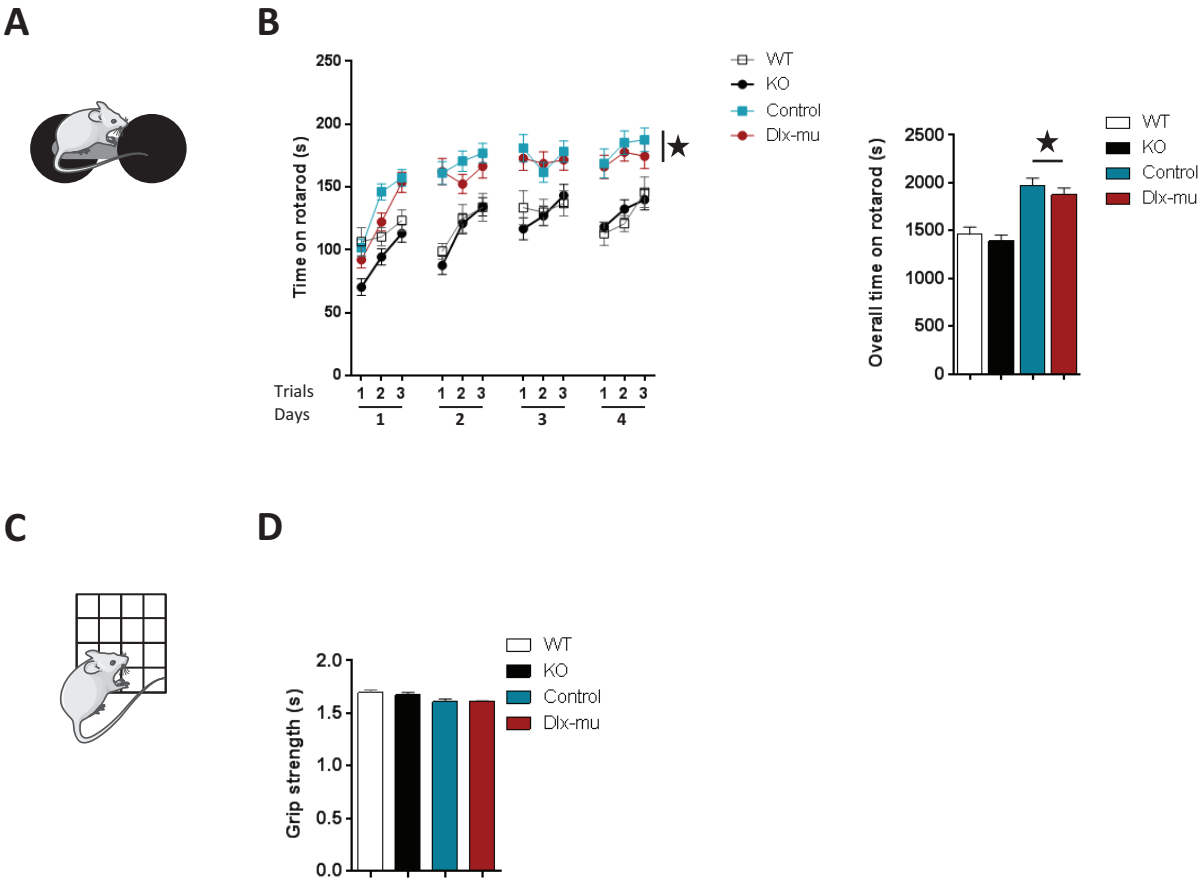

Figure S1. Motor functions assessed in rotarod (**A-B**) and grip (**C-D**) tests. (**B**) The ability to stay on the rotarod is weaker in Dlx-mu mice compared to Control mice, but there is no differences between WT and KO. (**D**) n=11-20 per group. Black stars represent significant difference between Control and Dlx-mu groups. One star, $p<0.05$ (one-way RM ANOVA).

Statistical analysis

All statistical tests were performed using Prism6 (GraphPad Software). The effect of genotype was analysed by a one-way repeated measures ANOVA for Rotarod test and classical one-way ANOVA for the grip test. Significant genotype effect was followed by multiple comparisons test.

II. Results

Dlx-mu mice show decreased motor functions compared to Control

We examined motor functions using the rotarod and the grip test. In the rotarod experiment, the time the mouse stays on the accelerating rotarod was measured for each trial in each session (**Figure S1A**). One-way repeated measures ANOVA revealed a genotype effect [$F_{(1.667, 18.33)}$=61.46, p<0.001]. *Post hoc* multiple comparisons analysis showed a difference between Control and Dlx-mu mice (p<0.05). In the grip test, the strength of the mice forepaws is measured. One-way repeated measures ANOVA revealed a small genotype effect [$F_{(3, 8)}$=4.48, p<0.040]. *Post hoc* multiple comparisons analysis showed no differences between genotypes when comparing one by one (p<0.05).

III. Discussion and perspectives

Impairment in motor performance and coordination is a secondary symptom of ASD (Kopp et al., 2010). We did not reproduce the deficit in motor coordination in the rotarod that our team previously showed in mu total knockout animals (Becker et al., 2014). A small decrease in motor coordination was detected in Dlx-mu mice compared with littermate Control. Forelimb muscular strength is unchanged in both mu total and conditional KO, as previously shown for KO in (Becker et al., 2014). Because animals from all genotypes performed extremely well in the test, we will perform new rotarod assays using conditions that render the task more difficult, in order to (i) reproduce the total mu KO deficit in motor coordination observed in our previous study and (ii) determine whether Dlx-mu mice also show a deficit under those conditions. This will assess the potential participation of mu receptor GABAergic forebrain neurons in motor coordination.

Additionally, we will evaluate other ASD features in our model. For instance, stereotyped behavior is a key symptom of autistic-like behavior (DSM V). This repetitive behavior can be easily examined in mouse models (Crawley, 2012). One other core symptom is the lack of communication. It has been shown that invalidation of mu receptor gene can impact the pups' communication by

decreasing vocalizations when separated from their mother (Moles et al., 2004). We could also perform vocalization studies to assess the role of mu receptor in GABAergic forebrain neurons in this behavior. Furthermore, we could complete our social behavior experiments by assessing social CPP in KO and conditional KO mice. Altogether, this study will help deciphering the implication of the mu opioid receptor in ASD.

PART III

Target glutamatergic forebrain mu receptors in adult mice

I. Introduction

1. The mu opioid receptor in glutamatergic neurons

As described in previous chapters, the mu opioid receptor is predominantly expressed in GABAergic neurons. However, mu receptors are also expressed in other neuronal types. In particular, receptor-containing glutamatergic neurons have been described in the PAG (Rodríguez-Muñoz et al., 2012). In this study, biochemical studies demonstrate that mu and NMDA receptors coexist and interact to cross-regulate pain responses (Rodríguez-Muñoz et al., 2012). Further, electrophysiological studies show modulation of glutamate signalling by mu receptors. Chieng and Christie showed that mu receptor agonists inhibit GABA and glutamatergic components of postsynaptic potentials in single PAG neurons (Chieng and Christie, 1994). In the dorsal horn, mu receptors presynaptically inhibit glutamatergic transmission (Wrigley et al., 2010) and also inhibit glutamatergic transmission in the rat anterior cingulate cortex (Zheng, 2010). Although the latter studies do not establish direct modulation of glutamatergic neurons by the mu opioid receptor, it is likely that part of mu opioid receptor activity operates within glutamatergic neurons. One approach to address this question is to target the *Oprm1* gene in this particular neuronal population, and study the functional consequences of the genetic manipulation.

2. CaMKII gene

Intracellular domains of ionotropic and metabotropic glutamate receptors interact with protein kinases such as CaMKII (Ca^{2+}/calmodulin-dependent protein kinase type II) (for review, see Mao et al., 2014). Postsynaptically, CaMKII phosphorylation in a constitutive or activity-dependent manner regulates glutamate receptor properties. The highly abundant serine/threonine kinase CaMKII has four isoforms, namely α, β, γ and δ, that are differentially distributed within the rat brain (Takaishi et al., 1992). The anatomical localization of the different CaMKII isoforms plays a major role in regulation of enzyme function (Liu and Murray, 2012). CaMKII α and β are the predominant isoforms in the brain. The α isoform has a particular pattern of expression, being expressed only on excitatory cells of the brainstem and spinal cord (Liu and Murray, 2012); this isoform is expressed in glutamatergic but not GABAergic synapses in the thalamus and cortex (Liu and Jones, 1996) as well as in the CA1 of rat hippocampus (Liu and Jones, 1997). Moreover, CaMKII has been shown to be contained only in

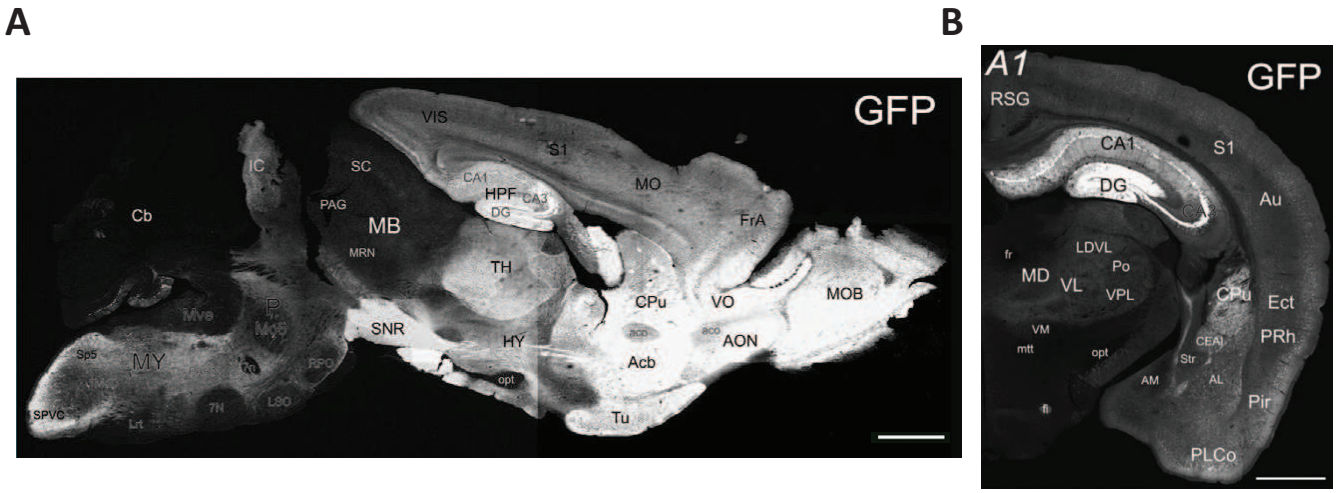

Figure 8. Images of CaMKIIα-GFP adult mouse brain. (**A**) Sagittal view. Confocal image montage shows GFP in a 30 µm sagittal section (lateral1.10mm). (**B**) Coronal view. Image of GFP in a 30 µm coronal section (Bregma -2.22 mm). Scale bars = 500 µm. Adapted from Wang et al., 2013.

Abbreviations: 7n, facial nucleus root; 7N, facial nucleus; Acb, accumbens nucleus; Aco, anterior commissure; AM, amygdalar nucleus, medial; AL, amygdalar nucleus, lateral; Ang, angular thalamic nucleus; AON, anterior olfactory nucleus; ArcD, arcuate hypothalamic nucleus, dorsal part; ArcL, arcuate hypothalamic nucleus, lateral part; Au, auditory cortex; CA1, field CA1; CA3, field CA3; Cb, cerebellum; CEAl, central amygdalar nucleus, lateral; CL, central lateral nucleus of the thalamus; CM, central medial nucleus of the thalamus; CPu, caudoputamen; DG, dentate gyrus; DM, dorsal medial nucleus of the hypothalamus; Ect, ectorhinal cortex; Fr, fasciculus retroflexus; FrA, frontal association cortex; Ge5, gelatinous layer of the caudal spinal trigeminal nucleus; gr, granule layer of cerebellum; GrDG, granular layer of dentate gyrus; HPF, hippocampal formation; HY, hypothalamus; IC, inferior collicullus; IMD, infer mediodorsal nucleus of the thalamus; LDDM, laterodorsal thalamic nucleus, dorsomedial part; LDVL, laterodorsal thalamic nucleus, ventrolateral part;LPMR, lateral posterior thalamic nucleus, mediorostral part; LH, lateral hypothalamus area; Lmol, stratum lacunosummolecular; Lrt, lateral reticular nucleus; LSO, lateral superior olive; MB, midbrain; MO, motor cortex; MDC, mediodorsal nucleus of the thalamus,central part; MdD, medullary reticular nucleus, dorsal part; MDL, mediodorsal nucleus of the thalamus, dorsal part; MDM, mediodorsal nucleus of the thalamus, medial part; ME, median eminence; mmt, mammilo thalmic tract; Mo5, motor trigeminal nucleus; MOB, main olfactory bulb; MoDG, dentate gyrus, molecular layer; MRN, midbrain reticular nucleus; MY, Medulla; MVe, medial vestibular nucleus; Opt, optictract; Or, stratum oriens; P, pons; Pa, paraventricular hypothalamic nucleus; PARN, parvi cellular reticular nucleus; PAG, periaqueductal gray; PC, paracentralnucleus; Pir, piriform cortex; Pc, purkinje cell layer of cerebellum; PLCo, posterolateral cortical amygdaloid nucleus; Po, posterior complex of the thalamus; PoDG, polymorph layer of the dentate gyrus; PRh, perirhinal cortex; Rad, stratum radiatum; Re, nucleus of reunions; RPO, rostal periolivary region; RSG, retrosplenial granular cortex; RT, reticular nucleus of the thalamus; S1, primary somatosensory cortex; SC, superior colliculus; Slu, stratum lucidum; SNR, substantia nigra, reticular part of amygdaloid area; Sp5, spinal trigeminal nucleus; SPVC, spinal nucleus of the trigeminal, caudal part; Str, striatum terminals; Sub, subparafascicular nucleus; TH, thalamus; Tu, olfactory tubercle; VIS, visual cortex; VL, ventrolateral nucleus of thalamus; VO, ventral orbital cortex; VPM, ventral postero medial nucleus of thalamus; VPL, ventral posterolateral nucleus of thalamus; Wm, whitematter.

pyramidal neurons and GABA to be contained only in non-pyramidal cells of the basolateral amygdala (McDonald et al., 2002). In the forebrain, CaMKII is restricted to excitatory glutamatergic neurons and absent from GABA-containing neurons (Benson et al., 1992; Jones et al., 1994). Some studies have demonstrated exceptions of non-conventional distribution of CaMKIIα in which CaMKIIα is not restricted to excitatory cells in all the brain regions. Indeed, in the mouse olfactory bulb, CamKIIα immunoreactivity was positive in the GABAergic granule cells, and was positive in glutamatergic neurons in the piriform cortex (Zou et al., 2002). Recently, a CaMKII FRET sensor was developed, permitting more precise localization of the protein's activity (Shibata et al., 2015). The generation of a CaMKIIα-GFP mouse line has been very useful to study the regional and cellular distribution of the kinase (Wang et al., 2013) (**Figure 8**). No overlap between GFP and GABA immunoreactivity was found in the neocortex, thalamus, CA1 and 3 of the hippocampus, piriform cortex, caudate putamen and hypothalamus, but a very high overlap was observed in the granule cells of the olfactory bulb, as previously demonstrated (Zou et al., 2002). Thus, the unique distribution of CaMKIIα establishes this gene as an excellent tool to study glutamatergic cell specific populations.

3. Aim of the study: target glutamatergic forebrain mu receptors in adult mice

To study the role of mu opioid receptors in glutamate neuronal populations, we developed a new mouse line in which Cre recombinase is expressed under the control of the CaMKIIα gene promoter that targets glutamatergic forebrain neurons. This Cre is fused with ER^{T2} protein and permits expression of the enzyme only after tamoxifen treatment. To evaluate this new molecular tool, I characterized the Cre recombinase pattern of expression using a reporter mouse line following tamoxifen injections, and attempted to obtain a conditional deletion of the *Oprm1* gene in glutamatergic neurons.

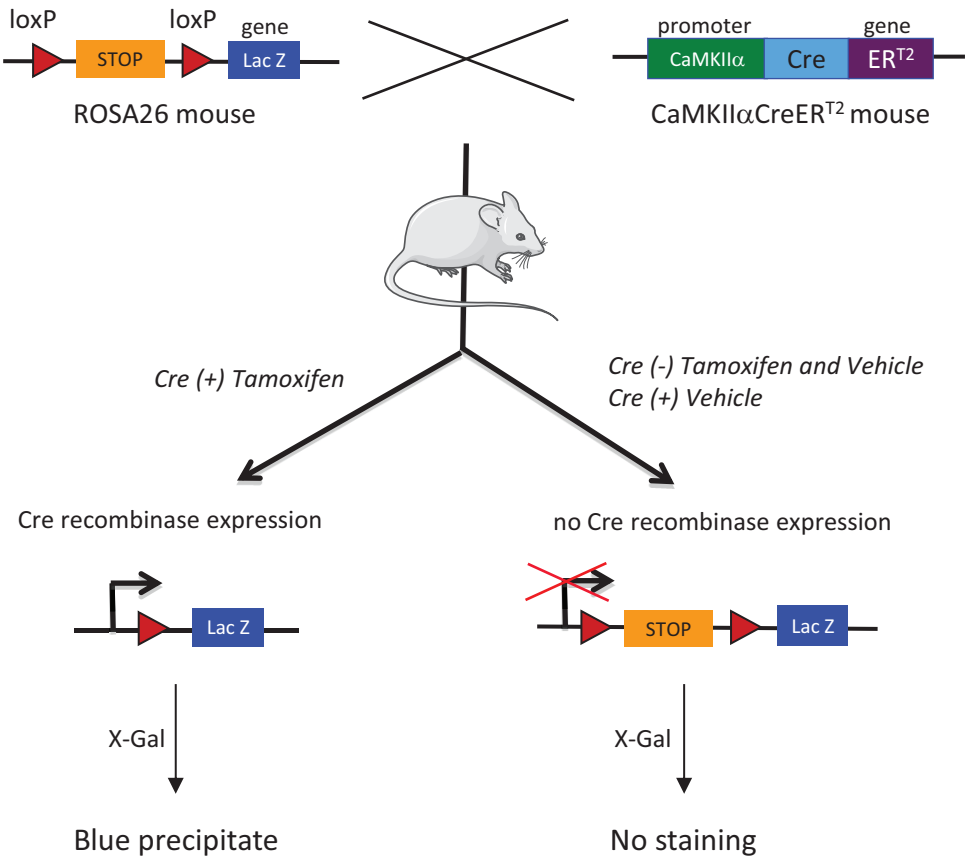

Figure 9. **CaMKIIαCreER^{T2} ROSA26 mouse line to study the Cre recombinase activity.**
We bred the Cre recombinase reporter ROSA26 mice with CaMKIIαCreER^{T2} mice to obtain CaMKIIαCreER^{T2} ROSA26 mouse line. Cre recombinase positive animals were treated with tamoxifen (2 mg/day, 15 days) to induce Cre recombinase activation, leading to excision of the stop sequence. The *LacZ* gene will then be expressed and will code for the β-galactosidase enzyme that produces a blue precipitate in presence of its substrate X-Gal in Cre-expressing cells.

II. Materials and methods

Animals

Experiments were performed on male and female mice aged 8 weeks at the beginning of the study. CaMKIIα-CreER^{T2} line was successfully used in a recent study to conditionally invalidate *Nae1* gene (Vogl et al., 2015). To generate a conditional knockout for *Oprm1* in glutamatergic forebrain neurons, the CaMKIIα-CreER^{T2}-*Oprm1*$^{-/-}$ mouse line was created at the ICS-IGBMC (Institut Clinique de la Souris - Institut de Génétique et de Biologie Moléculaire et Cellulaire, Illkirch, France) by breeding the CaMKIIα-CreER^{T2} mice (ICS) with mu floxed mice. The mu floxed mouse line (*Oprm1*$^{fl/fl}$) has been previously described by our group (Weibel et al., 2013). Briefly, exons 2 and 3 of the mu receptor gene *Oprm1* were flanked by loxP sites. *Oprm1*$^{fl/fl}$ mice show intact mu receptor expression (Weibel et al., 2013). Resulting Cre positive (Cre(+), CaMKIIα-CreER^{T2}-*Oprm1*$^{-/-}$) animals are called CaMKIIα-mu and Cre negative (Cre(-), *Oprm1*$^{fl/fl}$) are Controls. CaMKIIα-mu and littermate controls have the same genetic background (35% C57BL/6J - 20% C57BL/6N - 45% 129SvPas).

CMV-Cre-*Oprm1*$^{-/-}$ (CMV-mu) mice were used as total knockout for the mu receptor gene, by breeding *Oprm1*$^{fl/fl}$ mice with CMV-Cre mice, expressing the Cre recombinase under the control of the cytomegalovirus (CMV, ubiquitous) promoter (Metzger and Chambon, 2001). This line has a 75% C57BL/6J-25% 129SvPas background.

For the Cre recombinase activity reporter line, we created the CaMKIIα-CreER^{T2}-ROSA26 mouse line. We obtained this new line by crossing the CaMKIIα-CreER^{T2} mice (ICS) with the Cre activity reporter transgenic line ROSA26 (Soriano, 1999).

All experiments were carried out according to the recommendations of the NIH Guide for Care and Use of Laboratory Animals. The study protocol was approved by the Local Bioethics Committee (Strasbourg, France). All animals were housed in a room maintained at 21±2°C and 45±5% humidity, with a 12h light-dark cycle. Food and water were available *ad libitum*.

LacZ staining

The Cre-expression pattern in CaMKIIα-mu mice was characterized by crossing that Cre(+) line with the ROSA26 reporter mouse line (**Figure 9**). Resulting mice were treated with tamoxifen or vehicle (see treatment), and sacrificed by cervical dislocation 4 weeks later. Brains were extracted, rinsed in 1X PBS (phosphate-buffered saline solution, Sigma), embedded in OCT (Optimal Cutting Temperature medium, Thermo Scientific), frozen and stored at -80°C. Frozen brains were cut in a cryostat (CM 3000,

Leica) to obtain coronal 25-µm thick sections. They were subsequently collected on slides (Micro Slides Precleaned X-Tra™ Adhesive, Surgipath) and kept at -80°C until use.

After 30-min warm up at room temperature, slides were incubated in a fixative solution (formaldehyde 2%; glutaraldehyde 0.2%; Tween 20 0.1% in 1X PBS) for a minute and then washed at room temperature 2 X 5 min in PBST (1X PBS; Tween 20 0.1%). Slides were incubated at 37°C in the dark in a staining solution (potassium ferricyanide 5 mM; potassium hexacyanoferrate 5 mM; MgCl2 2 mM, X-Gal 1mg/mL (Euromedex) in 1X PBS) until a blue color developed. Next, slides were successively washed 3 times (2 X 10 min; 1 X 1h) in PBST at room temperature. Slides were then immersed in demineralized water for 10 sec and dehydrated in 100% ethanol for 10 sec. Slides were allowed to dry overnight. Sections were observed with a bright field macroscope (M420, Leica) and images were recorded using CoolSNAP software.

Treatment

Cre recombinase activity was induced by a 15-day treatment of 100 µL tamoxifen (10 mg/mL, i.p., twice daily). Tamoxifen powder was dissolved in 10%-ethanol containing sunflower oil. The exact same solution without tamoxifen was used as a control (vehicle treated animals).

Genotyping-PCR

PCR analysis on genomic DNA were performed in order to genotype the mice for presence of 1) Cre recombinase, 2) loxP sites and 3) excision of *Oprm1*. PCR was carried out on DNA obtained from the collected mouse digits digested with Proteinase K (NaCl 0.2M; Tris-HCl 100 mM pH8.5; EDTA 5mM; SDS 0.2%; proteinase K (Sigma) 10 mg/mL;) overnight at 55°C.

The Cre PCR reaction was performed by adding 0.5 µL lysate to 49.5 µL reaction mix (1X PCR buffer (Sigma); $MgCl_2$ (Sigma) 2.5 mM; dNTPs 0.2 mM (Thermo Scientific); TAQ DNA polymerase 2.5 U (Sigma); forward *Cre* primer (5'-GAT CGC TGC CAG GAT ATA CG-3'), reverse *Cre* primer (5'-CAT CGC CAT CTT CCA GCA G-3'), forward *myosin* gene primer (5'-TTA CGT CCA TCG TGG ACA GC-3'), reverse *myosin* gene primer (5'-TGG GCT GGG TGT TAG CCT TA-3') 0.5 µM). PCR reaction was performed with temperature cycling parameters consisting of initial denaturation at 94°C for 5 min followed by 30 cycles of denaturation at 94°C for 1 min, annealing at 62°C for 1 min, extension at 72°C for 1 min, and a final incubation at 72°C for 10 min.

The loxP sites PCR reaction was performed by adding 0.5 µL lysate to 49.5 µL reaction mix (1X PCR buffer GoTaq (Promega); $MgCl_2$ (Sigma) 1 mM; dNTPs 0.4 mM (Thermo Scientific); TAQ DNA

polymerase 2.5 U (Promega); forward *mu floxed* gene primer (5'-GTT ACT GGA GAA TCC AGG CCA AGC-3'), reverse *mu floxed* gene primer (5'-TGC TAG AAC CTG CGG AGC CAC A-3') 1 µM). PCR reaction was performed with temperature cycling parameters consisting of initial denaturation at 94°C for 5 min followed by 30 cycles of denaturation at 95°C for 1 min, annealing at 60°C for 1 min, extension at 72°C for 1 min, and a final incubation at 72°C for 10 min.

The mu excision PCR reaction was performed by adding 0.2 µL lysate to 49.8 µL reaction mix (1X PCR buffer (Sigma); $MgCl_2$ (Sigma) 2.5 mM; dNTPs 0.2 mM (Thermo Scientific); TAQ DNA polymerase 2.5 U (Sigma); forward excision primer (5'-ACC AGT ACA TGG ACT GGA TGT GCC-3'), reverse excision primer (5'-GAG ACA AGG CTC TGA GGA TAG TAA C-3'), forward *myosin* gene primer (5'-TTA CGT CCA TCG TGG ACA GC-3'), reverse *myosin* gene primer (5'-TGG GCT GGG TGT TAG CCT TA-3') 0.5 µM). PCR reaction was performed with temperature cycling parameters consisting of initial denaturation at 94°C for 5 min followed by 35 cycles of denaturation at 94°C for 30 sec, annealing at 61°C for 30sec, extension at 72°C for 30 sec, and a final incubation at 72°C for 10 min.

Tissue collection for mRNA analysis

Mice were sacrificed by cervical dislocation. Brains were extracted, rinsed in cold 1X PBS (phosphate-buffered saline solution, Sigma) and 1-mm thick slices were cut with a stainless steel coronal brain matrix chilled on ice (Harvard apparatus, Holliston, MA, USA). Different brain regions were collected from 3 to 4 mice per genotype and treatment, according to the stereotaxic atlas of mouse brain (Paxinos and Franklin, 2001). The CPu (caudate putamen) was bilaterally punched using a 2-mm diameter tissue corer; NAc (nucleus accumbens), BNST (bed nucleus of the stria terminalis), EC (entorhinal cortex), amygdala, and LH (lateral hypothalamus) were bilaterally punched with a 1.2-mm corer; PCF (prefrontal cortex), Cg (cingular cortex), VMH (ventromedial hypothalamic nucleus), thalamus and PAG (periacqueducal grey) were centrally punched using a 2-mm diameter tissue corer; VMPO (ventromedial preoptic nucleus), Arc (arcuate hypothalamic nucleus), Hb (habenula), IP (interpeduncular nucleus) and DRN (dorsal raphe nucleus) were centrally punched using a 1.2-mm diameter tissue corer; and the Hp (hippocampus), SC (spinal cord), tail and small intestine were dissected. Samples were immediately frozen on dry ice and kept at -80°C until processing.

Quantitative real-time PCR

Samples were processed to extract total RNA, using TRIzol reagent (Invitrogen, Cergy Pontoise, France) according to the manufacturer's instructions. The quality and quantity of RNA was measured

with ND-1000 NanoDrop (Thermo Fisher Scientific, Wilmington, USA) spectrophotometer. Reverse transcription of 800 ng to 1 µg total RNA was performed on bilateral pooled brain samples in triplicate, in a 20 µL final volume, with Superscript II kit (Superscript II RT, Invitrogen). Real-time PCR was performed on the resulting cDNA using a Light Cycler 480 apparatus (Roche, Meylan, France) and iQ SYBR Green supermix (Biorad, Marnes-la-Coquette, France). Primers sequences were: CCGAAATGCCAAAATTGTCA (*Oprm1* forward), GGACCCCTGCCTGTATTTTGT (*Oprm1* reverse), GACGGCCAGGTCATCACTAT (*β-actin* forward), CCACCGATCCACACAGAGTA (*β-actin* reverse), TGAGATTCGGGATATGCTGTTG (*arbp* gene "36B4" forward), TTCAATGGTGCCTCTGGAGAT (*arbp* gene "36B4" reverse), TGACACTGGTAAAACAATGCA (*HPRT* forward), GGTCCTTTTCACCAGCAAGCT (*HPRT* reverse). Thermal cycling parameters were 1 min at 95°C followed by 40 amplification cycles of 15 sec at 95°C, 15 sec at 60°C and 30 sec at 72°C. Expression levels were normalized to *β-actin* housekeeping gene levels. Two reference genes (*HPRT*, *arbp*) were tested in each run as an internal control. The $2^{-\Delta\Delta Ct}$ method was used to evaluate differential expression levels (Livak and Schmittgen, 2001) of Control, and CaMKIIα-mu mice. Control vehicle Cre(-) animals were used as baseline to normalize.

Statistical analysis

Statistical tests for quantitative real-time PCR were performed using Prism6 (GraphPad Software). Comparison of mu receptor transcripts in the four groups of genotypes (Cre(-) vehicle, Cre(-) tamoxifen, Cre(+) vehicle, Cre(+) tamoxifen) was performed by t-tests and corrected for multiple comparisons using the Holm-Sidak method.

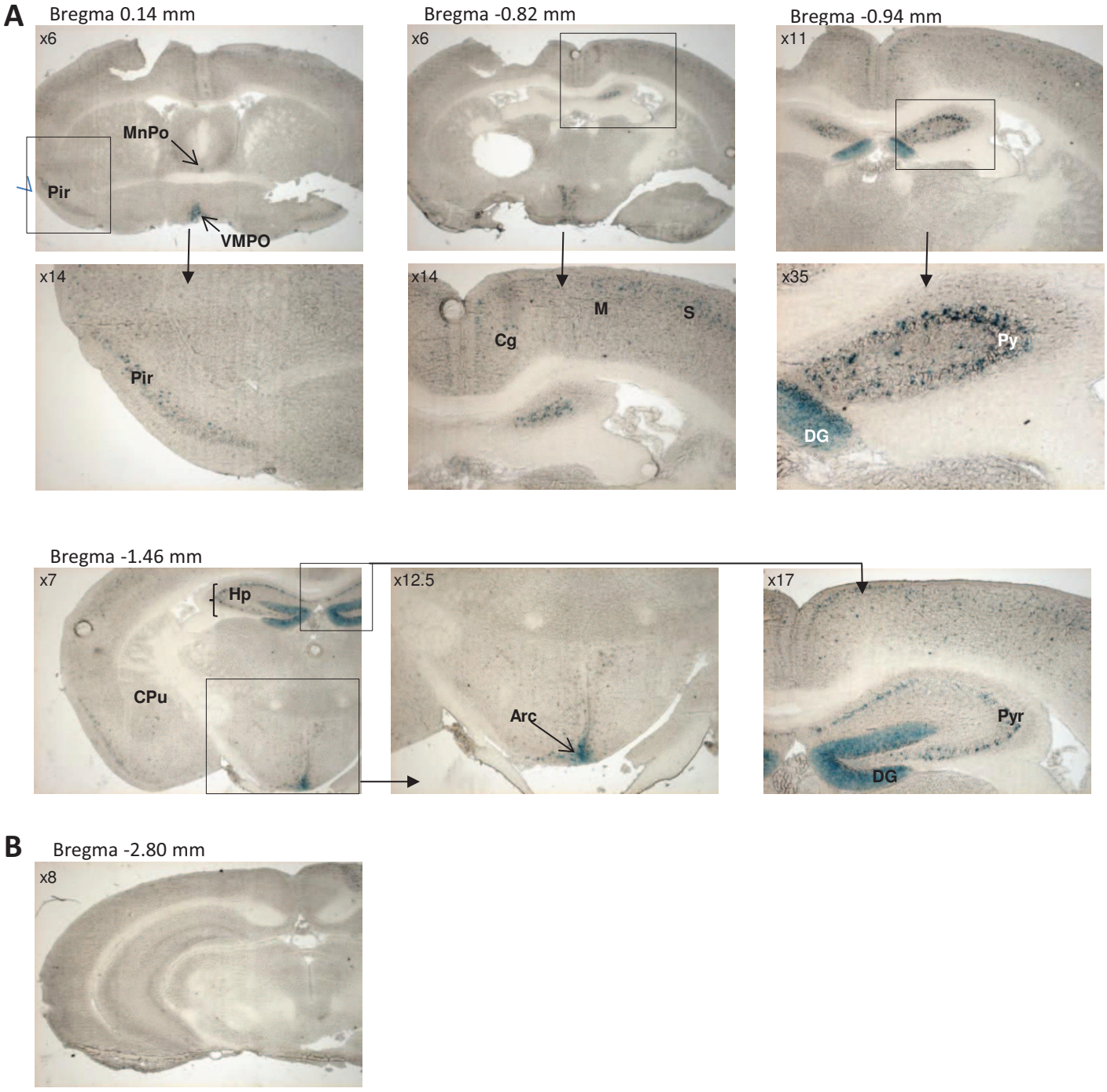

Figure 10. Pattern of Cre recombinase activity of CaMKIIαCreER^{T2} mice using ROSA26 reporter line. Images of CaMKIIαCreER^{T2} ROSA26 brain sections stained after X-Gal application of tamoxifen (**A**) and vehicle-treated (**B**) mice. Few cells were stained, compared to the literature (Choi et al, 2014).
Abbreviations: Arc, arcuate hypothalamic nucleus; Cg, cingulate cortex; CPu, caudate putamen; DG, dentate gyrus; Hp, hippocampus; M, motor cortex; MnPo, median preoptic nucleus; Pir, piriform cortex; Pyr, pyramidal cell layer of the hippocampus; S, primary somatosensory cortex ; VMPO, ventromedial preoptic nucleus.

III. Results

1. *In vivo* Cre activity pattern of the CaMKIIα-CreER^{T2} mouse line

Before breeding the CaMKIIα-CreER^{T2} mouse line to conditionally delete the mu receptor, we explored the Cre recombinase expression pattern. A CaMKIIα-Cre mouse line was previously used to conditionally inactivate the Go-alpha receptor in forebrain neurons and male germ cells, and the Cre recombinase activity pattern was also studied using ROSA26 reporter line (Choi et al., 2014).

We bred the CaMKIIα-CreER^{T2} line with the reporter mouse line ROSA26 (**Figure 9**). This reporter line is composed of a floxed stop cassette upstream of the *β-galactosidase* (lacZ) gene at the ROSA locus. Resulting mice received a twice-daily 1 mg tamoxifen treatment during 15 days. Four weeks after the end of the treatment (tamoxifen or vehicle), mice were sacrificed and brain tissues were collected. In presence of X-Gal, the *β-galactosidase* enzyme substrate, the brain slices showed a blue precipitate in Cre-positive cells. Staining results are shown in **Figure 10A** and are summarized in **Table 1**. We observed the most intense LacZ staining in the pyramidal cell layer of the hippocampus (Pyr), dentate gyrus (DG), arcuate hypothalamic nucleus (Arc) and ventromedial hypothalamic nucleus (VMH). Labeling was detected in the piriform cortex (pir), lateral hypothalamus (LH), interpeduncular nucleus (IP), medial mammillary nucleus, medial part (MM), dorsal raphe nucleus (DRN), and median (MnPO) and ventromedial (VMPO) preoptic nucleus. A weak staining was observed in the basolateral amygdala (BLA), cingulate (Cg), motor (M), orbital, prefrontal (PFC) and somatosensorial (S) cortices, bed nucleus of the stria terminalis (BNST), supramammillary nucleus, medial part (SuMM), different parts of anterior olfactory nucleus (dorsal AOD, lateral AOL, medial AOM parts) and paraventricular thalamic nucleus (PV). No staining was detected in the control groups (Cre positive animals treated with vehicle and vehicle/tamoxifen-treated Cre negative mice) (**Figure 10B**).

We next used this transgenic CaMKIIα-CreER^{T2} mouse line to target the *Oprm1* gene in glutamatergic forebrain neurons.

2. Conditional knockout of the mu receptor in CaMKIIα-mu mouse line

Using the Cre-loxP system, we deleted the mu receptor, encoded by the *Oprm1* gene, specifically in glutamatergic forebrain neurons. To this end, we bred the mu floxed mouse line

Brain regions	Cre recombinase expression levels
Basolateral amygdala (BLA)	+
Cingulate (Cg), motor (M), orbital, prefrontal (PFC), and somatosensorial (S) cortices	+
Piriform cortex (Pir)	++
Hippocampal pyramidal cells (Pyr)	+++
Dentate gyrus (DG)	+++
Lateral hypothalamus (LH)	++
Nucleus accumbens (NAc)	0
Caudate putamen (CPu)	0
Bed nucleus of the stria terminalis (BNST)	+
Arcuate hypothalamic nucleus (Arc)	+++
Ventromedial hypothalamic nucleus (VMH)	+++
Interpeduncular nucleus (IP)	++
Medial mammillary nucleus, medial part (MM)	++
Dorsal raphe nucleus (DR)	++
Supramammillary nucleus, medial part (SuMM)	+
Median (MnPO) and ventromedial (VMPO) preoptic nucleus	++
Anterior olfactory nucleus (dorsal AOD, lateral AOL, medial AOM parts)	+
Paraventricular thalamic nucleus (PV)	+

Table 1. Expression level of the Cre recombinase activity in CaMKIIαCreER^{T2} ROSA26 mice.
CaMKIIαCreER^{T2} ROSA26 mice displayed X-Gal mediated blue staining, corresponding to Cre activity, in numerous brain nucleuses. Expression levels: 0, no expression; +, weak; ++, high; +++, very high.

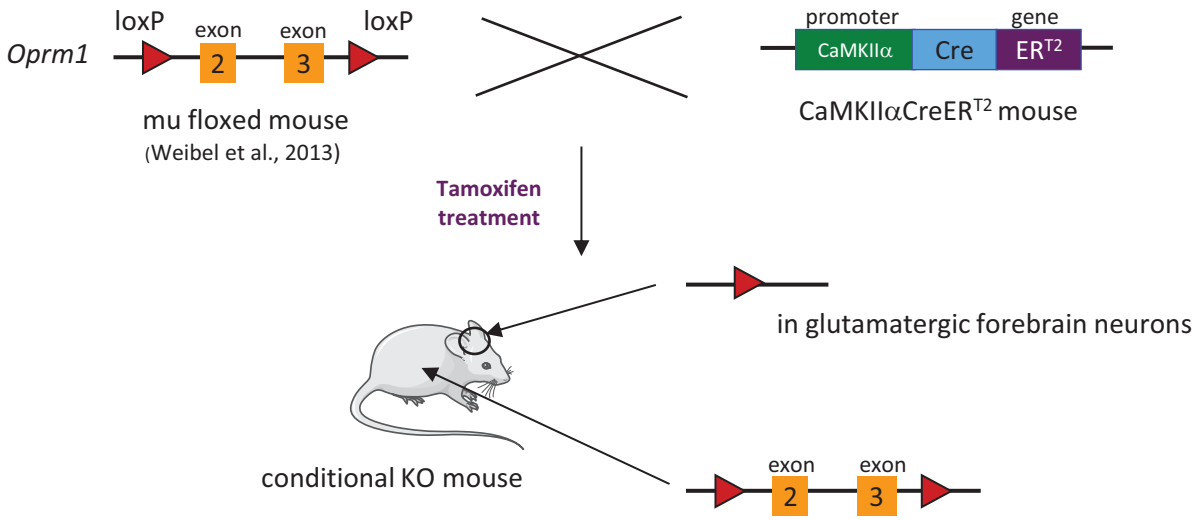

Figure 11. CaMKIIα-mu mouse line creation: breeding strategy and treatment.
We bred floxed mu receptor mice with CaMKIIαCreER^{T2} mice to obtain our conditional knockout (KO) line. Cre recombinase positive animals were treated with tamoxifen to induce Cre recombinase activation, leading to excision of *Oprm1* in glutamatergic forebrain neurons.

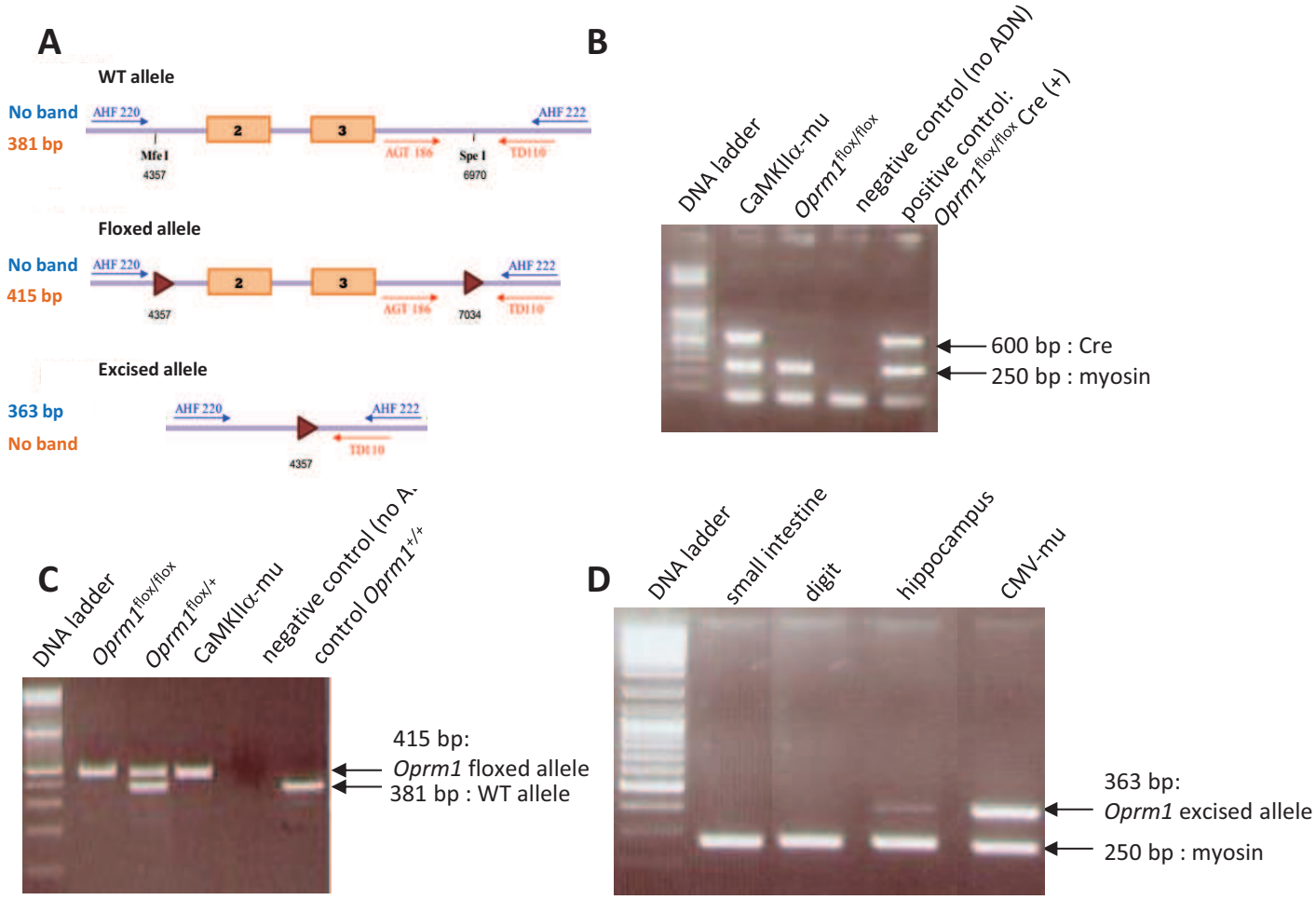

Figure 12. PRC strategies for *Oprm1* floxed allele detection and *Oprm1* excision detection (A) and PCR amplification showing presence of the Cre recombinase (B), lox P sites (C) and excision of mu (D) in CaMKIIα-mu mice treated with tamoxifen. PCR of digit biopsies of CaMKIIα-mu mice: Cre locus presence (**B**) is revealed by BBY14/BBY15 primers, ADV28/ADV30 primers showed myosin presence and served as control; loxP sites presence (**C**) is detected by AGT 186/TD 110 primers. Presence of the *Oprm1* excised allele in different regions is represented in (**D**). There is no *Oprm1* excision in the small intestine or the digit, but an excision band in the hippocampus was detected. Digit biopsy CMV-mu PCR amplification served as control for *Oprm1* excision.

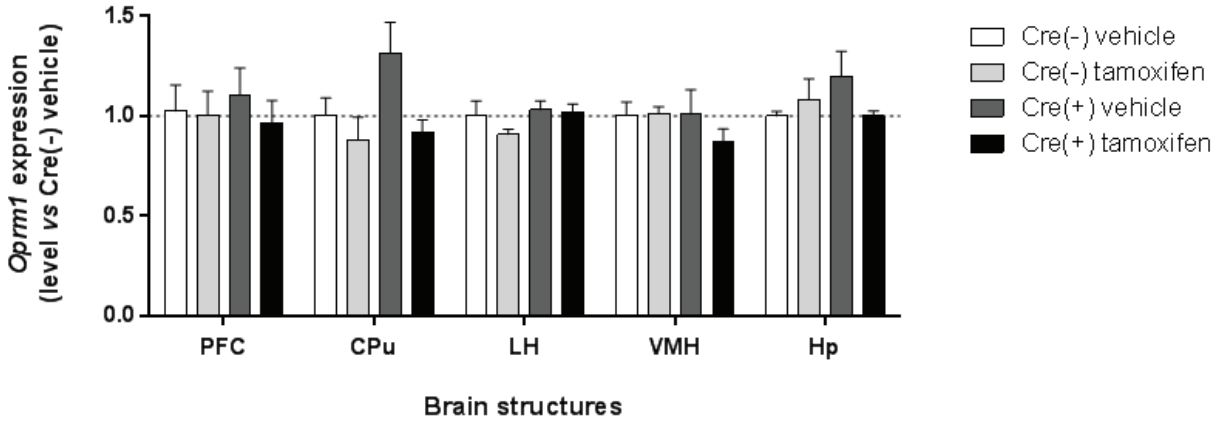

Figure 13. Neuroanatomical characterization of the conditional knockout animals. Quantitative real-time polymerase chain reaction. *Oprm1* messenger RNA in CaMKIIα-mu (conditional knockout) mice is represented according to the expression in vehicle-treated Control (=1, dotted line), normalized using *β-actin* as housekeeping gene. n=3-4 per group. CPu, caudate putamen; Hp, hippocampus; LH, lateral hypothalamus; PFC, prefrontal cortex; VMH, ventromedial hypothalamic nucleus .

(*Oprm1*$^{fl/fl}$) with the CaMKIIα-CreER^{T2} mouse line, to generate the conditional knockout line CaMKIIα-CreER^{T2}-*Oprm1*$^{-/-}$ (or CaMKIIα-mu) (**Figure 11**).

We first genotyped these animals for the presence of the Cre recombinase (**Figure 12B**) and the presence of loxP sites flanking exon 2-3 of the *Oprm1* gene (**Figure 12C**) in genomic DNA from digit biopsies. To assess the specific deletion of mu receptor in the brain, we tested the presence of the *Oprm1* excised allele in different anatomical regions: small intestine, tail and hippocampus (**Figure 12D**). No band at 363 bp, corresponding to the mu receptor's excised allele, was detected in the small intestine and digit, and a weak band was observed for *Oprm1* in the hippocampus. Comparing intensity of this band with the *Oprm1* excised allele band from CMV-mu mouse biopsy (positive control) suggests that excision of *Oprm1* in the hippocampus is partial (**Figure 12D**).

Next, we analysed *Oprm1* mRNA expression from homozygous mu floxed animals (Control) and conditional knockout CaMKIIα-mu mice treated with tamoxifen or vehicle (**Figure 13**) by qRT-PCR. Multiple t-tests showed no differences between groups. Conditional deletion of *Oprm1* was thus, undetectable in all the tested regions (PFC, CPu, LH, VMH, Hp; $p>0.05$).

IV. Discussion

The glutamatergic transmission has been shown to play an important role in addiction (Chartoff and Connery, 2014; Quintero, 2013; van Huijstee and Mansvelder, 2015) and pain control (Rodríguez-Muñoz et al., 2012), two well-established mu receptor implicated behaviors. The mu opioid receptor is predominantly expressed in GABAergic neurons. In the striatum, GABA-containing medium spiny neurons represent 90-95% of the neuronal populations; the other subtypes are GABA and cholinergic interneurons (Kawaguchi et al., 1995). In the brain, mu opioid receptors have also been demonstrated to be expressed in glutamatergic neurons (Chartoff and Connery, 2014). A substantial mu receptor population is localized in the NAc, derived from cortical projection glutamatergic neurons (Groenewegen et al., 1999). This result is consistent with our finding that following the conditional deletion of GABAergic mu receptors, in Dlx-mu mice (manuscript, Part I), a remaining population of mu receptor protein is observed in the NAc despite a complete deletion of the mu receptor mRNA in the same region.

In rats, CaMKIIα mRNA is localized in the forebrain, specifically in the piriform and entorhinal cortices, hippocampus (CA1, CA2, CA3 and dentate gyrus), amygdala (posteromedial and lateral, basomedial and lateral posterior nucleus), neocortex and a weaker expression in the nucleus accumbens, septum, hypothalamus, inferior colliculus and dorsal thalamus (Benson et al., 1992). This distribution is consistent with our LacZ staining results, showing an overlap of CaMKIIα and Cre recombinase. However, the Cre recombinase expression pattern in our animals appeared scarce compared to X-Gal staining from another reporter CaMKIIα-Cre mouse line (Choi et al., 2014). In this report, most cells in nucleus accumbens, hippocampus, caudate putamen, cortex, globus pallidus, hypothalamus, main olfactory bulb and septal nucleus showed intense X-gal staining. Of note, the CaMKIIα-Cre used by Choi and coll. was not inducible, and weak LacZ staining observed in our conditional mice could be due to an ineffective tamoxifen treatment.

The CreER^{T2} technology enables the temporal control of the Cre recombinase driver, via ligand-dependent recombinase (Brocard et al., 1998). The action of tamoxifen treatment leads to translocation of the Cre recombinase-ER^{T2} complex and provokes activation of the enzyme (**Figure 14**). Numerous tamoxifen regiments have been reported in the literature. For example, to induce the deletion of the CaMKIIα at adult stage in the entire brain, Achterberg and collaborators used four daily injections of tamoxifen at 20 mg/mL during 4 consecutive days at a dose of 0.10 mg/g bodyweight (Achterberg et al., 2014). In the first report of CreER^{T2} technology in transgenic rats, animals were injected with seven

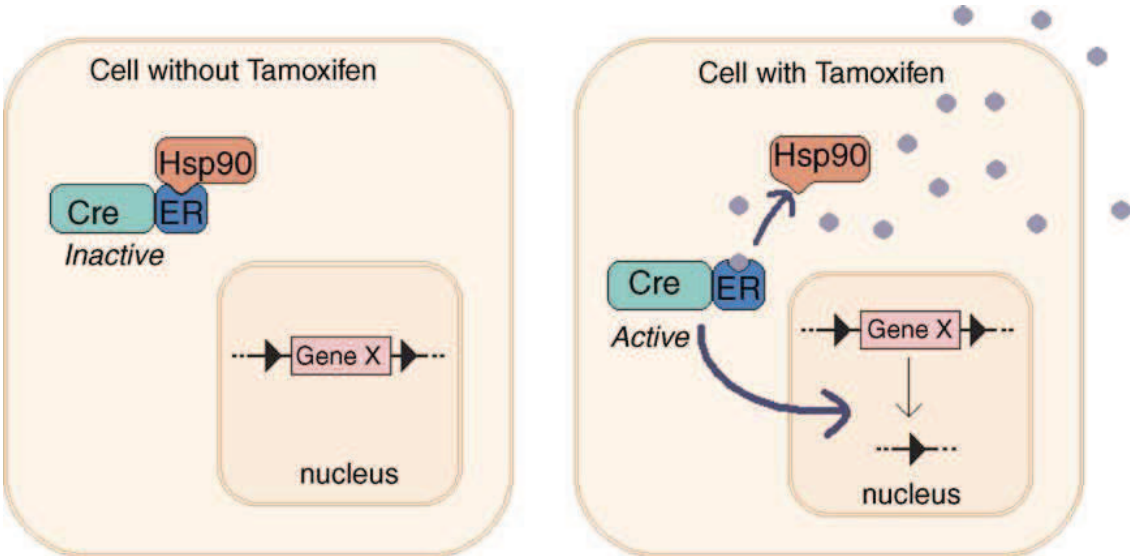

Figure 14. Cre activity in the CreER^{T2} fusion protein is inducible by 4-OH-tamoxifen. In the absence of tamoxifen, CreER is bound to Hsp90 and located in the cytoplasm. Tamoxifen preferentially binds to the Estrogen Receptor (ER), displacing Hsp90 and inducing translocation of CreER to the nucleus, hence activating Cre. Adapted from Tian et al., 2006.

tamoxifen (40 mg/kg, i.p.) injections over five consecutive days (Schonig et al., 2012). Ten days after the last tamoxifen injection, animals were analysed to assess the genetic invalidation (Schonig et al., 2012). To date, there has been only one study investigating a CamKIIα-CreER^{T2} mouse line that has utilized tamoxifen-food pellets at P35 during a week (week 7/8) and analysed conditional deletion of the gene of interest at week 11/12 (Vogl et al., 2015). Oral tamoxifen treatment is a convenient alternative to injections, and has been reviewed in (Kiermayer et al., 2007). In another experiment, tamoxifen treatment consisted in 2.5 mg tamoxifen per gram of food, 5% sucrose, 4 weeks, or intraperitoneal injections of 1 mg of tamoxifen for 5 days into 12-week-old mice, leading to a deletion of the gene of interest at only 5-10% of the total recombination possible (Casanova et al., 2002). In our study, we first used twice daily injections of 1 mg tamoxifen during 5 days, as reported for several inducible knockout lines (Erdmann et al., 2007; Friedel et al., 2011), but did not succeed to produce a knockout of *Oprm1* (no *Oprm1* allele excised band from hippocampus, not shown). Here, we used a longer treatment, which consists in twice daily injections of 1 mg tamoxifen during 15 consecutive days. We have also tried to double the dose by doubling the volume of injection, but this experiment led to 100% lethality (n=4), indicating that tamoxifen is highly toxic at this dose. Altogether, it is very difficult to define satisfying experimental conditions for gene targeting in the brain (Casanova et al., 2002). Since CaMKIIα mRNA expression starts only postnatally in the forebrain, the risk at obtaining developmental defects is weak (Burgin et al., 1990; Tsien et al., 1996). In our case, multiple protocols for tamoxifen treatment remained ineffective, and future studies of the role of mu receptors in glutamatergic forebrain neurons will require other methods, as for example use of a non-inducible CaMKIIα-Cre driver mouse line.

PART IV

Create a Cre mouse line to target the extended amygdala

I. Introduction

The 'Extended Amygdala' (EA) is a neuroanatomical entity that interfaces the brain reward and stress systems and is involved in behavioral responses related to stress and anxiety (Smith and Aston-Jones, 2008). This complex neuronal circuit involves several basal forebrain structures such as the bed nucleus of stria terminalis (BNST), the central medial amygdala (CeA), and a transition zone in the posterior part of the medial nucleus accumbens (Heimer and Alheid, 1991). To date, there is no EA specific Cre mouse available. The highly complex anatomic organization of the central nervous system is a constant obstacle in the development of a transgenic mouse line expressing Cre recombinase in specific brain structures. The identification of promoter sequences that would drive Cre expression to targeted brain structures, such as EA, is the first step in developing new transgenic mouse lines.

Previous work of our team using a genome-wide approach led to the identification of genes with enriched expression in the EA (Becker et al., 2008). In this study, expression pattern of 49 candidate genes was further examined by *in situ* hybridization in the mouse brain. Among these genes, the Wolframin gene (*WFS1*) showed strong expression in the NAc, BNST and CeA whereas only weak or no expression was detected in most other brain regions. Notably, Wolframin transcripts were also detected in the CA1 field of the hippocampus and the piriform cortex. Mutations in the *WFS1* gene are responsible for the Wolfram syndrome (Inoue et al., 1998; Strom et al., 1998). This disease is a rare autosomal recessive disorder characterized by early-onset diabetes mellitus, progressive optic atrophy, diabetes insipidus and deafness (Rigoli et al., 2011). WFS1 is a protein of 890 amino acids primarily localized in the endoplasmic reticulum (ER) membrane (Takeda et al., 2001) whose role is not fully understood. Functional studies have indicated that WFS1 is involved in intracellular calcium homeostasis by modulating the filling state of ER calcium stores (Takei et al., 2006) and produced under conditions of altered homeostasis, including ER stress (Fonseca et al., 2005; Shang et al., 2014), and this regulation is found in both rodent and human cells (Fonseca et al., 2010). In the brain, WFS1 is mainly expressed in subpopulations of forebrain neurons but not in glial cells (Takeda et al., 2001). Studies using WFS1 knockout mice have notably suggested a role of *Wfs1* gene in growth (Kõks et al., 2009), fertility (Noormets et al., 2009), mood disorder (Kato et al., 2008) and behavioral adaptations to stressful environments (Luuk et al., 2009). Due to the restricted pattern of expression of WFS transcripts, we chose the promoter of the *Wfs1* gene as our best candidate to drive Cre expression within EA neurons.

In this study, the characterization of shWFS1-Cre-eGFP lines was performed by Olivier Gardon, and I characterized the inducible lines (shWFS6-eGFP-T2A-CreERT2 lines and shWFS-eGFP-CreER^{T2} lines).

II. Material and Methods

Generation of transgenic mice

The targeting vector was constructed by the ICS-MSC. PCR cloning of the Cre-eGFP fused to part of the intron 1 was performed in MCI vector (Mouse Clinical Institute) containing a SV40 polyA. After sequencing, PCR cloning of part of the short Wfs promoter plus the remaining portion of the intron was assessed. Then, the rest of the 5.7 kb promoter was cloned (PCR). This construct was further microinjected into the pronucleus of fertilized oocytes (C57Bl6/N) and led to the birth of 5 Cre positive mice further bred to evaluate germ line transmission. Following the confirmation of offspring having a Cre positive genotype: we obtained shWFS1-Cre-eGFP lines.

We next modified the previous construct by adding the ER^{T2} domain to create the shWFS-eGFP-CreER^{T2} lines. This construct was also microinjected (4 micro-injections) into the pronucleus of fertilized oocytes (C57Bl6/N) and led to the birth of founder Cre positive mice, further bred with C57Bl6/N mice to start a colony. Offspring from 6 mice had a Cre positive genotype. After observation of the eGFP distribution as an indicator of Cre expression, we selected the shWFS158-eGFP-CreERT2 line, as the Cre line that showed the best pattern of expression of Cre.

To generate a third line, we modified the first construct by inserting T2A (sequence GAGGGCAGAGGAAGTCTTCTAACATGCGGTGACGTGGAGGAGAATCCCGGCCCT) between eGFP and Cre, as well as ER^{T2} in frame and 3' to Cre. This construct was also microinjected into the pronucleus of fertilized oocytes (C57Bl6/N) and led to the birth of 21 Cre positive mice, further bred with C57Bl6/N mice. Offspring from 3 mice showed a Cre positive genotype. After observation of the eGFP distribution as an indication for Cre expression, we selected the shWFS6-eGFP-T2A-CreERT2 line, the Cre line having the best pattern of Cre expression.

For controls in the *in situ* hybridization experiments, we also used male wildtype mice with C57Bl6 background.

For the Cre recombinase activity report, we generated the shWFS1-Cre-eGFP-ROSA26 mouse line, by crossing the shWFS1-Cre-eGFP mice with the Cre activity reporter transgenic line ROSA26 (Soriano, 1999).

All experiments were carried out according to the recommendations of the NIH Guide for Care and Use of Laboratory Animals. The study protocol was approved by the Local Bioethics Committee (Strasbourg, France). All animals were housed in a room maintained at 21±2°C and 45±5% humidity, with a 12h light-dark cycle. Food and water were available ad libitum.

Genotyping

Animals were genotyped for the presence of Cre and/or the ROSA26 locus through PCR analysis. PCR was carried out on DNA from a mouse digested tail or digit sample (NaCl 0.2M; Tris-HCl 100 mM pH8.5; EDTA 5mM; SDS 0.2%; proteinase K (Sigma-Aldrich) 10 mg/mL) for overnight at 55°C. PCR was performed using 0.5 µL of lysate in a 50 µL final volume of reactive mix [PCR buffer 1x (Sigma-Aldrich); $MgCl_2$ 2.5 mM (Sigma-Aldrich); dNTPs 0.2 mM; 2.5 U Taq DNA polymerase (Sigma-Aldrich)] with specific primers (0.2 µM each): Cre (forward GATCGCTGCCAGGATATACG; reverse CATCGCCATCTTCCAGCAG) and Rosa (forward GTTAACCGTCACGAGCATCA; reverse TCACACTCGGGTGATTACGA) primers. Cycling conditions were: 1 cycle at 94°C for 3 min; 30 cycles at 94°C for 30 sec; 62°C for 30 sec; and 72°C for 30 sec. Primers allowing the detection of the myosin gene were also included (sense, TTACGTCCATCGTGGACAGC; reverse, TGGGCTGGGTGTTAGCCTTA) as an internal control in the PCR reaction mix.

The loxP sites PCR reaction was performed by adding 0.5 µL lysate to 49.5 µL reaction mix (1X PCR buffer GoTaq (Promega); MgCl2 (Sigma) 1 mM; dNTPs 0.4 mM (Thermo Scientific); TAQ DNA polymerase 2.5 U (Promega); sense mu floxed primer AGT186 (GTT ACT GGA GAA TCC AGG CCA AGC), antisense mu floxed primer TD110 (TGC TAG AAC CTG CGG AGC CAC A) 1 µM). Cycling conditions were: 1 X 5 min at 94°C; 30 X: 1 min at 95°C, 1 min at 60°C, 1 min at 72°C; 1 X 10 min at 72°C.

The mu excision PCR reaction was performed by adding 0.2 µL lysate to 49.8 µL reaction mix (1X PCR buffer (Sigma); MgCl2 (Sigma) 2.5 mM; dNTPs 0.2 mM (Thermo Scientific); TAQ DNA polymerase 2.5 U (Sigma); sense excision primer AHF220 (ACC AGT ACA TGG ACT GGA TGT GCC), antisense excision primer AHF222 (GAG ACA AGG CTC TGA GGA TAG TAA C), sense myosin gene primer ADV28 (TTA CGT CCA TCG TGG ACA GC), antisense myosin gene primer ADV30 (TGG GCT GGG TGT TAG CCT TA) 0.5 µM). Cycling conditions were: 1 X 5 min at 94°C; 35 X: 30 sec at 94°C, 30 sec at 61°C, 30 sec at 72°C; 1 X 10 min at 72°C.

In situ *hybridization*

Brain sections kept at -80°C were allowed to warm up to room temperature for 30 minutes. Brain sections were next fixed in a 4% paraformaldehyde solution (Sigma-Aldrich) dissolved in 1x PBS for 10 minutes. Tissues were acetylated with triethanolamine [triethanolamine 0.1M pH 8 (Merck); 0.25% acetic acid anhydrous (Sigma-Aldrich)] under agitation for 10 minutes. Next, slides were washed 2 x 10 minutes in 2xSSC (300mM NaCl; 30mM sodium citrate; pH 7) and dehydrated by immersion for 1 minute in successive baths of 60%, 75%, 95%, 100% ethanol, chloroform, ethanol 100% and finally ethanol 95%. For the hybridization step, the Wfs1 probe was diluted to a concentration of 1.5 ng/µL in the hybridization mix [formamide 50% (molecular biology grade, Sigma-Aldrich); dextran sulfate 10%; Denhardt's 1x; tRNA 10mg/mL (from Baker's yeast, Sigma-Aldrich); NaCl 300mM; Tris-HCl 20 mM ph 6.8; EDTA 5 mM; NaH_2PO_4 5.4 mM; Na_2HPO_4 4.6 mM]. After denaturation (70°C for 10 minutes), the Wfs1 probe (180 ng) was hybridized on each slide for 16 hours at 65°C in humidified chambers saturated by vapors of a solution of 50% formamide (Fluka) dissolved in 1x PBS. Slides were then washed 3 x 30 minutes at 65°C [formamide 50% (Fluka); SSC 0.1x (15 mM NaCl; 1,5 mM sodium citrate); Tween20 0.1% (Sigma-Aldrich); PBS 1x]. Slides were further incubated 2 x 30 min in MABT 1x (maleic acid 100mM; NaCl 125mM; Tween20 0.1%; ph 7.5) at room temperature. Blocking step was performed by adding 350µL of blocking solution [2% Blocking (Roche); 20% heat inactivated goat serum (Sigma-Aldrich); MABT 1x] per slide for 1 hour at room temperature. Slides were drained off and 100µl blocking solution containing an anti-DIG antibody (Roche, 1/1500 dilution), was added quickly to each slide. Finally, coverslips were added and slides further incubated at room temperature for 2 hours (or at 4°C overnight) in water-humidified chambers.

Immunohistochemistry for Wfs1-Cre-eGFP mice

Mice were anesthetized by intra-peritoneal injection of ketamine/xylazine (10/100 mg/Kg) and intra-cardially perfused at a rate of 3mL/min with 10mL of 9.25% sucrose followed by 50 ml of 4% paraformaldehyde in phosphate buffer (PB) 0.1M. Brains were next post-fixed 24 hours at 4°C in 4% paraformaldehyde in PB 0.1M. Further, tissue cryoprotection was performed through immersion of the brains in a 30% sucrose solution dissolved in phosphate buffer 0.1 M until sinking of the brains. Fixed brains were included in OCT and stored at -80°C until sectioning. Brain sections were cut at 20 µm in a cryostat and transferred in 1 mL of PB 0.1 M. The free floating brain sections were further incubated in a blocking solution (PB 0.1 M; normal goat serum 5% (Sigma-Aldrich); Triton X-100 0.5% (Sigma-Aldrich)) for 2 hours at room temperature followed by overnight incubation at 4°C with an anti-GFP antibody (Invitrogen) diluted at 1/1000 in blocking solution. After 4 x 5 minute washes with the washing solution

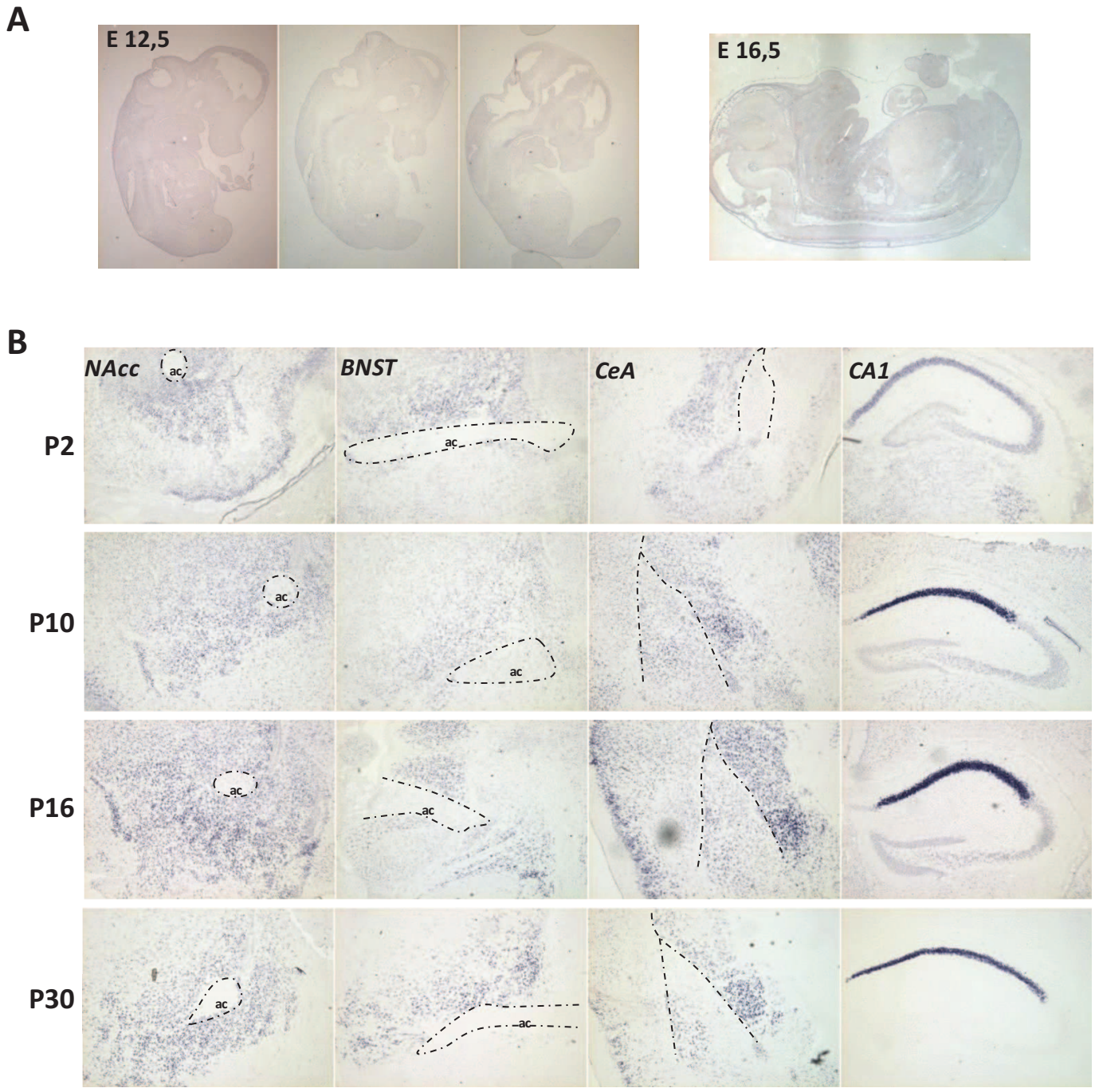

Figure 15. *Wfs1* expression pattern in the developing embryo and in the mouse brain during post-natal development by *in situ* hybridization. **(A)** No expression of the *WFS1* gene is detectable during embryonic development, as shown in the stages E12.5 and E16.5 (sagittal sections). **(B)** *Wfs1* expression in the mouse brain at different post-natal stages (coronal sections). Moderate levels of the *Wfs1* transcript are detected in the EA and the CA1 since post-natal day 2. The expression of *Wfs1* further increases with time and is comparable to adult expression at post-natal day 16.

ac, anterior commissure; BNST, bed nucleus of the stria terminalis; CA1, field CA1 of hippocampus; CeA, central amygdaloid nucleus; NAcc, nucleus accumbens.

(phosphate buffer 0.1 M; Triton X-100 0.5%), sections were incubated for 2 hours at room temperature with the secondary antibody GAR-Alexa488 (Molecular probes) diluted at 1/2000 in blocking solution. Finally, the free floating brain sections were washed 4 x 5 minutes in washing solution at room temperature and mounted on SuperFrost slides with Mowiol (Calbiochem) and DAPI (Sigma-Aldrich) (1:1000). Brain sections were observed under an epifluorescent microscope (Leica) and images were recorded using a CCD camera (CoolSNAP, Roper Scientific) and the CoolSNAP software.

Immunohistochemistry for shWFS158-eGFP-CreER^{T2} and shWFS6-eGFP-T2A-CreER^{T2} mice

Mice were anesthetized by intra-peritoneal injection of ketamine/xylazine (10/100 mg/kg) and intra-cardially perfused at a rate of 20mL/min with 10 mL PBS 1x followed by 100 mL of 4% paraformaldehyde in PB 0.1 M (PFA 4%). Brains were next post-fixed 24 to 48 hours at 4°C in PFA 4%. Further, tissue cryoprotection was performed through immersion of the brains in a 30% sucrose solution dissolved in PB 0.1 M. Fixed brains were blocked in OCT and stored at -80°C until sectioning. Brain sections were cut at 30 µm in a cryostat and transferred in PB 0.1M. Half of the brain slices were directly mounted onto a slide with Mowiol (Calbiochem) to observe direct fluorescence (no amplification). The remaining free floating brain sections were further incubated in a blocking solution [PB 0.1 M; normal goat serum 3% (Sigma-Aldrich); Tween20 0.2%] for 1 hour at room temperature followed by overnight incubation at 4°C with an anti-GFP antibody (Invitrogen) diluted at 1/1000 in blocking solution. After 3 x 10 minute washes with the washing solution (PB 0.1M; Tween20 0.2%), sections were incubated 2 hours at room temperature with the secondary antibody GAR-Alexa488 (Molecular probes) diluted at 1/2000 in washing solution. Finally, the free floating brain sections were washed 3 x 10 minutes in washing solution and once in milliQ water at room temperature and mounted on SuperFrost slides with Mowiol (Calbiochem) and DAPI (Sigma-Aldrich) (1:1000). Brain sections were observed under an epifluorescent microscope (Zeiss) and images were recorded using an Axiocam camera (Zeiss Axiocam MRm) and the AxioVision software.

III. Results

Early promoter activity may trigger developmental compensations or may lead to a lethal phenotype if the target gene is essential for development. Moreover, early promoter activity can lead to inadequate and/or widespread recombination if the pattern of expression is markedly different between embryonic and adult stages. Therefore, late promoters are preferred to study gene function in the adult

Figure 16. Schematic representation of the construct used to generate the transgenic WFS1-Cre-eGFP mouse line
A short transgene containing a cDNA encoding a fluorescent Cre-eGFP fusion protein under the control of 5.7 kb Wfs1 promoter was constructed and further microinjected into fertilized oocytes.

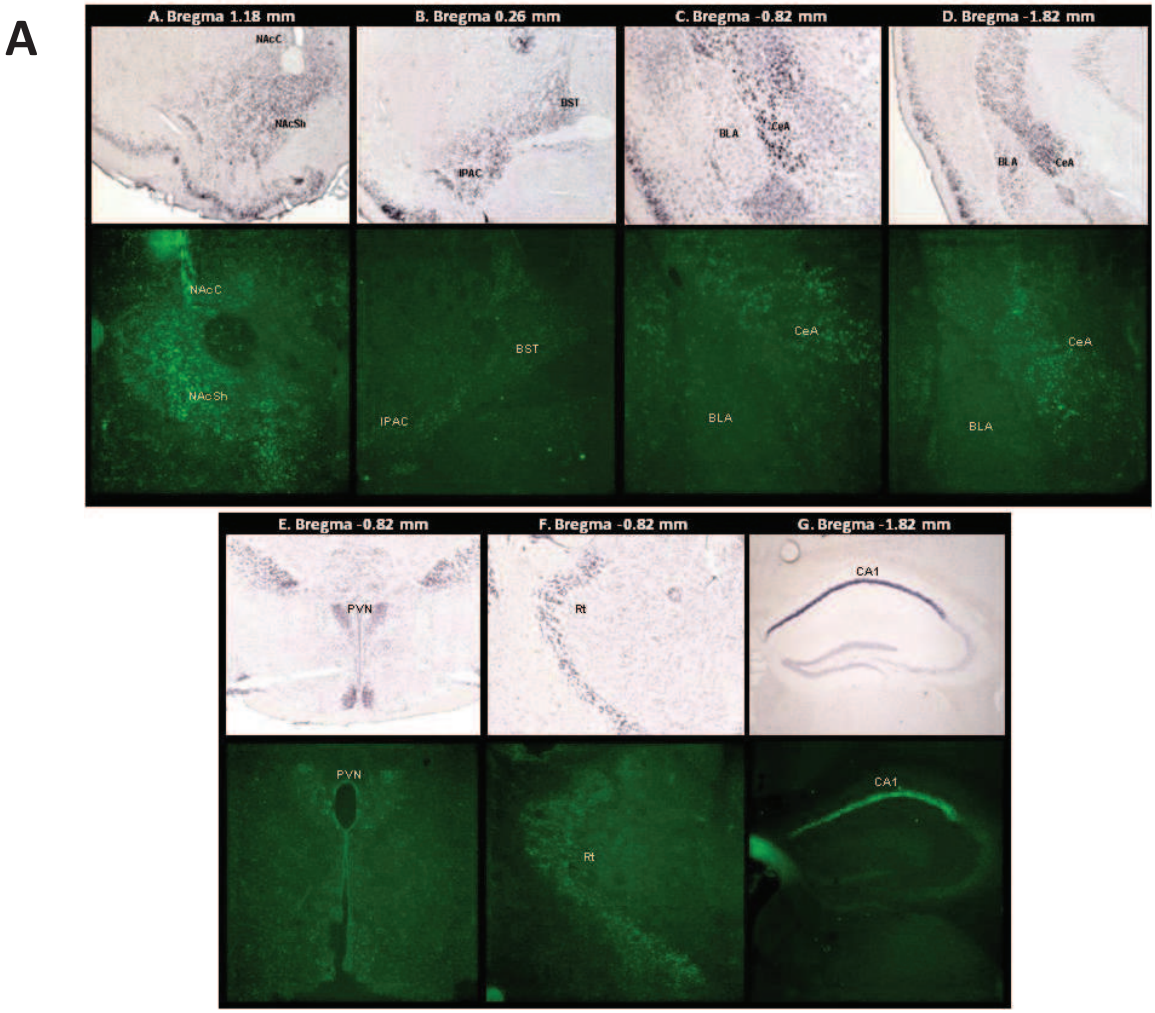

Figure 17. (A) Comparing expression patterns of *Wfs1* mRNA (WT mice) with the Cre-eGFP transgene (shWFS1-Cre-eGFP mice). The top panels depict brain sections of WT mice after *in situ* hybridization using a *Wfs1* probe whereas the bottom panels depict images of brain sections of shWFS1-Cre-eGFP1 mice after immunohistochemistry using an anti-GFP antibody. Images A to D correspond to different components of the EA, image E to the PVN, image F the Rt and image G to the CA1 field of the hippocampus.
BLA, basolateral amygdaloid nucleus, anterior part; BST, bed nucleus of the stria terminalis; CA1, field CA1 of hippocampus; CeA, central amygdaloid nucleus; IPAC, interstitial nucleus of the posterior limb of the anterior commissure; NAcC, nucleus accumbens core; NAcS, nucleus accumbens shell; PVN, paraventricular thalamic nucleus; Rt, reticular thalamic nucleus.

brain (Gavériaux-Ruff and Kieffer, 2007). In order to determine the onset of the *WFS1* promoter, we performed *in situ* hybridization experiments on sections of wild type mouse tissues (embryos or brain) collected during embryonic development and at different post-natal stages (**Figure 15**). No expression of *WFS1* was detectable by *in situ* hybridization at any of the embryonic developmental stages tested, including E12.5, E14.5, E16.5 and E21.5. At post-natal day 2 (P2), weak to moderate *Wfs1* expression is detectable in the NAc, BNST, CeA and CA1. Levels of *Wfs1* expression observed at later post-natal stages (P10, P16 and P30) were higher. At the P16 stage, *Wfs1* level of expression is comparable to expression observed in adult mice (starting P56). These results indicate that the WFS1 promoter activity is detectable starting around birth and that this expression increases with time, stabilizing at post-natal day 16. These results confirmed those from a study showing that WFS1 is only weakly expressed in the mouse brain at the day of birth and that this expression increases with a peak at P14 (Kawano et al., 2009). Altogether, these data demonstrate that the WFS1 promoter is a late promoter and is therefore a suitable candidate to drive Cre expression to the EA cells while avoiding developmental compensations.

To provide a tool allowing the study of gene function specifically in EA, we generated the shWFS1-Cre-eGFP transgenic mouse model. A short transgene containing a cDNA encoding a fluorescent Cre-eGFP fusion protein (Calmels et al., 2009) under the control of 5.7 kb WFS1 promoter was constructed (**Figure 16**). This construct was microinjected into the pronucleus of fertilized oocytes and led to the birth of 5 founder Cre positive mice that would potentially lead to 5 distinct Cre lines. These 5 founder mice were further bred in order to obtain germ line transmission. Offspring from 1 of the founder mice showed a Cre positive genotype, indicating that we have successfully established one shWFS1-Cre-eGFP transgenic mouse line.

To determine the pattern of Cre-eGFP mediated DNA recombination, we crossed shWFS1-Cre-eGFP transgenic animals with ROSA26 lacZ reporter mice (Soriano, 1999). Unfortunately, this breeding, using either males or females Cre(+) mice, failed to produce viable double mutant Cre(+)/ROSA26(+) animals. We thus took advantage of the eGFP reporter fused to the Cre recombinase to directly visualize the Cre-eGFP protein. Fluorescence imaging did not reveal any detectable signal. We therefore carried out anti-eGFP immunohistochemistry experiments in order to amplify eGFP signaling (**Figure 17**). Data shows that Cre-eGFP is expressed in all brain structures forming the EA (NAc, BNST, and CeA) in WFS1-Cre-eGFP animals. Moreover, eGFP is detected in other brain structures where WFS1 is expressed in WT animals (paraventricular nucleus of the hypothalamus, PVN; reticular thalamic nucleus, Rt; CA1) and is not detected in the brain regions that do not express *WFS1*. This experiment indicates that shWFS1-Cre-eGFP perfectly recapitulates the expression pattern of the *WFS1* gene.

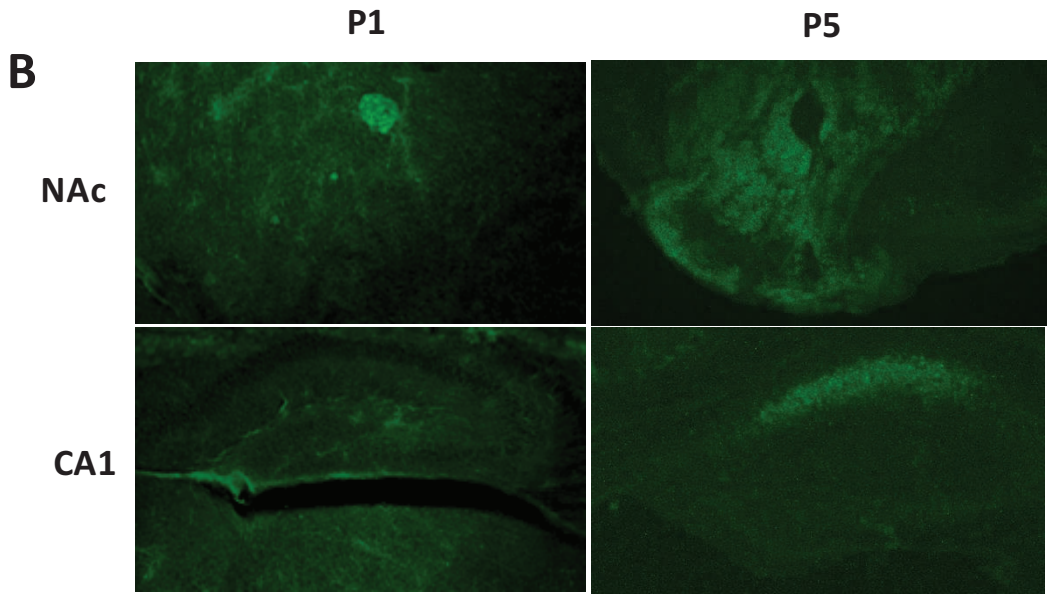

Figure 17. (B) Pattern of Cre-eGFP expression during the post-natal brain development. Anti-GFP immunohistochemistry revealed that Cre-eGFP protein is not yet present in Wfs1-Cre-EGFP mice at P1 stage, but is expressed in neurons of the NAc and CA1 at stage P5.
CA1, field CA1 of hippocampus; NAc, nucleus accumbens.

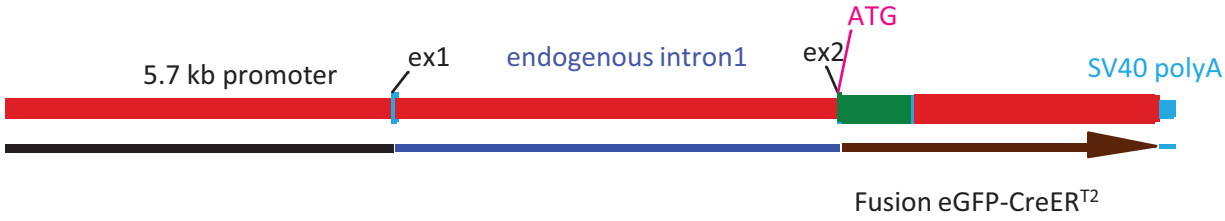

Figure 18. Schematic representation of the construct used to generate the transgenic shWFS1-eGFP-CreER^{T2} mouse line

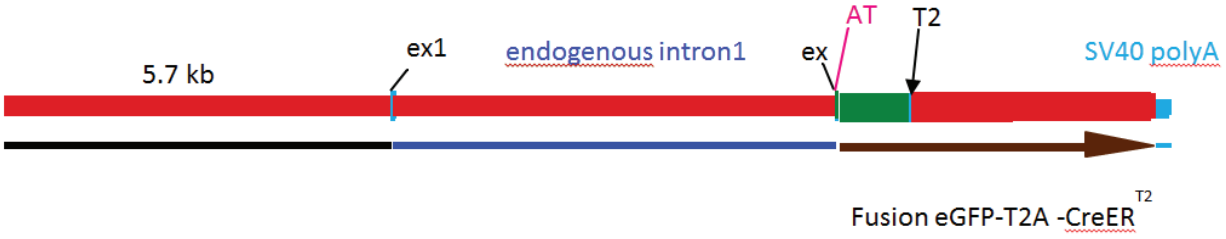

Figure 19. Schematic representation of the construct used to generate the transgenic shWFS1- eGFP-T2A-CreER^{T2} mouse line

Next, we performed immunohistochemistry experiments at different pre and post-natal stages (E12.5, P1, and P5) to characterize the temporal pattern of Cre expression in shWFS1-Cre-eGFP mice. Results for post-natal stages P1 and P5 are depicted in **Figure 17**. These experiments show that Cre-eGFP protein is not detectable in the brain of shWFS1-Cre-eGFP mice during the embryonic development. Also, no Cre-eGFP signal is detectable in the brain at stage P1. At stage P5, Cre-eGFP signal becomes observable and the distribution of the Cre-eGFP protein is similar to the distribution of the *Wfs1* mRNA in the WT brain at post-natal day 4 (P4) as described in (Kawano et al., 2009). In summary, the pattern of Cre-eGFP protein expression in the brain of Wfs1-Cre-eGFP mice is similar to the pattern of the *WFS1* gene expression seen by *in situ* hybridization in WT mice.

We next bred these animals with two different lines of floxed mice: mu opioid receptor floxed (*Oprm1* L2/L2) and GPR88 floxed (*Gpr88* L2/L2) mice. Animals from the first generation were expected to be heterozygous for the floxed gene (*Oprm1* or *GPR88*) and were genotyped for the presence of the Cre transgene only. Cre positive animals were further bred with floxed *Oprm1* or *Gpr88* animals, and their offspring genotyped for the presence of the Cre transgene and the status of the floxed gene allele. Unexpectedly, all animals derived from these breeding pairs were carrying at least one excised gene (*Oprm1* or *GPR88*) allele in tail or digit samples, which normally show no WFS1 expression in the adult. This was observed independently on whether we used male and female shWfs1-Cre-eGFP mice for breeding. The most likely explanation for these unexpected gene excision, in tail and digit biopsies, is that Cre-mediated recombination has occurred in both male and female gametes of Cre positive mice and produced heterozygous knockout animals after the first generation of breeding. Germline Cre transgene expression was already described in a line of CaMKIIα-Cre transgenic mice (Bastia et al., 2005; Choi et al., 2014; Dragatsis and Zeitlin, 2000). Unfortunately, this early Cre-mediated recombination occurring in gametes of shWFS1-Cre-eGFP mice makes this mouse line unsuitable for the generation of EA-specific knockout animals.

To overcome this issue, we further used the 5.7kb *Wfs1* promoter fragment to drive the expression of an inducible Cre-ER^{T2} protein (Brocard et al., 1998). The Cre-ER^{T2} system requires tamoxifen treatment to induce Cre activation. Transgene induction in the adult animal would then prevent the occurrence of Cre-mediated recombination in gametes and the subsequent generalized gene knockout. Two different constructs were produced. The first construct encodes a fusion eGFP-CreER^{T2} protein (**Figure 18**), and the second construct produces a fusion eGFP-T2A-CreER^{T2} permitting dissociation of Cre recombinase (nucleus) and eGFP (cytoplasm) upon cleavage of the T2A peptide by endogenous peptidases (**Figure 19**) (Yoshinari et al., 2012). We obtained 5 lines for classical construct

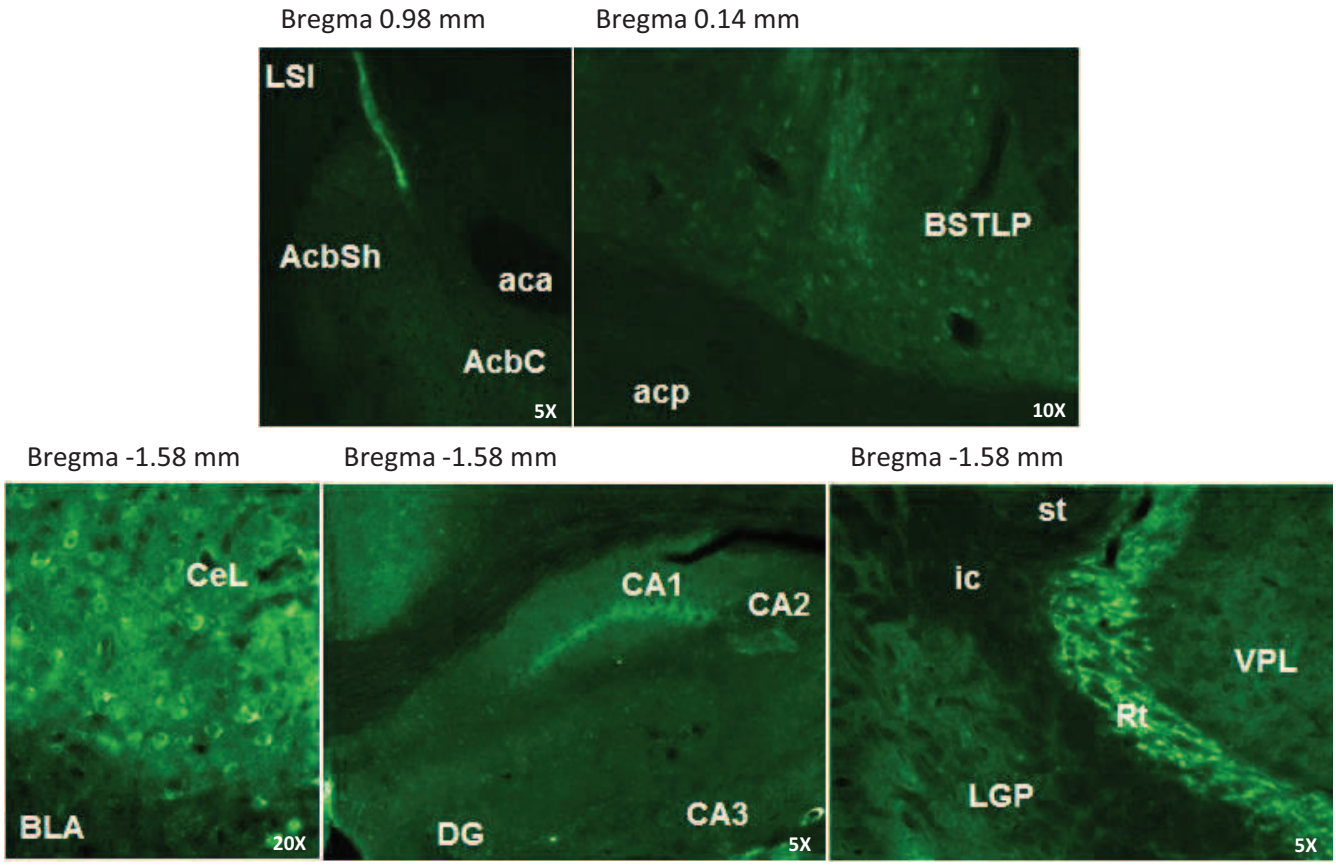

Figure 20. Cre-eGFP expression pattern revealed by anti-eGFP immunohistochemistry in the transgenic shWFS158-eGFP-CreER^{T2} mouse line (coronal sections).

aca, anterior commissure, anterior part; AcbC/Sh, accumbens nucleus, core/shell; acp, anterior commissure, posterior part; BLA, basolateral amygdaloid nucleus, anterior part; BSTLP, bed nucleus of the stria terminalis, lateral division, posterior part; CA1/2/3, field CA1/2/3 of hippocampus; CeL, central amygdaloid nucleus, lateral division; DG, dentate gyrus; ic, internal capsule; LGP, lateral globus pallidus; Rt, reticular thalamic nucleus; st, stria terminalis; VPL, ventral posterolateral thalamic nucleus.

and 3 lines for T2A construct. We characterized Cre expression using eGFP immunostaining for each line and selected one line for each construct, based on highest eGFP expression levels.

The shWFS-eGFP-CreER^{T2} mouse line (shWFS158, see **Figure 20**) showed no detectable eGFP fluorescence upon direct observation. Immunohistochemistry using an eGFP antibody permitted the observation of strong staining in the NAc shell, CeA, CA1 and Rt. The Cre-eGFP protein was also detectable in the granular cell layer of the olfactory bulb (GrO), NAc core, BNST, Rt and ventral posterolateral thalamic nucleus (VPL), and to a lesser extent in the anterior olfactory nucleus, caudal part of the basolateral amygdala (BLA) as well as the lateral hypothalamus (LH). The eGFP pattern, therefore, recapitulates anatomical distribution of *WFS1* gene expression. The shWFS-eGFP-T2A-CreER^{T2} mouse line (shWFS6T2A) showed an eGFP fluorescent signal that was detectable by direct observation in NAc, piriform cortex, CeA, and CA1 field of the hippocampus, suggesting stronger expression levels compared to the shWFS158 line. Further eGFP immunostaining (**Figure 21**) revealed strong staining in the NAc, CeA, CA1, BNST, anterior dorsal part of the medial amygdaloid nucleus (MeAD) and Rt. As for the shWFS158 line, therefore, this pattern recapitulates extremely well the expression pattern of the *WFS1* gene. No eGFP staining was detected by direct observation or following eGFP immunohistochemistry in Cre negative animals (data not shown).

IV. Discussion and perspectives

Methods using site-specific Cre-mediated recombination are invaluable to decipher gene function in targeted cell types, regions or circuits. Moreover, the use of promoters that drive gene knockout late in the development permits to avoid embryonic lethality often associated with global gene knockout. For some promoters, transient expression of the recombinase during germline or embryonic development may occur (Winkeler et al., 2012), in which case the use of inducible versions of the Cre recombinase is most appropriate. A most widely used inducible form of Cre recombinase is CreER^{T2}, where gene deletion occurs only after tamoxifen treatment (Brocard et al., 1998), although tamoxifen treatment is fairly inefficient to induce Cre activity in the brain due to poor blood brain barrier penetrance (Casanova et al., 2002). The use of inducible CreER^{T2} is discussed in the previous chapter (Part III).

Here, we have generated two viable mouse lines with CreER^{T2} expression mostly restricted to the EA. The next step will involve breeding of the transgenic driver line with mice harbouring floxed alleles for the gene of interest. Breeding is underway with mu opioid receptor floxed (*Oprm1* L2/L2) and

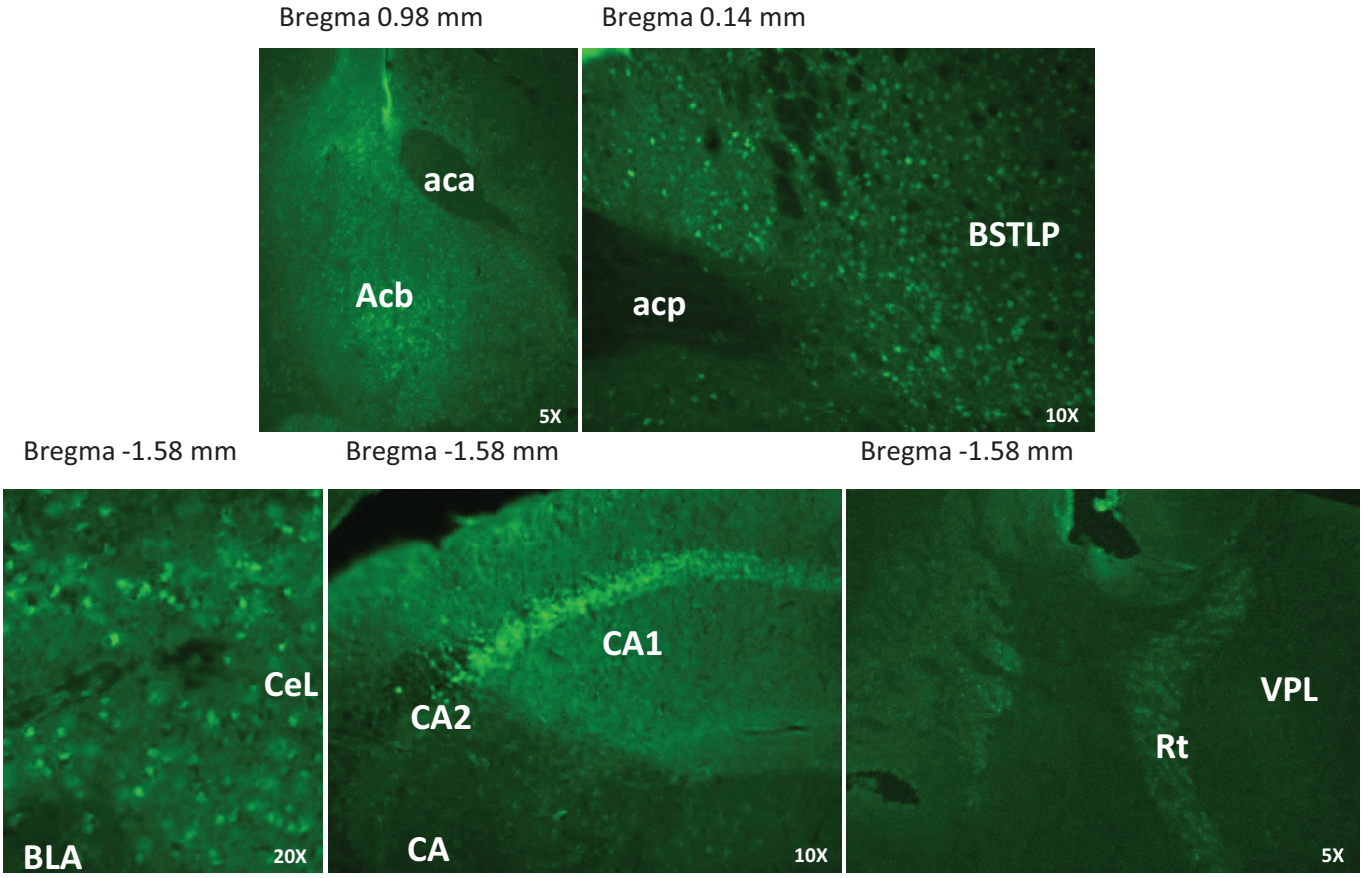

Figure 21. Cre-eGFP expression pattern revealed by anti-eGFP immunohistochemistry in the transgenic shWFS6-eGFP-T2A-CreERT2 mouse line (coronal sections).

aca, anterior commissure, anterior part; Acb, accumbens nucleus, core/shell; acp, anterior commissure, posterior part; BLA, basolateral amygdaloid nucleus, anterior part; BSTLP, bed nucleus of the stria terminalis, lateral division, posterior part; CA1/2/3, field CA1/2/3 of hippocampus; CeL, central amygdaloid nucleus, lateral division; Rt, reticular thalamic nucleus; VPL, ventral posterolateral thalamic nucleus.

GPR88 floxed (*Gpr88* L2/L2) mice, as previously done for the non-inducible WFS1-Cre line. The analysis of tamoxifen- and vehicle-treated adult mice will determine whether *Oprm1 and Gpr88* are efficiently inactivated specifically in the EA. Should this be successful, the two lines would represent a highly valuable mouse tool to target any gene of interest in the EA, in particular genes potentially involved in the negative affective state consequent to binge intoxication with drugs of abuse, drug craving or depressive states that characterize protracted abstinence.

These novel Cre driver lines will also be useful for other genetic manipulations. After breeding with a stop-floxed mouse line (a stop cassette flanked by loxP sites upstream of a gene of interest), these Cre lines would rescue expression of the target gene in the EA, as was shown for the rescue of the mu opioid receptor in pDyn-expressing neurons (Cui et al., 2014). Also, the Cre driver lines could be used in optogenetic approaches to activate (channelrhodopsin) or inactivate (halorhodopsin) (Fenno et al., 2011) the gene of interest in the EA. Altogether, the two WFS1-Cre-eGFP mouse lines reported in this study will be of general interest for genes and neural circuit research in the area of drug abuse and mood disorders.

GENERAL DISCUSSION

General aim of the thesis

The mu opioid receptor is of prime interest in neuroscience and healthcare. The mu receptor is the primary molecular target for morphine *in vivo* and mediates its multiple effects including analgesia, tolerance, dependence, respiratory depression, constipation. Also, in physiology, the mu receptor modulates cardiovascular and gastrointestinal functions, nociception, locomotion and natural rewards such as social behavior, sexual activity and food consumption. The use of total knockout mouse model for the mu receptor, as well as local pharmacology, was a powerful progress in opioid research. However, the precise role of mu receptors at the level of neural pathways remains unknown. To this aim, we targeted selected mu receptor populations using Cre-loxP based knockout technology and examined molecular, cellular and behavioral responses of conditional genetic mutant mice.

In Part I, I investigated the role of mu opioid receptors expressed in GABAergic forebrain neurons in opioid effects using Dlx-mu mice. Anatomical distribution of the *Oprm1* mRNA in this mutant showed a knockout in the striatum, amygdala and hippocampus. Behavioral assays showed no detectable role of the targeted mu receptors in analgesic effects and physical dependence induced by morphine, and rewarding properties of opiates were maintained. Interestingly however, the analysis of activity and operant behaviors revealed that GABAergic forebrain mu receptors are essential for locomotor effects of heroin and inhibit motivation to get heroin and chocolate.

In Part II, I examined the role of mu receptors in GABAergic forebrain neurons in autistic-like behaviors. Mu KO recapitulate an autistic-like phenotype (Becker et al., 2014). I evaluated core and secondary symptoms of autism spectrum disorder. Neither social behavior (core symptom) nor levels of defensive and conflict anxiety (secondary symptoms) were modified in the conditional mutants. This study therefore indicates that deletion of the mu opioid receptor in forebrain GABAergic neurons is not sufficient to produce social and anxiety-like behaviors, characterized in the full KO animals.

In Part III, we used a Cre recombinase fused with ER^{T2} under the control of a CaMKIIα gene promoter to target the *Oprm1* gene in glutamatergic forebrain neurons. Despite a Cre expression pattern matching the expected glutamatergic distribution, the Cre activity was too weak to produce detectable knockout of the mu receptor gene, likely due to poor efficiency of tamoxifen treatment in the brain.

In Part IV, we developed new transgenic Cre driver mouse lines that target the extended amygdala, a brain microcircuit involved in the negative emotional state associated to drug abuse. The first shWFS1-Cre-eGFP mouse line, showed EA-specific expression but triggered body-wide knockout of

the *Oprm1* gene due to a germline expression of the Cre. Two other lines were created (a classic and a T2A constructs) using the 5.7kb Wfs1 promoter fragment to drive the expression of the inducible Cre-ER^{T2} recombinase.

Perspective Parts I & II

It is interesting to note that there were no change in morphine and heroin conditioned place preference in Dlx-mu mice compared to controls, indicating that rewarding properties of opiates are maintained (Part I). Consistent with this finding, social interactions considered an important reward trigger (Calcagnetti and Schechter, 1992) were unchanged in these mutants (Part II). We further found that Dlx-mu mice show stronger motivation to get heroin and chocolate than controls. Should motivation to obtain drugs or undergo social interactions share common neurological pathways, we may then anticipate a higher social interaction score in Dlx-mu animals. We found however no modification of social interactions in Dlx-mu mice, at least under our experimental conditions. It may be of interest to test these animals under conditions of social operant responding (Martin et al., 2014), which would specifically address motivational aspects of social interactions involved in the social motivation theory of autism (Chevallier et al., 2012).

Animal models: relevance for human research

In this (very personal) section, I would like to discuss the importance of fundamental studies to better understand mental diseases, and their contribution to human research.

Animal models are key tools permitting valuable investigation in research. Reliable models are complex to build in psychiatric disorders (for comments and discussion, see (Nestler and Hyman, 2010)). To be the optimal model, an experimental design would meet 3 types of validity: face (similarity in observable outcomes, i.e. symptoms), construct (theoretical rationale), predictive (treatments will be effective in both model and humans) (Willner, 1986). To create animal models of neuropsychiatric disorders, several approaches can be considered, including genetics (i.e. mutations or transgenic mice), pharmacology (i.e. agonist or antagonist), environmental (i.e. chronic stress) or electrical stimulation and lesions (i.e. optogenetics) (Nestler and Hyman, 2010).

In the field of drugs of abuse, behavioral models have been developed that address different stages of the addiction process (see Introduction). DSM V criteria for substance use disorders are impaired control over substance use, social impairment, risky use of the substance, and pharmacological

criteria. Here, we didn't model addiction but we tried to examine several features/components of drug of abuse consumption; we investigated the implication of a gene in specific stages of addiction development, including drug taking and drug seeking (CPP, self-administration), physical dependence (sensitization, withdrawal) and relapse (cue-induced reinstatement) (O'Brien and Gardner, 2005). The advantage of the pathological drug use research is the reciprocity between animal models and humans. Animal models of addiction have remarkable face validity. For instance, a study by Deroche-Gamonet showed that the proportion of rats that becomes dependent to cocaine is equivalent to the human population (Deroche-Gamonet et al., 2004). One of the symptoms of addicted humans is having difficulties to interrupt consumption despite adverse consequences (DSM V). This is modeled by a resistance to punishment, which is the persistence of consumption when mild electric shocks are concomitantly given to rats with history of reinforcement (Pelloux et al., 2007). Also, when placed in an enriched environment, rodents display less psychostimulant self- administration (Bardo et al., 2001; Howes et al., 2000) and seeking (Hofford et al., 2014) compared to rats in isolated conditions. Thus animals are more prone to develop addiction-like behavior when they are alone, with no social or novel object stimulation, suggesting a protecting role of enriched environment against drug consumption (Puhl et al., 2012).

In mental illness research, most of the diseases are multifactorial, involving complex genetic and environmental conditions. It is by definition hard to produce a valuable mouse model with a single genetic mutation that recapitulates construct validity. Numerous human studies of twins, familial cases permitted to conclude that autism is not a single-gene disorder, but involve mutations, polymorphisms and epigenetic modifications (Banerjee et al., 2014; Crawley, 2012). Animal models are tremendous translational research tools to better understand biological aspect of autism. Monogenic ASD mouse models have been generated that recapitulate autism-relevant behavioral phenotypes (for review, please see Crawley, 2012; Oddi et al., 2013). Human symptoms, that include social interaction and social communication deficits, as well as restricted, repetitive patterns of behavior, interests or activities (DSM V), can be translated into mouse phenotypes (reciprocal social interaction, parental behavior, ultrasonic vocalization, motor functions and anxiety-like behavior).

Altogether, mice are valuable models of human mental disorders, are easy to genetically modify and are a social species. Those translational systems, with face and construct validity, are valuable tools to investigate new pharmacological and/or behavioral treatments.

BIBLIOGRAPHY

Achterberg, K.G., Buitendijk, G.H.S., Kool, M.J., Goorden, S.M.I., Post, L., Slump, D.E., Silva, A.J., van Woerden, G.M., Kushner, S. a, Elgersma, Y., 2014. Temporal and Region-Specific Requirements of αCaMKII in Spatial and Contextual Learning. J. Neurosci. 34, 11180–7. doi:10.1523/JNEUROSCI.0640-14.2014

Adler, M.W., Geller, E.B., Rogers, T.J., Henderson, E.E., Eisenstein, T.K., 1993. Opioids, receptors, and immunity. Adv. Exp. Med. Biol. 335, 13–20.

Akil, H., Owens, C., Gutstein, H., Taylor, L., Curran, E., Watson, S., 1998. Endogenous opioids: overview and current issues. Drug Alcohol Depend. 51, 127–140. doi:10.1016/S0376-8716(98)00071-4

Allouche, S., Noble, F., Marie, N., 2014. Opioid receptor desensitization: mechanisms and its link to tolerance. Front. Pharmacol. 5, 1–20. doi:10.3389/fphar.2014.00280

Atici, S., Cinel, I., Cinel, L., Doruk, N., Eskandari, G., Oral, U., 2005. Liver and kidney toxicity in chronic use of opioids: an experimental long term treatment model. J. Biosci. 30, 245–252. doi:10.1007/BF02703705

Austin, M.C., Kalivas, P.W., 1990. Enkephalinergic and GABAergic modulation of motor activity in the ventral pallidum. J. Pharmacol. Exp. Ther. 252, 1370–1377. doi:http://jpet.aspetjournals.org/content/252/3/1370.short

Banerjee, S., Riordan, M., Bhat, M. a, 2014. Genetic aspects of autism spectrum disorders: insights from animal models. Front. Cell. Neurosci. 8, 58. doi:10.3389/fncel.2014.00058

Bardo, M.T., Klebaur, J.E., Valone, J.M., Deaton, C., 2001. Environmental enrichment decreases intravenous self-administration of amphetamine in female and male rats. Psychopharmacology (Berl). 155, 278–284. doi:10.1007/s002130100720

Bastia, E., Xu, Y.-H., Scibelli, A.C., Day, Y.-J., Linden, J., Chen, J.-F., Schwarzschild, M. a, 2005. A crucial role for forebrain adenosine A(2A) receptors in amphetamine sensitization. Neuropsychopharmacology 30, 891–900. doi:10.1038/sj.npp.1300630

Becker, A., Grecksch, G., Kraus, J., Loh, H.H., Schroeder, H., Höllt, V., 2002. Rewarding effects of ethanol and cocaine in μ opioid receptor-deficient mice. Naunyn. Schmiedebergs. Arch. Pharmacol. 365, 296–302. doi:10.1007/s00210-002-0533-2

Becker, J. a J., Befort, K., Blad, C., Filliol, D., Ghate, a., Dembele, D., Thibault, C., Koch, M., Muller, J., Lardenois, a., Poch, O., Kieffer, B.L., 2008. Transcriptome analysis identifies genes with enriched expression in the mouse central extended amygdala. Neuroscience 156, 950–965. doi:10.1016/j.neuroscience.2008.07.070

Becker, J.A., Clesse, D., Spiegelhalter, C., Schwab, Y., Le Merrer, J., Kieffer, B.L., 2014. Autistic-Like Syndrome in Mu Opioid Receptor Null Mice is Relieved by Facilitated mGluR4 Activity. Neuropsychopharmacology 2049–2060. doi:10.1038/npp.2014.59

Beckerman, M. a., Glass, M.J., 2012. The NMDA-NR1 receptor subunit and the mu-opioid receptor are expressed in somatodendritic compartments of central nucleus of the amygdala neurons projecting to the bed nucleus of the stria terminalis. Exp. Neurol. 234, 112–126. doi:10.1016/j.expneurol.2011.12.034

Befort, K., 2015. Interactions of the opioid and cannabinoid systems in reward: Insights from knockout studies. Front. Pharmacol. 6, 1–15. doi:10.3389/fphar.2015.00006

Befort, K., Tabbara, L., Kling, D., Maigret, B., Kieffer, B.L., 1996. Role of aromatic transmembrane residues of the delta-opioid receptor in ligand recognition. J. Biol. Chem. 271, 10161–10168. doi:10.1074/jbc.271.17.10161

Benson, D.L., Isackson, P.J., Gall, C.M., Jones, E.G., 1992. Contrasting patterns in the localization of glutamic acid decarboxylase and Ca2+/calmodulin protein kinase gene expression in the rat central nervous system. Neuroscience 46, 825–849.

Berger, A.C., Whistler, J.L., 2011. Morphine-induced mu opioid receptor trafficking enhances reward yet prevents compulsive drug use. EMBO Mol. Med. 3, 385–397. doi:10.1002/emmm.201100144

Bergevin, A., Girardot, D., Bourque, M.J., Trudeau, L.E., 2002. Presynaptic μ-opioid receptors regulate a late step of the secretory process in rat ventral tegmental area GABAergic neurons. Neuropharmacology 42, 1065–1078. doi:10.1016/S0028-3908(02)00061-8

Berrendero, F., Kieffer, B.L., Maldonado, R., 2002. Attenuation of nicotine-induced antinociception, rewarding effects, and dependence in mu-opioid receptor knock-out mice. J. Neurosci. 22, 10935–10940. doi:22/24/10935 [pii]

Bodnar, R.J., 2014. Endogenous opiates and behavior: 2013. Peptides 62, 67–136. doi:10.1016/j.peptides.2014.09.013

Bohn, L.M., Lefkowitz, R.J., Gainetdinov, R.R., Peppel, K., Caron, M.G., Lin, F.T., 1999. Enhanced morphine analgesia in mice lacking beta-arrestin 2. Science 286, 2495–2498. doi:10.1126/science.286.5449.2495

Brady, L.S., Herkenham, M., Rothman, R.B., Partilla, J.S., König, M., Zimmer, A.M., Zimmer, A., 1999. Region-specific up-regulation of opioid receptor binding in enkephalin knockout mice. Mol. Brain Res. 68, 193–197. doi:10.1016/S0169-328X(99)00090-X

Briand, L. a., Hilario, M., Dow, H.C., Brodkin, E.S., Blendy, J. a., Berton, O., 2015. Mouse Model of OPRM1 (A118G) Polymorphism Increases Sociability and Dominance and Confers Resilience to Social Defeat. J. Neurosci. 35, 3582–3590. doi:10.1523/JNEUROSCI.4685-14.2015

Bridges, R.S., Grimm, C.T., 1982. Reversal of morphine disruption of maternal behavior by concurrent treatment with the opiate antagonist naloxone 218, 166–168.

Brocard, J., Feil, R., Chambon, P., Metzger, D., 1998. A chimeric Cre recombinase inducible by synthetic,but not by natural ligands of the glucocorticoid receptor. Nucleic Acids Res. 26, 4086–4090. doi:gkb657 [pii]

Brownstein, M.J., 1993. A brief history of opiates, opioid peptides, and opioid receptors. Proc. Natl. Acad. Sci. U. S. A. 90, 5391–5393. doi:10.1073/pnas.90.12.5391

Brusa, R., 1999. Genetically modified mice in neuropharmacology. Pharmacol. Res. 39, 405–419. doi:10.1006/phrs.1998.0457

Burgin, K.E., Waxham, M.N., Rickling, S., Westgate, S. a, Mobley, W.C., Kelly, P.T., 1990. In situ hybridization histochemistry of Ca2+/calmodulin-dependent protein kinase in developing rat brain. J. Neurosci. 10, 1788–1798.

Calcagnetti, D.J., Schechter, M.D., 1992. Place conditioning reveals the rewarding aspect of social interaction in juvenile rats. Physiol. Behav. 51, 667–672. doi:10.1016/0031-9384(92)90101-7

Calmels, N., Schmucker, S., Wattenhofer-Donzé, M., Martelli, A., Vaucamps, N., Reutenauer, L., Messaddeq, N., Bouton, C., Koenig, M., Puccio, H., 2009. The first cellular models based on frataxin missense mutations that reproduce spontaneously the defects associated with Friedreich ataxia. PLoS One 4. doi:10.1371/journal.pone.0006379

Capecchi, M.R., 1989. Altering the Genome Homologous Recombination by From ES Cells to Germ Line Chimera. Science (80-.). 236, 1288–1291.

Casanova, E., Fehsenfeld, S., Lemberger, T., Shimshek, D.R., Sprengel, R., Mantamadiotis, T., 2002. ER-based double iCre fusion protein allows partial recombination in forebrain. Genesis 34, 208–214. doi:10.1002/gene.10153

Cavalcanti, I., Carvalho, A., Musauer, M., Rodrigues, V., Migon, R., Figueiredo, N., Vane, L., 2014. Safety and tolerability of controlled-release oxycodone on postoperative pain in patients submitted to the oncologic head and neck surgery. Rev Col Bras Cir 41, 393–399.

Charbogne, P., Kieffer, B.L., Befort, K., 2013. 15 years of genetic approaches in vivo for addiction research: Opioid receptor and peptide gene knockout in mouse models of drug abuse. Neuropharmacology 1–14. doi:10.1016/j.neuropharm.2013.08.028

Chartoff, E.H., Connery, H.S., 2014. It's MORe exciting than mu: Crosstalk between mu opioid receptors and glutamatergic transmission in the mesolimbic dopamine system. Front. Pharmacol. 5 MAY, 1–21. doi:10.3389/fphar.2014.00116

Chefer, V.I., Denoroy, L., Zapata, a., Shippenberg, T.S., 2009. Mu opioid receptor modulation of somatodendritic dopamine overflow: GABAergic and glutamatergic mechanisms. Eur. J. Neurosci. 30, 272–278. doi:10.1111/j.1460-9568.2009.06827.x

Chevallier, C., Kohls, G., Troiani, V., Brodkin, E.S., Schultz, R.T., 2012. The social motivation theory of autism. Trends Cogn. Sci. 16, 231–238. doi:10.1016/j.tics.2012.02.007

Chieng, B., Christie, M.J., 1994. Inhibition by opioids acting on mu-receptors of GABAergic and glutamatergic postsynaptic potentials in single rat periaqueductal gray neurones in vitro. Br. J. Pharmacol. 113, 303–309.

Choi, C.-I., Yoon, S.-P., Choi, J.-M., Kim, S.-S., Lee, Y.-D., Birnbaumer, L., Suh-Kim, H., 2014. Simultaneous deletion of floxed genes mediated by CaMKIIα-Cre in the brain and in male germ cells: application to conditional and conventional disruption of Goα. Exp. Mol. Med. 46, e93. doi:10.1038/emm.2014.14

Chu Sin Chung, P., Keyworth, H.L., Martin-Garcia, E., Charbogne, P., Darcq, E., Bailey, A., Filliol, D., Matifas, A., Scherrer, G., Ouagazzal, A.-M., Gaveriaux-Ruff, C., Befort, K., Maldonado, R., Kitchen, I., Kieffer, B.L., 2015. A Novel Anxiogenic Role for the Delta Opioid Receptor Expressed in GABAergic Forebrain Neurons. Biol. Psychiatry 77, 404–415. doi:10.1016/j.biopsych.2014.07.033

Cinque, C., Pondiki, S., Oddi, D., Di Certo, M.G., Marinelli, S., Troisi, a, Moles, a, D'Amato, F.R., 2012. Modeling socially anhedonic syndromes: genetic and pharmacological manipulation of opioid neurotransmission in mice. Transl. Psychiatry 2, e155. doi:10.1038/tp.2012.83

Connery, H.S., 2015. Medication-Assisted Treatment of Opioid Use Disorder. Harv. Rev. Psychiatry 23, 63–75. doi:10.1097/HRP.0000000000000075

Contarino, A., Picetti, R., Matthes, H.W., Koob, G.F., Kieffer, B.L., Gold, L.H., 2002. Lack of reward and locomotor stimulation induced by heroin in ??-opioid receptor-deficient mice. Eur. J. Pharmacol. 446, 103–109. doi:10.1016/S0014-2999(02)01812-5

Coolen, L.M., Allard, J., Truitt, W. a., McKenna, K.E., 2004. Central regulation of ejaculation. Physiol. Behav. 83, 203–215. doi:10.1016/j.physbeh.2004.08.023

Corder, G., R, D., ..., Taylor, B.K., 2013. Constitutive m -Opioid Receptor Activity leads to long-term endogenous analgesia and dependence. Science (80-.). 1394, 1394–1400. doi:10.1126/science.1239403

Crabbe, J.C., Harris, R.A., Koob, G.F., 2011. Preclinical studies of alcohol binge drinking. Ann. N. Y. Acad. Sci. 1216, 24–40. doi:10.1111/j.1749-6632.2010.05895.x

Crawley, J.N., 2012. Translational animal models of autism and neurodevelopmental disorders. Dialogues Clin. Neurosci. 14, 293–305.

Crews, K.R., Gaedigk, a, Dunnenberger, H.M., Leeder, J.S., Klein, T.E., Caudle, K.E., Haidar, C.E., Shen, D.D., Callaghan, J.T., Sadhasivam, S., Prows, C. a, Kharasch, E.D., Skaar, T.C., 2014. Clinical Pharmacogenetics Implementation Consortium guidelines for cytochrome P450 2D6 genotype and codeine therapy: 2014 update. Clin. Pharmacol. Ther. 95, 376–82. doi:10.1038/clpt.2013.254

Cui, Y., Ostlund, S.B., James, A.S., Park, C.S., Ge, W., Roberts, K.W., Mittal, N., Murphy, N.P., Cepeda, C., Kieffer, B.L., Levine, M.S., Jentsch, J.D., Walwyn, W.M., Sun, Y.E., Evans, C.J., Maidment, N.T., Yang, X.W., 2014. Targeted expression of μ-opioid receptors in a subset of striatal direct-pathway neurons restores opiate reward. Nat. Neurosci. 17, 254–61. doi:10.1038/nn.3622

Daunais, J.B., Letchworth, S.R., Sim-Selley, L.J., Smith, H.R., Childers, S.R., Porrino, L.J., 2001. Functional and anatomical localization of mu opioid receptors in the striatum, amygdala, and extended amygdala of the nonhuman primate. J. Comp. Neurol. doi:10.1002/cne.1154

Davis, M.P., 2012. Twelve Reasons for Considering Buprenorphine as a Frontline Analgesic in the Management of Pain. J. Support. Oncol. doi:10.1016/j.suponc.2012.05.002

Deroche-Gamonet, V., Belin, D., Piazza, P.V., 2004. Evidence for addiction-like behavior in the rat. Science 305, 1014–1017. doi:10.1126/science.1099020

Dragatsis, I., Zeitlin, S., 2000. CaMKII??-cre transgene expression and recombination patterns in the mouse brain. Genesis 26, 133–135. doi:10.1002/(SICI)1526-968X(200002)26:2<133::AID-GENE10>3.0.CO;2-V

Ellegood, J., Anagnostou, E., Babineau, B. a, Crawley, J.N., Lin, L., Genestine, M., DiCicco-Bloom, E., Lai, J.K.Y., Foster, J. a, Peñagarikano, O., Geschwind, D.H., Pacey, L.K., Hampson, D.R., Laliberté, C.L., Mills, a a, Tam, E., Osborne, L.R., Kouser, M., Espinosa-Becerra, F., Xuan, Z., Powell, C.M., Raznahan, a, Robins, D.M., Nakai, N., Nakatani, J., Takumi, T., van Eede, M.C., Kerr, T.M., Muller, C., Blakely, R.D., Veenstra-VanderWeele, J., Henkelman, R.M., Lerch, J.P., 2014. Clustering autism: using neuroanatomical differences in 26 mouse models to gain insight into the heterogeneity. Mol. Psychiatry 20, 118–125. doi:10.1038/mp.2014.98

Elsabbagh, M., Divan, G., Koh, Y.J., Kim, Y.S., Kauchali, S., Marcín, C., Montiel-Nava, C., Patel, V., Paula, C.S., Wang, C., Yasamy, M.T., Fombonne, E., 2012. Global Prevalence of Autism and Other Pervasive Developmental Disorders. Autism Res. 5, 160–179. doi:10.1002/aur.239

Erb, S., Shaham, Y., Stewart, J., 1996. Stress reinstates cocaine-seeking behavior after prolonged extinction and a drug-free period. Psychopharmacology (Berl). 128, 408–412. doi:10.1007/s002130050150

Erbs, E., Faget, L., Scherrer, G., Matifas, A., Filliol, D., Vonesch, J.L., Koch, M., Kessler, P., Hentsch, D., Birling, M.C., Koutsourakis, M., Vasseur, L., Veinante, P., Kieffer, B.L., Massotte, D., 2014. A mu-delta opioid receptor brain atlas reveals neuronal co-occurrence in subcortical networks. Brain Struct. Funct. 1–26. doi:10.1007/s00429-014-0717-9

Erdmann, G., Schütz, G., Berger, S., 2007. Inducible gene inactivation in neurons of the adult mouse forebrain. BMC Neurosci. 8, 63. doi:10.1186/1471-2202-8-63

Fenno, L., Yizhar, O., Deisseroth, K., 2011. The development and application of optogenetics. Annu. Rev. Neurosci. 34, 389–412. doi:10.1146/annurev-neuro-061010-113817

Fields, H.L., Margolis, E.B., 2015. Understanding opioid reward. Trends Neurosci. 1–9. doi:10.1016/j.tins.2015.01.002

Filliol, D., Ghozland, S., Chluba, J., Martin, M., Matthes, H.W., Simonin, F., Befort, K., Gavériaux-Ruff, C., Dierich, a, LeMeur, M., Valverde, O., Maldonado, R., Kieffer, B.L., 2000. Mice deficient for delta-

and mu-opioid receptors exhibit opposing alterations of emotional responses. Nat. Genet. 25, 195–200. doi:10.1038/76061

Fonseca, S.G., Fukuma, M., Lipson, K.L., Nguyen, L.X., Allen, J.R., Oka, Y., Urano, F., 2005. WFS1 is a novel component of the unfolded protein response and maintains homeostasis of the endoplasmic reticulum in pancreatic beta-cells. J. Biol. Chem. 280, 39609–39615. doi:10.1074/jbc.M507426200

Fonseca, S.G., Ishigaki, S., Oslowski, C.M., Lu, S., Lipson, K.L., Ghosh, R., Hayashi, E., Ishihara, H., Oka, Y., Permutt, M.A., Urano, F., 2010. Wolfram syndrome 1 gene negatively regulates ER stress signaling in rodent and human cells. Program 120. doi:10.1172/JCI39678.744

Ford, C.P., Mark, G.P., Williams, J.T., 2006. Properties and opioid inhibition of mesolimbic dopamine neurons vary according to target location. J. Neurosci. 26, 2788–2797. doi:10.1523/JNEUROSCI.4331-05.2006

Fredriksson, R., Lagerström, M.C., Lundin, L.-G., Schiöth, H.B., 2003. The G-protein-coupled receptors in the human genome form five main families. Phylogenetic analysis, paralogon groups, and fingerprints. Mol. Pharmacol. 63, 1256–1272. doi:10.1124/mol.63.6.1256

Friedel, R., Wurst, W., Wefers, B., Kühn, R., 2011. Generating Conditional Knockout Mice. Methods Mol. Biol. 693, 37–56. doi:10.1007/978-1-60761-974-1

Galli-Taliadoros, L. a, Sedgwick, J.D., Wood, S. a, Körner, H., 1995. Gene knock-out technology: a methodological overview for the interested novice. J. Immunol. Methods 181, 1–15. doi:10.1016/0022-1759(95)00017-5

Gavériaux-Ruff, C., Kieffer, B.L., 2007. Conditional gene targeting in the mouse nervous system: Insights into brain function and diseases. Pharmacol. Ther. 113, 619–634. doi:10.1016/j.pharmthera.2006.12.003

Gavériaux-Ruff, C., Matthes, H.W., Peluso, J., Kieffer, B.L., 1998. Abolition of morphine-immunosuppression in mice lacking the mu-opioid receptor gene. Proc. Natl. Acad. Sci. U. S. A. 95, 6326–6330.

Ghozland, S., Chu, K., Kieffer, B.L., Roberts, A.J., 2005. Lack of stimulant and anxiolytic-like effects of ethanol and accelerated development of ethanol dependence in mu-opioid receptor knockout mice. Neuropharmacology 49. doi:10.1016/j.neuropharm.2005.04.006

Ghozland, S., Matthes, H.W.D., Simonin, F., Filliol, D., Kieffer, B.L., Maldonado, R., 2002. Motivational effects of cannabinoids are mediated by mu-opioid and kappa-opioid receptors. J. Neurosci. 22, 1146–1154.

Gossen, M., Bujardt, H., 1992. Tight control of gene expression in mammalian cells by tetracycline-responsive promoters. PNAS 89, 5547–5551.

Granier, S., Manglik, A., Kruse, A.C., Kobilka, T.S., Thian, F.S., Weis, W.I., Kobilka, B.K., 2012. Structure of the δ-opioid receptor bound to naltrindole. Nature 485, 400–404. doi:10.1038/nature11111

Groenewegen, H.J., Wright, C.I., Beijer, a. V.J., Voorn, P., 1999. Convergence and segregation of ventral striatal inputs and outputs. Ann. N. Y. Acad. Sci. 877, 49–63. doi:10.1111/j.1749-6632.1999.tb09260.x

Groer, C.E., Schmid, C.L., Jaeger, A.M., Bohn, L.M., 2011. Agonist-directed interactions with specific β-arrestins determine μ-opioid receptor trafficking, ubiquitination, and dephosphorylation. J. Biol. Chem. 286, 31731–31741. doi:10.1074/jbc.M111.248310

Gu, H., Zou, Y., Rajewsky, K., 1993. Independent Control of lmmunoglobulin Switch Recombination at Individual Switch Regions Evidenced through Cre- / oxP-Mediated Gene Targeting. Cell 73, 1155–1164. doi:10.1016/0092-8674(93)90644-6

Gutkowska, J., Strick, D.M., Pan, L., McCann, S.M., 1993. Effect of morphine on urine output: possible role of atrial natriuretic factor. Eur. J. Pharmacol. 242, 7–13. doi:10.1016/0014-2999(93)90003-Z

Hadley, G., Derry, S., Moore, R.A., Wiffen Philip, J., 2013. Transdermal fentanyl for cancer pain. Cochrane Database Syst. Rev. doi:10.1002/14651858.CD010270.pub2

Haghparast, A., Taslimi, Z., Ramin, M., Azizi, P., Khodagholi, F., Hassanpour-Ezatti, M., 2011. Changes in phosphorylation of CREB, ERK, and c-fos induction in rat ventral tegmental area, hippocampus and prefrontal cortex after conditioned place preference induced by chemical stimulation of lateral hypothalamus. Behav. Brain Res. 220, 112–118. doi:10.1016/j.bbr.2011.01.045

Hall, F.S., Li, X.F., Goeb, M., Roff, S., Hoggatt, H., Sora, I., Uhl, G.R., 2003. Congenic C57BL/6 mu opiate receptor (MOR) knockout mice: baseline and opiate effects. Genes. Brain. Behav. 2, 114–121. doi:10.1034/j.1601-183X.2003.00016.x

Hall, F.S., Sora, I., Uhl, G.R., 2001. Ethanol consumption and reward are decreased in mu-opiate receptor knockout mice. Psychopharmacology (Berl). 154, 43–49.

Heimer, L., Alheid, G.F., 1991. The Basal Forebrain 295. doi:10.1007/978-1-4757-0145-6

Hjelmstad, G.O., Xia, Y., Margolis, E.B., Fields, H.L., 2013. Opioid modulation of ventral pallidal afferents to ventral tegmental area neurons. J. Neurosci. 33, 6454–9. doi:10.1523/JNEUROSCI.0178-13.2013

Hofford, R.S., Darna, M., Wilmouth, C.E., Dwoskin, L.P., Bardo, M.T., 2014. Environmental enrichment reduces methamphetamine cue-induced reinstatement but does not alter methamphetamine reward or VMAT2 function. Behav. Brain Res. 270, 151–158. doi:10.1016/j.bbr.2014.05.007

Holland, P.W.H., 2013. Evolution of homeobox genes. Wiley Interdiscip. Rev. Dev. Biol. 2, 31–45. doi:10.1002/wdev.78

Howes, S.R., Dalley, J.W., Morrison, C.H., Robbins, T.W., Everitt, B.J., 2000. Leftward shift in the acquisition of cocaine self-administration in isolation-reared rats: Relationship to extracellular levels of dopamine, serotonin and glutamate in the nucleus accumbens and amygdala-striatal FOS expression. Psychopharmacology (Berl). 151, 55–63. doi:10.1007/s002130000451

Hsu, D.T., Sanford, B.J., Meyers, K.K., Love, T.M., Hazlett, K.E., Wang, H., Ni, L., Walker, S.J., Mickey, B.J., Korycinski, S.T., Koeppe, R. a, Crocker, J.K., Langenecker, S. a, Zubieta, J.-K., 2013. Response of the μ-opioid system to social rejection and acceptance. Mol. Psychiatry 18, 1211–7. doi:10.1038/mp.2013.96

Huang, P., CHen, C., Liu-Chen, L.-Y., 2015. Opioid Receptors. Methods mol biol 1230, 141–154. doi:10.1007/978-1-4939-1708-2

Ide, S., Sora, I., Ikeda, K., Minami, M., Uhl, G.R., Ishihara, K., 2010. Reduced emotional and corticosterone responses to stress in μ-opioid receptor knockout mice. Neuropharmacology 58, 241–247. doi:10.1016/j.neuropharm.2009.07.005

Inoue, H., Tanizawa, Y., Wasson, J., Behn, P., Kalidas, K., Bernal-Mizrachi, E., Mueckler, M., Marshall, H., Donis-Keller, H., Crock, P., Rogers, D., Mikuni, M., Kumashiro, H., Higashi, K., Sobue, G., Oka, Y., Permutt, M. a, 1998. A gene encoding a transmembrane protein is mutated in patients with diabetes mellitus and optic atrophy (Wolfram syndrome). Nat. Genet. 20, 143–148. doi:10.1038/2441

Jaferi, a., Pickel, V.M., 2009. Mu-opioid and corticotropin-releasing-factor receptors show largely postsynaptic co-expression, and separate presynaptic distributions, in the mouse central amygdala and bed nucleus of the stria terminalis. Neuroscience 159, 526–539. doi:10.1016/j.neuroscience.2008.12.061

Jalabert, M., Bourdy, R., Courtin, J., Veinante, P., Manzoni, O.J., Barrot, M., Georges, F., 2011. Neuronal circuits underlying acute morphine action on dopamine neurons. Proc. Natl. Acad. Sci. 108, 16446–16450. doi:10.1073/pnas.1105418108

Jhou, T.C., Geisler, S., Marinelli, M., Degarmo, B. a., Zahm, D.S., 2009. The mesopontine rostromedial tegmental nucleus: A structure targeted by the lateral habenula that projects to the ventral tegmental area of Tsai and substantia nigra compacta. J. Comp. Neurol. 513, 566–596. doi:10.1002/cne.21891

Johnson, C.P., Myers, S.M., 2007. Identification and evaluation of children with autism spectrum disorders. Pediatrics 120, 1183–1215. doi:10.1542/peds.2007-2361

Johnson, S.W., North, R. a, 1992. Opioids excite dopamine neurons by hyperpolarization of local interneurons. J. Neurosci. 12, 483–488.

Jones, E.G., Huntley, G.W., Benson, D.L., 1994. Alpha calcium/calmodulin-dependent protein kinase II selectively expressed in a subpopulation of excitatory neurons in monkey sensory-motor cortex: comparison with GAD-67 expression. J. Neurosci. 14, 611–629.

Kato, T., Ishiwata, M., Yamada, K., Kasahara, T., Kakiuchi, C., Iwamoto, K., Kawamura, K., Ishihara, H., Oka, Y., 2008. Behavioral and gene expression analyses of Wfs1 knockout mice as a possible animal model of mood disorder. Neurosci. Res. 61, 143–158. doi:10.1016/j.neures.2008.02.002

Kawaguchi, Y., Wilson, C.J., Augood, S.J., Emson, P.C., 1995. Striatal interneurones: chemical, physiological and morphological characterization. Trends Neurosci. 18, 527–535. doi:10.1016/0166-2236(95)98374-8

Kawano, J., Fujinaga, R., Yamamoto-Hanada, K., Oka, Y., Tanizawa, Y., Shinoda, K., 2009. Wolfram syndrome 1 (Wfs1) mRNA expression in the normal mouse brain during postnatal development. Neurosci. Res. 64, 213–230. doi:10.1016/j.neures.2009.03.005

Kieffer, B.L., 1999. Opioids: First lessons from knockout mice. Trends Pharmacol. Sci. 20, 19–26. doi:10.1016/S0165-6147(98)01279-6

Kiermayer, C., Conrad, M., Schneider, M., Schmidt, J., Brielmeier, M., 2007. Optimization of Spatiotemporal Gene Inactivation in Mouse Heart by Oral Application of Tamoxifen Citrate. Genesis 45, 418–426. doi:10.1002/dvg

Kitchen, I., Slowe, S.J., Matthes, H.W., Kieffer, B., 1997. Quantitative autoradiographic mapping of mu-, delta- and kappa-opioid receptors in knockout mice lacking the mu-opioid receptor gene. Brain Res. 778, 73–88.

Koch, T., Höllt, V., 2008. Role of receptor internalization in opioid tolerance and dependence. Pharmacol. Ther. 117, 199–206. doi:10.1016/j.pharmthera.2007.10.003

Kõks, S., Soomets, U., Paya-Cano, J.L., Fernandes, C., Luuk, H., Plaas, M., Terasmaa, a, Tillmann, V., Noormets, K., Vasar, E., Schalkwyk, L.C., 2009. Wfs1 gene deletion causes growth retardation in mice and interferes with the growth hormone pathway. Physiol. Genomics 37, 249–259. doi:10.1152/physiolgenomics.90407.2008

Komatsu, H., Ohara, A., Sasaki, K., Abe, H., Hattori, H., Hall, F.S., Uhl, G.R., Sora, I., 2011. Decreased response to social defeat stress in μ-opioid-receptor knockout mice. Pharmacol. Biochem. Behav. 99, 676–682. doi:10.1016/j.pbb.2011.06.008

Koob, G.F., Kenneth Lloyd, G., Mason, B.J., 2009. Development of pharmacotherapies for drug addiction: a Rosetta stone approach. Nat. Rev. Drug Discov. 8, 500–515. doi:10.1038/nrd2828

Koob, G.F., Volkow, N.D., 2010. Neurocircuitry of addiction. Neuropsychopharmacology 35, 217–238. doi:10.1038/npp.2010.4

Kopp, S., Beckung, E., Gillberg, C., 2010. Developmental coordination disorder and other motor control problems in girls with autism spectrum disorder and/or attention-deficit/hyperactivity disorder. Res. Dev. Disabil. 31, 350–361. doi:10.1016/j.ridd.2009.09.017

Kudo, T., Konno, K., Uchigashima, M., Yanagawa, Y., Sora, I., Minami, M., Watanabe, M., 2014. GABAergic neurons in the ventral tegmental area receive dual GABA/enkephalin-mediated inhibitory inputs from the bed nucleus of the stria terminalis. Eur. J. Neurosci. 39, 1796–1809. doi:10.1111/ejn.12503

Kupchik, Y.M., Scofield, M.D., Rice, K.C., Cheng, K., Roques, B.P., Kalivas, P.W., 2014. Cocaine dysregulates opioid gating of GABA neurotransmission in the ventral pallidum. J. Neurosci. 34, 1057–66. doi:10.1523/JNEUROSCI.4336-13.2014

LaBuda, C.J., Sora, I., Uhl, G.R., Fuchs, P.N., 2000. Stress-induced analgesia in mu-opioid receptor knockout mice reveals normal function of the delta-opioid receptor system. Brain Res. 869, 1–5. doi:S0006-8993(00)02196-X [pii]

Lê, a. D., Quan, B., Juzytch, W., Fletcher, P.J., Joharchi, N., Shaham, Y., 1998. Reinstatement of alcohol-seeking by priming injections of alcohol and exposure to stress in rats. Psychopharmacology (Berl). 135, 169–174. doi:10.1007/s002130050498

Le Merrer, J., Becker, J. a J., Befort, K., Kieffer, B.L., 2009. Reward processing by the opioid system in the brain. Physiol. Rev. 89, 1379–1412. doi:10.1152/physrev.00005.2009

Lecca, S., Melis, M., Luchicchi, A., Muntoni, A.L., Pistis, M., 2012. Inhibitory Inputs from Rostromedial Tegmental Neurons Regulate Spontaneous Activity of Midbrain Dopamine Cells and Their Responses to Drugs of Abuse. Neuropsychopharmacology 37, 1164–1176. doi:10.1038/npp.2011.302

Li, X., Shorter, D., Kosten, T.R., 2004. Buprenorphine in the treatment of opioid addiction: opportunities, challenges and strategies. Eur. Neuropsychopharmacol. 14, 205.

Liu, X., Jones, E.G., 1997. Alpha isoform of calcium-calmodulin dependent protein kinase II (CAM II kinase-alpha) restricted to excitatory synapses in the CA1 region of rat hippocampus. Neuroreport 8, 1475–1479.

Liu, X.B., Jones, E.G., 1996. Localization of alpha type II calcium calmodulin-dependent protein kinase at glutamatergic but not gamma-aminobutyric acid (GABAergic) synapses in thalamus and cerebral cortex. Proc. Natl. Acad. Sci. U. S. A. 93, 7332–7336. doi:10.1073/pnas.93.14.7332

Liu, X.-B., Murray, K.D., 2012. Neuronal excitability and calcium/calmodulin-dependent protein kinase type II: location, location, location. Epilepsia 53 Suppl 1, 45–52. doi:10.1111/j.1528-1167.2012.03474.x

Livak, K.J., Schmittgen, T.D., 2001. Analysis of relative gene expression data using real-time quantitative PCR and the 2(-Delta Delta C(T)) Method. Methods 25, 402–408. doi:10.1006/meth.2001.1262

Loh, H.H., Liu, H.C., Cavalli, A., Yang, W., Chen, Y.F., Wei, L.N., 1998. μ opioid receptor knockout in mice: Effects on ligand-induced analgesia and morphine lethality. Mol. Brain Res. 54, 321–326. doi:10.1016/S0169-328X(97)00353-7

Lowe, J.D., Bailey, C.P., 2014. Functional selectivity and time-dependence of mu-opioid receptor desensitization at nerve terminals in the mouse ventral tegmental area. Br. J. Pharmacol. 1–46. doi:10.1111/bph.12605

Lutz, P.-E., Kieffer, B.L., 2013. Opioid receptors: distinct roles in mood disorders. Trends Neurosci. 36, 195–206. doi:10.1016/j.tins.2012.11.002

Luuk, H., Plaas, M., Raud, S., Innos, J., Sütt, S., Lasner, H., Abramov, U., Kurrikoff, K., Kõks, S., Vasar, E., 2009. Wfs1-deficient mice display impaired behavioural adaptation in stressful environment. Behav. Brain Res. 198, 334–345. doi:10.1016/j.bbr.2008.11.007

MacDonald, R.B., Pollack, J.N., Debiais-Thibaud, M., Heude, E., Coffin Talbot, J., Ekker, M., 2013. The ascl1a and dlx genes have a regulatory role in the development of GABAergic interneurons in the zebrafish diencephalon. Dev. Biol. 381, 276–285. doi:10.1016/j.ydbio.2013.05.025

Maldonado, R., Saiardi, a, Valverde, O., Samad, T. a, Roques, B.P., Borrelli, E., 1997. Absence of opiate rewarding effects in mice lacking dopamine D2 receptors. Nature 388, 586–589. doi:10.1038/41567

Manglik, A., Kruse, A.C., Kobilka, T.S., Thian, F.S., Mathiesen, J.M., Sunahara, R.K., Pardo, L., Weis, W.I., Kobilka, B.K., Granier, S., 2012. Crystal structure of the μ-opioid receptor bound to a morphinan antagonist. Nature 485, 321–326. doi:10.1038/nature10954

Mansour, a, Fox, C. a, Burke, S., Meng, F., Thompson, R.C., Akil, H., Watson, S.J., 1994. Mu, delta, and kappa opioid receptor mRNA expression in the rat CNS: an in situ hybridization study. J. Comp. Neurol. 350, 412–438. doi:10.1002/cne.903500307

Mansour, A., Fox, C.A., Thompson, R.C., Akil, H., Watson, S.J., 1994. mu-Opioid receptor mRNA expression in the rat CNS: comparison to mu-receptor binding. Brain Res. 643, 245–265.

Mansour, S.L., Thomas, K.R., Capecchi, M.R., 1988. Disruption of the proto-oncogene int-2 in mouse embryo-derived stem cells: a general strategy for targeting mutations to non-selectable genes. Nature 336, 348–352. doi:10.1038/336348a0

Manzke, T., Guenther, U., Ponimaskin, E.G., Haller, M., Dutschmann, M., Schwarzacher, S., Richter, D.W., 2003. 5-HT4(a) receptors avert opioid-induced breathing depression without loss of analgesia. Science 301, 226–229. doi:10.1126/science.1084674

Mao, L.-M., Jin, D.-Z., Xue, B., Chu, X.-P., Wang, J.Q., 2014. Phosphorylation and regulation of glutamate receptors by CaMKII 66, 365–372. doi:10.13294/j.aps.2014.0044

Martin, L., Sample, H., Gregg, M., Wood, C., 2014. Validation of operant social motivation paradigms using BTBR T+tf/J and C57BL/6J inbred mouse strains. Brain Behav. 4, 754–764. doi:10.1002/brb3.273

Matsui, a., Williams, J.T., 2011. Opioid-Sensitive GABA Inputs from Rostromedial Tegmental Nucleus Synapse onto Midbrain Dopamine Neurons. J. Neurosci. 31, 17729–17735. doi:10.1523/JNEUROSCI.4570-11.2011

Matsui, A., Jarvie, B.C., Robinson, B.G., Hentges, S.T., Williams, J.T., 2014. Separate GABA afferents to dopamine neurons mediate acute action of opioids, development of tolerance, and expression of withdrawal. Neuron 82, 1346–1356. doi:10.1016/j.neuron.2014.04.030

Matthes, H.W., Maldonado, R., Simonin, F., Valverde, O., Slowe, S., Kitchen, I., Befort, K., Dierich, a, Le Meur, M., Dollé, P., Tzavara, E., Hanoune, J., Roques, B.P., Kieffer, B.L., 1996. Loss of morphine-induced analgesia, reward effect and withdrawal symptoms in mice lacking the mu-opioid-receptor gene. Nature. doi:10.1038/383819a0

McDonald, A.J., Muller, J.F., Mascagni, F., 2002. GABAergic innervation of alpha type II calcium/calmodulin-dependent protein kinase immunoreactive pyramidal neurons in the rat basolateral amygdala. J. Comp. Neurol. 446, 199–218. doi:10.1002/cne.10204

Mehendale, S.R., Yuan, C.S., 2006. Opioid-induced gastrointestinal dysfunction. Dig. Dis. doi:10.1159/000090314

Metzger, D., Chambon, P., 2001. Site- and time-specific gene targeting in the mouse. Methods 24, 71–80. doi:10.1006/meth.2001.1159

Meye, F.J., Ramakers, G.M.J., Adan, R. a H., 2014. The vital role of constitutive GPCR activity in the mesolimbic dopamine system. Transl. Psychiatry 4, e361. doi:10.1038/tp.2013.130

Michel, M.C., Wieland, T., Tsujimoto, G., 2009. How reliable are G-protein-coupled receptor antibodies? Naunyn. Schmiedebergs. Arch. Pharmacol. 379, 385–388. doi:10.1007/s00210-009-0395-y

Mickiewicz, A.L., Dallimore, J.E., Napier, T.C., 2009. The ventral pallidum is critically involved in the development and expression of morphine-induced sensitization. Neuropsychopharmacology 34, 874–886. doi:10.1038/npp.2008.111

Miranda-Paiva, C.M., Ribeiro-Barbosa, E.R., Canteras, N.S., Felicio, L.F., 2003. A role for the periaqueductal grey in opioidergic inhibition of maternal behaviour. Eur. J. Neurosci. 18, 667–674. doi:10.1046/j.1460-9568.2003.02794.x

Miura, M., Saino-Saito, S., Masuda, M., Kobayashi, K., Aosaki, T., 2007. Compartment-specific modulation of GABAergic synaptic transmission by mu-opioid receptor in the mouse striatum with green fluorescent protein-expressing dopamine islands. J. Neurosci. 27, 9721–9728. doi:10.1523/JNEUROSCI.2993-07.2007

Modesto-Lowe, V., Brooks, D., Petry, N., 2010. Methadone deaths: Risk factors in pain and addicted populations. J. Gen. Intern. Med. 25, 305–309. doi:10.1007/s11606-009-1225-0

Moles, A., Kieffer, B.L., D'Amato, F.R., 2004. Deficit in attachment behavior in mice lacking the mu-opioid receptor gene. Science 304, 1983–1986. doi:10.1126/science.1095943

Monory, K., Massa, F., Egertová, M., Eder, M., Blaudzun, H., Westenbroek, R., Kelsch, W., Jacob, W., Marsch, R., Ekker, M., Long, J., Rubenstein, J.L., Goebbels, S., Nave, K.A., During, M., Klugmann, M., Wölfel, B., Dodt, H.U., Zieglgänsberger, W., Wotjak, C.T., Mackie, K., Elphick, M.R., Marsicano, G.,

Lutz, B., 2006. The Endocannabinoid System Controls Key Epileptogenic Circuits in the Hippocampus. Neuron 51, 455–466. doi:10.1016/j.neuron.2006.07.006

Napier, T.C., Mitrovic, I., 1999. Opioid modulation of ventral pallidal inputs. Ann. N. Y. Acad. Sci. 877, 176–201. doi:10.1111/j.1749-6632.1999.tb09268.x

Nathan, P.J., Bullmore, E.T., 2009. From taste hedonics to motivational drive: central μ-opioid receptors and binge-eating behaviour. Int. J. Neuropsychopharmacol. 12, 995–1008. doi:10.1017/S146114570900039X

Nestler, E.J., Hyman, S.E., 2010. Animal models of neuropsychiatric disorders. Nat. Neurosci. 13, 1161–1169. doi:10.1038/nn.2647

Nguyen, A.T., Marquez, P., Hamid, A., Lutfy, K., 2012. The role of mu opioid receptors in psychomotor stimulation and conditioned place preference induced by morphine-6-glucuronide. Eur. J. Pharmacol. 682, 86–91. doi:10.1016/j.ejphar.2012.02.021

Nieh, E.H., Kim, S.Y., Namburi, P., Tye, K.M., 2013. Optogenetic dissection of neural circuits underlying emotional valence and motivated behaviors. Brain Res. 1511, 73–92. doi:10.1016/j.brainres.2012.11.001

Noormets, K., Kõks, S., Kavak, A., Arend, A., Aunapuu, M., Keldrimaa, A., Vasar, E., Tillmann, V., 2009. Male mice with deleted Wolframin (Wfs1) gene have reduced fertility. Reprod. Biol. Endocrinol. 7, 82. doi:10.1186/1477-7827-7-82

O'Brien, C.P., Gardner, E.L., 2005. Critical assessment of how to study addiction and its treatment: human and non-human animal models. Pharmacol. Ther. 108, 18–58. doi:10.1016/j.pharmthera.2005.06.018

Oddi, D., Crusio, W.E., D'Amato, F.R., Pietropaolo, S., 2013. Monogenic mouse models of social dysfunction: Implications for autism. Behav. Brain Res. 251, 75–84. doi:10.1016/j.bbr.2013.01.002

Olds, M.E., 1982. Reinforcing effects of morphine in the nucleus accumbens. Brain Res. 237, 429–440. doi:10.1016/0006-8993(82)90454-1

Olmstead, M.C., Ouagazzal, A.M., Kieffer, B.L., 2009. Mu and delta opioid receptors oppositely regulate motor impulsivity in the signaled nose poke task. PLoS One 4. doi:10.1371/journal.pone.0004410

Papaleo, F., Kieffer, B.L., Tabarin, A., Contarino, A., 2007. Decreased motivation to eat in μ-opioid receptor-deficient mice. Eur. J. Neurosci. 25, 3398–3405. doi:10.1111/j.1460-9568.2007.05595.x

Pattinson, K.T.S., 2008. Opioids and the control of respiration. Br. J. Anaesth. 100, 747–758. doi:10.1093/bja/aen094

Paxinos, G., Franklin, K.B.J., 2001. The mouse brain in stereotaxic coordinates. Acad. Press 1–350.

Peciña, S., Smith, K.S., 2010. Hedonic and motivational roles of opioids in food reward: Implications for overeating disorders. Pharmacol. Biochem. Behav. 97, 34–46. doi:10.1016/j.pbb.2010.05.016

Pelloux, Y., Everitt, B.J., Dickinson, A., 2007. Compulsive drug seeking by rats under punishment: Effects of drug taking history. Psychopharmacology (Berl). 194, 127–137. doi:10.1007/s00213-007-0805-0

Pergolizzi, J., Boger, R.H., Budd, K., Dahan, A., Erdine, S., Hans, G., Kress, H.G., Langford, R., Likar, R., Raffa, R.B., Sacerdote, P., 2008. Opioids and the management of chronic severe pain in the elderly: consensus statement of an International\nExpert Panel with focus on the six clinically most often used World Health Organization Step\nIII opioids (buprenorphine, fentanyl, hydromorphone, m. Pain Pr. 8, 287–313.

Persico, A.M., Bourgeron, T., 2006. Searching for ways out of the autism maze: genetic, epigenetic and environmental clues. Trends Neurosci. 29, 349–358. doi:10.1016/j.tins.2006.05.010

Pert, C.B., Snyder, S.H., 1973. Opiate receptor: demonstration in nervous tissue. Science 179, 1011–1014. doi:10.1126/science.179.4077.1011

Poulin, J.-F., Arbour, D., Laforest, S., Drolet, G., 2009. Neuroanatomical characterization of endogenous opioids in the bed nucleus of the stria terminalis. Prog. Neuropsychopharmacol. Biol. Psychiatry 33, 1356–1365. doi:10.1016/j.pnpbp.2009.06.021

Pradhan, A. a., Smith, M.L., Kieffer, B.L., Evans, C.J., 2012. Ligand-directed signalling within the opioid receptor family. Br. J. Pharmacol. 167, 960–969. doi:10.1111/j.1476-5381.2012.02075.x

Puhl, M.D., Blum, J.S., Acosta-Torres, S., Grigson, P.S., 2012. Environmental enrichment protects against the acquisition of cocaine self-administration in adult male rats, but does not eliminate avoidance of a drug-associated saccharin cue. Behav. Pharmacol. 23, 43–53. doi:10.1097/FBP.0b013e32834eb060

Quintero, G.C., 2013. Role of nucleus accumbens glutamatergic plasticity in drug addiction. Neuropsychiatr. Dis. Treat. 9, 1499–1512. doi:10.2147/NDT.S45963

Raehal, K.M., Schmid, C.L., Groer, C.E., Bohn, L.M., 2011. Functional Selectivity at the mu-Opioid Receptor : Implications for Understanding Opioid Analgesia. Pharmacol. Rev. 63, 1001–1019. doi:10.1124/pr.111.004598.the

Raffa, R.B., Pergolizzi, J. V., Segarnick, D.J., Tallarida, R.J., 2010. Oxycodone combinations for pain relief. Drugs of Today 46, 379–398. doi:10.1358/dot.2010.46.6.1470106

Rigoli, L., Lombardo, F., Di Bella, C., 2011. Wolfram syndrome and WFS1 gene. Clin. Genet. 79, 103–117. doi:10.1111/j.1399-0004.2010.01522.x

Roberts, a J., McDonald, J.S., Heyser, C.J., Kieffer, B.L., Matthes, H.W., Koob, G.F., Gold, L.H., 2000. mu-Opioid receptor knockout mice do not self-administer alcohol. J. Pharmacol. Exp. Ther. 293, 1002–1008.

Rodríguez-Muñoz, M., Sánchez-Blázquez, P., Vicente-Sánchez, A., Berrocoso, E., Garzón, J., 2012. The Mu-Opioid Receptor and the NMDA Receptor Associate in PAG Neurons: Implications in Pain Control. Neuropsychopharmacology 37, 338–349. doi:10.1038/npp.2011.155

Sanchis-Segura, C., Spanagel, R., 2006. Behavioural assessment of drug reinforcement and addictive features in rodents: An overview. Addict. Biol. 11, 2–38. doi:10.1111/j.1369-1600.2006.00012.x

Scherrer, G., Tryoen-Tóth, P., Filliol, D., Matifas, A., Laustriat, D., Cao, Y.Q., Basbaum, A.I., Dierich, A., Vonesh, J.-L., Gavériaux-Ruff, C., Kieffer, B.L., 2006. Knockin mice expressing fluorescent delta-opioid receptors uncover G protein-coupled receptor dynamics in vivo. Proc. Natl. Acad. Sci. U. S. A. 103, 9691–9696. doi:10.1073/pnas.0603359103

Schonig, K., Weber, T., Frommig, A., Wendler, L., Pesold, B., Djandji, D., Bujard, H., Bartsch, D., 2012. Conditional Gene Expression Systems in the Transgenic Rat Brain. BMC Biol. 10, 77. doi:10.1186/1741-7007-10-77

Schuller, a G., King, M. a, Zhang, J., Bolan, E., Pan, Y.X., Morgan, D.J., Chang, a, Czick, M.E., Unterwald, E.M., Pasternak, G.W., Pintar, J.E., 1999. Retention of heroin and morphine-6 beta-glucuronide analgesia in a new line of mice lacking exon 1 of MOR-1. Nat. Neurosci. 2, 151–156. doi:10.1038/5706

Shaham, Y., Rajabi, H., Stewart, J., 1996. Relapse to heroin-seeking in rats under opioid maintenance: the effects of stress, heroin priming, and withdrawal. J. Neurosci. 16, 1957–1963.

Shang, L., Hua, H., Foo, K., Martinez, H., Watanabe, K., Zimmer, M., Kahler, D.J., Freeby, M., Chung, W., LeDuc, C., Goland, R., Leibel, R.L., Egli, D., 2014. β-cell dysfunction due to increased ER stress in a stem cell model of wolfram syndrome. Diabetes 63, 923–933. doi:10.2337/db13-0717

Shibata, A.C.E., Maebashi, H.K., Nakahata, Y., Nabekura, J., Murakoshi, H., 2015. Development of a Molecularly Evolved, Highly Sensitive CaMKII FRET Sensor with Improved Expression Pattern. PLoS One 10, e0121109. doi:10.1371/journal.pone.0121109

Simon, E.J., Hiller, J.M., Edelman, I., 1973. Stereospecific binding of the potent narcotic analgesic (3H) Etorphine to rat-brain homogenate. Proc. Natl. Acad. Sci. U. S. A. 70, 1947–1949. doi:10.1073/pnas.70.7.1947

Smith, R.J., Aston-Jones, G., 2008. Noradrenergic transmission in the extended amygdala: Role in increased drug-seeking and relapse during protracted drug abstinence. Brain Struct. Funct. 213, 43–61. doi:10.1007/s00429-008-0191-3

Sora, I., Elmer, G., Funada, M., Pieper, J., Li, X.F., Hall, F.S., Uhl, G.R., 2001. μ Opiate receptor gene dose effects on different morphine actions: Evidence for differential in vivo μ receptor reserve. Neuropsychopharmacology 25, 41–54. doi:10.1016/S0893-133X(00)00252-9

Sora, I., Takahashi, N., Funada, M., Ujike, H., Revay, R.S., Donovan, D.M., Miner, L.L., Uhl, G.R., 1997. Opiate receptor knockout mice define mu receptor roles in endogenous nociceptive responses and

morphine-induced analgesia. Proc. Natl. Acad. Sci. U. S. A. 94, 1544–1549. doi:10.1073/pnas.94.4.1544

Soriano, P., 1999. Generalized lacZ expression with the ROSA26 Cre reporter strain. Nat. Genet. 21, 70–71. doi:10.1038/5007

Spetea, M., Asim, M.F., Wolber, G., Schmidhammer, H., 2013. The Opioid Receptor and Ligands Acting at the and Potential Therapeutics Opioid Receptor , as Therapeutics. Curr. Pharm. Des. 19, 7415–7434.

Stein, C., Clark, J.D., Oh, U., Vasko, M.R., Wilcox, G.L., Overland, A.C., Vanderah, T.W., Spencer, R.H., 2009. Peripheral mechanisms of pain and analgesia. Brain Res. Rev. 60, 90–113. doi:10.1016/j.brainresrev.2008.12.017

Straube, C., Derry, S., Kc, J., Pj, W., Rf, B., Strassels, S., Straube, S., 2014. Codeine , alone and with paracetamol (acetaminophen), for cancer pain (Review) SUMMARY OF FINDINGS FOR THE MAIN COMPARISON. Cochrane Database Syst. Rev.

Strom, T.M., Hörtnagel, K., Hofmann, S., Gekeler, F., Scharfe, C., Rabl, W., Gerbitz, K.D., Meitinger, T., 1998. Diabetes insipidus, diabetes mellitus, optic atrophy and deafness (DIDMOAD) caused by mutations in a novel gene (wolframin) coding for a predicted transmembrane protein. Hum. Mol. Genet. 7, 2021–2028. doi:ddb264 [pii]

Takaishi, T., Saito, N., Tanaka, C., 1992. Evidence for distinct neuronal localization of gamma and delta subunits of Ca2+/calmodulin-dependent protein kinase II in the rat brain. J. Neurochem. 58, 1971–1974.

Takeda, K., Inoue, H., Tanizawa, Y., Matsuzaki, Y., Oba, J., Watanabe, Y., Shinoda, K., Oka, Y., 2001. WFS1 (Wolfram syndrome 1) gene product: predominant subcellular localization to endoplasmic reticulum in cultured cells and neuronal expression in rat brain. Hum. Mol. Genet. 10, 477–484. doi:10.1093/hmg/10.5.477

Takei, D., Ishihara, H., Yamaguchi, S., Yamada, T., Tamura, A., Katagiri, H., Maruyama, Y., Oka, Y., 2006. WFS1 protein modulates the free Ca2+ concentration in the endoplasmic reticulum. FEBS Lett. 580, 5635–5640. doi:10.1016/j.febslet.2006.09.007

Tejedor-Real, P., Mico, J. a., Maldonado, R., Roques, B.P., Gibert-Rahola, J., 1995. Implication of endogenous opioid system in the learned helplessness model of depression. Pharmacol. Biochem. Behav. 52, 145–152. doi:10.1016/0091-3057(95)00067-7

Terenius, L., 1973. Characteristics of the “receptor” for narcotic analgesics in synaptic plasma membrane fraction from rat brain. Acta Pharmacol. Toxicol. (Copenh). 33, 377–384.

Thomas, K.R., Capecchi, M.R., 1987. Site-directed mutagenesis by gene targeting in mouse embryo-derived stem cells. Cell 51, 503–512. doi:10.1016/0092-8674(87)90646-5

Tian, B.M., Broxmeyer, H.E., Fan, Y., Lai, Z., Zhang, S., Aronica, S., Cooper, S., Bigsby, R.M., Steinmetz, R., Engle, S.J., Mestek, A., Pollock, J.D., Lehman, M.N., Jansen, H.T., Ying, M., Stambrook, P.J., Tischfield, J. a, Yu, L., 1997. Altered hematopoiesis, behavior, and sexual function in mu opioid Receptor – deficient Mice. J. Exp. Med. 185, 1517–1522.

Troisi, A., Frazzetto, G., Carola, V., Di Lorenzo, G., Coviello, M., D'Amato, F.R., Moles, A., Siracusano, A., Gross, C., 2011. Social hedonic capacity is associated with the A118G polymorphism of the mu-opioid receptor gene (OPRM1) in adult healthy volunteers and psychiatric patients. Soc. Neurosci. 6, 88–97. doi:10.1080/17470919.2010.482786

Tsien, J.Z., Chen, D.F., Gerber, D., Tom, C., Mercer, E.H., Anderson, D.J., Mayford, M., Kandel, E.R., Tonegawa, S., 1996. Subregion- and Cell Type – Restricted Gene Knockout in Mouse Brain. Cell 87, 1317–1326.

Tzschentke, T.M., 2007. Measuring reward with the conditioned place preference (CPP) paradigm: Update of the last decade. Addict. Biol. 12, 227–462. doi:10.1111/j.1369-1600.2007.00070.x

Van der Schier, R., Roozekrans, M., van Velzen, M., Dahan, A., Niesters, M., 2014. Opioid-induced respiratory depression: reversal by non-opioid drugs. F1000Prime Rep. 6, 1–8. doi:10.12703/P6-79

Van Furth, W.R., Wolterink, G., Van Ree, J.M., 1995. Regulation of masculine sexual behavior: Involvement of brain opioids and dopamine. Brain Res. Rev. 21, 162–184. doi:10.1016/0165-0173(96)82985-7

Van Huijstee, A.N., Mansvelder, H.D., 2015. Glutamatergic synaptic plasticity in the mesocorticolimbic system in addiction. Front. Cell. Neurosci. 8, 1–13. doi:10.3389/fncel.2014.00466

Van Ree, J.M., Gerrits, M. a, Vanderschuren, L.J., 1999. Opioids, reward and addiction: An encounter of biology, psychology, and medicine. Pharmacol. Rev. 51, 341–396. doi:10.1016/S0924-977X(98)80013-8

Vogl, A.M., Brockmann, M.M., Giusti, S. a, Maccarrone, G., Vercelli, C. a, Bauder, C. a, Richter, J.S., Roselli, F., Hafner, A.-S., Dedic, N., Wotjak, C.T., Vogt-Weisenhorn, D.M., Choquet, D., Turck, C.W., Stein, V., Deussing, J.M., Refojo, D., 2015. Neddylation inhibition impairs spine development, destabilizes synapses and deteriorates cognition. Nat. Neurosci. 18, 239–251. doi:10.1038/nn.3912

Waldhoer, M., Bartlett, S.E., Whistler, J.L., 2004. Opioid receptors. Annu. Rev. Biochem. 73, 953–990. doi:10.1146/annurev.biochem.73.011303.073940

Walters, C.L., Cleck, J.N., Kuo, Y.C., Blendy, J. a., 2005. ??-opioid receptor and CREB activation are required for nicotine reward. Neuron 46, 933–943. doi:10.1016/j.neuron.2005.05.005

Wang, X., Zhang, C., Szábo, G., Sun, Q.Q., 2013. Distribution of CaMKIIα expression in the brain in vivo, studied by CaMKIIα-GFP mice. Brain Res. 1518, 9–25. doi:10.1016/j.brainres.2013.04.042

Ward, H.G., Nicklous, D.M., Aloyo, V.J., Simansky, K.J., 2006. Mu-opioid receptor cellular function in the nucleus accumbens is essential for hedonically driven eating. Eur. J. Neurosci. 23, 1605–1613. doi:10.1111/j.1460-9568.2006.04674.x

Watabe-Uchida, M., Zhu, L., Ogawa, S.K., Vamanrao, A., Uchida, N., 2012. Whole-Brain Mapping of Direct Inputs to Midbrain Dopamine Neurons. Neuron 74, 858–873. doi:10.1016/j.neuron.2012.03.017

Weibel, R., Reiss, D., Karchewski, L., Gardon, O., Matifas, A., Filliol, D., Becker, J. a J., Wood, J.N., Kieffer, B.L., Gaveriaux-Ruff, C., 2013. Mu Opioid Receptors on Primary Afferent Nav1.8 Neurons Contribute to Opiate-Induced Analgesia: Insight from Conditional Knockout Mice. PLoS One 8, 1–18. doi:10.1371/journal.pone.0074706

Weissmann, C., Büeler, H., Fischer, M., Aguet, M., 1993. Role of the PrP gene in transmissible spongiform encephalopathies. Intervirology 35, 164–175.

Wermeling, D.P., 2015. Review of naloxone safety for opioid overdose: practical considerations for new technology and expanded public access. Ther. Adv. Drug Saf. 6, 20–31. doi:10.1177/2042098614564776

Wiffen, P.J., Wee, B., Moore, R. a., 2013. Oral morphine for cancer pain (Review). Cochrane Libr.

Williams, J.T., Christie, M.J., Manzoni, O., 2001. Cellular and synaptic adaptations mediating opioid dependence. Physiol. Rev. 81, 299–343.

Williams, J.T., Ingram, S.L., Henderson, G., Chavkin, C., Zastrow, M. Von, Schulz, S., Koch, T., Evans, C.J., Christie, M.J., 2013. Regulation of m -Opioid Receptors : Desensitization , Phosphorylation , Internalization , and Tolerance 223–254.

Willner, P., 1986. Criteria for Animal Models of Human Mental Disorders : 677.

Winkeler, C.L., Kladney, R.D., Maggi, L.B., Weber, J.D., 2012. Cathepsin K-Cre causes unexpected germline deletion of genes in mice. PLoS One 7. doi:10.1371/journal.pone.0042005

Wittert, G., Hope, P., Pyle, D., 1996. Tissue distribution of opioid receptor gene expression in the rat. Biochem. Biophys. Res. Commun. 218, 877–881. doi:10.1006/bbrc.1996.0156

Wrigley, P.J., Jeong, H.-J., Vaughan, C.W., 2010. Dissociation of μ- and δ-opioid inhibition of glutamatergic synaptic transmission in superficial dorsal horn. Mol. Pain 6, 71. doi:10.1186/1744-8069-6-71

Wu, H., Wacker, D., Mileni, M., Katritch, V., Han, G.W., Vardy, E., Liu, W., Thompson, A. a., Huang, X.-P., Carroll, F.I., Mascarella, S.W., Westkaemper, R.B., Mosier, P.D., Roth, B.L., Cherezov, V., Stevens, R.C., 2012. Structure of the human κ-opioid receptor in complex with JDTic. Nature 485, 327–332. doi:10.1038/nature10939

Xia, Y., Driscoll, J.R., Wilbrecht, L., Margolis, E.B., Fields, H.L., Hjelmstad, G.O., 2011. Nucleus accumbens medium spiny neurons target non-dopaminergic neurons in the ventral tegmental area. J. Neurosci. 31, 7811–7816. doi:10.1523/JNEUROSCI.1504-11.2011

Yoo, J.-H., Lee, Loh, Ho, Jang, C.-G., 2004a. Loss of Nicotine-Induced Behavioral Sensitization in □ -Opioid Receptor. Synapse 223, 219–223. doi:10.1002/syn.10303

Yoo, J.-H., Lee, S.-Y., Loh, H.H., Ho, I.K., Jang, C.-G., 2004b. Altered emotional behaviors and the expression of 5-HT1A and M1 muscarinic receptors in micro-opioid receptor knockout mice. Synapse 54, 72–82. doi:10.1002/syn.20067

Yoo, J.-H., Yang, E.-M., Lee, S.-Y., Loh, H.H., Ho, I.K., Jang, C.-G., 2003. Differential effects of morphine and cocaine on locomotor activity and sensitization in μ-opioid receptor knockout mice. Neurosci. Lett. 344, 37–40. doi:10.1016/S0304-3940(03)00410-5

Yoshinari, N., Ando, K., Kudo, A., Kinoshita, M., Kawakami, A., 2012. Colored medaka and zebrafish: Transgenics with ubiquitous and strong transgene expression driven by the medaka β-actin promoter. Dev. Growth Differ. 54, 818–828. doi:10.1111/dgd.12013

Yu, M., Xi, Y., Pollack, J., Debiais-Thibaud, M., MacDonald, R.B., Ekker, M., 2011. Activity of dlx5a/dlx6a regulatory elements during zebrafish GABAergic neuron development. Int. J. Dev. Neurosci. 29, 681–691. doi:10.1016/j.ijdevneu.2011.06.005

Zheng, W., 2010. Activation of mu opioid receptor inhibits the excitatory glutamatergic transmission in the anterior cingulate cortex of the rats with peripheral inflammation. Eur. J. Pharmacol. 628, 91–95. doi:10.1016/j.ejphar.2009.11.041

Zhou, L., Bohn, L.M., 2014. Functional selectivity of GPCR signaling in animals. Curr. Opin. Cell Biol. 27, 102–108. doi:10.1016/j.ceb.2013.11.010

Zou, D.J., Greer, C. a., Firestein, S., 2002. Expression pattern of ??CaMKII in the mouse main olfactory bulb. J. Comp. Neurol. 443, 226–236. doi:10.1002/cne.10125

RÉSUMÉ EN FRANÇAIS

La morphine est l'analgésique le plus utilisé en clinique, malgré de nombreux effets indésirables. Elle produit ses effets en activant le récepteur opioïde mu, encodé par le gène *Oprm1*. Notre équipe s'intéresse aux caractéristiques génétiques, moléculaires et cellulaires du système opioïde et tente de mieux comprendre son rôle dans l'addiction aux drogues. Le système opioïde est composé de trois récepteurs (mu, delta et kappa) et de peptides endogènes (enképhalines, endorphine et dynorphines). Les approches pharmacologiques et l'analyse de souris génétiquement modifiées ont montré que ces récepteurs ont des rôles distincts dans les mécanismes de l'addiction (Kieffer and Gavériaux-Ruff, 2002). Notamment, la caractérisation de souris knockout (invalidées, KO) pour le gène *Oprm1* a permis de montrer que le récepteur mu est responsable à la fois de l'effet analgésique de la morphine et de ses autres effets: dépression respiratoire, constipation et potentiel addictif. Aussi, les souris mu KO montrent un comportement proche du syndrome autistique (Moles *et al*., 2004 ; Becker *et al*., 2014). Le récepteur mu est largement exprimé dans le système nerveux, essentiellement dans des neurones GABAergiques. Ce récepteur est particulièrement abondant dans les voies de la récompense (structures mésocorticolimbiques, comme le cortex, le striatum, l'aire tegmentale ventrale [VTA] ou l'amygdale étendue [AE]) et dans les circuits nociceptifs (aires thalamiques, tronc cérébral et moelle épinière). L'objectif général de mon projet est de 1) caractériser une lignée de souris transgénique visant spécifiquement les récepteurs mu des neurones GABAergiques afin de déterminer leur contribution 2) dans les activités analgésiques et addictives des opiacés et 3) dans les comportements sociaux altérés dans le syndrome de l'autisme (ASD), 4) développer un nouveau modèle transgénique visant le récepteur mu des neurones glutamatergiques, 5) initier un outil génétique ciblant l'amygdale étendue.

Objectif 1 : Caractérisation moléculaire et anatomique de la lignée Dlx-mu

Notre laboratoire a construit une lignée de souris mu knockout conditionnelle, en utilisant la technologie Cre-LoxP, avec pour objectif l'inactivation sélective du gène *Oprm1* dans les neurones GABAergiques du cerveau antérieur (Dlx-mu). Nous avons d'une part créé une lignée dont le récepteur mu est flanqué de 2 sites loxP autour des exons 2 et 3 (Weibel *et al*., 2013). Lorsque la Cre recombinase reconnaît ces sites, elle induit une délétion de la séquence floxée. Nous avons d'autre part obtenu une lignée de souris transgénique exprimant la Cre sous le contrôle du promoteur Dlx 5/6, spécifiquement exprimé dans les neurones GABAergiques du cerveau antérieur (collaboration, voir Monory *et al*., 2006). Nous avons croisé cette lignée transgénique avec la lignée mu-floxé et obtenu la lignée de souris Dlx-mu que nous avons caractérisée.

L'analyse de la distribution de l'expression du récepteur mu par qRT-PCR montre que son expression est maintenue dans la majorité des régions du cerveau analysées (niveaux d'expression *vs* souris contrôles proches de 1). Par contre, le récepteur mu n'est pas exprimé dans le striatum (noyau accumbens et noyau caudé putamen) (niveaux d'expression *vs* souris contrôles de 0.07 et 0.02, respectivement) et très peu exprimé dans l'amygdale et l'hippocampe (0.16 et 0.31, respectivement). L'autoradiographie de ligand radiomarqué ([^{3}H] DAMGO) a révélé une baisse remarquable de récepteur mu dans le striatum (collaboration, Helen Keyworth dans l'équipe du Professeur Ian Kitchen, UK). Une étude électrophysiologique au niveau de la VTA (collaboration, Aya Matsui dans l'équipe du Docteur Veronica Alvarez, Washington) a permis de démontrer l'absence de mu au niveau des terminaisons GABAergiques du noyau accumbens projetant sur la VTA.

Objectif 2 : Addiction et analgésie opioïdes chez les souris Dlx-mu

J'ai examiné les réponses des souris mutantes à des composés opiacés (morphine et héroïne), afin d'évaluer la contribution des récepteurs mu exprimés dans les neurones GABAergiques dans les fonctions analgésiques et addictives. L'étude de l'analgésie morphinique, grâce aux tests d'immersion et de retrait de la queue et du test de la plaque chaude, ne montre aucun changement dans les réponses en comparaison avec les souris contrôles. La dépendance physique à la morphine, mesurée par un sevrage précipité par la naloxone, n'est pas non plus modifiée. L'ensemble de ces résultats est conforme à nos attentes, l'expression du récepteur mu étant maintenue au niveau des régions du cerveau impliquées dans les réponses analgésiques et le sevrage.

J'ai mesuré l'effet récompensant de la morphine et de l'héroïne sur les souris Dlx-mu en utilisant le test de préférence de place conditionnée. De façon surprenante, la préférence de place conditionnée à la morphine (10 mg/kg) ainsi qu'à l'héroïne (2 et 10 mg/kg) est intacte (respectivement 63%, 68% et 74%) malgré l'absence du récepteur dans le striatum, région décrite comme fortement impliquée dans ces processus. La caractérisation de l'effet appétitif de la morphine a été complétée en collaboration avec l'équipe du Pr. Maldonado (Elena Martin-Garcia, UPF, Barcelona) dans un comportement opérant (auto-administration). Les souris Dlx-mu montrent une augmentation de la motivation à obtenir de l'héroïne et du chocolat (point limite, rétablissement de la consommation induit par un indice). Il semble donc que l'absence du récepteur mu dans les neurones striataux ne diminue pas, mais au contraire augmente l'appétence pour l'opiacé et la nourriture sucrée.

Par ailleurs l'héroïne n'a pas d'effet hyperlocomoteur chez les mutants, comme classiquement observé chez les souris contrôles, mais présente une activité cataleptique puissante. En effet, l'hyperlocomotion induite par l'héroïne est abolie aux trois doses testées (0.5, 2 et 10 mg/kg), tout comme la locomotion verticale (redressement) (héroïne 10 mg/kg), mais la catalepsie induite par l'héroïne (10 mg/kg) mesurée dans le test de la barre est nettement supérieure à celle des contrôles. Afin de vérifier l'intégrité du système dopaminergique chez ces souris, j'ai vérifié le niveau d'expression des récepteurs dopaminergiques grâce à des qRT-PCR visant les récepteurs D1 et D2 dans striatum (noyau accumbens et noyau caudé putamen). J'ai également étudié l'effet hyperlocomoteur induit par l'amphétamine (à 2.5 et 5 mg/kg). Cet effet est maintenu chez les souris Dlx-mu par rapport aux contrôles, traduisant un système dopaminergique fonctionnel chez les mutants. Aussi, une analyse d'imagerie c-Fos montre que l'activation neuronale dans le striatum et la VTA sont modifiés chez les Dlx-mu, indiquant une altération significative de la réponse à l'héroïne au niveau cellulaire.

En conclusion, l'ensemble de nos observations indique que l'ablation des récepteurs mu dans une population neuronale ciblée, les neurones GABAergiques du striatum, augmente les effets de l'héroïne. Ce résultat, apparemment paradoxal, révèle une nouvelle fonction du récepteur et un nouveau mécanisme de régulation des circuits mesolimbiques dopaminergiques. Nous proposons en effet que les récepteurs mu exprimés dans les neurones GABAergiques striataux exercent un frein (anti-motivation) sur le mécanisme classique de désinhibition dopaminergique, classiquement décrit pour les récepteurs mu de la VTA (pro-motivation). Un manuscrit est en préparation : : *Mu opioid receptors in GABAergic forebrain neurons are necessary for heroin hyperlocomotion and reduce motivation for heroin and palatable food*. Charbogne P, Gardon O, Martín-García E, Keyworth H, Matsui A, Matifas A, Befort K, Kitchen I, Bailey A, Alvarez VA, Maldonado R, Kieffer BL.

Objectif 3 : Le syndrome autistique chez les souris Dlx-mu

Les souris KO mu totales présentent un phénotype de type « autistique » (Becker *et al*., 2014), et j'ai évalué ces comportements chez les souris Dlx-mu. L'interaction sociale (contact du museau, temps de contact, temps de toilettage) n'est pas affectée par l'invalidation de mu dans les neurones GABAergiques du cerveau antérieur. L'anxiété dans le test d'enfouissement des billes est équivalente chez les souris Dlx-mu et les contrôles, contrairement aux KO totales qui sont plus anxieuses. Dans un test de conflit, la prise de nourriture supprimée par la nouveauté, qui est très forte chez les KO totales, n'est pas modifiée chez les souris Dlx-mu. Ces résultats suggèrent que les récepteurs mu des neurones

GABAergiques du cerveau antérieur ne sont pas responsables des aspects socio-émotionnels de l'ASD observés chez les KO. Nous complétons actuellement l'évaluation d'autres caractéristiques du syndrome autistique. D'autres projets au laboratoire vont étudier la contribution de mu au phénotype autistique dans d'autres circuits. Un manuscrit est en préparation : *Mu opioid receptors in GABAergic forebrain neurons are not involved in autistic-like symptoms*. Charbogne P, Matifas A, Befort K, Kieffer BL.

Objectif 4 : Cibler les récepteurs mu des neurones glutamatergiques

Nous avons construit une lignée de souris mu KO conditionnelle et inductible, dans laquelle le gène *Oprm1* est inactivé sélectivement dans les neurones glutamatergiques du cerveau antérieur (CaMKIIαCreER^{T2}-mu) après traitement au tamoxifène. J'ai étudié le profil d'expression de la Cre grâce à une lignée rapportrice d'activité (ROSA26, gène lacZ). Les souris sont traitées au tamoxifène (10mg/mL) deux fois par jours pendant quinze jours (injections intra-péritonéales). Après 4 semaines, l'analyse du profil d'expression de la Cre a montré un marquage dans plusieurs noyaux hypothalamiques, les cellules pyramidales de l'hippocampe et quelques cellules éparses du cortex. Cependant, l'analyse de l'ADN génomique par PCR révèle une excision très partielle du récepteur mu chez les souris CaMKIIαCreER^{T2}-mu traitées au tamoxifène au niveau du cerveau uniquement. Enfin, l'analyse par qRT-PCR n'a malheureusement pas permis de détecter une diminution significative de l'expression de mu dans les différentes structures étudiées. Il semble donc que le tamoxifène ne puisse pas créer une excision du gène suffisamment efficace pour créer un animal utilisable pour l'étude. Nous avons abandonné ce projet.

Objectif 5 : Créer une lignée transgénique Cre pour cibler l'amygdale étendue

L'amygdale étendue (AE, noyau du lit de la strie terminale, amygdale centrale et noyau accumbens médian) est une région importante dans l'induction de l'état émotionnel négatif associé au développement de l'addiction. Suite à une analyse du génome effectuée dans notre équipe (Becker *et al*., 2008), nous avons identifié un gène fortement enrichi dans l'AE, codant pour la wolframine (*Wfs1*). Nous avons développé plusieurs lignées de souris transgéniques permettant une expression de la Cre sous le contrôle du promoteur de la wolframine ; nous les avons croisées avec des souris mu-floxé et avons obtenu un KO total. Ceci est probablement dû à une expression très précoce du gène *Wfs1* que nous n'avions pu détecter (stade gamète). Nous avons ensuite développé des lignées inductibles Cre-

ER^{T2} utilisant une version courte du promoteur *Wfs1* et portant le gène de la protéine fluorescence verte eGFP. L'une d'elle, exprimant une fusion eGFP-$CreER^{T2}$, montre le profil d'expression attendu dans l'amygdale étendue. Une autre construction, exprimant une fusion eGFP-T2A-$CreER^{T2}$ permettant une dissociation de la Cre et de l'eGFP a donné lieu à 4 fondateurs présentant également un profil d'expression limité à l'AE.

L'approche d'inactivation génétique conditionnelle nous a permis de découvrir un rôle nouveau pour le récepteur mu dans les aspects addictifs et locomoteurs des opiacés (morphine, héroïne) au niveau du circuit mésolimbique dopaminergique. Les études futures indiqueront si cette fonction « anti-récompense » du récepteur mu opère également pour d'autres drogues d'abus. Par ailleurs, la génération de souris transgéniques ciblant l'amygdale étendue sera un outil unique pour le ciblage de gènes dans une structure cérébrale essentielle pour les réponses au stress, les addictions et les troubles de l'humeur.

FIGURES AVEC
LÉGENDES EN FRANÇAIS

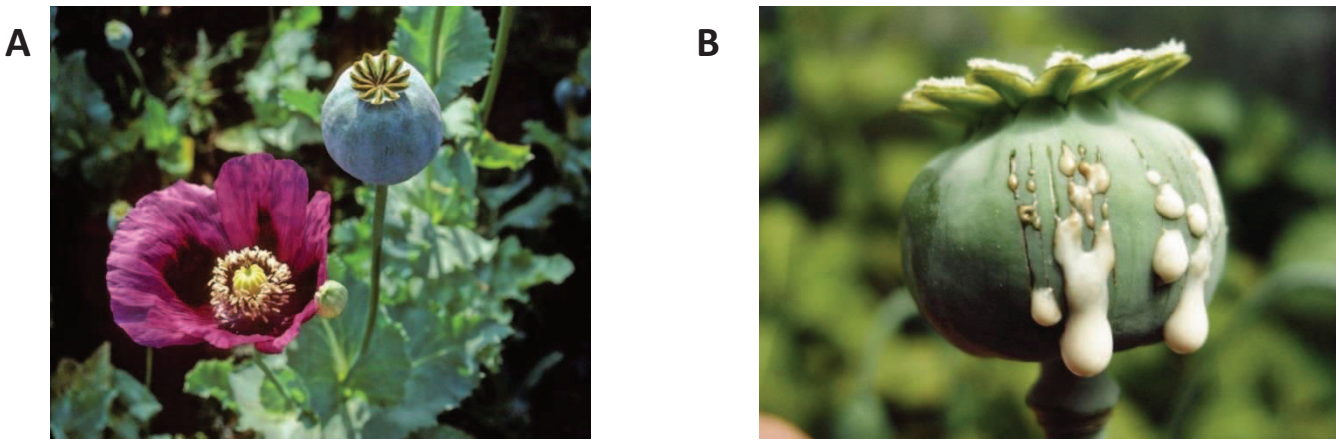

Figure 1. Pavot
(**A**) Fleur de pavot (*Papaver somniferum*)
(**B**) Après incision de la cosse verte, le latex est collecté. Les alkaloïdes sont extraits à partir de la matière sèche.

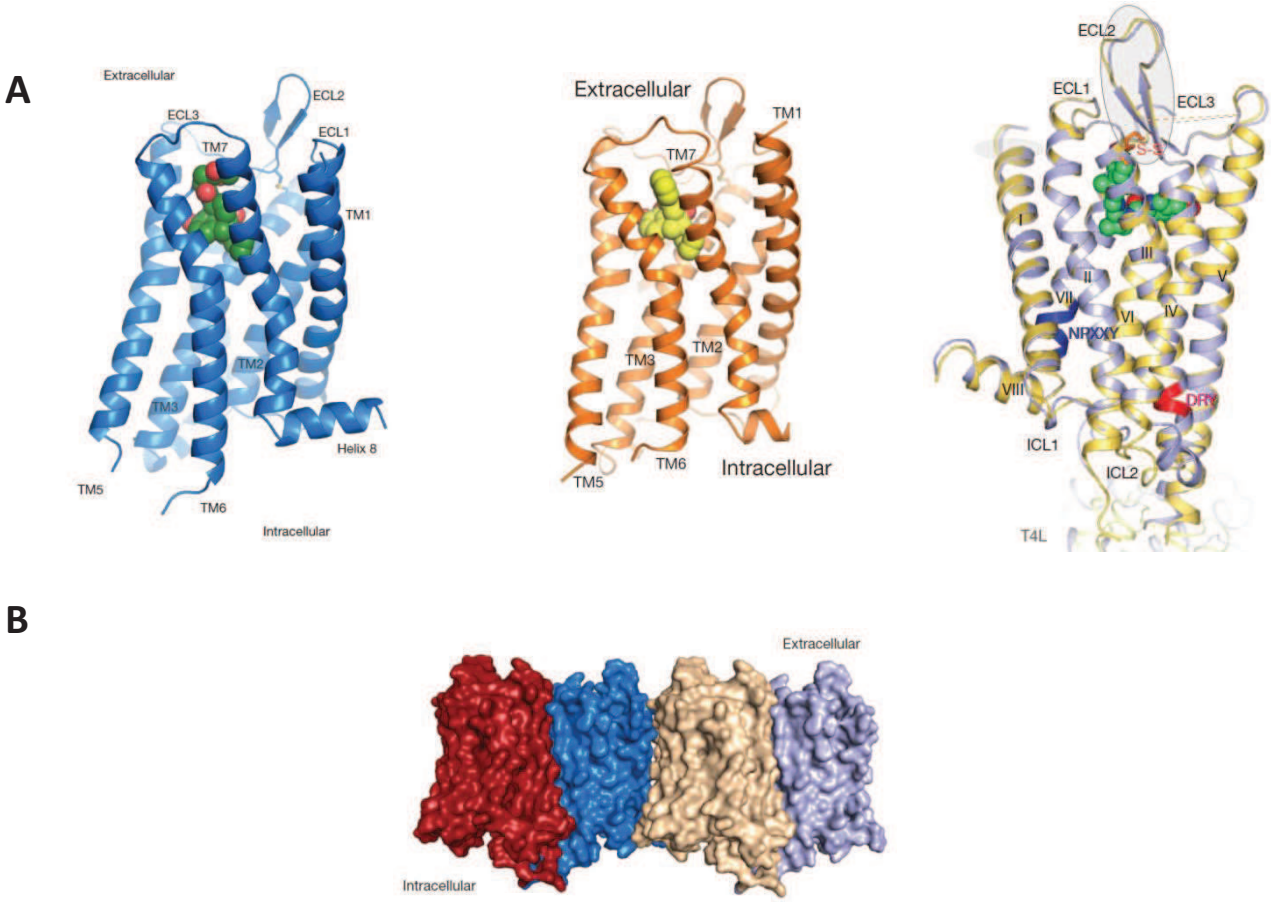

Figure 2. Vue d'ensemble de la structure des récepteurs opioïdes mu, delta et kappa.
(**A**) Les vues du plan de la membrane montrent l'architecture typique des RCPG à sept domaines transmembranaires des récepteurs opioïdes mu, delta et kappa (Adapté de Manglik et al., 2012, Granier et al., 2012 et Wu et al., 2012).
(**B**) Arrangement oligomérique du récepteur mu (Adapté de Manglik et al., 2012).

A

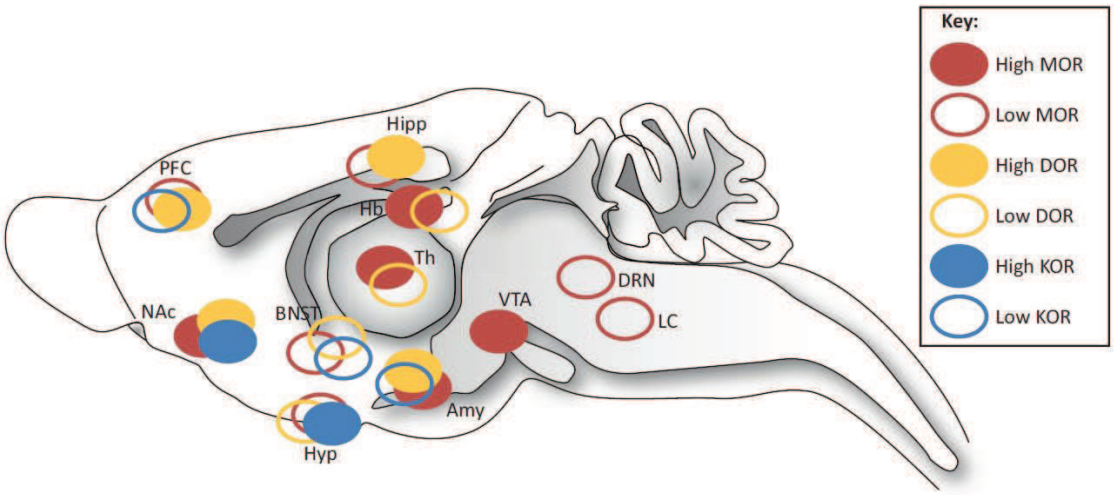

Amy, amygdale; BNST, noyau du lit de la strie terminale; DRN, noyau raphé dorsal; Hb, habenula; Hipp, hippocampe; Hyp hypothalamus; LC locus coeruleus; Th, thalamus; VTA, aire tegmentale ventrale.

B

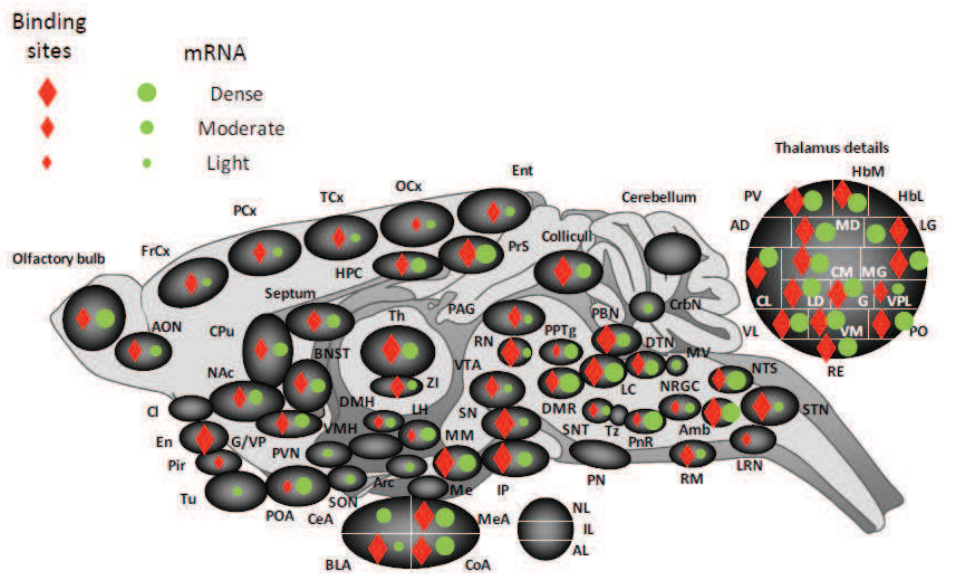

Abbreviations

Amb, nucleus ambiguus; AD, anterodorsal thalamus; AL, anterior lobe, pituitary; AON, anterior olfactory nucleus; Arc, arcuate nucleus, hypothalamus; BLA, basolateral nucleus, amygdala; BNST, bed nucleus of the stria terminalis; CeA, central nucleus, amygdala; Cl, claustrum; CL, centrolateral thalamus; CM, centromedial thalamus; CoA, cortical nucleus, amygdala; CPu, caudate putamen; CrbN, cerebellar nuclei; DMH, dorsomedial hypothalamus; DMR, dorsal and medial raphe' ; DTN, dorsal tegmental nucleus; En, endopiriform cortex; Ent, entorhinal cortex; FrCx, frontal cortex; G, nucleus gelatinosus, thalamus; G/VP, globus pallidus/ventral pallidum; HbL, lateral habenula; HbM, medial habenula; HPC, hippocampus; IL, intermediate lobe, pituitary; IP, interpeduncular nucleus; LC, locus coeruleus; LD, laterodorsal thalamus; LG, lateral geniculate, thalamus; LH, lateral hypothalamus; LRN, lateral reticular nucleus; MD, mediodorsal thalamus; Me, median eminence; MEA, median nucleus, amygdala; MG, medial geniculate; MM, medial mammillary nucleus; MV, medial vestibular nucleus; NAc, nucleus accumbens; NL, neuronal lobe, pituitary; NRGC, nucleus reticularis gigantocellularis; NTS, nucleus tractus solitarius; OCx, occipital cortex; PAG, periaqueductal gray; PCx, parietal cortex; Pir, piriform cortex; PN, pontine nucleus; PnR, pontine reticular; PO, posterior thalamus; POA, preoptic area; PPTg, pedunculopontine nucleus; PrS, presubiculum; PV, paraventricular thalamus; PVN, paraventricular hypothalamus; RE, reuniens thalamus; RN, red nucleus; RM, raphe' magnus; SON, supraoptic nucleus; SN, substancia nigra; SNT, sensory trigeminal nucleus; STN, spinal trigeminal nucleus; TCx, temporal cortex; Th, thalamus; Tu, olfactory tubercle; Tz, trapezoid nucleus; VL, ventrolateral thalamus; VM, ventromedial thalamus; VMH, ventromedial hypothalamus; VPL, ventroposterolateral thalamus; VTA, ventral tegmental area; ZI, zona incerta

Figure 3. Distribution des récepteur opioïdes

(**A**) Les protéines récepteurs mu, delta et kappa montrent une distribution qui se recoupe, mais distincte. (Adapté de Lutz and Kieffer, 2013)

(**B**) La protéine et l'ARNm du récepteur mu montrent une distribution anatomique qui coïncide, mais des différences ont été trouvées dans plusieurs structures, suggérant que des récepteurs présynaptiques sont transportés dans des aires de projection (Adapté de Olivier Gardon and Le Merrer et al, 2009)

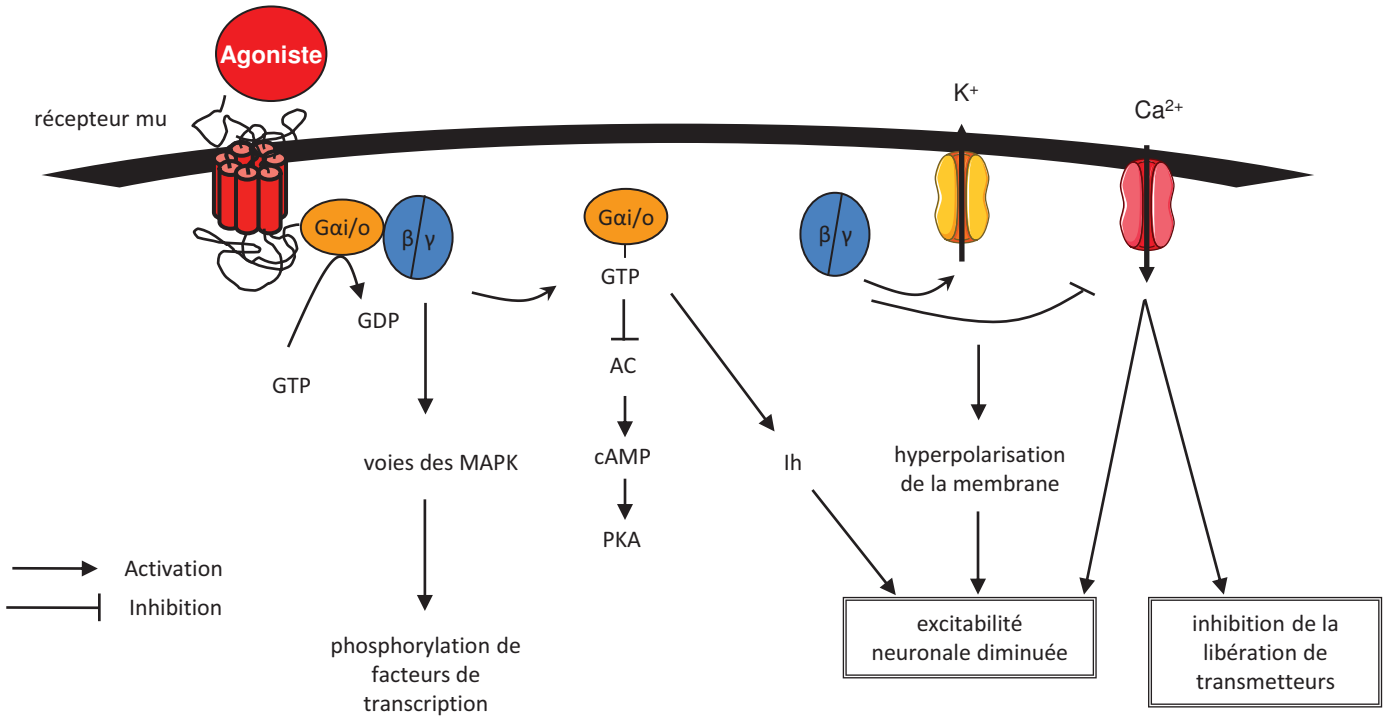

Figure 4. Transduction du signal induit par l'activation du récepteur mu
L'activation du récepteur mu induite par le ligand entraîne l'activation des sous-unités de la protéine G. Les consequences sont l'inhibition de l'AC, l'activation de la conductance potassique, l'inhibition de la conductance calcique et l'inhibition de la libération de transmetteurs. (Adapté de Williams *et al*., 2001)
AC, adénylate cyclase; cAMP, adénosine monophosphate cyclique ; GDP, guanosine diphosphate; GTP, guanosine triphosphate; Ih, courant voltage-dependant; MAPK, protéine kinase activée par des mitogènes; PKA, protéine kinase A.

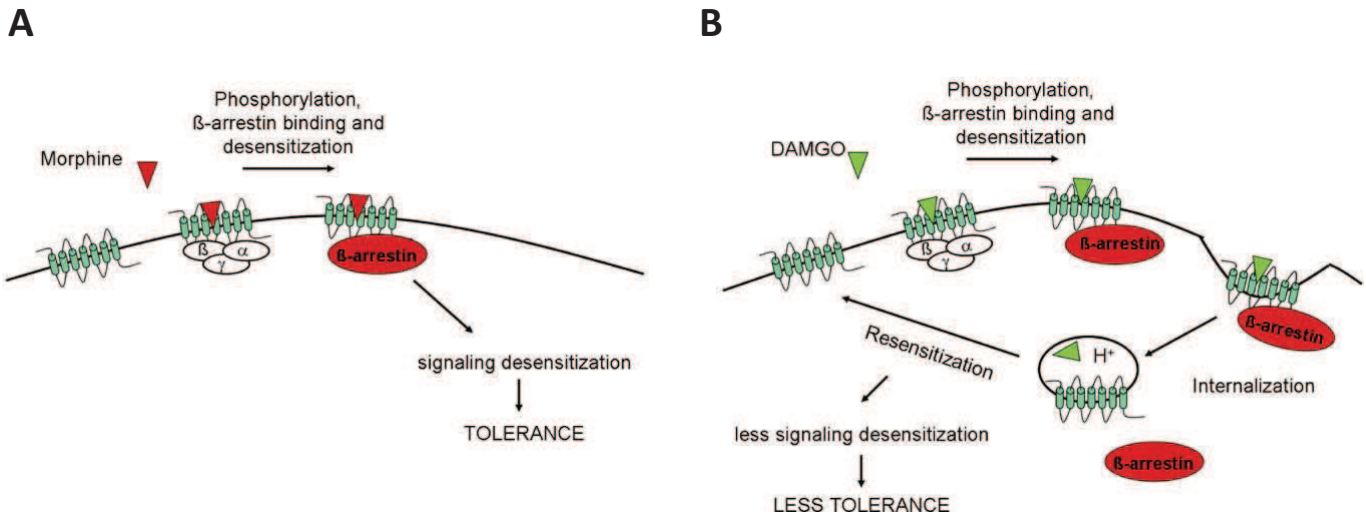

Figure 5. Différents potentiels d'internalisation de la morphine (**A**) et du DAMGO (**B**). (Adapté de Koch et al., 2008)

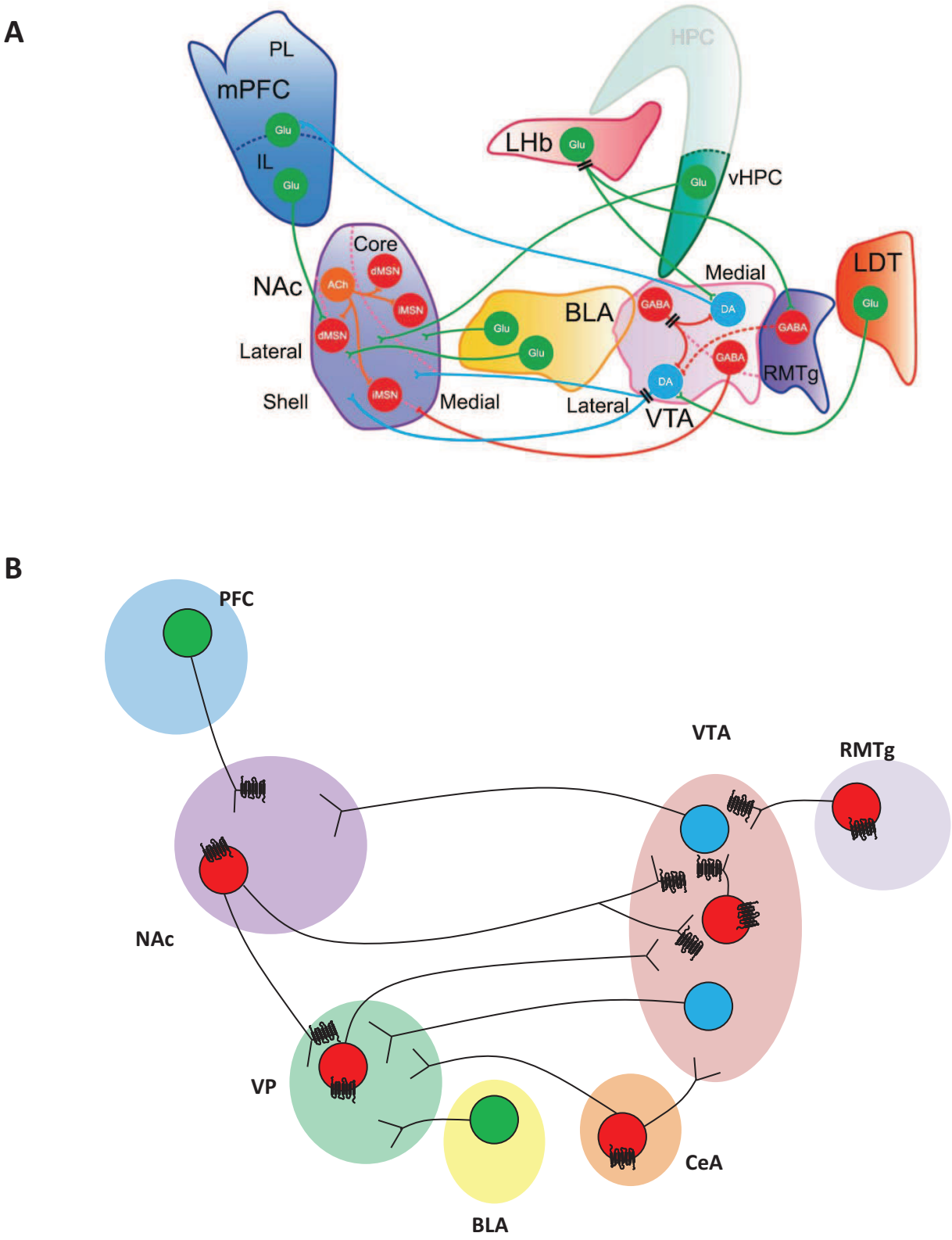

Figure 6. Le système dopaminergique mésolimbique
(**A**) caracterisé par optogénétique (Adapté de Nieh et al., 2013)
(**B**) avec position des récepteurs mu ( )(pour description, voir texte) (Adapté de Meye et al., 2014)

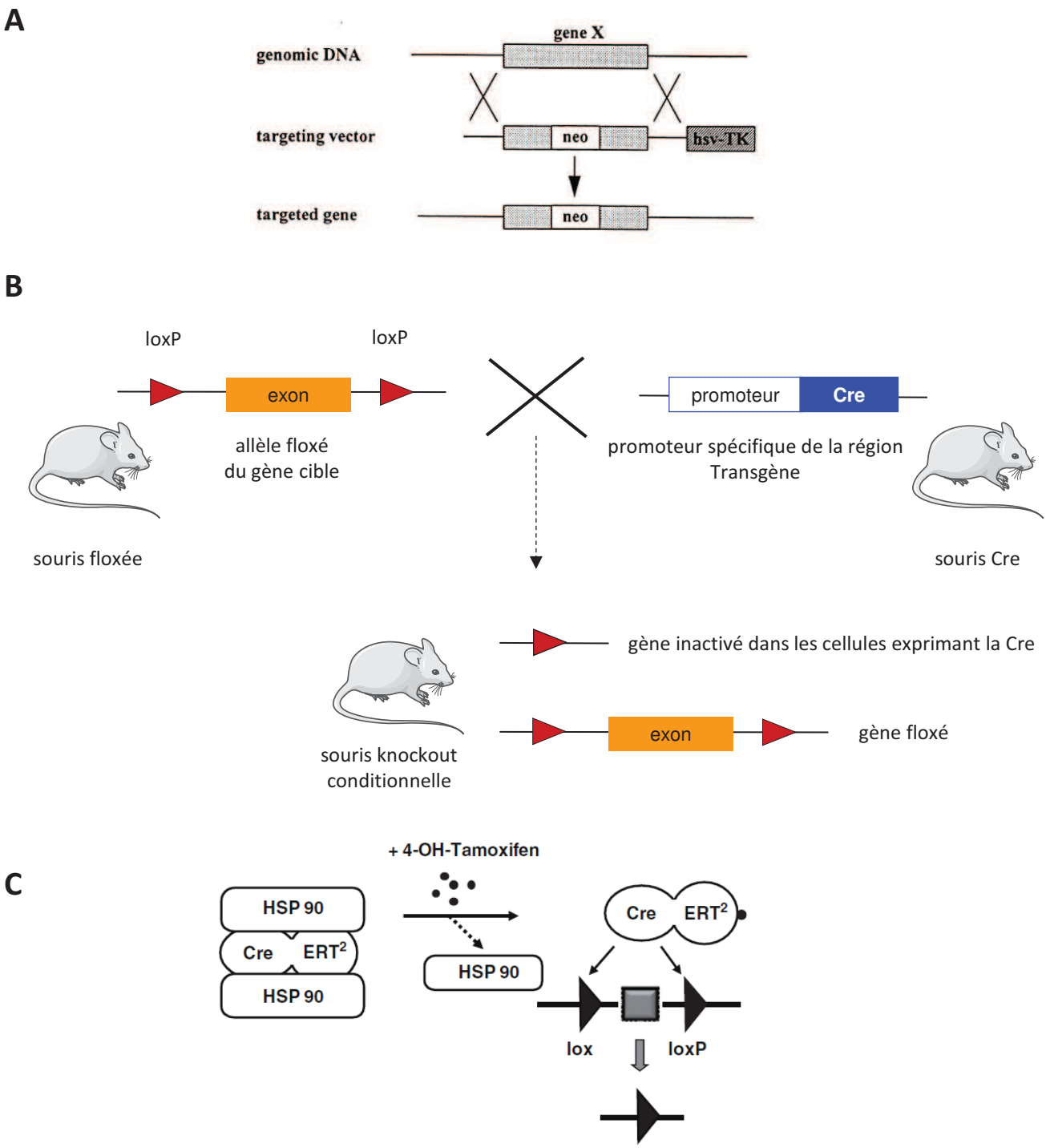

Figure 7. Approches génétiques de création de modèles murins

(**A**) Inactivation (KO) par recombinaison homologue : un gène est remplacé par une version interrompue du gène par recombinaison homologue. La cassette Neo est utilisée pour interrompre le gène. (Adapté de Brusa et al., 1999)

(**B**) Inactivation spécifique d'un gène par le système Cre-loxP. Le promoteur conduit l'expression de la Cre recombinase, qui excise la séquence entre 2 sites loxP du gène d'intérêt. (Adapté de Gavériaux-Ruff and Kieffer, 2007)

(**C**) Inactivation spécifique d'un gène par le système CreER^{T2} inductible par le tamoxifène. La protéine Cre-ER^{T2} est exprimée de façon constitutive dans la population cellulaire ciblée, mais reste inactive. Le 4-OH-tamoxifène (le tamoxifène est métabolisé en 4-OH-tamoxifène par le foie) active ER^{T2}, menant à la dissociation de HSP90 et levant l'interférence induite par HSP90. (Adapté de Friedel et al., 2011)

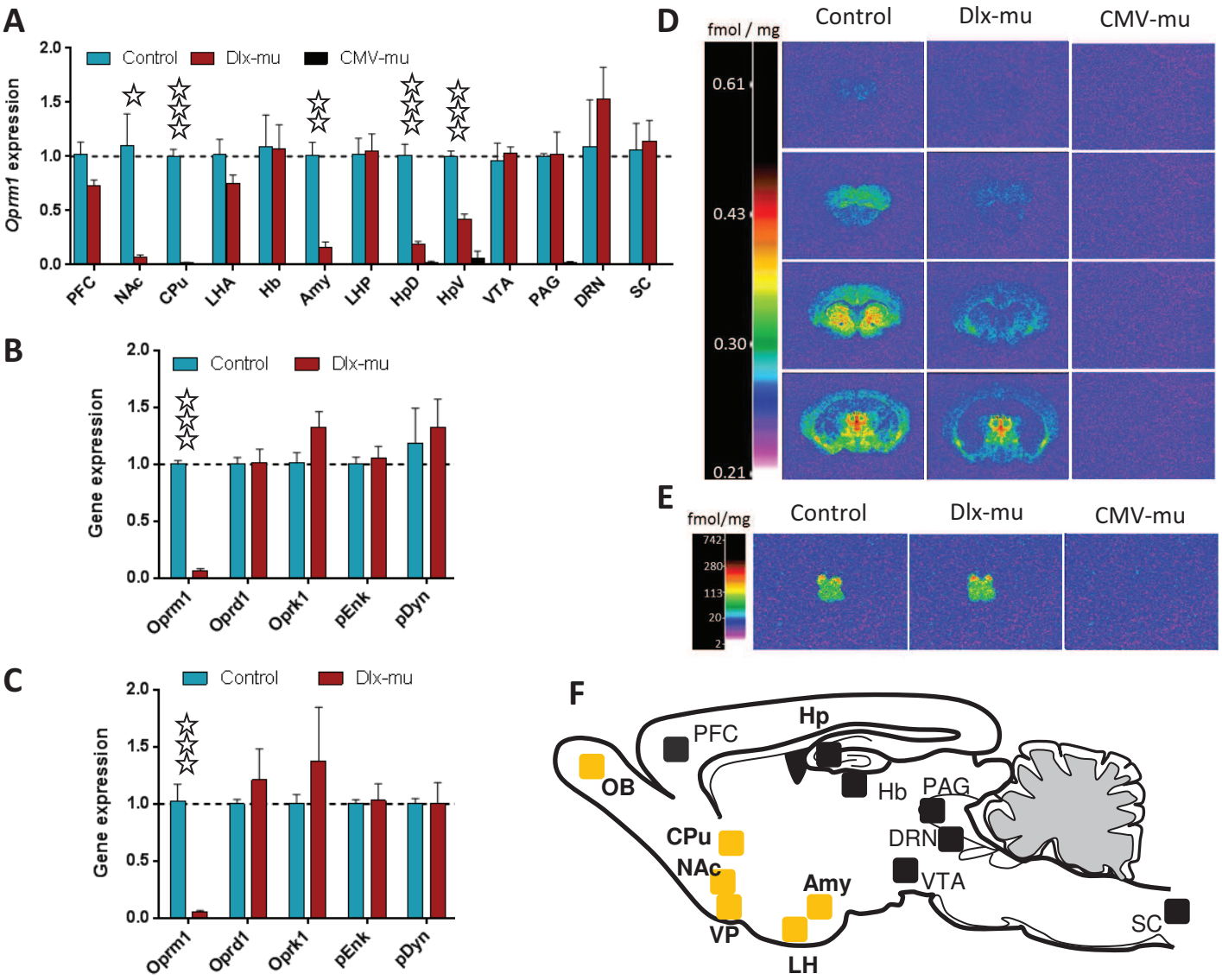

Figure 1. Caractérisation neuroanatomique des animaux invalidés conditionnels. (**A-C**) Réaction en chaîne par polymérase quantitative en temps réel. L'ARN messager du gène du récepteur mu (*Oprm1*) des souris Dlx-mu (knockout conditionnel) et CMV-mu (knockout constitutif) est représenté en fonction de l'expression chez les contrôles (Control=1, ligne en pointillés) (**A**), normalisé par la β-actine comme gène de référence. L'expression de l'ARN messager des gènes du système opioïde chez les souris Dlx-mu est représenté selon l'expression chez les contrôles (Control=1, ligne en pointillés) dans le CPu (**B**) et le NAc (**C**). Aucune expression de l'ARNm de *Oprm1* n'a été détectée chez les souris Dlx-mu. Aucun changement de l'expression de l'ARNm des autres gènes n'a été détecté chez les souris (ANOVA à une voie). (**D, E**) Autoradiogrammes de sections de cerveaux (**D**) et de moelles épinières (**E**) chez les souris Control, Dlx-mu et CMV-mu. Le récepteur mu est marqué avec du [^{3}H]DAMGO. Les barres de couleur montrent une interprétation de la densité relative des images noir et blanc, calibrées en fmol/mg de tissu. La liaison non-spécifique est homogène et à des niveaux de bruit de fond. Les sections des trois génotypes ont été traités en parallèle pour la liaison et le développement des autoradiogrammes. (**F**) Résumé de la suppression de la protéine mu chez les souris Dlx-mu par rapport aux Control, adapté de **Tableau 1**. Les régions cérébrales en jaune correspondent aux structures des souris Dlx-mu qui montrent un réduction significative de la protéine mu par rapport aux souris Control. n=3-4 par groupe. Les étoiles blanches représentent une différence significative entre les souris Control et Dlx-mu. Une étoile, $p<0.05$; deux étoiles, $p<0.01$; trois étoiles, $p<0.001$ (test t). Amy, amygdale; CPu, noyau caudé putamen; DRN, noyau raphé dorsal; Hb, habenula; Hp, hippocampe; LH, hypothalamus lateral; NAc, noyau accumbens; OB, bulbes olfactifs ; PAG, matière grise périaqueductale; PFC, cortex préfrontal; SC, moelle épinière; VP, pallidum ventral; VTA, aire tegmentale ventrale.

Tableau 1. Quantification de la liaison spécifique de [^{3}H]DAMGO sur des sections cérébrales de souris Control et knockout conditionnelles

		liaison spécifique [^{3}H]DAMGO (fmol/mg tissu)		
Région	**Bregma**	**Control (n=3)**	**Dlx-mu (n=4)**	**% changement**
Olfactory bulb	3.56			
External plexiform Layer		21.4 ± 9.1	0.0 ± 0.0 ***	-100
Internal granular layer		21.8 ± 8.5	0.0 ± 0.1 ***	-100
Cortical areas				
Motor	2.1			
Superficial layers		41.8 ± 15.4	27.7 ± 9.6	-33.8
Deep layers		46.7 ± 6.9	30.2 ± 9.4	-35.4
Orbital	2.1			
Superficial layers		48.8 ± 14.6	57.2 ± 10.5	17.2
Deep layers		49.0 ± 9.0	48.1 ± 9.8	-1.7
Frontal	1.98			
Superficial layers		27.9 ± 10.4	29.9 ± 9.2	7.2
Deep layers		33.7 ± 10.6	34.4 ± 10.3	2.3
Cingulate	1.1			
Superficial layers		28.8 ± 10.9	32.1 ± 9.4	11.6
Deep layers		30.6 ± 2.6	32.7 ± 11.0	7.1
Frontal-Parietal	1.1			
Superficial layers		17.1 ± 3.7	25.9 ± 10.2	51.9
Deep layers		25.8 ± 6.2	31.4 ± 10.2	21.7
Rostral sosmatosensory	1.1			
Superficial layers		14.3 ± 4.3	22.2 ± 8.3	55.3
Deep layers		27.2 ± 7.0	28.3 ± 9.1	3.9
Parietal	-1.46			
Superficial layers		17.0 ± 9.1	16.0 ± 6.3	-5.9
Deep layers		25.0 ± 9.4	23.1 ± 8.1	-7.4
Caudal somatosensory	-2.06			
Superficial layers		14.9 ± 5.2	15.6 ± 5.1	4.7
Deep layers		25.8 ± 8.0	24.0 ± 8.3	-7
Retrosplenial	-2.06			
Superficial layers		22.6 ± 6.4	24.1 ± 8.5	6.6
Deep layers		38.0 ± 5.6	25.6 ± 7.1	-32.5
Temporal	-2.06			
Superficial layers		22.8 ± 6.6	25.7 ± 5.1	12.7
Deep layers		35.0 ± 8.8	36.9 ± 9.3	5.2
Auditory	-2.54			
Superficial layers		22.5 ± 6.7	23.3 ± 7.6	3.2
Deep layers		33.3 ± 11.1	35.6 ± 8.7	7.1
Visual	-3.52			
Superficial layers		32.9 ± 15.9	14.7 ± 7.1	-55.3
Deep layers		26.6 ± 7.2	18.1 ± 7.7	-31.8
Entorhinal	-3.64	53.5 ± 17.8	77.8 ± 9.5	45.5

Les valeurs de la liaison spécifique de [^{3}H]DAMGO représentent la moyenne ± SEM fmol/mg de tissu dans les régions cérébrales de souris Control et de souris knockout conditionnelles pour le récepteur mu. Les coordonnées Bregma ont été choisies selon The Mouse Brain Atlas de Franklin et Paxinos (1997). La liaison spécifique a été calculée après soustraction de la liaison non-spécifique à la liaison totale de [^{3}H]DAMGO. Le pourcentage de changement dans la liaison indique le changement chez les souris knockout conditionnelles par rapport aux souris Control. N indique le nombre d'animaux par groupe. L'ANOVA à deux voies a révélé un effet significatif du génotype, de la région et de génotype X région, tous p<0.001. Les comparaisons multiples (*post hoc)* Holm- ídák ont révélé des différences significatives intrarégions par rapport aux souris Control. Une étoile, p<0.05; deux étoiles, *p*<0.01; trois étoiles, *p*<0.001.

Tableau 1. Suite

		liaison spécifique [^{3}H]DAMGO (fmol/mg tissu)		
Région	**Bregma**	**Control (n=3)**	**Dlx-mu (n=4)**	**% changement**
Nucleus accumbens	1.18			
Core		119.5 ± 4.5	33.7 ± 5.3 ***	-71.8
Shell		102.6 ± 4.9	32.2 ± 4.4 ***	-68.6
Caudate putamen	1.1	56.8 ± 12.7	27.2 ± 2.3 *	-52.1
Dorsal endopiriform nucleus	1.1	66.6 ± 7.3	73.3 ± 10.4	10.1
Septum	0.74			
Medial		56.6 ± 4.7	25.2 ± 8.1 *	-55.4
Lateral		35.6 ± 5.6	18.2 ± 6.7	-49
Vertical limb of the diagonal band		49.0 ± 8.2	21.9 ± 8.1	-55.4
Ventral pallidum	-0.22	66.4 ± 22.9	12.5 ± 1.3 ***	-81.1
Preoptic area	-0.22	53.4 ± 7.6	15.8 ± 6.6 *	-70.4
Amygdala	-1.46			
Basolateral		98.5 ± 14.9	104.5 ± 17.7	6.1
Basomedial		70.6 ± 13.9	32.2 ± 10.9 *	-54.4
Medial		59.6 ± 11.8	49.5 ± 13.7	-28.9
Medial habenula	-1.46	190.0 ± 19.4	221.0 ± 21.6	16.3
Thalamus	-1.46	61.0 ± 11.8	48.8 ± 11.1	-19.9
Central lateral		132.6 ± 17.5	112.1 ± 14.7	-15.5
Central medial		155.4 ± 28.3	140.8 ± 15.4	-9.4
Intermediodorsal thalamic nucleus		142.9 ± 37.2	157.8 ± 20.1	10.5
Reuniens		103.9 ± 26.5	69.6 ± 18.4	-33
Hypothalamus	-1.46	62.6 ± 10.7	24.8 ± 7.7 *	-60.4
Hippocampus	-2.06	26.1 ± 3.7	10.7 ± 7.0	-59
Dorsal hippocampus	-3.8	41.1 ± 20.2	23.9 ± 8.9	-41.8
Substantia nigra	-3.4	68.6 ± 12.5	40.1 ± 11.5	-41.6
Ventral tegmental area	-3.4	86.8 ± 9.0	67.7 ± 6.3	-22
Superficial grey	-3.4			
Superficial layer		83.0 ± 14.5	78.6 ± 7.9	-5.3
Intermediate layer		87.3 ± 7.7	74.6 ± 5.1	-14.4
Medial geniculate nucleus	-3.4	48.5 ± 12.7	11.7 ± 3.0 *	-75.9
Periaqueductal grey	-3.4	59.1 ± 6.0	39.4 ± 9.2	-33.3
Interpeduncular nucleus	-3.64	83.1 ± 18.7	67.1 ± 33.9	-19.2
Spinal cord				
Cervical (C6)				
Whole section		41.7 ± 15.9	55.3 ± 12.8	32.5
Superficial layers (lamina I and II)		80.3 ± 22.9	95.0 ± 12.9	18.3
Laminas III-IV		36.0 ± 8.5	50.7 ± 7.8	40.9
Lamina X		39.6 ± 18.6	48.2 ± 10.3	21.9
Ventral horn (laminas VII -IX)		33.2 ± 8.9	46.1 ± 7.5	38.5

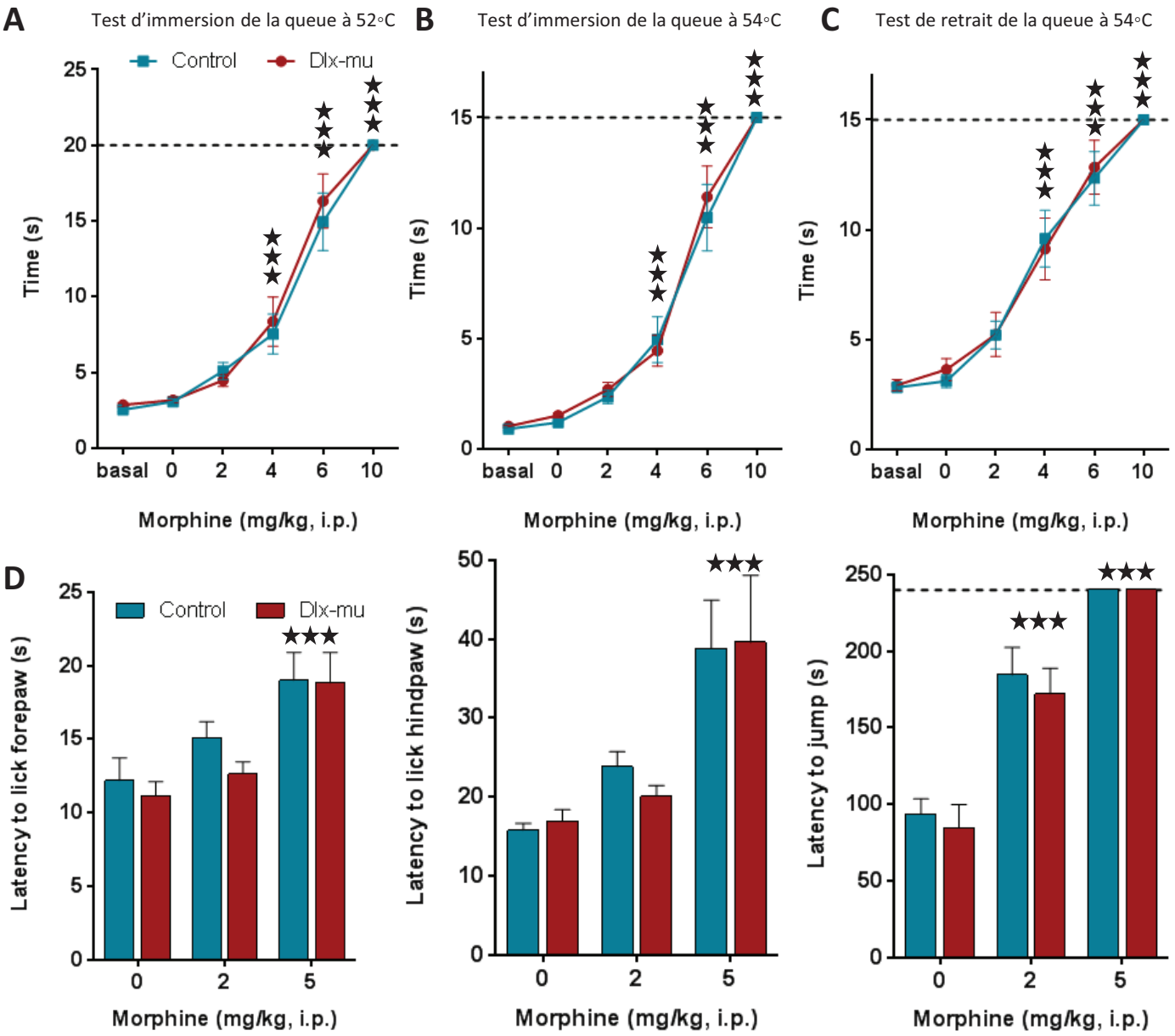

Figure 2. Analgésie et dépendance physique induites par la morphine. (**A**). L'analgésie morphinique mesurée par la latence de retrait de la queue dans le test d'immersion de la queue à 52◦C (**A**) et 54◦C (**B**) et dans le test de retrait de la queue (**C**) à 54◦C est conservée pour tous les génotypes. (**D**) L'analgésie morphinique dans le test de la plaque chaude, mesurée par la latence de léchage de pattes avant, pattes arrière et de saut (s) est maintenue chez les souris Dlx-mu. (**E**) Les signes comportementaux de sevrage induit par la naloxone après traitement à la morphine ne sont pas différents chez les souris Control et Dlx-mu. Un score global est déterminé selon Berrendero *et al.*, 2003 pour la somme des 20 minutes post-injection de naloxone et donnant un poids relatif à chaque paramètre mesuré. n=5-15 par groupe. Les étoiles représentent un effet significatif du traitement par rapport aux groupes saline. Trois étoiles, $p<0.001$ (ANOVA à deux voies).

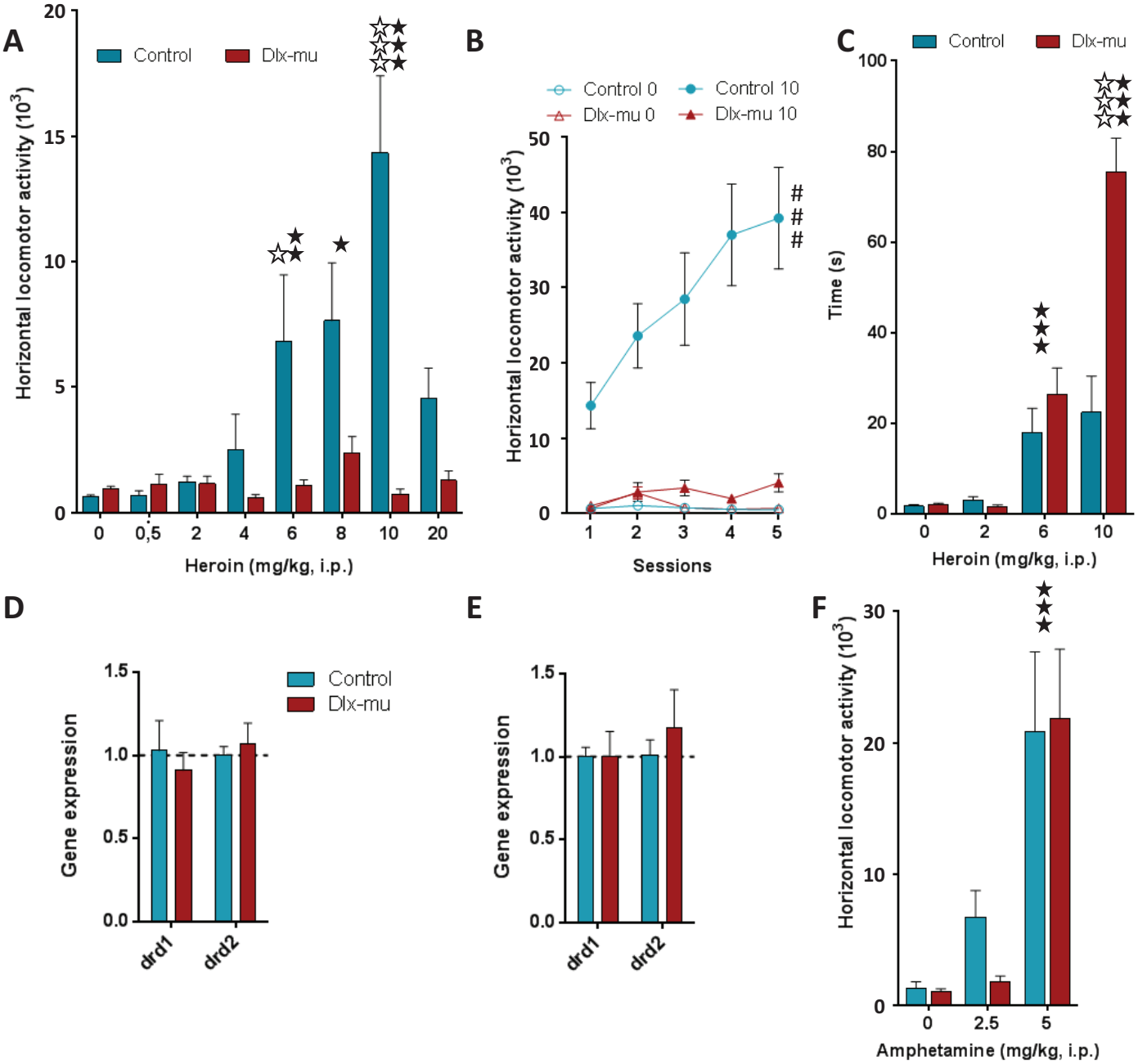

Figure 3. **Modification pharmacologique de la locomotion, sensibilisation à l'hyperlocomotion et catalepsie**. Les panneaux supérieurs montrent les effets locomoteurs de l'héroïne, les panneaux inférieurs montrent les effets locomoteurs de l'amphétamine. (**A**) L'activité après injection intraperitonéale d'héroïne est mesurée durant une session de deux heures. L'héroïne augmente l'activité locomotrice chez les souris Control à 6, 8 et 10 mg/kg, mais pas chez les souris Dlx-mu. Une différence entre les génotypes apparaît à 6 et 10 mg/kg. (**B**) La sensibilisation à l'effet locomoteur de l'héroïne à 10 mg/kg est mesurée pendant 5 sessions de 2h. Les souris Control montrent une sensibilisation locomotrice mais pas les animaux Dlx-mu. (**C**) La catalepsie est évaluée dans le test de la barre, 30 min après une administration intrapéritonéale d'héroïne. L'héroïne produit de la catalepsie chez les deux génotypes à 6 et 10 mg/kg, et cet effet est plus fort chez les souris Dlx-mu à la plus grande dose testée. (**D**) L'expression de l'ARNm des gènes des récepteurs dopaminergiques chez les souris Dlx-mu est représentée selon l'expression chez les Control (=1, ligne en pointillés) dans le CPu (**D**) et le NAc (**E**). Aucun changement dans l'expression de l'ARNm des récepteurs à la dopamine n'est détecté (ANOVA à une voie). (**F**) L'activité après injection ip d'amphétamine est mesurée pendant une session de 2h. L'amphétamine augmente l'activité locomotrice chez les souris Control et Dlx-mu à 5 mg/kg. Aucune différence entre génotype n'est observée. n=5-33 par groupe. Les étoiles noires représentent un effet significatif du traitement par rapport aux groupes saline, les blanches une différence significative entre génotypes, # une différence significative entre les groupes. 1 symbole, p<0.05; 2 symboles, *p*<0.01; 3 symboles, *p*<0.001 (ANOVA à 2 voies pour la locomotion et le bar test, à 3 voies pour la sensibilisation).

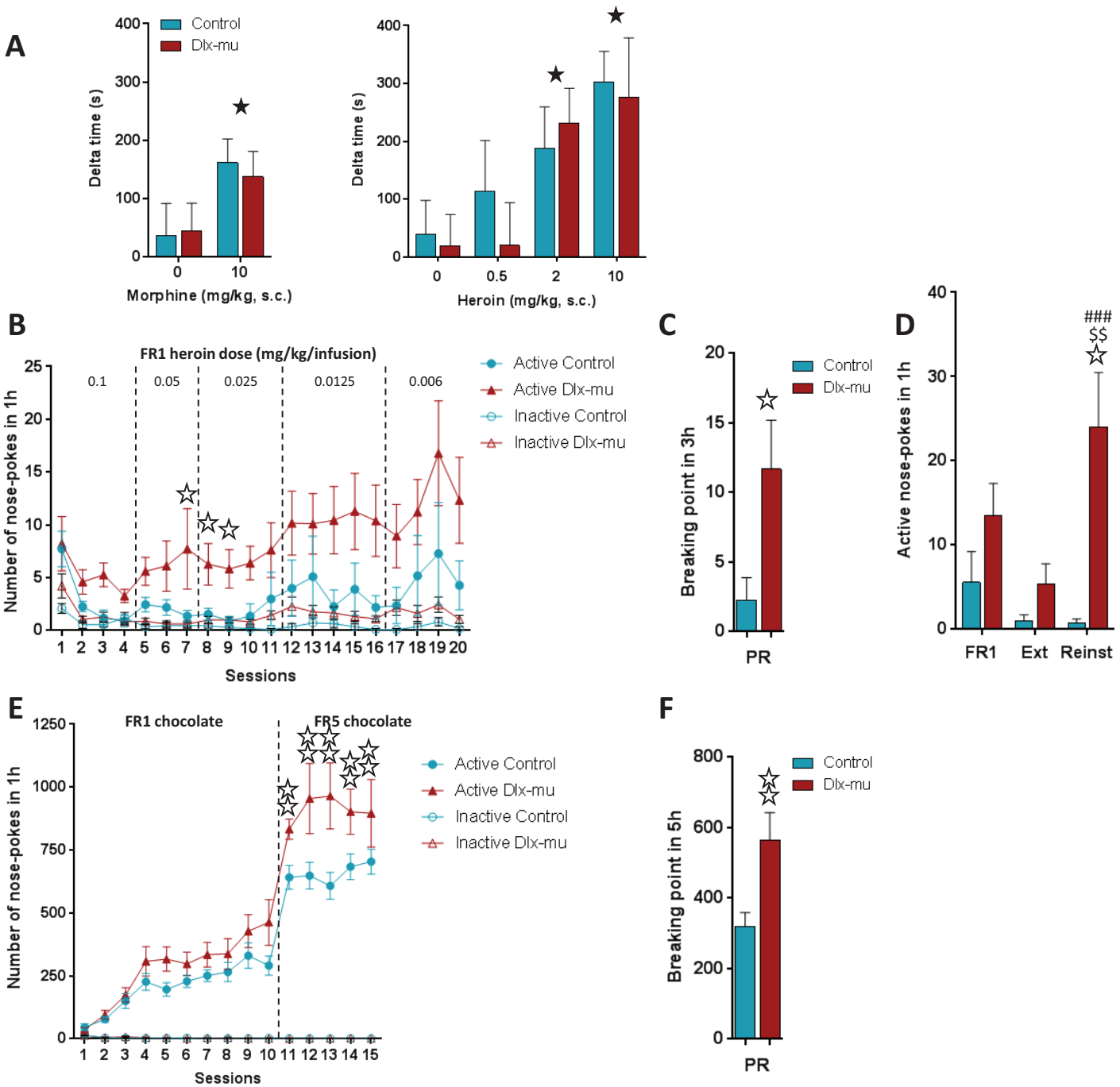

Figure 4. **Récompense et comportement motivé**. (**A**) La récompense induite par les opiacés est mesurée dans un test de préférence de place conditionnée (CPP) de 6 sessions. La CPP est représentée en delta temps (temps passé dans le compartiment associé à la drogue durant le pré-conditionnement moins post-conditionnement). A gauche, la morphine est récompensante à 10 mg/kg (s.c) chez les deux génotypes. A droite, l'héroïne induit une préférence de place à 2 et 10 mg/kg (s.c.) et cet effet n'est pas différent selon le génotype. (**B**) Le conditionnement opérant maintenu par l'héroïne est testé afin de mesurer les effets renforçants primaires de la drogue. L'acquisition de l'auto-administration d'héroïne commence a être significativement plus grande chez les souris Dlx-mu aux sessions 7-9 à une dose de 0.025 mg/kg/infusion et est maintenue dans les doses suivantes plus faibles. (**C**) Motivation pour l'héroïne (0.0125 mg/kg/inf). Le point de rupture atteint en une session de 3h de PR révèle une motivation pour l'héroïne augmentée chez les souris Dlx-mu. (**D**) Rechute induite par un indice (acquisition à 0.006 mg/kg/inf). Après une phase d'extinction, la rechute induite par un indice est observée uniquement chez les souris Dlx-mu. (**E**) Conditionnement opérant maintenu par le chocolat. Le nombre moyen de nose-pokes actifs et inactifs (session journalière d'une heure) pendant 10 jours de FR1 est équivalent dans les deux génotypes, mais lors des 5 jours de FR5 ce nombre est supérieur chez les souris Dlx-mu. (**F**) Motivation pour le chocolat. Le point de rupture moyen atteint en une session unique de 5h de PR révèle une motivation pour le chocolat augmentée chez les souris Dlx-mu. n=4-21 par groupe en CPP, n=11-20 par groupe en tests opérants. Les étoiles noires représentent un effet significatif du traitement par rapport aux groupes saline, les blanches une différence significative entre génotypes, $ une différence avec l'acquisition, # une différence avec l'extinction. 1 symbole, $p<0.05$; 2 symboles, $p<0.01$; 3 symboles, $p<0.001$ (ANOVA à 2 voies en CPP, ANOVA à 1 voie en auto-administration). FR, ratio fixe; PR, ratio progressif; ext, extinction; Reinst, rechute.

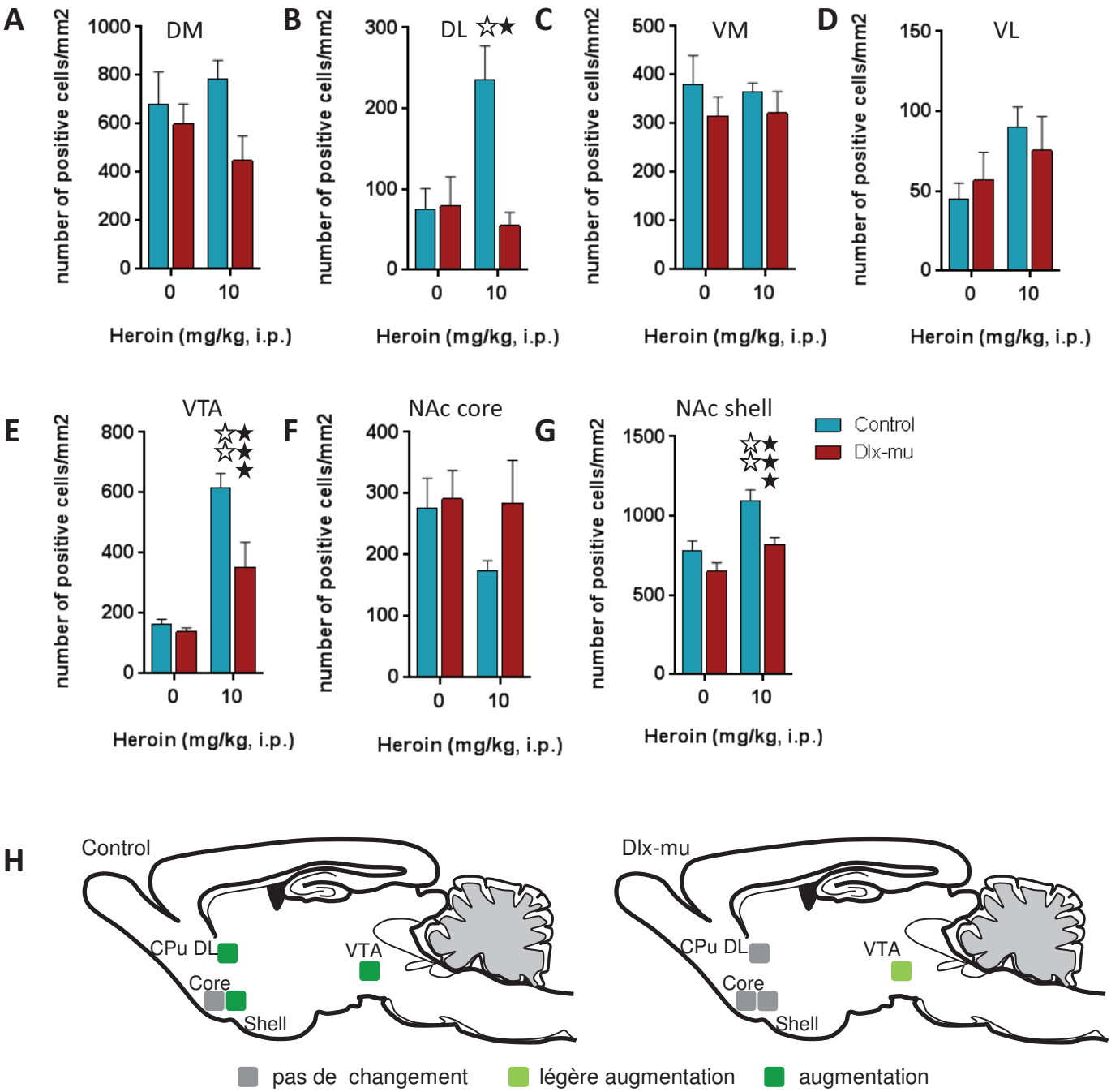

Figure 5. Immunoréactivité c-Fos chez les souris Control et Dlx-mu. L'immunohistochimie pour la protéine c-Fos est testée sur des sections de cerveaux d'animaux perfusés 2h après administration de solution saline ou héroïne (10 mg/kg, i.p.). Le nombre de neurones positifs est relevé manuellement dans des régions définies et les données sont exprimées en cellules positives pour c-Fos par mm2. L'héroïne induit l'expression de c-Fos dans le CPu dorsolatéral (**B**), la VTA (**E**) et le shell du NAc (**G**) du groupe Control, et dans la VTA du groupe Dlx-mu. Le traitement n'a pas d'effet sur l'induction de c-Fos dans le CPu dorsmédial (**A**), ventrolatéral (**D**) et ventromédial (**C**) et dans le core du NAc (**F**). Résumé schématique de l'immunoréactivité c-Fos chez les groupes Control et Dlx-mu après administration d'héroïne (**H**).

n=5-6 par groupe. Les étoiles noires représentent un effet significatif du traitement, les blanches une différence significative entre génotypes. Une étoile, $p<0.05$; deux étoiles, $p<0.01$; trois étoiles, $p<0.001$ (ANOVA à 2 voies). CPu, noyau caudé putamen; DL, dorsolatéral; DM, dorsomédial; NAc, noyau accumbens; VL, ventrolatéral; VM, ventromédial; VTA, aire tegmentale ventrale.

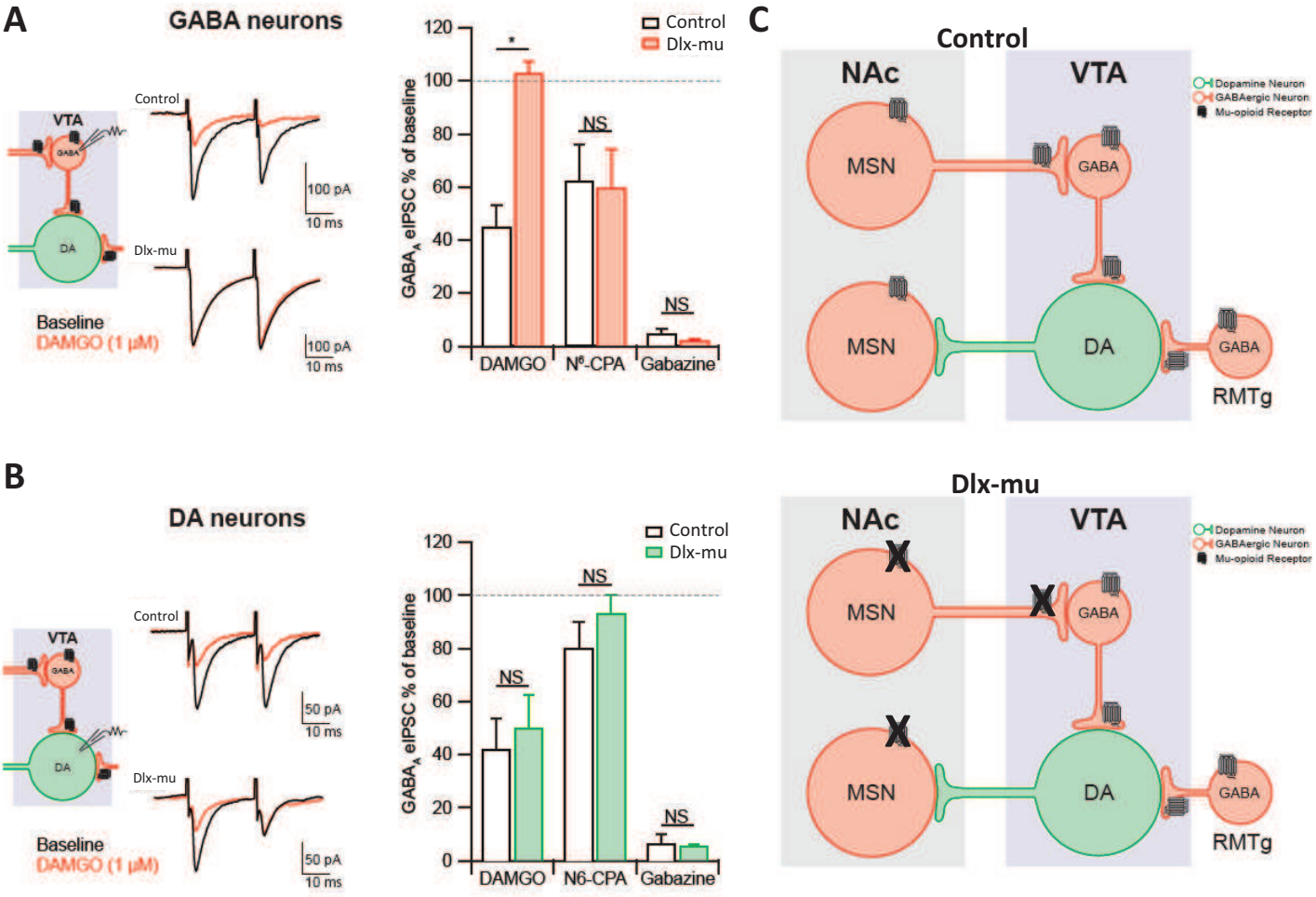

Figure 6. Caractérisation électrophysiologique des neurones de la VTA des animaux knockout conditionnels. (**A**) IPSC évoqués des neurones GABAergiques de la VTA. L'amplitude des IPSCs GABA-A est diminuée après application de DAMGO (1 µM) chez les animaux Control mais pas chez les Dlx-mu. Les différences de eIPSCs entre génotypes n'ont pas été observées après application d'un agoniste adénosine (N6-CPA, 1 µM). (**B**) IPSC évoqués des neurones dopaminergiques de la VTA. L'amplitude des IPSCs GABA-A est diminuée après application de DAMGO (1 µM) et de N6-CPA (1 µM) de la même façon chez les animaux Control et chez les Dlx-mu. (**C**) Représentation schématique de la localisation du récepteur mu (noir) sur les neurones dopaminergiques (vert) et GABAergique (rouge) de la VTA et du NAc. Panneau supérieur, localisation chez les Control; panneauinférieur, localisation chez les Dlx-mu. n=8-10 par groupe. Les étoiles représentent une différence significative entre les souris Control et Dlx-mu. Une étoile, $p<0.05$ (test t). DA, dopamine; NAc, noyau accumbens; VTA, aire tegmentale ventrale.

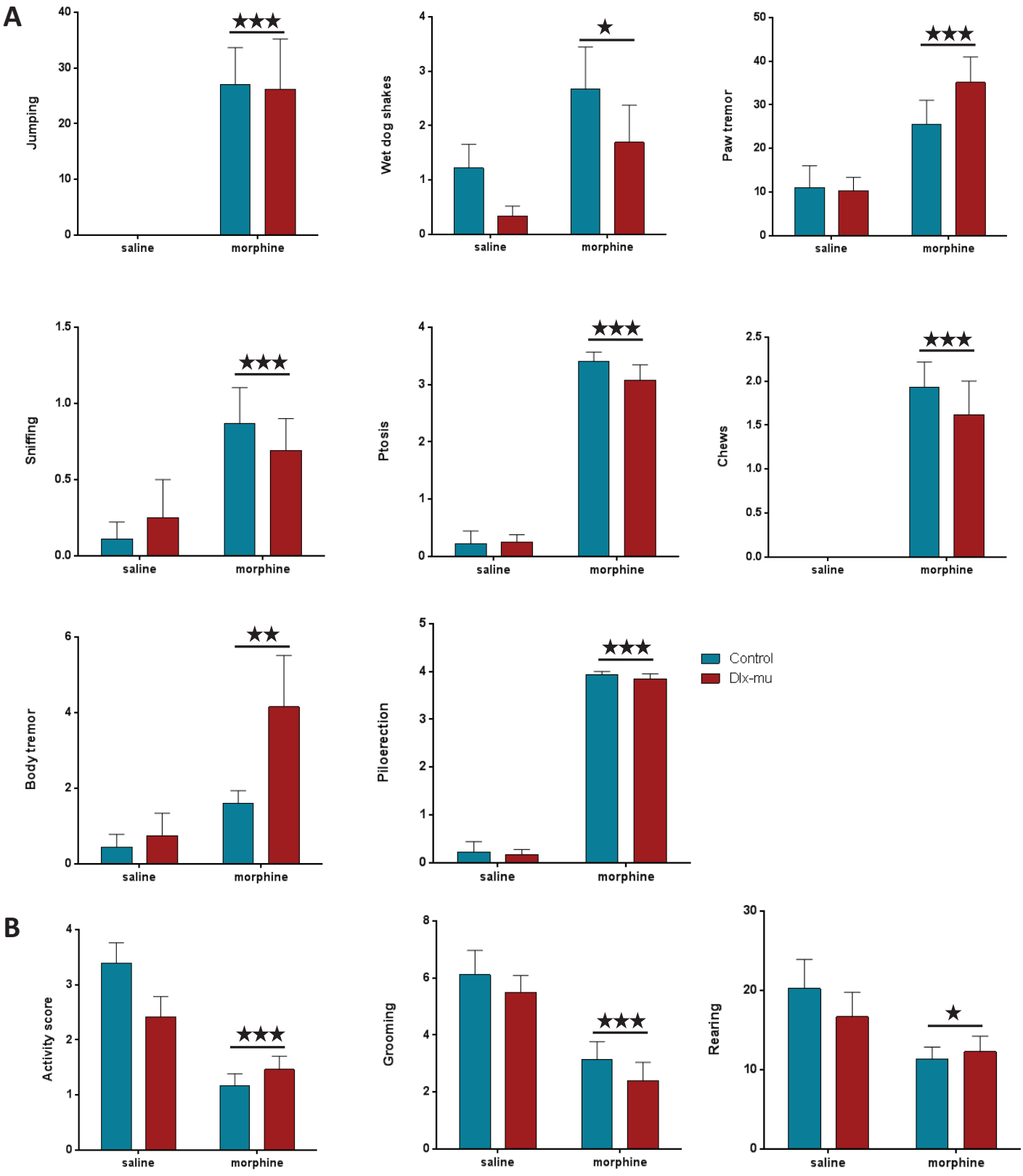

Figure S1. Signes comportementaux de sevrage induit par la naloxone après un traitement chronique à la morphine chez les souris Control et Dlx-mu. Chaque signe est relevé 5 min avant et 20 min après l'injection de naloxone. Les données montrent la somme des 20 min après l'injection de naloxone. **(A)** Signes inclus dans le score global. **(B)** Signes supplémentaires relevés. n=9-15 par groupe. Les étoiles représentent un effet du traitement. Une étoile, *p<0.05*; deux étoiles, *p<0.01*; trois étoiles, *p<0.001* (ANOVA à deux voies).

		Df1	Df2	F	*p*-value	
Jump	genotype	1	45	0.004335	0.9478	
	treatment	1	45	17.11	0.0002	***
	genotype x treatment	1	45	0.004335	0.9478	
Wet dog shake	genotype	1	45	2.117	0.1526	
	treatment	1	45	4.792	0.0338	*
	genotype x treatment	1	45	0.004454	0.9471	
Paw tremor	genotype	1	45	0.7086	0.4043	
	treatment	1	45	14.01	0.0005	***
	genotype x treatment	1	45	0.9686	0.3303	
Sniffing	genotype	1	45	0.006059	0.9383	
	treatment	1	45	6.91	0.0117	*
	genotype x treatment	1	45	0.4726	0.4953	
Ptosis	genotype	1	45	0.5199	0.4746	
	treatment	1	45	215	<0.0001	****
	genotype x treatment	1	45	0.7339	0.3962	
Chews	genotype	1	45	0.3364	0.5648	
	treatment	1	45	41.9	<0.0001	****
	genotype x treatment	1	45	0.3364	0.5648	
Body tremor	genotype	1	45	2.976	0.0914	
	treatment	1	45	7.566	0.0085	**
	genotype x treatment	1	45	1.84	0.1817	
Piloerection	genotype	1	45	0.3456	0.5596	
	treatment	1	45	926.5	<0.0001	****
	genotype x treatment	1	45	0.01696	0.897	
Activity	genotype	1	45	1.303	0.2597	
	treatment	1	45	28.67	<0.0001	****
	genotype x treatment	1	45	4.56	0.0382	
Grooming	genotype	1	45	0.9898	0.3251	
	treatment	1	45	19.87	<0.0001	****
	genotype x treatment	1	45	0.010147	0.9203	
Rearing	genotype	1	45	0.2776	0.6008	
	treatment	1	45	7.214	0.01	*
	genotype x treatment	1	45	0.8326	0.3663	

Tableau S1. Analyse statistique (ANOVA à deux voies) des signes comportementaux de sevrage induit par la naloxone après traitement à la morphine chez les animaux Control et Dlx-mu. Tableau supérieur, signes inclus dans le score global; tableau inférieur, signes supplémentaires relevés.

A

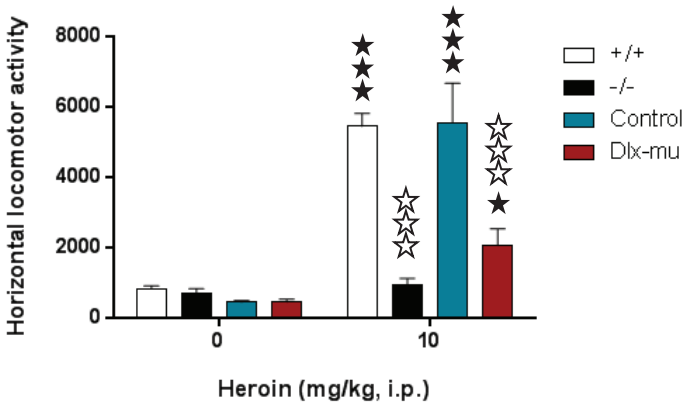

B

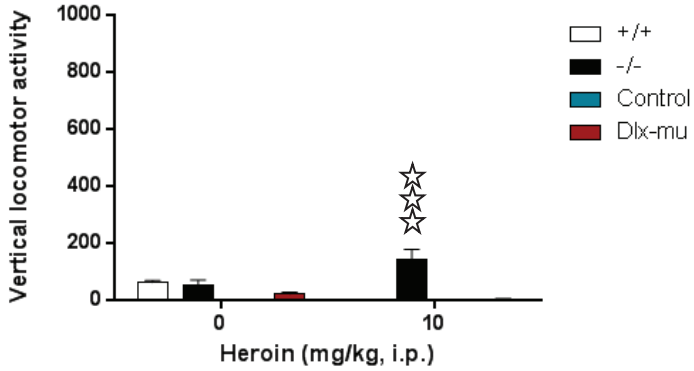

Figure S2. Activité hyperlocomotrice induite par l'héroïne durant une session de 2h. **(A)** L'activité horizontale après injection intrapéritonéale d'héroïne est mesurée durant une session de 2h. L'héroïne augmente l'activité locomotrice chez les souris +/+, Control et Dlx-mu à 10 mg/kg, mais pas chez les souris -/-. Les animaux -/- et Dlx-mu à 10 mg/kg d'héroïne diffèrent des animaux +/+ et Control. **(B)** L'activité verticale après injection intrapéritonéale d'héroïne est mesurée durant une session de 2h. L'héroïne augmente l'activité verticale seulement chez les souris -/-. La différence est trouvée entre les -/- et les autres génotypes.

n=6-11 par groupe. Les étoiles noires représentent un effet significatif du traitement par rapport aux groupes saline, les blanches représentent une différence significative entre les génotypes. Une étoile, $p<0.05$; deux étoiles, $p<0.01$; trois étoiles, $p<0.001$ (ANOVA à deux voies).

	Three-way ANOVA			
	Acquisition 0.1 mg/kg/inf		Acquisition 0.05 mg/kg/inf	
	F-value	*P*-value	*F*-value	*P*-value
Genotype	$F_{(1,26)}$ = 3.61	*n.s.*	$F_{(1,27)}$ = 2.55	*n.s.*
Hole	$F_{(1,26)}$ = 20.40	*P* < 0.001	$F_{(1,27)}$ = 6.27	*P* < 0.001
Day	$F_{(3,78)}$ = 8.73	*P* < 0.001	$F_{(2,54)}$ =0.04	*n.s.*
Genotype × Hole	$F_{(1,26)}$ = 2.63	*n.s.*	$F_{(1,27)}$ = 2.05	*n.s.*
Genotype × Day	$F_{(3,78)}$ = 0.36	*n.s.*	$F_{(2,54)}$ = 0.43	*n.s.*
Hole × Day	$F_{(3,78)}$ = 1.58	*n.s.*	$F_{(2,54)}$ = 007	*n.s.*
Genotype × Hole × Day	$F_{(3,78)}$ = 7.14	*n.s.*	$F_{(2,54)}$ = 058	*n.s.*
	Acquisition 0.025 mg/kg/inf		Acquisition 0.0125 mg/kg/inf	
	F-value	*P*-value	*F*-value	*P*-value
Genotype	$F_{(1,2)}$ = 5.44	*P* < 0.05	$F_{(1,27)}$ = 2.81	*n.s.*
Hole	$F_{(1,2)}$ = 10.08	*P* < 0.01	$F_{(1,27)}$ = 8.64	*P* < 0.001
Day	$F_{(2,54)}$ = 0.19	*n.s.*	$F_{(5,135)}$ = 1.53	*n.s.*
Genotype × Hole	$F_{(1,2)}$ = 4.75	*P* < 0.05	$F_{(1,27)}$ = 1.91	*n.s.*
Genotype × Day	$F_{(2,54)}$ = 0.02	*n.s.*	$F_{(5,135)}$ = 0.72	*n.s.*
Hole × Day	$F_{(2,54)}$ = 0.28	*n.s.*	$F_{(5,135)}$ = 1.10	*n.s.*
Genotype × Hole × Day	$F_{(2,54)}$ = 0.01	*n.s.*	$F_{(5,135)}$ = 1.34	*n.s.*
	Acquisition 0.006 mg/kg/inf		Extinction and cue-induced reinstatement	
	F-value	*P*-value	*F*-value	*P*-value
Genotype	$F_{(1,27)}$ = 1.92	*n.s.*	$F_{(1,27)}$ = 5.88	*P* < 0.05
Hole	$F_{(1,27)}$ = 73.78	*P* < 0.01	$F_{(1,27)}$ = 10.46	*P* < 0.01
Day/Experimental phase	$F_{(3,81)}$ = 25.50	*P* < 0.01	$F_{(2,54)}$ = 4.97	*P* < 0.05
Genotype × Hole	$F_{(1,27)}$ = 1.94	*n.s.*	$F_{(1,27)}$ = 5.29	*P* < 0.05
Genotype × Day	$F_{(3,81)}$ = 1.80	*n.s.*	$F_{(2,54)}$ = 5.80	*P* < 0.01
Hole × Day	$F_{(3,81)}$ = 24.30	*P* < 0.05	$F_{(2,54)}$ = 4.06	*P* < 0.05
Genotype × Hole × Day	$F_{(3,81)}$ = 1.91	*n.s.*	$F_{(2,54)}$ = 4.61	*P* < 0.05

Three-way ANOVA with genotype as between-subjects factor and repeated measures in the factors day/experimental phase and hole (active/inactive). See materials and methods for details. *n.s.:* non significant

Tableau S2. Réponse opérante maintenue par l'héroïne pendant l'acquisition (0.1, 0.05, 0.025, 0.0125 et 0.006 mg/kg par injection, i.v.), l'extinction et la rechute induite par un indice.

	Three-way ANOVA			
	Acquisition FR1		Acquisition FR5	
	F-value	*P*-value	*F*-value	*P*-value
Genotype	$F_{(1,31)} = 2.87$	*n.s.*	$F_{(1,31)} = 6.88$	$P < 0.01$
Hole	$F_{(1,31)} = 122.15$	$P < 0.001$	$F_{(1,31)} = 259.91$	$P < 0.001$
Day	$F_{(9,279)} = 31.40$	$P < 0.001$	$F_{(4,124)} = 0.81$	*n.s.*
Genotype × Hole	$F_{(1,31)} = 2.79$	*n.s.*	$F_{(1,31)} = 6.80$	$P < 0.05$
Genotype × Day	$F_{(9,279)} = 1.75$	*n.s.*	$F_{(4,124)} = 1.55$	*n.s.*
Hole × Day	$F_{(9,279)} = 34.46$	$P < 0.001$	$F_{(4,124)} = 0.78$	*n.s.*
Genotype × Hole × Day	$F_{(9,279)} = 1.83$	*n.s.*	$F_{(4,124)} = 1.56$	*n.s.*

Three-way ANOVA with genotype as between-subjects factor and repeated measures in the factors day and hole (active/inactive). See materials and methods for details. *n.s.:* non significant

Tableau S3. Réponse opérante maintenue par le chocolat pendant l'acquisition à FR1 et FR5.

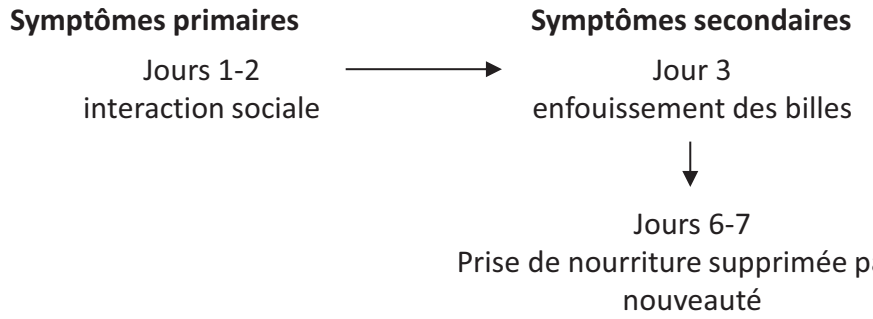

Figure 1. Déroulement chronologique de la batterie de tests de comportements associés à l'ASD.

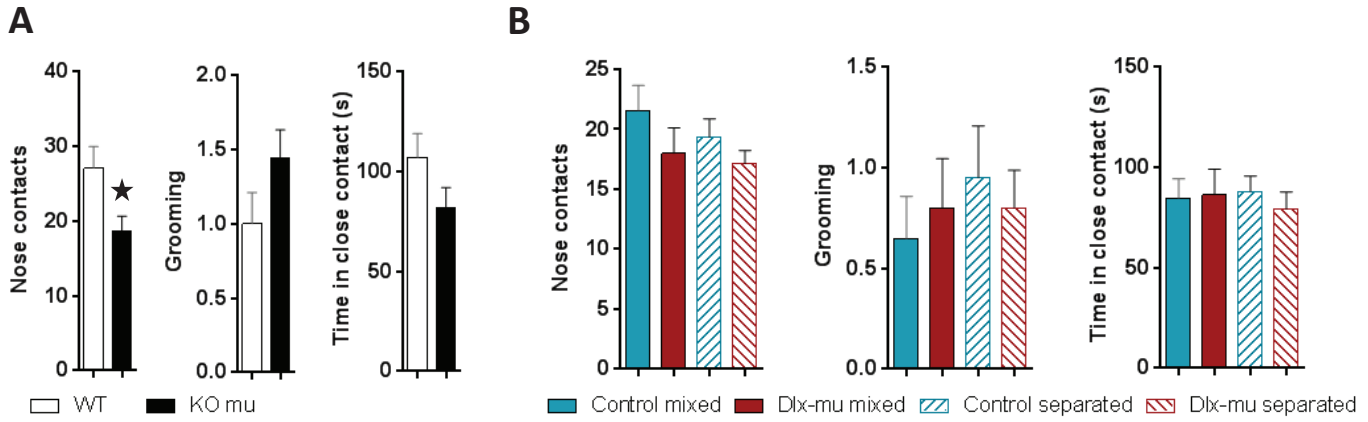

Figure 2. Capacités sociale mesurées dans le test d'interaction sociale. (**A**) n=17-18 par groupe. (**B**) n=15-20 par groupe. Un déficit d'interaction sociale est trouvé chez les souris KO ais pas chez les souris Dlx-mu, qu'elles soient élevées mélangées ou séparées. Les étoiles noires représentent une différence significative par rapport au groupe WT. Une étoile, $p<0.05$ (test t).

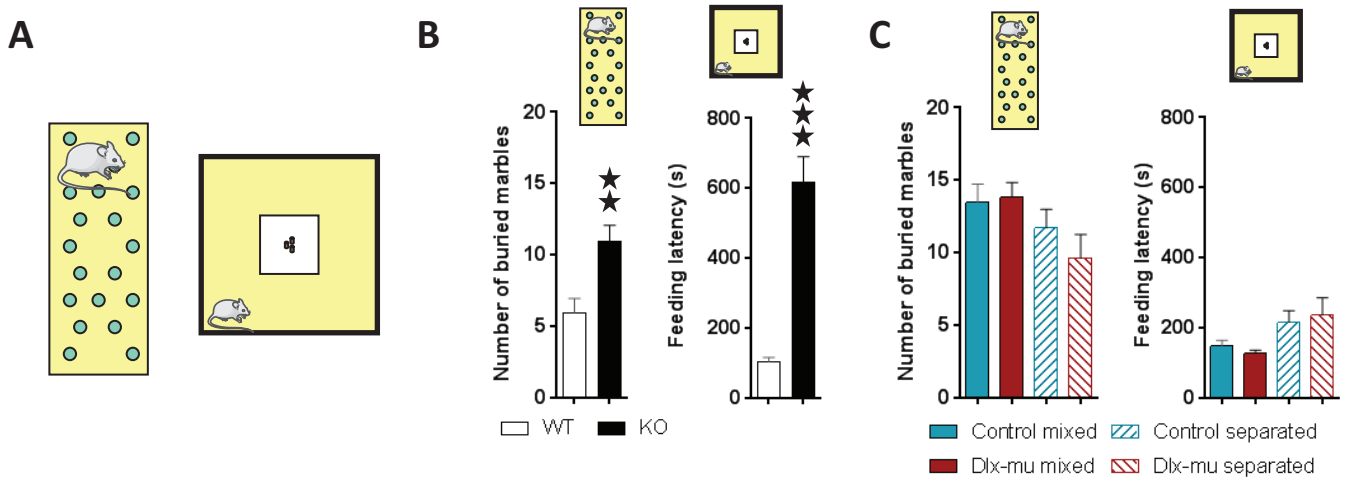

Figure 3. Le comportement pseudo-anxieux est évalué grâce aux tests d'enfouissement des billes (**A, gauche**) et de la prise de nourriture supprimée par la nouveauté (NSF) (**A, droite**). (**B**) Les tests d'enfouissement des billes et de NSF montrent une augmentation du comportement pseudo-anxieux chez les souris KO par rapport aux WT. (**C**) Aucune différence n'est trouvée dans le comportement défensif entre les Control et les Dlx-mu, mélangés ou séparés, et ce pour les deux tests. *(**A, gauche**) n=15-18 par groupe. (**A, droite**) n=10-20 par groupe*. Les étoiles noires représentent une différence significative par rapport au groupe WT. Deux étoiles, $p<0.01$; trois étoiles, $p<0.001$ (test t).

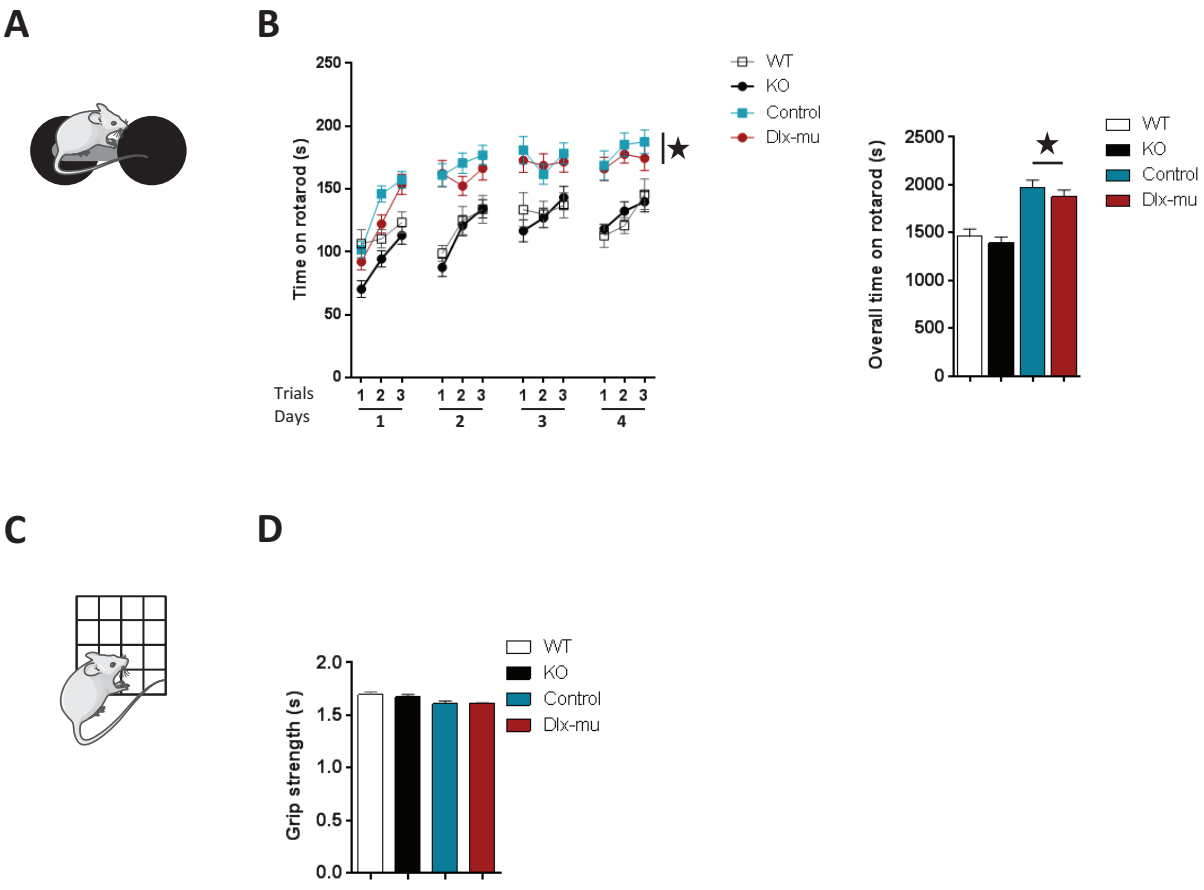

Figure S1. Fonctions motrices testées dans le rotarod (**A-B**) et le test de grip (**C-D**). (**B**) La capacité à rester sur le rotarod est plus faible che les souris Dlx-mu par rapport aux Control, mais il n'y a pas de différence entre les WT et les KO. (**D**) n=11-20 par groupe. Les étoiles noires représentent une différence significative entre les animaux Control et Dlx-mu. Une étoile, $p<0.05$ (ANOVA à une voie sur mesures répétées).

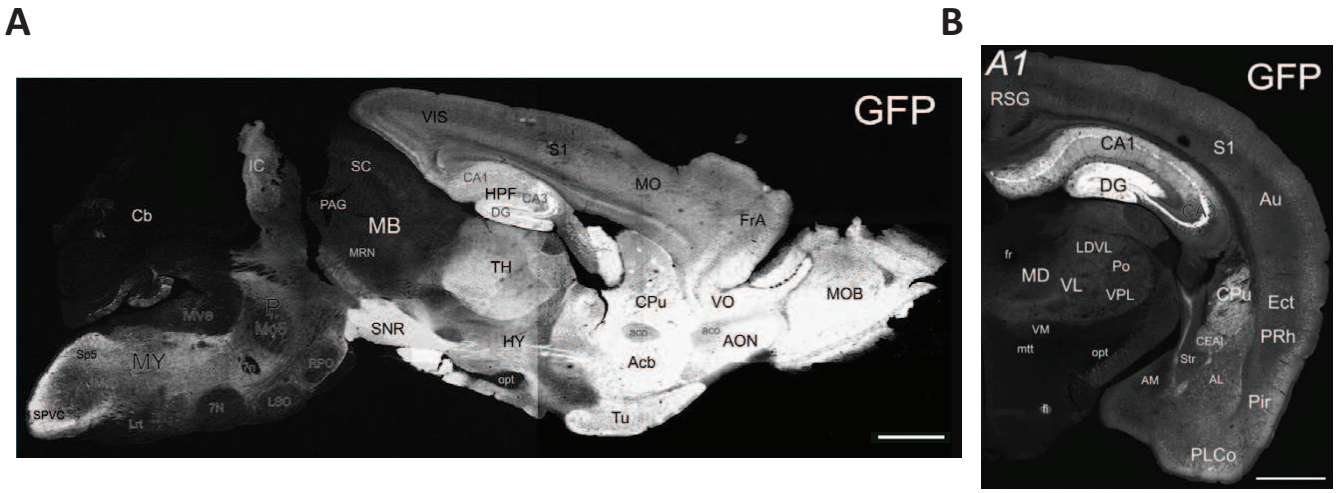

Figure 8. Images de cerveau de souris adulte CaMKIIα-GFP. (**A**) Vue sagittale. Le montage d'images confocales montre la GFP sur des sections sagittales de 30 µm (latéral 1.10mm). (**B**) Vue coronale. Image de GFP sur des sections coronales de 30 µm (Bregma -2.22 mm). Échelle = 500 µm. Adapté de Wang et al., 2013.

Abbreviations: 7n, facial nucleus root; 7N, facial nucleus; Acb, accumbens nucleus; Aco, anterior commissure; AM, amygdalar nucleus, medial; AL, amygdalar nucleus, lateral; Ang, angular thalamic nucleus; AON, anterior olfactory nucleus; ArcD, arcuate hypothalamic nucleus, dorsal part; ArcL, arcuate hypothalamic nucleus, lateral part; Au, auditory cortex; CA1, field CA1; CA3, field CA3; Cb, cerebellum; CEAl, central amygdalar nucleus, lateral; CL, central lateral nucleus of the thalamus; CM, central medial nucleus of the thalamus; CPu, caudoputamen; DG, dentate gyrus; DM, dorsal medial nucleus of the hypothalamus; Ect, ectorhinal cortex; Fr, fasciculus retroflexus; FrA, frontal association cortex; Ge5, gelatinous layer of the caudal spinal trigeminal nucleus; gr, granule layer of cerebellum; GrDG, granular layer of dentate gyrus; HPF, hippocampal formation; HY, hypothalamus; IC, inferior collicullus; IMD, infer mediodorsal nucleus of the thalamus; LDDM, laterodorsal thalamic nucleus, dorsomedial part; LDVL, laterodorsal thalamic nucleus, ventrolateral part;LPMR, lateral posterior thalamic nucleus, mediorostral part; LH, lateral hypothalamus area; Lmol, stratum lacunosummolecular; Lrt, lateral reticular nucleus; LSO, lateral superior olive; MB, midbrain; MO, motor cortex; MDC, mediodorsal nucleus of the thalamus,central part; MdD, medullary reticular nucleus, dorsal part; MDL, mediodorsal nucleus of the thalamus, dorsal part; MDM, mediodorsal nucleus of the thalamus, medial part; ME, median eminence; mmt, mammilo thalmic tract; Mo5, motor trigeminal nucleus; MOB, main olfactory bulb; MoDG, dentate gyrus, molecular layer; MRN, midbrain reticular nucleus; MY, Medulla; MVe, medial vestibular nucleus; Opt, optictract; Or, stratum oriens; P, pons; Pa, paraventricular hypothalamic nucleus; PARN, parvi cellular reticular nucleus; PAG, periaqueductal gray; PC, paracentralnucleus; Pir, piriform cortex; Pc, purkinje cell layer of cerebellum; PLCo, posterolateral cortical amygdaloid nucleus; Po, posterior complex of the thalamus; PoDG, polymorph layer of the dentate gyrus; PRh, perirhinal cortex; Rad, stratum radiatum; Re, nucleus of reunions; RPO, rostal periolivary region; RSG, retrosplenial granular cortex; RT, reticular nucleus of the thalamus; S1, primary somatosensory cortex; SC, superior colliculus; Slu, stratum lucidum; SNR, substantia nigra, reticular part of amygdaloid area; Sp5, spinal trigeminal nucleus; SPVC, spinal nucleus of the trigeminal, caudal part; Str, striatum terminals; Sub, subparafascicular nucleus; TH, thalamus; Tu, olfactory tubercle; VIS, visual cortex; VL, ventrolateral nucleus of thalamus; VO, ventral orbital cortex; VPM, ventral postero medial nucleus of thalamus; VPL, ventral posterolateral nucleus of thalamus; Wm, whitematter.

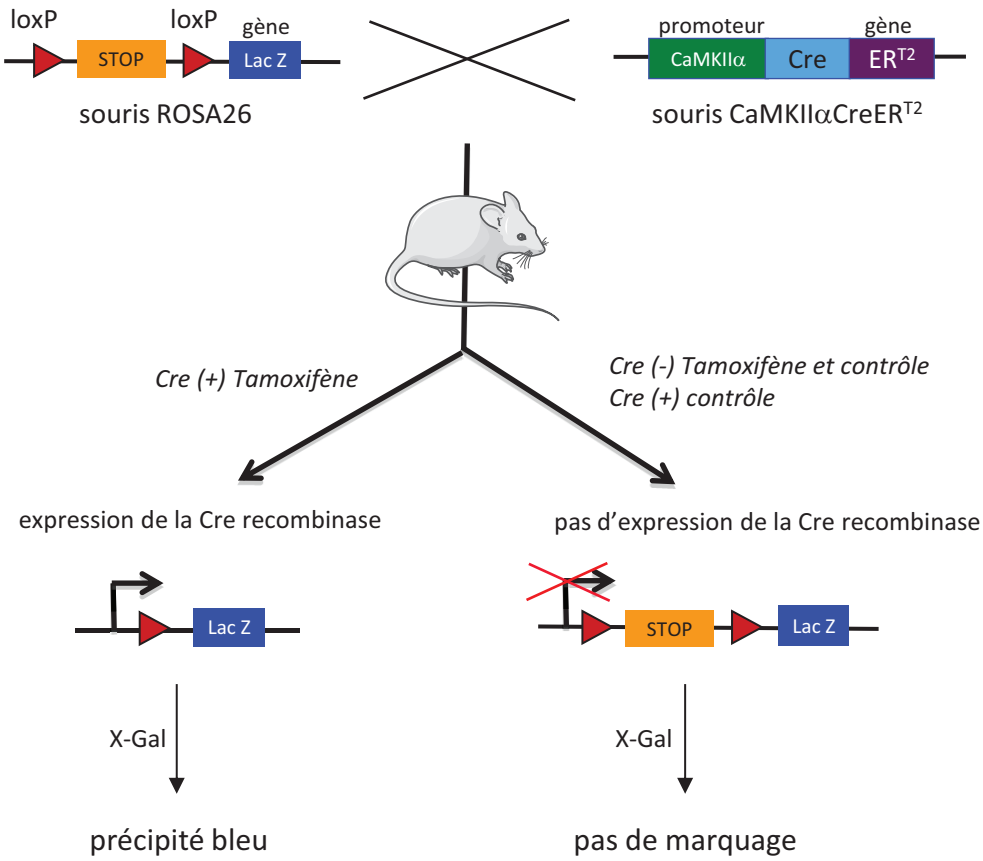

Figure 9. **Utilisation de la lignée de souris CaMKIIαCreER^{T2} ROSA26 pour étudier l'activité Cre recombinase.**
Nous avons croisé la souris rapportrice Cre recombinase ROSA26 avec la lignée de souris CaMKIIαCreER^{T2} pour obtenir la lignées CaMKIIαCreER^{T2} ROSA26. Les animaux positifs pour la Cre recombinase sont traités au tamoxifène (2 mg/jour, 15 jours) pour induire l'activation de la Cre recombinase, menant à l'excision de la séquence stop. Le gène *LacZ* est alors exprimé et code pour l'enzyme β-galactosidase, qui produit, dans les cellules exprimant la Cre, un précipité bleu en présence de son substrat X-Gal.

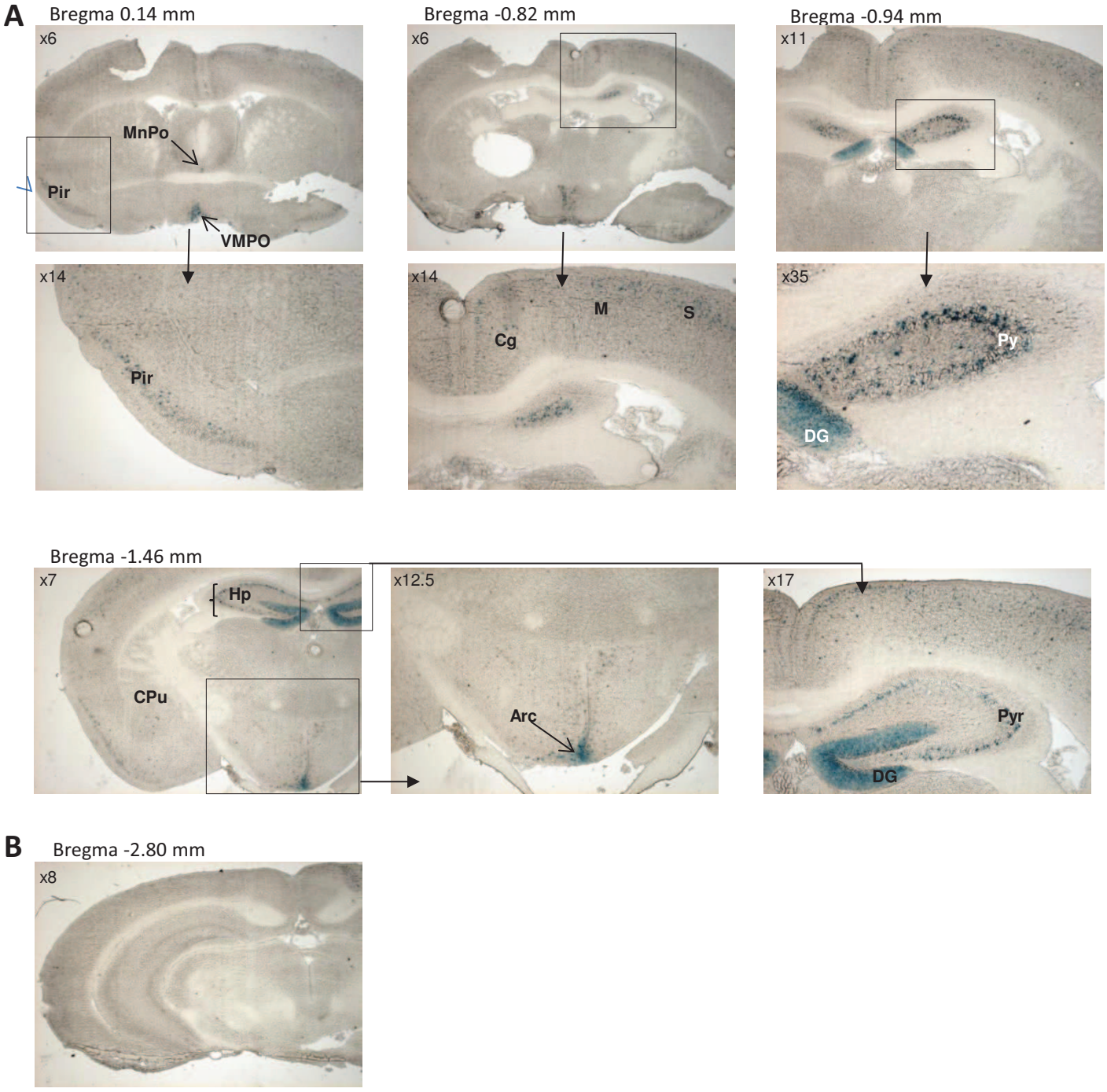

Figure 10. Pattern d'activité de la Cre recombinase des souris CaMKIIαCreER^{T2} en utilisant la lignée rapportrice ROSA26. Images de sections de cerveau CaMKIIαCreER^{T2} ROSA26 marquées après application de X-Gal pour des souris traitées au tamoxifène (**A**) ou contrôle (**B**). Peu de cellules sont marquées par rapport à la littérature (Choi et al, 2014).

Abréviations : Arc, noyau arqué de l'hypothalamus; Cg, cortex cingulaire; CPu, noyau caudé putamen; DG, gyrus denté ; Hp, hippocampe; M, cortex moteur ; MnPo, noyau préoptique médian; Pir, cortex piriforme ; Pyr, cellules pyramidales de l'hippocampe; S, cortex somatosensoriel primaire; VMPO, noyau préoptique ventromédial.

Régions cérébrales	Niveaux d'expression de la Cre recombinase
Basolateral amygdala (BLA)	+
Cingulate (Cg), motor (M), orbital, prefrontal (PFC), and somatosensorial (S) cortices	+
Piriform cortex (Pir)	++
Hippocampal pyramidal cells (Pyr)	+++
Dentate gyrus (DG)	+++
Lateral hypothalamus (LH)	++
Nucleus accumbens (NAc)	0
Caudate putamen (CPu)	0
Bed nucleus of the stria terminalis (BNST)	+
Arcuate hypothalamic nucleus (Arc)	+++
Ventromedial hypothalamic nucleus (VMH)	+++
Interpeduncular nucleus (IP)	++
Medial mammillary nucleus, medial part (MM)	++
Dorsal raphe nucleus (DR)	++
Supramammillary nucleus, medial part (SuMM)	+
Median (MnPO) and ventromedial (VMPO) preoptic nucleus	++
Anterior olfactory nucleus (dorsal AOD, lateral AOL, medial AOM parts)	+
Paraventricular thalamic nucleus (PV)	+

Table 1. Niveau d'expression de la Cre recombinase chez les souris CaMKIIαCreER^{T2} ROSA26.
Les souris CaMKIIαCreER^{T2} ROSA26 affichent un marquage bleu dû au X-Gal, qui correspond à l'activité de la Cre, dans de nombreux noyaux cérébraux. Niveaux d'expression : 0, pas d'expression; +, faible; ++, fort; +++, très fort.

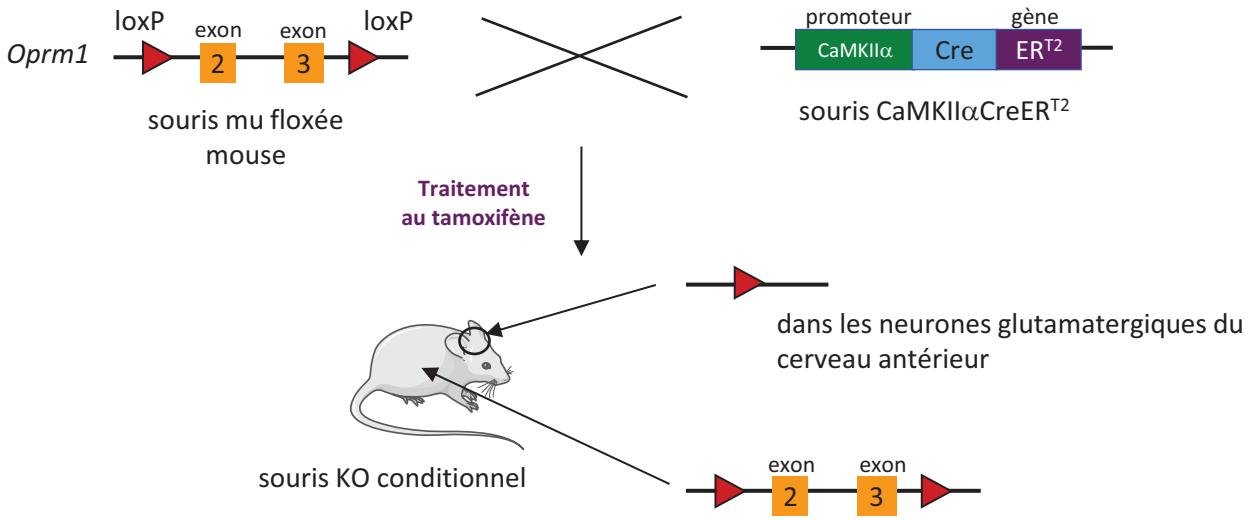

Figure 11. Création de la lignée de souris CaMKIIα-mu : stratégie de croisement et traitement.
Nous avons croisé les souris mu floxées avec les souris CaMKIIαCreER^{T2} pour obtenir notre lignée de souris knockout conditionnelles. Les animaux positifs pour la Cre recombinase sont traités au tamoxifène pour induire l'activation de la Cre recombinase, menant à l'excision de *Oprm1* dans les neurones glutamatergiques du cerveau antérieur.

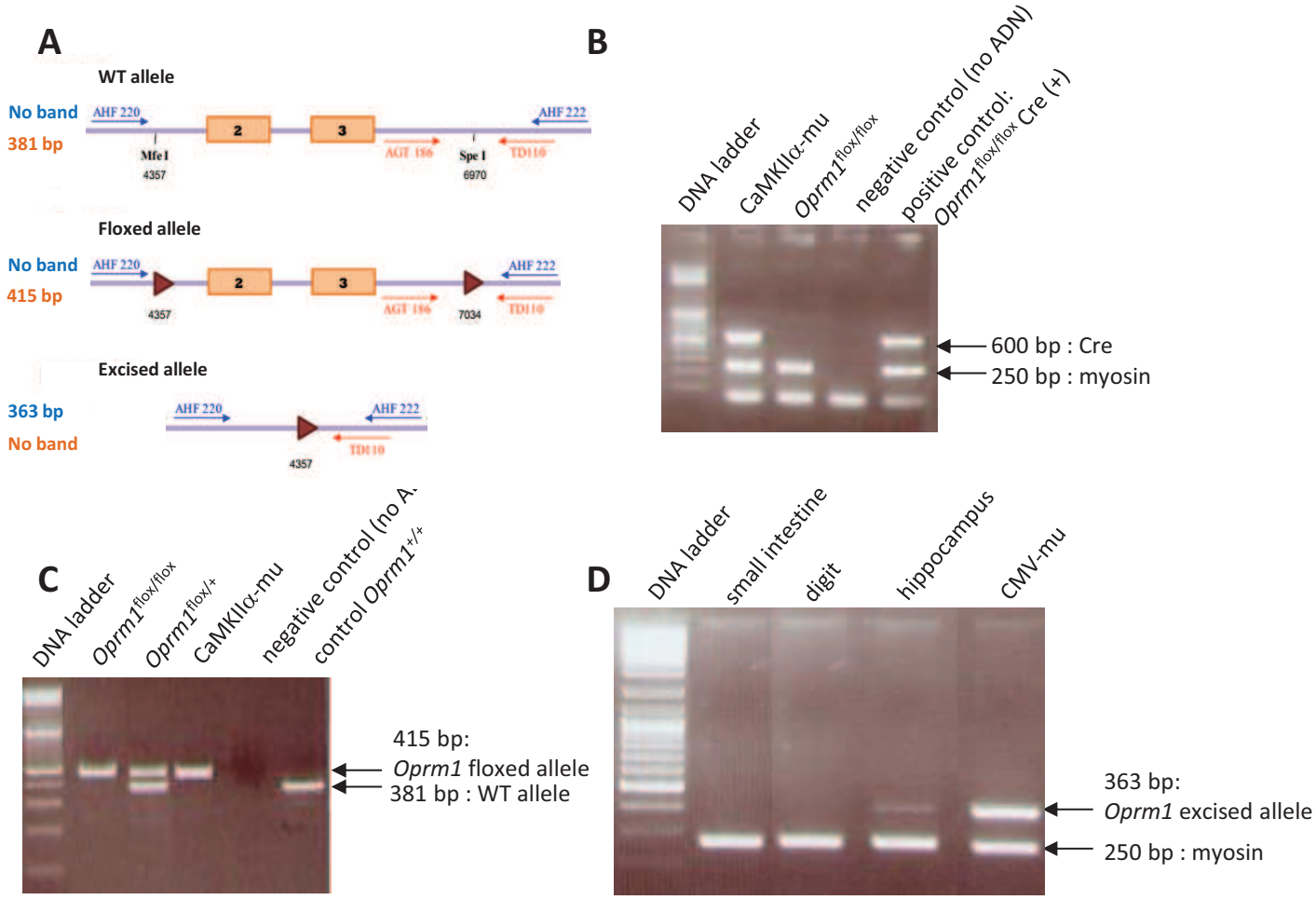

Figure 12. Stratégies PRC pour la détection des allèles *Oprm1* floxé et excisé (A) et amplification PCR montrant la présence de la Cre recombinase (B), des sites loxP (C) et de l'excision de mu (D) chez les souris CaMKIIα-mu traitées au tamoxifène. PCR de biopsies de doigts de souris CaMKIIα-mu : la présence du locus Cre (**B**) est révélé par les amorces BBY14/BBY15, les amorces ADV28/ADV30 montrent la présence de la myosine qui sert de contrôle; la présence des sites loxP (**C**) est détectée par les amorces AGT186/TD110. La présence de l'allèle *Oprm1* excisé dans différentes régions est représentée en (**D**). Il n'y a pas d'excision de *Oprm1* dans l'intestin grêle ou le doigt, mais une bande d'excision est détectée dans l'hippocampe. L'amplification PCR des biopsies de doigts de souris CMV-mu sert de contrôle pour l'excision de *Oprm1*.

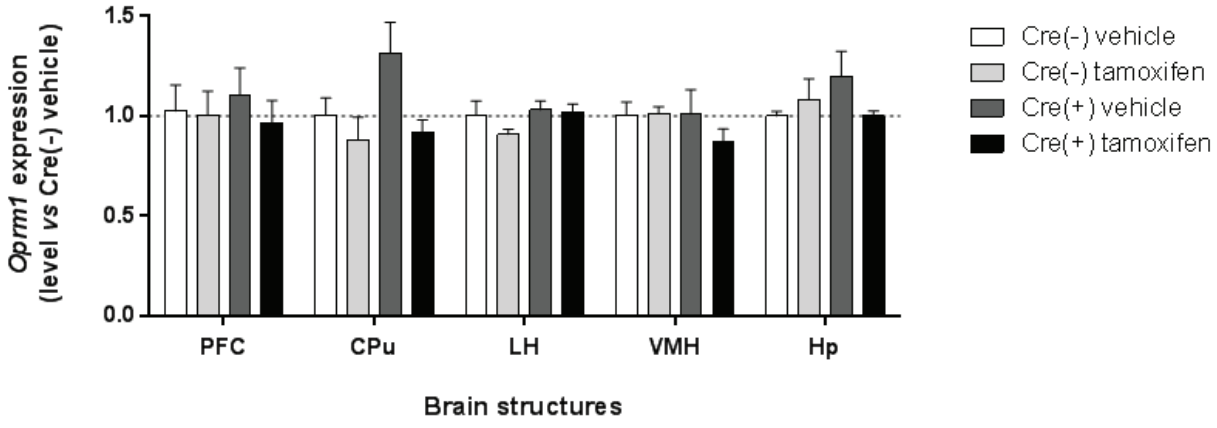

Figure 13. Caractérisation neuroanatomique des animaux KO conditionnels. PCR quantitative en temps réel. L'ARNm de *Oprm1* chez les souris CaMKIIα-mu (knockout conditionnel) est représenté selon l'expression chez les animaux Control injectés contrôle (*vehicle*; =1, ligne en pointillés), normalisé grâce à la *β-actine* comme gène de référence. n=3-4 par groupe. CPu, noyau caudé putamen; Hp, hippocampe; LH, hypothalamus latéral; PFC, cortex préfrontal; VMH, noyau hypothalamique ventromédial.

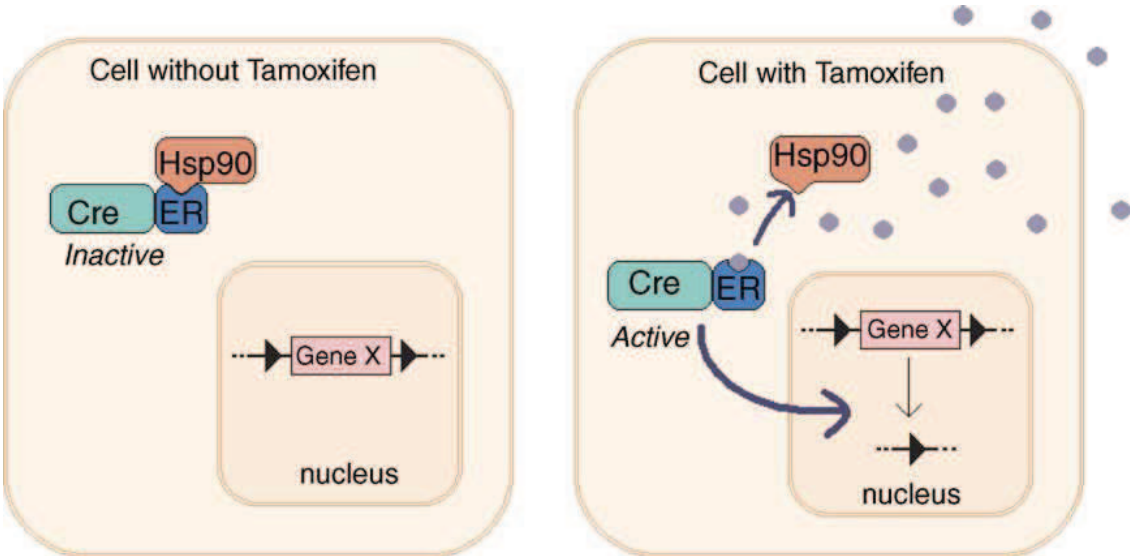

Figure 14. L'activité Cre de la protéine de fusion CreER^{T2} est inductible par 4-OH-tamoxifène. Sans tamoxifène, CreER est lié à Hsp90 et localisé dans le cytoplasme. Le tamoxifène se lie préférentiellement au récepteur de l'œstrogène (ER), déplaçant Hsp90 et induisant la translocation de CreER dans le noyau, activant à son tour Cre. Adapté de Tian et al., 2006.

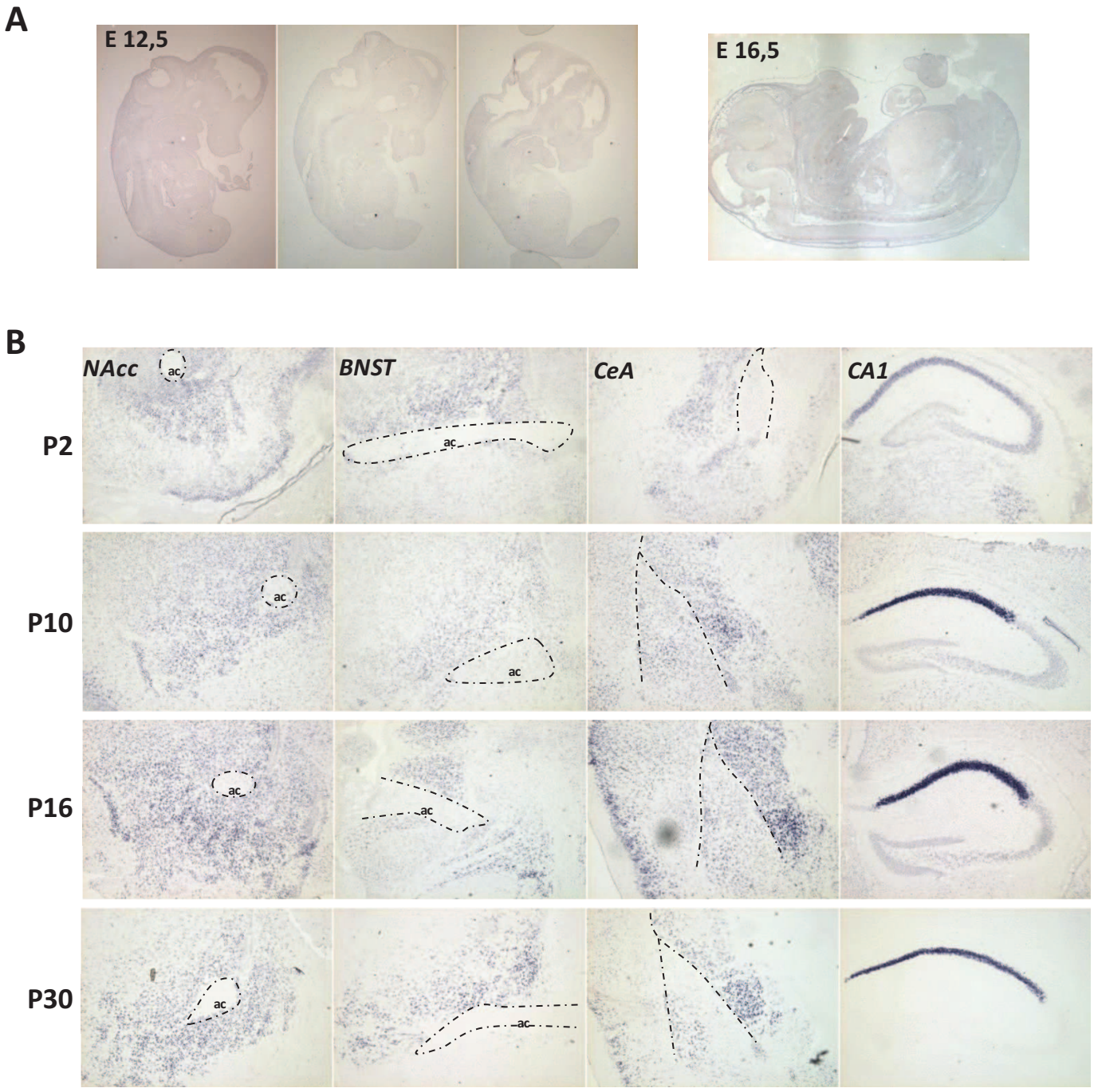

Figure 15. Pattern d'expression de *Wfs1* au court du développement embryonnaire dans l'organisme entier et postnatal dans le cerveau de souris par hybridation *in situ*. (A) L'expression du gène *WFS1* n'est pas détectable pendant le développement embryonnaire, comme montré sur les sections sagittales aux stades E12,5 et E16,5. **(B)** Expression de *Wfs1* dans le cerveau de souris à différents stades postnataux, en sections coronales. Des niveaux modérés de transcrit *Wfs1* sont détectés dans l'amygdale étendue et le CA1 à partir du jour postnatal 2. L'expression de *Wfs1* augmente de plus en plus avec le temps et est comparable à l'expression chez l'adulte à P16.
ac, commissure antérieure; BNST, noyau du lit de la strie terminale; CA1, CA1 de l'hippocampe; CeA, noyau amygdaloïde central; NAcc, noyau accumbens.

Figure 16. Représentation schématique de la construction utilisée pour générer la lignée transgénique de souris WFS1-Cre-eGFP
Un court transgène, contenant un ADNc qui encode une protéine de fusion Cre-eGFP fluorescente sous le contrôle d'un promoteur Wfs1 de 5,7kb, a été construit et microinjecté dans des oocytes fertilisés.

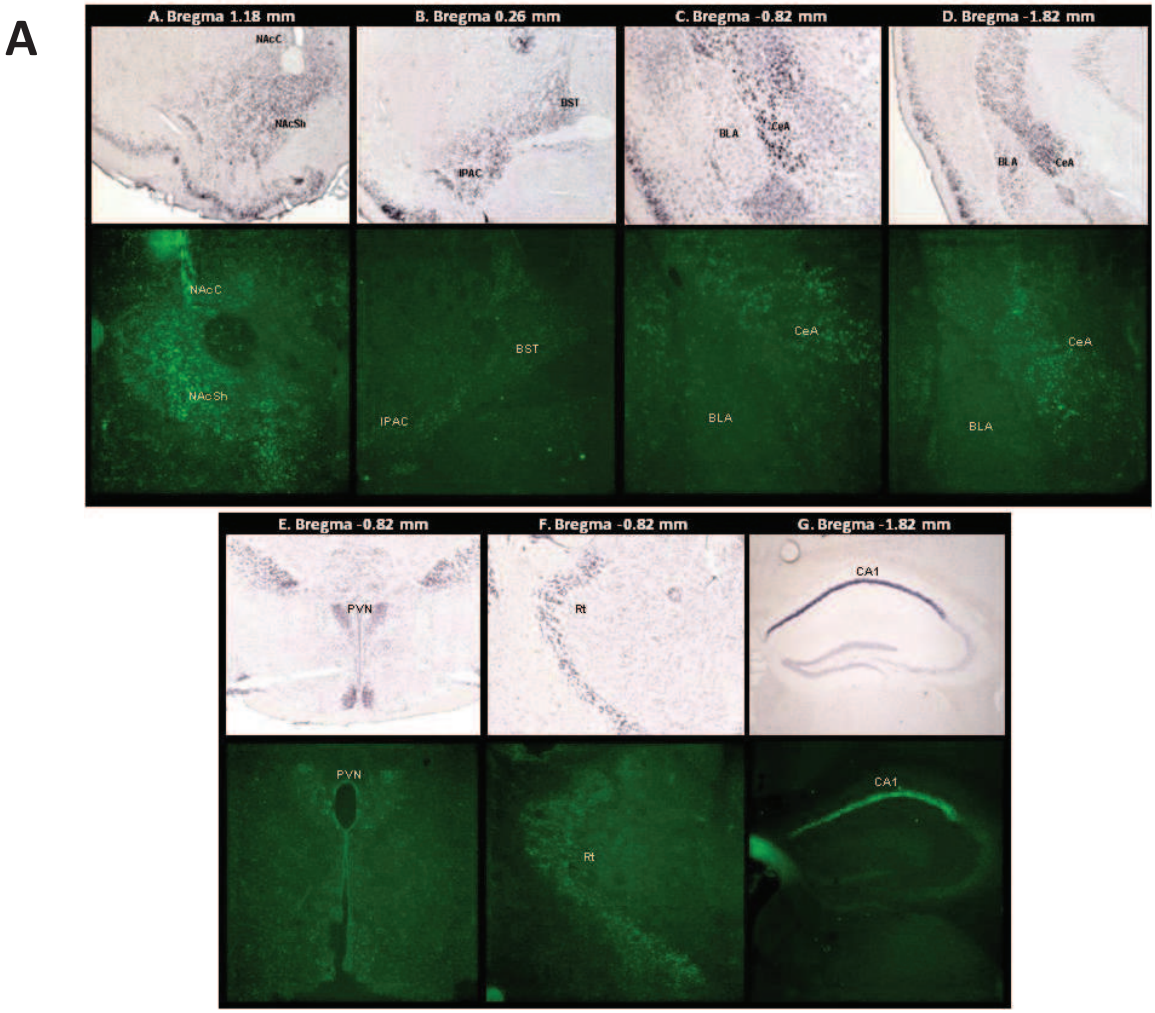

Figure 17. (A) Comparaison des patterns d'expression de l'ARNm de *Wfs1* (souris WT) avec le transgène Cre-eGFP (souris shWFS1-Cre-eGFP). Les panneaux supérieurs représentent des images de sections de cerveaux de souris WT après hybridation en utilisant une sonde *Wfs1*, alors que les panneaux inférieurs représentent des images de sections de cerveaux de souris shWFS1-Cre-eGFP1 après immunohistochimie avec anticorps anti-GFP. Les images A à D correspondent à différents composants de l'EA, l'image E au PVN, l'image F le Rt et l'image G au CA1.
BLA, noyau amygdaloïde basolatéral, partie antérieure; BST, noyau du lit de la strie terminale; CA1, CA1 de l'hippocampe; CeA, noyau amygdaloïde central; IPAC, noyau interstitiel du bras postérieur de la commissure antérieure; NAcC, core du noyau accumbens; NAcS, shell du noyau accumbens; PVN, noyau thalamique paraventriculaire; Rt, noyau thalamique réticulaire.

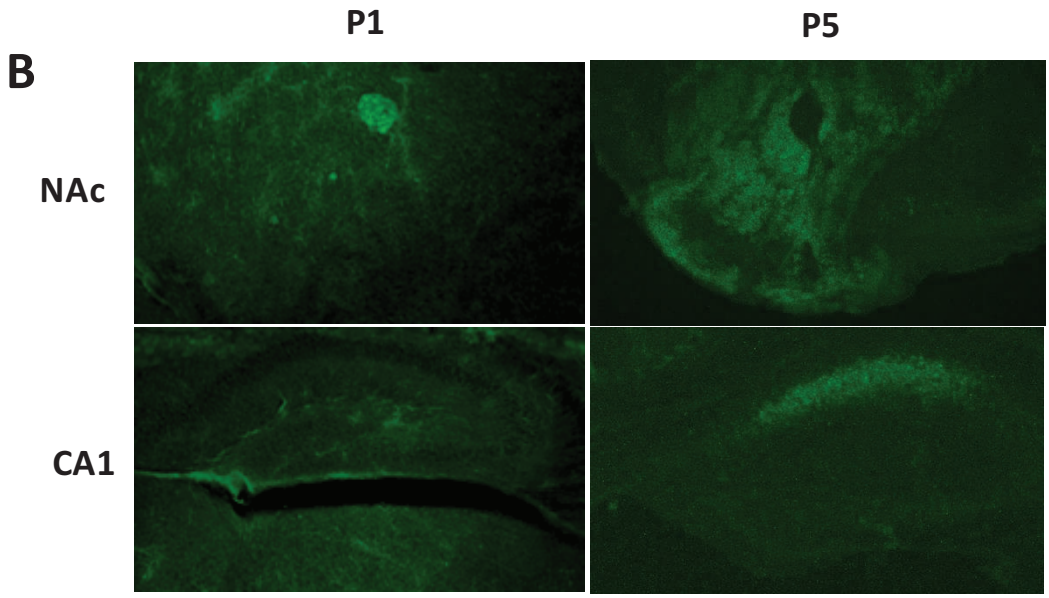

Figure 17. (B) Pattern d'expression de Cre-eGFP pendant le développement postnatal du cerveau. L'immunohistochimie anti-GFP révèle que la protéine Cre-eGFP n'est pas encore présente chez les souris Wfs1-Cre-EGFP au stade P1, mais est exprimée dans les neurones du NAc et du CA1 au stade P5.
CA1, CA1 de l'hippocampe; NAc, noyau accumbens.

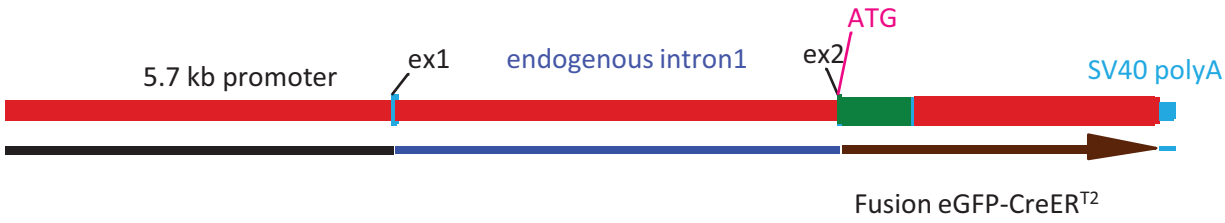

Figure 18. . Représentation schématique de la construction utilisée pour générer la lignée transgénique de souris shWFS1-eGFP-CreER^{T2}

Figure 19. . Représentation schématique de la construction utilisée pour générer la lignée transgénique de souris shWFS1- eGFP-T2A-CreER^{T2}

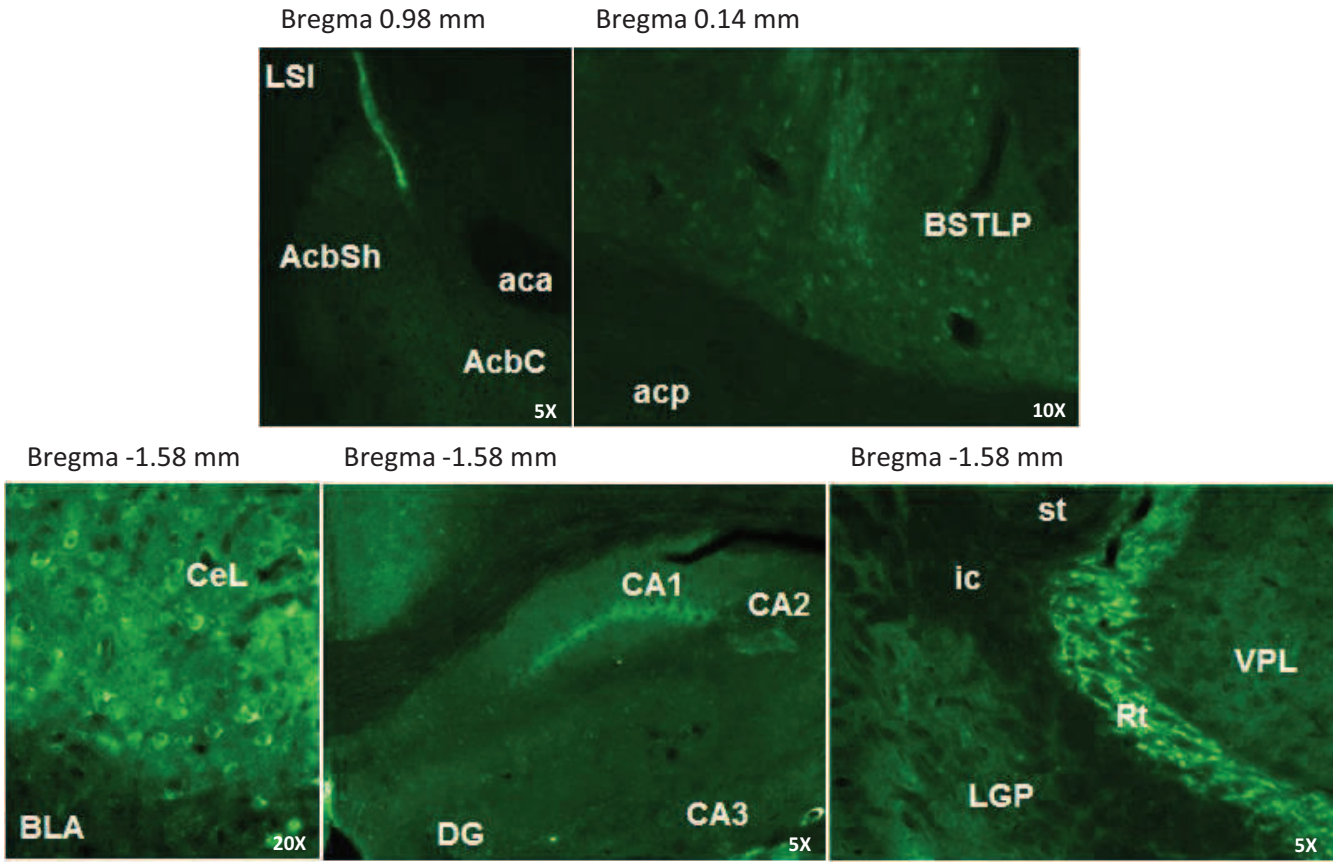

Figure 20. Pattern d'expression de la Cre-eGFP révélé par immunohistochimie anti-eGFP chez la lignée de souris transgénique shWFS158-eGFP-CreER^{T2} (sections coronales).

aca, commissure antérieure, partie antérieure; AcbC/Sh, noyau accumbens, core/shell; acp, commissure antérieure, partie postérieure; BLA, noyau amygdaloïde basolatéral, partie antérieure; BSTLP, noyau du lit de la strie terminale, division latérale, partie postérieure; CA1/2/3, CA1/2/3 de l'hippocampe; CeL, noyau amygdaloïde central, division latérale; DG, gyrus denté; ic, capsule interne; LGP, globus pallidus latéral; Rt, noyau thalamique réticulaire; st, strie terminale; VPL, noyau thalamique ventral postérolatéral.

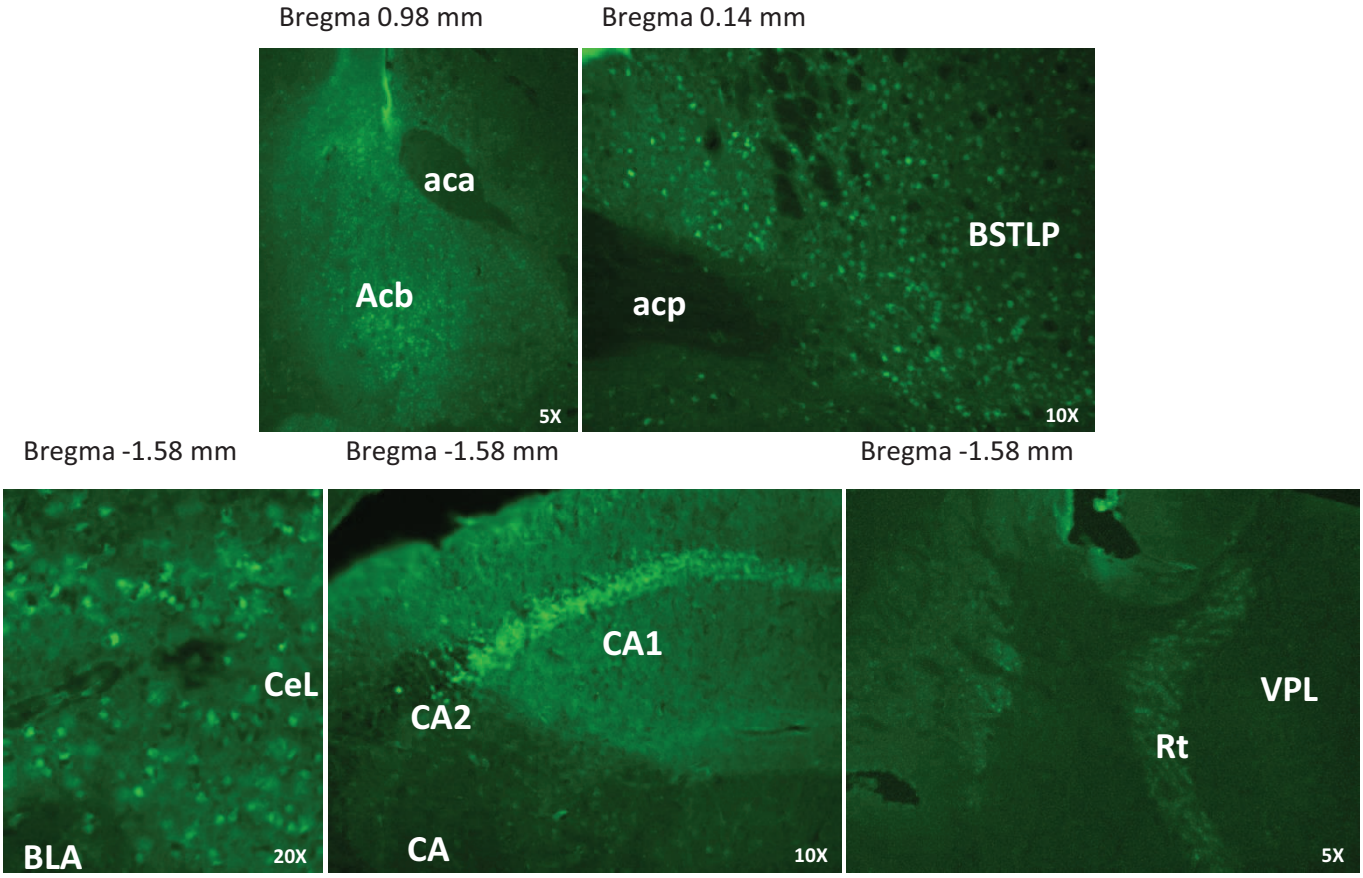

Figure 21. Pattern d'expression de la Cre-eGFP révélé par immunohistochimie anti-eGFP chez la lignée de souris transgénique shWFS6-eGFP-T2A-CreERT2 (sections coronales).

aca, commissure antérieure, partie antérieure; Acb, noyau accumbens, core/shell; acp, commissure antérieure, partie postérieure; BLA, noyau amygdaloïde basolatéral, partie antérieure; BSTLP, noyau du lit de la strie terminale, division latérale, partie postérieure; CA1/2/3, CA1/2/3 de l'hippocampe; CeL, noyau amygdaloïde central, division latérale; Rt, noyau thalamique réticulaire; VPL, noyau thalamique ventral postérolatéral.

Pauline CHARBOGNE

Mu opioid receptors and neuronal circuits of addiction: genetic approaches in mice

Résumé

Le récepteur opioïde mu est responsable des propriétés analgésiques et addictives puissantes de la morphine et de l'héroïne, mais son mode d'action à l'échelle des circuits neuronaux est mal connu et a été peu étudié par des approches génétiques. Le récepteur mu est largement exprimé dans le système nerveux, essentiellement dans des neurones GABAergiques. Le premier objectif de mon projet a été d'inactiver le gène codant pour le récepteur mu dans les neurones GABAergiques du cerveau antérieur et d'en étudier les conséquences comportementales. Notre étude montre que ces récepteurs ne sont pas impliqués dans l'analgésie et la dépendance physique à la morphine, mais qu'ils sont essentiels à l'effet hyperlocomoteur de l'héroïne. De plus, nos résultats indiquent que ces récepteurs limitent la motivation à consommer de l'héroïne et du chocolat, révélant un rôle entièrement nouveau pour cette population particulière de récepteurs (Manuscrit 1 : *Mu opioid receptors in GABAergic forebrain neurons are necessary for heroin hyperlocomotion and reduce motivation for heroin and palatable food*). Aussi, cette population de récepteurs mu n'est pas responsable du syndrome autistique décrit chez les souris knockout totales (Manuscrit 2 : *Mu opioid receptors in GABAergic forebrain neurons are not involved in autistic-like symptoms*). Enfin, nous avons développé un nouveau modèle transgénique visant l'inactivation génétique du récepteur mu dans les neurones glutamatergiques, mais qui n'a pas abouti à un knockout conditionnel détectable. Nous avons aussi initié la création d'une lignée transgénique Cre pour l'inactivation de gènes d'intérêt dans l'amygdale étendue, qui permettra notamment d'étudier le rôle du récepteur mu dans ce microcircuit.

Mots-clés : récepteur opioïde mu, souris knockout conditionnelles, récompense, nociception, trouble autistique, amygdale étendue.

Résumé en anglais

Mu opioid receptors mediate the strong analgesic and addictive properties of morphine and heroin; however mu receptor function at circuit levels is not well understood and has been poorly studied by genetic approaches. These receptors are widely expressed throughout the nervous system, essentially in GABAergic neurons. The first aim of my project was to genetically inactivate the mu receptor gene in GABAergic forebrain neurons and study the behavioral consequences. Our study shows that these mu receptors are not implicated in morphine-induced analgesia and physical dependence, but are essential for locomotor effects of heroin. Moreover, our data show that these receptors inhibit motivation to consume heroin and chocolate, revealing an entirely new role for this particular population of mu receptors (Manuscript 1: *Mu opioid receptors in GABAergic forebrain neurons are necessary for heroin hyperlocomotion and reduce motivation for heroin and palatable food*). Also, mu receptors expressed in forebrain GABAergic neurons are not responsible for the autistic syndrome described in total mu receptor knockout mice (Manuscript 2: *Mu opioid receptors in GABAergic forebrain neurons are not involved in autistic-like symptoms*). Finally, we developed a new transgenic model targeting the mu receptor gene in glutamatergic neurons, but receptor deletion was not detectable in conditional mice. We also initiated the creation of a transgenic Cre driver line to knockout genes of interest in the extended amygdala, and this tool will enable us to study mu receptor function within this microcircuit.

Key words: mu opioid receptor, conditional knockout mice, reward, nociception, autism spectrum disorder, extended amygdala.